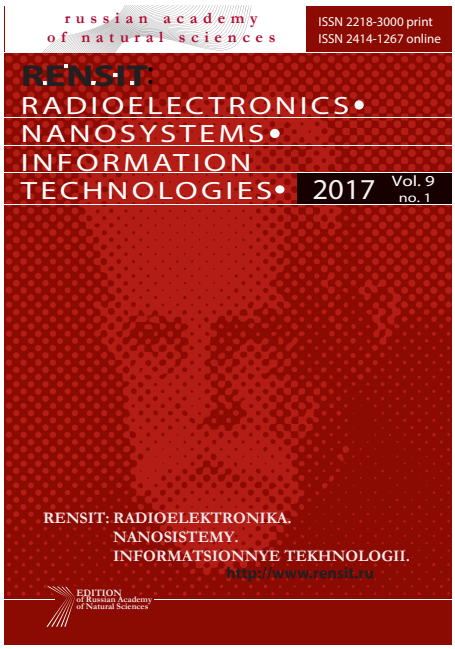

RENSIT:
RadioElektronika. NanoSistemy. Informatsionnye Tekhnologii

Journal "Radioelektronika. Nanosistemy. Informatsionnye Tekhnologii" (abbr. RENSIT)
publishes original articles, reviews and brief reports, not previously published, on topical problems in **radioelectronics (including biomedical) and fundamentals of information, nano- and biotechnologies and adjacent areas of physics and mathematics.**

Designed for **researchers, graduate students, physics students of senior courses and teachers**.
It turns out **2 times a year** (that includes 2 issues)

Authors of journal are academicians, corresponding members and foreign members of Russian Academy of Natural Sciences (RANS) and their colleagues,
as well as other russian and foreign authors on presentation of their manuscripts by the members of RANS, which can be obtained by authors before sending articles to editors.
And also after its receiving - on recommendation of a member of editorial board of journal, or another member of Academy of Natural Sciences, that gave her opinion on article at request of editor.
The editors will accept articles in both **Russian and English** languages.

Articles are internally peer reviewed (**double-blind peer review**) by members of the Editorial Board.
Some articles undergo external review, if necessary.

Journal RENSIT is included in the **AJ and DB VINITI RAS** (http://www.viniti.ru),
in the international abstracts database - **Ulrich's International Periodicals Directory**,
(USA, New York, http://www.ulrichsweb.com);
and DB **Russian Science Citation Index (RSCI** http://elibrary.ru/project_risc.asp).
Full-text content is posted in the DB of the **Russian Scientific Electronic Library**
- information resource on the Internet http://elibrary.ru and is available for registered users.
And also - in Open Access **KIBERLENINKA NEB**, the Russian Federation
http://cyberleninka.ru.
On the journal's website http://www.rensit.ru posted metadata publications
and RENSIT: Radioelectronics. Nanosystems. Information Technologies
– english version (cover-to-cover translation) of journal, which is a party to **CrossRef.**

The founder - the **Russian Academy of Natural Sciences**
Publisher - Publishing Center of the Russian Academy of Natural Sciences
Publisher Address: 119002 Moscow, per. Sivtsev Vrazhek 29/16

CONTENTS

RUSSIAN ACADEMY OF NATURAL SCIENCES

DEPARTMENT OF RADIOELECTRONICS, NANOPHYSICS AND INFORMATION TECHNOLOGIES PROBLEMS

RENSIT:

RADIOELECTRONICS. NANOSYSTEMS. INFORMATION TECHNOLOGIES.
2017, VOL. 9, № 1

FOUNDED IN 2009
2 ISSUES PER YEAR
MOSCOW

ISSN 2414-1267
The journal on-line is registered by the Ministry of Telecom and Mass Cjmmunications of the Russian Federation. Certificate El. no. FS77-60275 on 19.12.2014

EDITORIAL BOARD ADDRESS
218-219 of., 7 b., 11, Mokhovaya str.,
125009 MOSCOW, RUSSIAN FEDERATION,
TEL. +7 495 629 3368
FAX +7 495 629 3678 FOR GRACHEV

SCIENTIFIC-TECHNOLOGICAL FORECASTING

Vladimir I. Grachev

Kotel'nikov Institute of Radioengineering and Electronics, Russian Academy of Sciences, http://www.cplire.ru
Moscow 125009, Russian Federation
Editor-in-Chief of journal "Radioelectronics. Nanosystems. Information Technologies" (RENSIT)
grachev@cplire.ru

Sergey P. Gubin

Kurnakov Institute of General and Inorganic Chemistry, Russian Academy of Sciences, http://www.igic.ras.ru
Moscow 119991, Russian Federation
Deputy Chief of journal RENSIT
gubin@igic.ras.ru

Abstract. **The editorial board of the journal RENSIT announces one of the most important principles of publishing policy of the journal is the publication of the materials researches having the character of scientific-technological forecasting. As a first experience of such publications in the present issue of the journal a series of articles on researches into low energy nuclear reactions (LENR) in Russia is represented.**

Keywords: **scientific-technological forecasting, low energy nuclear reactions**

UDC 001.18

Received 14.06.2017

RENSIT, 2017, 9(1):3-4 **DOI: 10.17725/rensit.2017.09.003**

Issue of the journal, which we offers readers is thematic. But it's not just a compilation of articles with a specific theme of researches. We believe that the material presented can serve as a basis for long-range forecasting of scientific-technological forecasting of energetic in the future.

The word "forecast" in a literal translation from the Greek means "before knowledge", ie before there will be real knowledge (observation) of an object or phenomenon, before the event occurs. In the Russian language synonyms of the forecasting are the words "foresight, prediction".

Innovation activity, about which so much talk lately, requires presence of scientific-technological forecasting of development of society as a whole and its separate parts. A number of techniques and methods, which enable with varying degree of probability to predict the development of separate fields of human activity are developed and used. It is, essentially, a kind of extrapolation. Such forecasting allows you to put the always limited means (resources) to the development of individual directions on a fairly limited time frame in the hope to get effective result.

Wide, but still "until skyline" the forecast usually goes something like this. "The new technological revolution in .... at the turn of the 20...-20... years will lead to the creation ..... Tasks that will be addressed by one agency, will be relevant to other directions. The typical approach of experts and managers: it is necessary to develop "a road map" that is applicable to the widest possible circle of recipients of high-tech industries. As a result, will provide a concentration of resources and development of competence centres..."

In other words – is the work "until skyline". There are methods to rise "higher" and thus move the skyline, but go out beyond the skyline such methods as a rule do not allow.

In our opinion, the most interesting is what there is namely the beyond the skyline. For such an forecasting "beyond skyline" are necessary inmost knowledge and nonstandard thinking plus intuition. Is usually not under force to one person, but a group of people with nonstandard-critical thinking, as experience shows, allows for such "beyond skyline" forecasting.

Scientific-technological forecasting is a form of knowing of the future, it is a special kind of

scientific activity. The forecast, which is discussed here is the forecast of phenomenon. Such scientific-technological forecasting, by definition, should be out-departmental, interdisciplinary.

But herewith the problem arises – how to go between Scylla of vast array of science fiction literature on the one hand and the Charybdis of the so-called "pseudoscience" on the other. The main condition of success – the composition of the participants forecasting. It should be well-qualified specialists, which along with in-depth knowledge in a particular fields, have the ability broad vision, the ability to go beyond their narrow areas.

In this journal issue we make an attempt to implement such approach and to submit scientific-technological forecasting in the area of energetic of the future – the most acute problem of humanity. Our authors in their articles persuasively demonstrate the perspectivity of low-energy nuclear reactions in the quality an energy source and method of obtaining stable isotopes. At the intensive development of works in this direction could will be to go to an principly new level of energy development.

About the quality and significance of what was get of our attempt – not by us to judge. We would be grateful to anyone who will wants to express their opinion in one form or another on the issues raised in this issue of our journal.

What is the efficiency of such a forecast? What are the possible consequences of its use? Who needs to will perceive it? Whom is addressed it?

To these questions are difficult to answer now. In the case of conventional departmental forecasts such addressee always there is – it appropriate management structures. Probable consumer of here submitted forecast must be structures of strategic planning. In what measure the interaction with them will be fruitful - time will tell.

With publications in the present issue of the journal we hope to open (start) the publications of a series of materials on various aspects of interdisciplinary scientific-technological forecasting. We hope that readers take an active part in the discussions of questions raised in this issue of the journal, will share their critical remarks and suggestions on the further development of this topic. If necessary, we are ready to open in the next issues our journal a special discussion section. With regard to the theme cold transformation of chemical elements ("cold fusion" – the biting expression of journalists), raised in this issue of journal we have every confidence that if at least one-hundredth share of what is here set out, - is reality, then it will can to provide humanity with energy for many centuries ahead.

LENR IN RUSSIA

Anri A. Rukhadze
Prokhorov General Physics Institute, Russian Academy of Sciences, http://www.gpi.ru
Moscow 119991, Russian Federation
rukh@fpl.gpi.ru

Vladimir I. Grachev
Kotel'nikov Institute of Radioengineering and Electronics, Russian Academy of Sciences, http://www.cplire.ru
Moscow 125009, Russian Federation
grachev@cplire.ru

Abstract. **Provides information on research into low energy nuclear reactions, held in Russia. Shows a great variety of methodological approaches, which is typical for Russian studies in this area. Lists the most vivid experiments, the problem of low reproducibility of their results also provided the basic theoretical work that illustrate attempts of interpretation of the known experimental results. Formulated possible at the moment understanding low-energy nuclear reactions, collective nuclear transformations occurring at energies unacceptably low for conventional nuclear reactions, and give a variation of the isotopic composition and high heat in the absence of residual radioactivity.**

Keywords: **cold transformation of nuclears, the reproducibility of the experimental results, the attempts of theoretical interpretation**

УДК 530.145, 539.17

Bibliography – 8 references *Received 20.06.2017*

RENSIT, 2017, 9(1):5-7 **DOI: 10.17725/rensit.2017.09.005**

Contents

1. INTRODUCTION

From the first steps of nuclear physics, its development has been largely, in General, in two directions – of high- and low-energetic. E. Rutherford (1871-1937), the "father" of nuclear physics who discovered (1919) artificial "transmutation of elements" – nuclei ($^{14}_{7}N + {}^{4}_{2}He \rightarrow {}^{17}_{8}O + {}^{1}_{1}H$ [1, 2]) by fast alpha particles, have inter-preted this "modern alchemistry" as the area of high-energy processes, which opening the era of nuclear power.

Available by the time the works on nuclear transmutations of stable isotopes in natural conditions, and primarily the receipt by the american chemists K. Irion and J. Wendt (1922) of helium in alpha-decay of tungsten, induced of electric explosion [3], Rutherford declared as error [4]. Then low-energetic ("cold") transmutation of nucleuses for many years turned "pseudoscience".

Nevertheless, reports of studies of low-energy nuclear reactions occasionally appeared. Including, among others, the famous 1956 I.V. Kurchatov lecture on thermonuclear reactions in gas discharge in Harwell (England), E.I. Zababakhin bubble thermonuclear fusion [5], as well as the world's first reactor LENR 1957 of moscow constructor I.S. Filimonenko, which generating the heat excess in the system "the palladium-deuterium", etc.

And after the publication in 1989 M. Fleischmann and S. Pons (USA) in Journal of Electroanalytical Chemistry [6] and their interview on March 23, 1989 in the newspaper "Financial Times" in which they stated that it is possible to create the energy source of the industrial scale based on the fusion of nuclei of heavy hydrogen at room temperature, such researches have widely developing in many laboratories around the world under the trenchant title "cold fusion", coined by journalists.

Are appeared generators JET-MIT "NANOR" (MIT, USA), Patterson (USA), Mayer (USA), J.

Arata (Japan), Y. Iwamura Japan), Shoulders (USA), R. Mills USA), A. Rossi nickel-hydrogen reactor (Italy), etc.

In countries such as USA, Japan, Italy, China and other, these studies are funded by the state programs and the largest firms.

Since 1990, are conducted annual International Conferences on Cold Fusion (ICCF, since 2007 – International Conferences on Condensed Matter Nuclear Science) in the United States, Japan, Italy, France, China, Korea, India and other countries.

2. LENR IN RUSSIA

In Russia during these studies have included the moscow RRC "Kurchatov Institute", the dubna Joint Institute for nuclear research, sarov RFNC, novosibirsk INP SB RAS, Institute of physical chemistry RAS, etc.

The studies are used the term "low energy nuclear reactions" (LENR) and conducted at a wide variety of methodological approaches (that is typical for Russian studies in this area).

These are Parkhomov's analogies of the reactor A. Rossi, Klimov's plasma vortex reactor (JIHT RAS), Kirkinskii's deuterium heat generator (IGM SB RAS), Bazhutov's heatgeneraror of plasma electrolyte (IZMIRAN), Urutskoev's electric explosion of foil, Krymsky's nano-pulse generator, Savvatimova's glow discharge, Nigmatulin-Taleyarkhan deuterated acetone, Shafeev's laser quenching of radioactivity (IOF RAS), Kornilova's transmutation of elements in biological systems (Lomonosov MSU) and many others.

I.e. the phenomenon of low-energy nuclear reactions was discovered in various experimental facilities.

This are reactions in the crystal lattice of metals induced by electrolysis or by saturating it with hydrogen, and reactions in the crystal lattice, induced by impact, the different reactions by diffusion through the membrane. This is a whole class of experiments using electric discharge, electric explosion, ultrasound in a gas or liquid. This are reactions induced corpuscular and wave action on condensed media, and finally, reactions in biological systems.

For many works in this area is characterized by a low reproducibility of the experimental results. This is due to the fact that while still fail to find the key parameter that controls the process, because there is no understanding of the physical model of the phenomenon and the conditions of implementation regimes that promote low-energy reactions

There is also a lot of fairly elaborate theoretical models which tend to focus on resolution of the presence of anomalously large transparency of the Coulomb barrier and practically do not consider other equally important features of low-energy nuclear reactions, such as the lack of daughters radioactive isotopes, as well as the features of concomitant radiations.

Of the currently available results it follows that low energy nuclear reactions are not synthesis or decay, but, apparently, they are some collective nuclear transformations that occur at unacceptably low energies for thermonuclear reactions, and give the variation of the isotopic composition and high heatgeneration at the absence of residual radioactivity.

3. THE PUBLICATIONS OF THIS ISSUE

The editorial Board of the journal "Radioelectronics. Nanosystems. Information technology" (RENSIT) provides the pages of his issue for publishing a series of review materials on the studies of low energy nuclear reactions, held in Russia.

Formed the sampling includes three theoretical overview of V.A. Andreev (Lebedev Physical Institute of RAS), of S.F. Timashev (Karpov Institute of Physical Chemistry) and V.I. Vysotsky (T.Shevchenko Kiev national university) who have been developing their approaches on the foundations of modern quantum theory and five experimental works A.A. Kornilova (Lomonosov MSU), A.G. Shafeev (Prokhorov IOF RAS), A.G. Parkhomov (OIG "K. I. T."), G.V. Mishinsky (JINR), V.V. Krymsky (UrSU), the results of which are obtained by using modern experimental and diagnostic techniques.

Under the cover of one of the issue was not possible to place equally interesting results of other authors [7]. But and done sampling gives an idea about the level and scope of Russian research in this area.

4. CONCLUSION

Presented works indicate a significant advancement in the understanding of weak nuclear processes and can serve as a promising subject of fruitful discussions, the broad expert consideration of the phenomenon of nuclear reactions at low energies.

It is obvious that the mastery of low-energy nuclear reactions will allow to solve many applied tasks, including the creation of a cheap stand-alone energetical plants, high-performance technologies of deactivation of nuclear waste, obtaining rare isotopes and transformation of chemical elements.

REFERENCES

1. Rutherford E. Collision of α-particles with light atoms. I. Hydrogen. II. Velocity of the hydrogen atom. III. Nitrogen and oxygen atoms. IV. An anomalous effect in nitrogen. – *London, Edinburg and Dublin Philos. Mag. and J. Sci.*, London, 1919, ser. 6, 37, p. 537-585.
2. Rutherford E. Sovremennaya alkhimiya [Modern alchemistry]. *UFN*, 1938, 19(1):18-48 (in Russ.).
3. Wendt GL, Irion CE. Experimental attempts to decompose tungsten at high temperatures. *J.of the American Chemical Society,* 1922, 44(9):1887-1894.
4. Rutherford E. Identification of a missing element. *Nature*, London, 1922, 109:781.
5. Kurchatov IV. O vozmozhnosti sozdaniya termoyadernykh reactsiy v gazovom razryade [About possibility of creation of thermonuclear reactions in gas discharge]. *UFN*, 1956, 59(4):603-618.
6. Zababakhin EI, Zababakhin IE. *Yavleniya neogranichennoy kumulyatsii* [Phenomena of unlimited cumulation]. Moscow, Nayka Publ., 1988, 161 p.
7. Fleishmann M, Pons S, Hawkins M. Electrochemically induced nuclear fusion of deuterium. *J. Electroanal. Chem.*, 1989, 261:301-308.
8. Erlikh GV, Andreev SN. *Istoriya yadernoy fiziki v zerkale alkhimii* [The history of nuclear physics in the mirror of alchemistry]. Moscow, Lenand Publ., 2017, 232 p.

HARMONIC OSCILLATOR AND RELATED STATES WITH LARGE VALUE OF UNCERTAINTY

Vladimir A. Andreev

P.N. Lebedev Physical Institute, Russian Academy of Sciences, http://www.lebedev.ru
Moscow 119991, Russian Federation
andrvlad@yandex.ru

Abstract. **A review is given of the properties of two types of quantum states, which have great uncertainty in the coordinate and momentum. Both are obtained from the states of a harmonic oscillator by means of certain transformations. The first type is correlated states, they are obtained from coherent states with a help of the Bogolyubov transform. The variances of the coordinate and momentum of such a state depend on the Bogolyubov transform parameters and can, in general, take arbitrarily large values. Their specific values are determined by the physical processes with which the Bogolyubov transform is realized. A concrete example of such physical process is considered. Another type are stretched states. Formally, they arise when the n-partial state of a harmonic oscillator undergoes a transform associated with a scale transformation of the phase space. The dispersion of the coordinate and momentum of these states depends on the scale transformation parameter and can also take arbitrarily large values. Physically stretched states can be obtained by passing n-photon states through a quantum amplifier. The role of the scale transformation of the phase space is played by the gain of the quantum amplifier.**

Keywords: **harmonic oscillator, correlated states, compressed states, stretched states, uncertainty relations, Planck constant**

PACS 03.65.−w, 23.20.Lv
Bibliography – 33 references *Received 22.04.2017*
RENSIT, 2017, 9(1):8-20 **DOI: 10.17725/rensit.2017.09.008**

Contents

1. INTRODUCTION

This review aims to systematize the disparate facts related to the field of low energy nuclear reactions (LENR), as well as some unusual phenomena associated with electromagnetic field. Until recently, this area was outside of wide scientific discussion

The most of the observed phenomena of this type have no theoretical explanation, and are in contradiction with well-established ideas about the physics of processes of this kind. For this reason they were blamed for the lack of cleanliness of experiments, small statistics and low, in the opinion of critics, qualification of the authors.

In addition, some of the authors did not give the detailed description of their devices and experimental conditions, which made it impossible to verify the results independently. This raised doubts about their scrupulosity. Therefore the studies of this kind did not get support in authoritative academic community, and as the result did not get necessary financial and administrative support. They acquired an odious shade and were discarded in the marginal area.

In recent years, the situation has changed. First, the quantity turned into quality, and the abundance of results obtained in authoritative scientific centers in different countries no longer allowed to be dismissed. Secondly, and more importantly, it turned out that the development of

this topic promises an inexhaustible, safe source of energy. And it opens the way to cheap and rapid decontamination of radioactive isotopes arising from operation of nuclear reactors.

This stimulated the activity of theoreticians in this field, which led to understanding that such phenomena and processes do not contradict the basic laws of nature and many of them can be described using traditional theoretical approaches. Here we give references to some accessible and informative sources on this topic [1-6], if desired; this list can be significantly expanded.

One of the first works in which the problem of LENR was discussed is [7].

At the same time, in our opinion, in order to explain some facts it is necessary to go beyond traditional methods and to look more broadly at the laws of nature and on the consequences that follow from them. This seems quite natural, because the range of phenomena that we discuss is very wide, and it is difficult to expect that all of them can be described in the frame of one model. In this review, we will analyze two such models: the model of correlated states and the model of stretched states.

These models are built within the framework of traditional quantum mechanics and don't use any additional physical assumptions that are different from those generally accepted. Previously they were used in other problems. In this review we describe their formal structure, but don't discuss their possible applications.

One of the phenomena that are actively discussed in connection with LENR is the tunnel effect. It is known that the probability of the occurrence of nuclear reactions involving charged particles of low or medium energies is determined, to a large extent, by the existence of a Coulomb barrier. The charged particles can pass this barrier due to the tunneling effect. The probability of the occurrence of nuclear reactions is determined by the probability of passage of charged particles through the barrier. Therefore it is of interest to consider those factors that can increase this probability.

One of these factors is the connection between product of position and momentum dispersions with the probability of particle passing through a potential barrier. It is assumed that increase of the product of the position and momentum dispersions leads to increase of transparency of the barrier. This in turn increases the probability of nuclear reactions at low energy of the interacting particles. Generally speaking, this statement can not be considered absolutely fair, something like a mathematical theorem, sometimes it can be fulfilled, and sometimes it does not. Everything depends on the specific situation.

In this work we consider two types of states for which the uncertainties of the position and momentum can take arbitrarily large values. We didn't discuss the problem whether these states arise in atomic nucleus, and if they arise, whether they stimulate the low-energy nuclear reactions conducive.

But first we give the basic information concerning the uncertainty relations. This is necessary for unification of terminology and notation, which we will use in the future.

2. THE UNCERTAINTY RELATIONS

The uncertainty relations are the most important characteristic of quantum states, which distinguishes them from classical states. For quantum states one can't measure simultaneously some observable with arbitrary precision. This fact limits our possibilities in localizing this state, but on the other hand, it makes it possible to detect it outside the region of classical localization.

We give the basic facts concerning the uncertainty relations. Here we follow, basically, [8].

Let there be an observable A and operator $\hat{A}$ is associated with it. By "uncertainty" of the value A one understand its root-mean-square deviation, assuming

$$\Delta A = \sqrt{\sigma_A}. \quad (1)$$

Here σ_A is the dispersion of the quantity A

$$\sigma_A = \left\langle \hat{A}^2 \right\rangle - \left\langle \hat{A} \right\rangle^2. \quad (2)$$

$$\left\langle \hat{A} \right\rangle = \int \psi^* \hat{A} \psi dV. \quad (3)$$

If the state is mixed and is described by a density matrix $\hat{\rho}$, then

$$\left\langle \hat{A} \right\rangle = Sp(\hat{\rho}\hat{A}). \quad (4)$$

The Heisenberg uncertainty relation was derived in 1927 for position and momentum operators. It reads [9]

$$\sigma_p \sigma_x \geq \frac{\hbar^2}{4}. \quad (5)$$

In 1930, independently, Robertson and Schrödinger derived an inequality, which is valid for arbitrary Hermitian operators and [10, 11].

$$\sigma_A \sigma_B - \sigma_{AB}^2 \geq \frac{\hbar^2}{4} \left| \left\langle \left[\hat{A}, \hat{B} \right] \right\rangle \right|. \quad (6)$$

Here

$$\sigma_{AB} = \frac{1}{2} \left\langle \hat{A}\hat{B} + \hat{B}\hat{A} \right\rangle - \left\langle \hat{A} \right\rangle \left\langle \hat{B} \right\rangle. \quad (7)$$

The inequality (6) is called the Robertson-Schrödinger inequality. For the position and momentum operators it reads

$$\sigma_p \sigma_x - \sigma_{px}^2 \geq \frac{\hbar^2}{4}. \quad (8)$$

The inequalities (5) and (6) are valid for any quantum states, but in a number of cases they can be clarified. Namely, by considering certain classes of states, or even single state, one can find out that for these states the left-hand sides of the inequalities exceed the minimum values of uncertainties. First of all, we note that the inequalities (5), (6) can be transformed into equalities for pure states. If, on the other hand, the state is mixed and is described by a density matrix $\hat{\rho}$, then the inequalities (5), (6) take the form

$$\sigma_p \sigma_x \geq \frac{\hbar^2}{4} \Phi(\mu),$$

$$\sigma_A \sigma_B - \sigma_{AB}^2 \geq \frac{\hbar^2}{4} \left| \left\langle \left[\hat{A}, \hat{B} \right] \right\rangle \right| \Phi(\mu). \quad (9)$$

Here μ - is a purity

$$\mu = Sp(\hat{\rho}^2), 0 < \mu \leq 1. \quad (10)$$

The quantity $\Phi(\mu)$ is a function that grows monotonically with decreasing of the parameter μ, such that $\Phi(1) = 1$. For pure states $\rho^2 = \rho$ and $\mu = 1$.

However even for pure states the left-hand side of the uncertainty relations may be greater than the minimum value. As an example, consider the N-particle states of a harmonic oscillator $|N\rangle$. For such states the relation (5) reads

$$\sigma_p \sigma_x = (2N+1) \frac{\hbar^2}{4}. \quad (11)$$

And for some other more complicated states one can obtain estimates for corresponding uncertainty relations.

So, in the case of correlated states, the right-hand side of the inequalities (5), (6) is multiplied by a value $1/(1 - r^2)$, where $0 \leq r < 1$ is the correlation coefficient. And in the case of the stretched states the right-hand side of the inequalities (5), (6) is multiplied by a value λ^{-2}, where $0 < \lambda \leq 1$ is the scale transformation coefficient in the phase space. We will discuss below these states in detail. Now we note only that in all these cases one can introduce a value $\hbar_{eff}$ - the effective Planck constant.

$$\hbar_{eff} = \hbar\sqrt{\Phi(\mu)}, \hbar_{eff} = \frac{\hbar}{\sqrt{(1-r^2)}}, \hbar_{eff} = \frac{\hbar}{\lambda}. \quad (12)$$

In the context of ideology of this work an increase of the uncertainty of certain states can be associated with increase of the probability of passage of quantum states through the potential barrier. The hope that such dependence exists is due to the fact that, with the appropriate election of the purity parameter μ and the correlation r and the scale transformation coefficient λ, the value of the effective Planck constant $\hbar_{eff}$ can significantly exceed the value of the usual Planck constant $\hbar$.

This indicates that fluctuations of position and momentum of a corresponding quantum state increase, and with the help of these fluctuations it can jump over a potential barrier. In addition, if we examine the formula for tunnel transition probability, we can see that the larger

Planck constant, the greater the probability of a tunnel transition.

However some examples show that there is no direct connection between the uncertainty and the probability of passing through a potential barrier. So, in particular, if one has a wave function $\psi = c_1\psi_1 + c_2\psi_2$, that is a superposition of two wave functions whose amplitude maxima are located on the axis X on one side of the potential barrier, then the transmission T through a potential barrier for such a function reads

$$T = |c_1|^2 T_1 + |c_2|^2 T_2, \quad (13)$$

here T_1 and T_2 are the transmission coefficients, which correspond separately to wave functions ψ_1 and ψ_2.

The expression (13) does not depend on localization of the wave packets in relation to each other, but the uncertainty relation for the function ψ depends on it. By expanding the locations of localization of the wave packets relative to each other, one can increase the uncertainty of the wave function, but the transmission coefficient (13) will not change. It is the exact result, and it shows that in each particular case the relationship between the uncertainty of the wave function and the probability of passing through the potential barrier must be studied separately.

This problem was studied also in [12, 13]. In Ref. [12] the evolution of Gaussian wave packet was studied in presence of the repulsive delta-potential barrier. For the initial packet localized far enough from the barrier, the transmission coefficient was determined as the probability of detecting a particle on the whole semi axis on the other side of the barrier. This coefficient depends on two dimensionless parameters: the normalized ratio of the force of the potential to the initial average value of the pulse and the ratio of the initial dispersion of the pulse to the initial average value of the pulse.

It was shown that for small values of the second parameter the result reduces to the known transparency formula for the delta barrier obtained in the plane wave approximation by solving the stationary Schrödinger equation. For large values of the second parameter the transmission coefficient can be much larger than that calculated in the plane-wave approximation.

In Ref. [13] the problem of tunneling a wave packet through Coulomb barrier was considered. It was shown that the value of the transmission coefficient can differ greatly from the standard expression obtained in the plane wave approximation (WKB), and can exceed it many times. It is established that the value of the transmission coefficient depends strongly on the shape of the packet.

We also note the paper [14], in which the relationship between the Heisenberg uncertainty relation and the measurement-perturbation error relation was studied.

In fact, in addition to the above, there are many other states with a large uncertainty. Our interest in correlated and stretched states is due to the fact that the processes with which they can be generated are known.

So, in particular, about 20-30 years ago many scientific groups, both in Russia and abroad, studied the squeezed light and developed ways of generating it. But they interested only in squeezing ratio, and did not notice the correlation coefficient. It seems to us interesting to analyze now these works on the subject of what correlation coefficients arise in their states.

3. THE SQUEEZED AND CORRELATED STATES

One can try to explain LENR with the help of squeezed and correlated states. From a formal point of view these states are special generalizations of the coherent states of harmonic oscillator. The important fact that for these states, the dispersions of position and momentum can take different values, depending on the parameters of the states. These values can be arbitrarily large, which makes it possible

to connect these states to phenomena of an increase of the probability of passage of particles through a potential barrier.

The real and imaginary parts of the electromagnetic field in a coherent state $|\alpha\rangle$ undergo fluctuations with equal dispersions. The ground state of a harmonic oscillator is a special case of a coherent state with $\alpha = 0$. For these states, the region of distribution of the canonical variables in the phase space has the form of a circle. The wave packet of the coherent state moves in the oscillator potential between the classical turning points, preserving its shape. The width of this wave packet is identical to the width of the wave packet of the ground state of the oscillator.

There exist states in which distribution of the canonical variables in the phase space is deformed in such a way that dispersion of one canonical variable decreases due to increase of dispersion of the other canonical variable. The domain of distribution of the canonical variables takes an oval shape, similar to an ellipse. Such deformation of a distribution region is called "squeezing", and such states themselves are called the "squeezed states." In contrast to coherent states, the width of the wave packet of squeezed states oscillates when these packets move back and forth in the oscillator potential.

The squeezed states were actively investigated, both theoretically and experimentally. Various methods for their generation have been proposed and realized. However, the fact that they are often also the correlated states remained in the shadows. Of course, this fact was noted by some authors, but it was not used in any way. At present, the presence of internal correlations in such states attracts attention to them. It is this fact that is used in [15-17] to explain the LENR.

In this section, we describe the main properties of squeezed and correlated states, as well as some methods for their generation.

Let us give a formal definition of the squeezed and correlated states, and describe their main properties [8,18]. As was already noted, these states are a generalization of coherent state. Let's consider a one-dimensional harmonic oscillator. Its Hamiltonian has the form

$$\hat{H} = -\frac{\hbar^2}{2m}\frac{d^2}{dx^2} + \frac{m\omega^2}{2}x^2 = \frac{1}{2m}(\hat{p}^2 + m^2\omega^2\hat{q}^2) = \hbar\omega\left(\hat{a}^\dagger\hat{a} + \frac{1}{2}\right), \quad (14)$$

The position and momentum operators $\hat{q}$ and $\hat{p}$, as well as the creation and annihilation operators, have the form

$$\hat{p} = -i\hbar\frac{d}{dx}, \hat{q} = x, \quad (15)$$

$$\hat{a}^\dagger = \sqrt{\frac{m\omega}{2\hbar}}\hat{q} - i\sqrt{\frac{1}{2m\omega\hbar}}\hat{p}, \hat{a} = \sqrt{\frac{m\omega}{2\hbar}}\hat{q} + i\sqrt{\frac{1}{2m\omega\hbar}}\hat{p}. \quad (16)$$

The operators (15), (16) satisfy the commutation relations

$$[\hat{p}, \hat{q}] = -i\hbar, \left[\hat{a}, \hat{a}^\dagger\right] = 1. \quad (17)$$

The position and momentum operators are connected with creation-annihilation operators as follows

$$\hat{q} = \sqrt{\frac{\hbar}{2m\omega}}(\hat{a}^\dagger + \hat{a}), \hat{p} = i\sqrt{\frac{m\omega\hbar}{2}}(\hat{a}^\dagger - \hat{a}). \quad (18)$$

The n - partial states $|n\rangle$ of the harmonic oscillator are eigenfunctions of the Hamiltonian (14)

$$\hat{H}|n\rangle = \hbar\omega\left(n + \frac{1}{2}\right)|n\rangle. \quad (19)$$

The coherent states of a harmonic oscillator read

$$|\alpha\rangle = e^{-|\alpha|^2/2}\sum_{n=0}^{\infty}\frac{\alpha^n}{\sqrt{n!}}|n\rangle. \quad (20)$$

Here α - is an arbitrary complex number.

The states (20) satisfy the equation

$$\hat{a}|\alpha\rangle = \alpha|\alpha\rangle. \quad (21)$$

The relation (21) can be regarded as the definition of a coherent state.

The coherent state $|\alpha\rangle$ can be obtained from the vacuum state $|0\rangle$ with the help of the shift operator $\hat{D}(\alpha) = \exp(\alpha\hat{a}^\dagger - \alpha^*\hat{a})$.

$$|\alpha\rangle = \hat{D}(\alpha)|0\rangle. \quad (22)$$

Using the definition (18) of the operators $\hat{q}, \hat{p}$, one can find their mean values in the coherent state (20).

$$\langle\alpha|\hat{q}|\alpha\rangle = \sqrt{\frac{2\hbar}{m\omega}}\,\mathrm{Re}\,\alpha, \langle\alpha|\hat{p}|\alpha\rangle = \sqrt{2\hbar m\omega}\,Im\alpha. \quad (23)$$

One can also calculate the dispersions of operator $\hat{q}, \hat{p}$.

$$\sigma_q = \langle\alpha|\hat{q}^2|\alpha\rangle - \langle\alpha|\hat{q}|\alpha\rangle^2 = \frac{\hbar}{2m\omega},$$

$$\sigma_p = \langle\alpha|\hat{p}^2|\alpha\rangle - \langle\alpha|\hat{p}|\alpha\rangle^2 = \frac{1}{2}m\omega\hbar. \quad (24)$$

It follows from (24) that

$$\sigma_q\sigma_p = \frac{1}{4}\hbar^2. \quad (25)$$

Thus, we see that for the coherent states (20) the Heisenberg uncertainty relation takes the form of equality, i.e. these states have minimal uncertainty.

Let's consider a linear transformation of creation-annihilation operators.

$$\hat{b} = u\hat{a} + v\hat{a}^\dagger, \hat{b}^\dagger = v^*\hat{a} + u^*\hat{a}^\dagger. \quad (26)$$

In the case when the complex numbers *u, v* satisfy the relation

$$|u|^2 - |v|^2 = 1, \quad (27)$$

the operators $\hat{b}^\dagger, \hat{b}$ satisfy the commutation relation

$$\left[\hat{b}, \hat{b}^\dagger\right] = 1. \quad (28)$$

Such transform is called the Bogolyubov transform.

In this case the operators $\hat{b}^\dagger, \hat{b}$ can be considered as some new creation-annihilation operators. For these operators one can introduce a vacuum state $|0\rangle_\beta$ and a coherent state $|\beta\rangle$. These states are determined by the relations

$$\hat{b}|0\rangle_\beta = 0, \hat{b}|\beta\rangle = \beta|\beta\rangle, \langle\beta|\beta\rangle = 1. \quad (29)$$

The coherent state $|\beta\rangle$ can be obtained from the vacuum state $|0\rangle_\beta$ in a way similar to (22)

$$|\beta\rangle_\beta = \hat{D}(\beta)|0\rangle_\beta. \quad (30)$$

The shift operator reads $\hat{D}(\beta) = \exp(\beta\hat{b}^\dagger - \beta^*\hat{b})$. In the coordinate representation the state $|\beta\rangle$ reads

$$\psi_\beta(x) = \left[\frac{\omega(|u|+|v|)^2}{\pi\hbar}\right]^{1/4} \exp\left\{-\frac{\omega}{2\hbar}\frac{u-v}{u+v}\left[x - \left(\frac{2\hbar}{\omega}\right)^{1/2}\frac{\beta}{u+v}\right]^2\right\}. \quad (31)$$

When $u = 1$, $v = 0$ the expression (31) is the wave function of an ordinary coherent state.

The transformation (26) is given by two complex numbers $u = |u|e^{i\varphi_u}$ and $v = |v|e^{i\varphi_v}$, which satisfy the relation (27). Let's introduce the following notation

$$\varphi = \varphi_u, \quad \theta = -\varphi_u - \varphi_v, \quad \tau = \ln(|u| + |v|). \quad (32)$$

It follows from (27) that $\tau \geq 0$.

The mean values of the operators $\hat{q}, \hat{p}$, given by (18), for the coherent state (30) have the form.

$$\langle\beta|\hat{q}|\beta\rangle = \sqrt{\frac{2\hbar}{m\omega}}\left[(u^* - v^*)\beta + (u - v)\beta^*\right],$$

$$\langle\beta|\hat{p}|\beta\rangle = -i\sqrt{2\hbar m\omega}\left[(u^* - v^*)\beta - (u - v)\beta^*\right]. \quad (33)$$

The dispersions of the operators $\hat{q}, \hat{p}$ for the coherent state $|\beta\rangle$ have the form.

$$\sigma_q(\beta) = \frac{\hbar}{2m\omega}\left[ch(2\tau) - sh(2\tau)\cos(2\varphi + \theta)\right],$$

$$\sigma_p(\beta) = \frac{m\omega\hbar}{2}\left[ch(2\tau) + sh(2\tau)\cos(2\varphi + \theta)\right]. \quad (34)$$

The Heisenberg uncertainty relation for the state $|\beta\rangle$ reads

$$\sigma_q(\beta)\sigma_p(\beta) = \frac{\hbar^2}{4}\left[ch^2(2\tau) - sh^2(2\tau)\cos^2(2\varphi + \theta)\right] =$$

$$= \frac{\hbar^2}{4}\left[1 + sh^2(2\tau)\sin^2(2\varphi + \theta)\right] \geq \frac{\hbar^2}{4}. \quad (35)$$

One can see from formulas (34), (35) for the state (30) that the values of dispersions of position and momentum are changed, and the total value of the uncertainty is changed too. It is the result of transformation (26). In this case the dispersions can both increase and decrease depending on the values of the transformation parameters (32), but their product always increases, i.e. the uncertainty of the transformed coherent state (30) increases.

It is convenient to characterized the properties of such states $|\beta\rangle$ by two parameters: a correlation coefficient

$$r = \frac{Im(uv^*)}{\sqrt{(1/2+|v|^2)-(Re(uv^*))^2}} = \\ = \frac{\sin(\theta+2\varphi)}{\sqrt{cth^2 2\tau - \cos^2(\theta+2\varphi)}}, \quad (36)$$

and a squeezing ratio k

$$k = \frac{1/2+|v|^2 - (Re(uv^*))^2}{1/2+|v|^2 + (Re(uv^*))^2} = \\ \left[1-\frac{\cos(\theta+2\varphi)}{cth2\tau}\right]\left[1+\frac{\cos(\theta+2\varphi)}{cth2\tau}\right]^{-1}. \quad (37)$$

With the help of the expressions (36) and (37) one can express the product of the dispersions through the correlation coefficient

$$\sigma_q(\beta)\sigma_p(\beta) = \frac{\hbar^2}{4(1-r^2)}. \quad (38)$$

We see that the product of the dispersions that enters into the Heisenberg uncertainty relation depends on the correlation coefficient, but does not depend on the sqeezing ratio. By choosing the parameters (32) of the transformation (26) in the required manner one can obtain different values of correlation and squeezing coefficients.

So, for example, if $\theta + 2\varphi = 0$, we have

$$r = 0,\ k = e^{-4\tau}. \quad (39)$$

In this case the squeezed states are appeared, but they are uncorrelated. The values of the dispersion (34) read

$$\sigma_q(\beta) = \frac{\hbar}{2m\omega}e^{-2\tau}, \sigma_p(\beta) = \frac{m\omega\hbar}{2}e^{2\tau}. \quad (40)$$

We see that the value of the dispersion of position decreases and the value of the dispersion of momentum increases. If $\theta + 2\varphi = \pi/2$ then

$$\sigma_q(\beta) = \frac{\hbar}{2m\omega}e^{2\tau}, \sigma_p(\beta) = \frac{m\omega\hbar}{2}e^{-2\tau}. \quad (41)$$

In this case on the contrary, the dispersion of position increases, and the dispersion of momentum decreases. But in both cases (40) and (41) the Heisenberg uncertainty relation has the form (25).

If $\theta + 2\varphi = \pi/2$, then

$$r = \text{th}2\tau,\ k = 1. \quad (42)$$

Such states do not have squeezing, but there exist correlation. The dispersions (34) read

$$\sigma_q(\beta) = \frac{\hbar}{2m\omega}ch(2\tau), \sigma_p(\beta) = \frac{m\omega\hbar}{2}ch(2\tau). \quad (43)$$

The product of the dispersions (43) has the form

$$\sigma_q(\beta)\sigma_p(\beta) = \frac{\hbar^2}{4}ch^2 2\tau. \quad (44)$$

We see that for such states the region of distribution of the canonical variables in the phase space preserves the symmetric form of the circle, but the radius of this circle increases.

Let us now consider some methods of generating squeezed and correlated states.

4. THE EXITATION OF SQUEEZED AND CORRELATED STATES

From the formal point of view the simplest way to excite squeezed and correlated states is a parametric excitation of a harmonic oscillator. This is due to the fact that one can find exact solutions of the nonstationary Schrödinger equation for an oscillator with a variable frequency and analyze their properties.

Let's consider a nonstationary Schrödinger equation

$$i\hbar\frac{\partial\psi(x,t)}{\partial t} = \frac{1}{2}\left[-\frac{\partial^2}{\partial x^2} + \omega^2(t)x^2\right]\psi(x,t). \quad (45)$$

Its solution has a form

$$\psi_\beta(x,t) = \left[\frac{\omega_0}{\pi\hbar\epsilon^2(t)}\right]^{1/4} \times \\ \times\exp\left[\frac{i\dot{\epsilon}(t)}{2\hbar\epsilon(t)}x^2 + \left(\frac{2\omega_0}{\hbar}\right)^{1/2}\frac{\beta}{\epsilon(t)}x - \frac{\beta^2\epsilon^*(t)}{2\epsilon(t)} - \frac{|\beta|^2}{2}\right]. \quad (46)$$

The solution (46) depends on the function $\epsilon(t)$, which is a solution of the equation

$$\frac{d^2\epsilon(t)}{dt^2} + \omega^2(t)\epsilon(t) = 0, \quad (47)$$

with the initial condition

$$\epsilon(0) = 1,\ \dot{\epsilon}(0) = i\omega_0. \quad (48)$$

The solutions of equation (47) can not be written in an explicit form, but their properties are well investigated. If $\omega(t)$ is a periodic

function the equation (47) is reduced to the Mathieu and Hill equations.

We introduce the parameters

$$u=\frac{1}{2}\left(\frac{\dot{\epsilon}(t)}{i\omega_0}+\epsilon(t)\right),\ \ v=\frac{1}{2}\left(\frac{\dot{\epsilon}(t)}{i\omega_0}-\epsilon(t)\right) \qquad (49)$$

The quantities (49) satisfy the relation (27). Now the function (46) takes the form (31). With their help one can also find the correlation coefficient (36) and the squeezing ratio (37).

In practice, one can generate squeezed states with the help of nonlinear processes. As an example consider the degenerate parametric down-conversion process.

In this process, the light beam with a frequency ω_0 falls on a nonlinear crystal, and as a result of interaction, the photon with frequency ω_0 decays into two photons with frequency $\omega_1=\frac{1}{2}\omega_0$. It is assumed that the incident pump field is sufficiently intense to be considered as classical, but the produced photons must be considered in a quantum fashion. Under such assumptions, the interaction Hamiltonian reads [19]

$$\hat{H}=\hbar\hat{a}_1^{\dagger}\hat{a}_1+\hbar g(\hat{a}_1^{\dagger 2}v_0e^{-2i\omega_1 t}+v_0^{*}\hat{a}_1^{2}e^{2i\omega_1 t}). \qquad (50)$$

Here ν_0 - is the complex amplitude of the initial light beam, and *g* - is the real coupling constant, its value depends on the nonlinear susceptibility of the medium. The Heisenberg equation of motion for the operator $\hat{a}(t)$ reads

$$\frac{d}{dt}\hat{a}_1=\frac{1}{i\hbar}[\hat{a}_1,\hat{H}]=-i\omega_1\hat{a}_1-2ig\hat{a}_1^{\dagger 2}v_0e^{-2i\omega_1 t}. \qquad (51)$$

The general solution of the equation (51) has the form

$$\hat{a}_1(t)=\hat{a}_1(0)ch(2g\,|\,v_0\,|\,t)e^{-i\omega_1 t}-$$
$$-i\frac{v_0}{|\,v_0\,|}\hat{a}_1^{\dagger}(0)sh(2g\,|\,v_0\,|\,t)e^{-i\omega_1 t},$$
$$\hat{a}_1^{\dagger}(t)=\hat{a}_1^{\dagger}(0)ch(2g\,|\,v_0\,|\,t)e^{i\omega_1 t}+$$
$$+i\frac{v_0^{*}}{|\,v_0\,|}\hat{a}_1(0)sh(2g\,|\,v_0\,|\,t)e^{i\omega_1 t}. \qquad (52)$$

Comparing the expressions (26) and (52) one can see that solutions (52) have the form of Bogolyubov transform also. Therefore, in the process of a degenerate parametric down conversion, the creation-annihilation operators $\hat{a}_1^{\dagger}(t),\hat{a}_1(t)$ of the generated photons evolve in such a way that a vacuum state $|0\rangle_1$, such that $|\hat{a}_1(0)\rangle_1=0$, is transformed into a squeezed state. The other examples of non-linear processes, including non-degenerate parametric down conversion, which can also be used to generate squeezed states, can be found in the book [20].

Let us find now the values of the dispersions of the position and momentum (34) and the values of correlation and squeezing coefficients (36), (37) for the coherent state (30) corresponding to the creation-annihilation operators $\hat{a}_1^{\dagger}(t),\hat{a}_1(t)$ given by formulas (52).

In this case the quantities defining the Bogolyubov transform (26) have the form

$$u=ch(2g\,|\,d_0\,|\,t)e^{-i\omega_1 t},$$
$$v=-ie^{i\delta}sh(2g\,|\,d_0\,|\,t)e^{-i\omega_1 t};\ d_0=|\,d_0\,|e^{i\delta}. \qquad (53)$$

The parameters (32) read

$$\varphi=\varphi_u=-\omega_1 t,\ \theta=-\varphi_u-\varphi_v=-\delta+\pi/2,$$
$$\tau=\ln(|\,u\,|+|\,v\,|)=2g\,|\,d_0\,|\,t. \qquad (54)$$

The dispersions (34) are equal to

$$\sigma_q(\beta)=\frac{\hbar}{2m\omega}[ch(4g\,|\,d_0\,|\,t)-sh(4g\,|\,d_0\,|\,t)\sin\delta],$$
$$\sigma_p(\beta)=\frac{m\omega\hbar}{2}[ch(4g\,|\,d_0\,|\,t)+sh(4g\,|\,d_0\,|\,t)\sin\delta]. \qquad (55)$$

And the correlation and squeezing coefficients take the form

$$r=\frac{\cos\delta}{\sqrt{cth^2(4g\,|\,d_0\,|\,t)-\sin^2\delta}}, \qquad (56)$$

$$k=\frac{cth(4g\,|\,d_0\,|\,t)-\sin\delta}{cth(4g\,|\,d_0\,|\,t)+\sin\delta}. \qquad (57)$$

One can see from (55) - (57) that as time *t* increases, both correlation and squeezing coefficients tend to unity ($r,\ k\rightarrow 1$). Thus

in the given process, as the time increases, the correlation increases, dispersions and uncertainty grow, but squeezing decreases. The domain of distribution of canonical variables expands and becomes more and more symmetric.

We have considered the simplest scheme for generating squeezed and correlated states, but there are exist other nonlinear optical processes that also lead to appearance of such states [21]. For example, if a nonlinear medium is inserted into an optical cavity, then the process of generating sqeezed and correlated states will proceed more intensively. Four-wave mixing can also be used as a non-linear process.

5. THE STRETCHED STATES

In this section we consider a new approach to constructing quantum states that is arise in certain physical processes.

It was developed within the framework of cooperation between FIAN and the Serbian Academy of Sciences and Art. The main ideas of the method and the results obtained with its help are presented in Ref. [22-27].

The method is based on the quasi-probability distributions, which are used for description of quantum states. These distributions are defined at the phase space, and transformations of this space are compared to some physical processes. The transformations of the phase space induce transformations of functions that are defined at it. It is possible to find physical states that correspond to the transformed quasi-probability distributions, and after that one can find the result of the action of the physical process at the initial quantum state.

This is the general outline of our approach. In this paper the Husimi function is used as quasi-probability distribution, and amplification of quantum states is considered as a physical process. This process can be connected with a scale transformation of the phase space.

In the framework of this approach we consider the class of states for which the values of position and momentum dispersions depend on parameters of the processes by which these states are generated. In this respect they are similar to the correlated states. We will consider the states that arise when N-partial Fock states are subjected by the action of a quantum amplifier. We call such states - the stretched states.

The stretched states are arise as a result of scale transformation of the phase space

$$(q,p) \rightarrow (\lambda q, \lambda p);\ |\lambda|^2 \leq 1. \qquad (58)$$

It was proved in [22, 23] that if $Q(q, p)$ is a Hushimi function of a quantum state and $\lambda < 1$, then the quantity

$$Q_\lambda(q, p) = \lambda^2 Q(\lambda q, \lambda p) \qquad (59)$$

is also a Hushimi function of some quantum state.

For the states of a harmonic oscillator it is possible to find an exact result of such transformation. If we consider a pure state that is an arbitrary superposition of n-particle states, then as a result of this transformation it goes into a mixed state and one can find an explicit form of its density matrix.

This mixed λ-state contains an infinite set of pure states, and the probabilities with which these pure states enter into the mixed state form a negative binomial distribution. In the case when we are dealing initially with one N-particle state, the transformed state contains all $N, N+1, \ldots$,-particle states. The distribution of these pure states in the mixed state becomes the more smooth the smaller parameter λ^2.

Simply speaking, one can consider that λ-transformation (58) of a state $|N\rangle$ generates states with large $M > N$. We call such mixed

states — the "stretched states". The mean values of a particle number operator were found for them, and the von Neumann entropy was calculated. The form of the Heisenberg and Robertson-Schrödinger uncertainty relations for stretched states is also found. It is established that for such states the factor λ^{-4} appears in the right-hand side of the uncertainty relations. Therefore when the λ-transformation (58) is performed, the uncertainty of the states increases.

Let us define the Husimi function. Suppose there is a quantum state, which is determined by the density operator $\hat{\rho}$. Then with the help of coherent states (20) one can construct its Husimi function.

$$Q(\alpha,\alpha^*)=\frac{1}{\pi}\int\langle\alpha\,|\,x\rangle\rho(x,y)\langle y\,|\,\alpha\rangle dxdy. \qquad (60)$$

If a quantum state is pure and is described by a wave function $|\psi\rangle$, then its Husimi function reads

$$Q(q,p)=\langle\alpha\,|\,\psi\rangle\langle\psi\,|\,\alpha\rangle. \qquad (61)$$

The transformation (58) can be related to certain physical processes, for example, the passage of the state of the electromagnetic field through a quantum amplifier [28, 29]. The main idea can be understood by the example of a simple linear light amplifier. It consists of partially inverted two-level atoms.

The resonance interaction Hamiltonian of the field with atoms reads

$$\hat{H}=\hbar k\begin{pmatrix}0 & \hat{a}\\ \hat{a}^\dagger & 0\end{pmatrix}. \qquad (62)$$

This is the interaction Hamiltonian of the Jaynes-Cummings model; it has a number of interesting properties, in particular, the property of supersymmetry [30, 31]. With such a Hamiltonian, the equation for the density matrix of the electromagnetic field has in first approximation the form [32]

$$\frac{\partial\hat{\rho}}{\partial t}=-kN_1(\hat{a}\hat{a}^\dagger\hat{\rho}-2\hat{a}^\dagger\hat{\rho}\hat{a}+\hat{\rho}\hat{a}\hat{a}^\dagger)-$$
$$-kN_2(\hat{a}^\dagger\hat{a}\hat{\rho}-2\hat{a}\hat{\rho}\hat{a}^\dagger+\hat{\rho}\hat{a}^\dagger\hat{a}). \qquad (63)$$

Here $\hat{a}^\dagger,\hat{a}$ – are the creation-annihilation operators of the electromagnetic field, N_1, N_2 – the populations of upper and lower levels of two-level atoms, and k – is the gain.

Using the relation (60) between the density matrix and the Husimi function, one can pass from the operator equation (63) to an ordinary differential equation for Husimi function. With the help of this equation an expression for Husimi function of a state at output from a quantum amplifier was found in Ref. [28]. It has the form

$$Q_{out}(\alpha,t)=\frac{1}{G^2}Q_{in}(\alpha/G)=\left\langle\frac{\alpha}{G}\,|\,\hat{\rho}_{in}\,|\,\frac{\alpha}{G}\right\rangle, \qquad (64)$$

here

$$G(t)=\exp[2(N_1-N_2)kt]. \qquad (65)$$

One can see that if $\lambda = G^{-1}$ the expression (64) coincides with (59).

Thus, the scale transform (58) of the phase space turns out to be connected with the action of the quantum amplifier. The form of this transform is determined by the structure of the Hamiltonian (62). Accordingly, the action of the amplifier at an arbitrary quantum state can be described by means of a scale transform of the phase space.

Let us find the Heisenberg and Robertson-Schrödinger uncertainty relations for the stretched states. The new method for constructing Husimi symbols for operators was proposed in [24, 25]. It is especially effective for operator, which are polynomial of position $\hat{q}$ and momentum $\hat{p}$ operators. With such operators we will deal in this section.

Let's consider the Hamiltonian of a harmonic oscillator

$$\hat{H}=\frac{\hbar\omega}{2}(\hat{q}^2+\hat{p}^2). \qquad (66)$$

Its Husimi symbol reads

$$K_H(q,p)=q^2+p^2-1. \qquad (67)$$

The mean value $\bar{E}$ of the energy of a state, which is characterized by Hushimi function $Q(q, p)$, has the form

$$\bar{E} = \int \frac{\hbar\omega}{2}(q^2 + p^2 - 1)Q(q,p)dqdp = \\ = \int \frac{\hbar\omega}{2}(q^2 + p^2)Q(q,p)dqdp - \frac{\hbar\omega}{2}. \quad (68)$$

Let us find now the average value of the energy of a stretched state, which corresponds to a state with Husimi function $Q(q, p)$. The Husimi function of the stretched state has the form $Q_\lambda(q, p) = \lambda^2 Q(\lambda q, \lambda p)$, and the average value of energy $\bar{E}_\lambda$ of a state with such Husimi function is determined by the formula

$$\bar{E}_\lambda = \int K_H(q,p)Q_\lambda(q,p)dqdp = \\ = \int \frac{1}{\lambda^2}\frac{\hbar\omega}{2}((\lambda q)^2 + (\lambda p)^2 - 1)Q(\lambda q, \lambda p)d(\lambda q)d(\lambda p) = \\ = \frac{1}{\lambda^2}\bar{E} + \frac{1-\lambda^2}{\lambda^2}\frac{\hbar\omega}{2}. \quad (69)$$

The expression (69) is valid for all stretched states of harmonic oscillator. Since $|\lambda|^2 < 1$ it is clear that with the scale transform the energy of stretched states increases. For the Fock states the mean value of energy of corresponding stretched states can be found in explicit form. Thus, in the case of an arbitrary superposition of Fock states, we have

$$\bar{E}_{\Sigma\lambda} = \frac{1}{\lambda^2}\frac{\hbar\omega}{2}\sum_{k=0}^{\infty}|c_k|^2\, k + \frac{1-\lambda^2}{\lambda^2}\frac{\hbar\omega}{2}. \quad (70)$$

With the help of the expression for mean values of operators and using the Husimi functions, it is possible to find the form of the uncertainty relations for stretched states. We will consider the Heisenberg and Robertson-Schrödinger uncertainty relations. The relations (5), (8) are satisfied for any quantum states. Let us now establish what happens with these relations when one passes to stretched states. To do this it is necessary to calculate the quantities

$$\sigma_{qq} = \langle \hat{q}^2 \rangle - \langle \hat{q} \rangle^2, \sigma_{pp} = \langle \hat{p}^2 \rangle - \langle \hat{p} \rangle^2, \\ \sigma_{qp} = \frac{1}{2}\langle \hat{p}\hat{q} + \hat{q}\hat{p} \rangle - \langle \hat{q} \rangle \langle \hat{p} \rangle. \quad (71)$$

With the help of Husimi function, the dispersions σ_{qq}, σ_{pp} and the value σ_{qp} can be written in the form

$$\sigma_{qq} = \int \left(q^2 - \frac{1}{2}\right)Q(q,p)dqdp - \left(\int qQ(q,p)dqdp\right)^2, \\ \sigma_{pp} = \int \left(p^2 - \frac{1}{2}\right)Q(q,p)dqdp - \left(\int pQ(q,p)dqdp\right)^2, \\ \sigma_{qp} = \int qpQ(q,p)dqdp - \int qQ(q,p)dqdp \int qQ(q,p)dqdp. \quad (72)$$

For the stretched states the formulas (72) take the form

$$\sigma_{qq\lambda} = \int \left(q^2 - \frac{1}{2}\right)\lambda^2 Q(\lambda q, \lambda p)dqdp - \left(\int q\lambda^2 Q(\lambda q, \lambda p)dqdp\right)^2, \\ \sigma_{pp\lambda} = \int \left(p^2 - \frac{1}{2}\right)\lambda^2 Q(\lambda q, \lambda p)dqdp - \left(\int p\lambda^2 Q(\lambda q, \lambda p)dqdp\right)^2, \\ \sigma_{qp\lambda} = \int qp\lambda^2 Q(\lambda q, \lambda p)dqdp - \\ - \int q\lambda^2 Q(\lambda q, \lambda p)dqdp \int p\lambda^2 Q(\lambda q, \lambda p)dqdp. \quad (73)$$

The formulas (73) give the values σ_{qq}, σ_{pp}, σ_{qp} for the stretched states

$$\sigma_{qq\lambda} = \frac{1}{\lambda^2}\sigma_{qq} + \frac{1-\lambda^2}{\lambda^2}, \sigma_{pp\lambda} = \frac{1}{\lambda^2}\sigma_{pp} + \frac{1-\lambda^2}{\lambda^2}, \sigma_{qp\lambda} = \frac{1}{\lambda^2}\sigma_{qp}. \quad (74)$$

Using these expressions one can find how the Heisenberg and Robertson-Schrödinger uncertainty relations are modified upon transition to stretched states.

$$\sigma_{qq\lambda}\sigma_{pp\lambda} = \\ = \frac{1}{\lambda^4}(\sigma_{qq}\sigma_{pp} + \frac{1}{2}(1-\lambda^2)(\sigma_{qq} + \sigma_{pp}) + \frac{1}{4}(1-\lambda^2)^2) \geq \frac{1}{4\lambda^4}\hbar^2, \quad (75)$$

and

$$\sigma_{qq\lambda}\sigma_{pp\lambda} - \sigma_{qp\lambda}^2 = \\ = \frac{1}{\lambda^4}(\sigma_{qq}\sigma_{pp} - \sigma_{qp}^2 + \frac{1}{2}(1-\lambda^2)(\sigma_{qq} + \sigma_{pp}) + \frac{1}{4}(1-\lambda^2)^2) \geq \frac{1}{4\lambda^4}\hbar^2.$$

We see that the right-hand sides of the uncertainty relations (75) contain a factor λ^{-4}, so for $|\lambda| < 1$ its values increase and, generally speaking, can become arbitrarily large. In this respect, they are similar to correlated states. As well as in the case of correlated states, we can assume that a scale transform $(q, p) \rightarrow (\lambda q, \lambda p)$ leads to the appearance of an "effective Planck constant". For $\lambda << 1$ the effective Planck constant satisfies the inequality $\hbar_{eff} \gg \hbar$.

However, there is a significant difference between these two types of states: the correlated states are pure states, and the stretched states are mixed states. The density matrices of these mixed states were found in [26, 27].

6. CONCLUSION

In this article we give an overview of the states of two types: the correlated states and the stretched states. These states can possess a great uncertainty in position and momentum, and for them the left-hand sides of Heisenberg and Robertson-Schrödinger uncertainty relations can take values significantly exceeding the minimum value. These states are obtained from the states of a harmonic oscillator with the help of nonlinear processes or external energy effects.

In the case when these conditions are realized in the atomic nucleus, the appearance of states with large values of the position and momentum dispersions can increase the probability of the tunnel effect and lead to low-energy nuclear reactions. Formally, the increase of probability of a tunnel transition can be correlated with the "increase" of the Planck constant ħ, i.e. with the ability to use the value $\hbar_{eff} \gg \hbar$ instead of ħ.

It was proposed in Ref. [15-17, 33] to use this property of correlated states to describe low-energy nuclear reactions. The stretched states also have great uncertainty, but they arise in other physical processes. We hope that they also will find application in nuclear physics and in other fields where there is an increase probability of a tunnel effect.

REFERENCES

1. Vysotskii VI, Kornilova AA. *Yaderny sintez i transmutatsiya izotopov v biologicheskikh sistemakh* [Nuclear fusion and transmutation of isotopes in biological systems]. Moscow, MIR Publ., 2003, 302 p., ISBN 5-03-003647-4 OCLC 67158435.
2. Ratis YuL. Upravlyaemy "termoyad" ili kholodny sintez? Drama idey [Controlled "fusion" or cold synthesis? Drama ideas]. http://electrosad.ru›files/LENR/cold.pdf (in Russ.).
3. LENR ore not LENR? http://geektimes.ru›post/275724/ (in Russ.).
4. Zhigalov V. Russkaja mozaika LENR (nizkoenergeticheskie yadernye reaktsii) [Russian mosaic LENR]. http://electrosad.ru›files/LENR/Zhigalov Vlad.pdf/ (in Russ.).
5. LENR - "kholodny sintez" ili "effekt Fleyshmana-Ponsa" ["Cold fusion" or "effect...]. http://genveles.livejournal.com/213196.html/ (in Russ.).
6. V zashchitu kholodnogo yadernogo sinteza [In defense of cold nuclear fusion (LENR)]. http://ss69100.livejournal.com/ (in Russ.).
7. Zel'dovich YaB, Gershtein SS. Yadernye reaktsii v kholodnom vodorode. 1. Mezonny kataliz [Nuclear reactions in cold hydrogen. I. Mesonic catalysis]. *UFN*, 1960, 71:581-630 (in Russ.).
8. Dodonov VV, Man'ko VI. Invariants and correlated states of nonstationary quantum systems. *Proc. Lebedev Physics Institute,* 1989, 183:71-181. In: Markov MA (ed.). *Invariants and the Evolution of Nonstationary Quantum Systems*, Commack, NY (USA); Nova Science Publishers, Inc., 1989.
9. Heisenberg W. *Ztschr. Phys.*, 1927, 43:172-198.
10. Robertson HP. *Phys. Rev.,* 1929, 34:163-164; Phys. Rev. A, 1930, 35(5);667.
11. Schrödinger E. About Heisenberg Uncertainty Relation (Eng. transl.) *Berl. Königlich Akad. Wiss.*, Berlin, 1930: 296-303.
12. Dodonov VV, Dodonov AV. Transmission of correlated Gaussian packets through a delta-potential. *J. Russ. Laser Res.*, 2014, 35(1):39-46.
13. Dodonov AV, Dodonov VV. Tunneling of slow quantum packets throw the high

Coulomb barrier. *Physics Letters A,* 2014, 378:1071-1073.
14. Vorontsov YuI. Uncertainty relation and the measurement error-perturbation relation. *Sov.Phys.Usp.*, 2005, 48(10):999-1013.
15. Vysotskii VI, Vysotskyy MV, Adamenko SV. Formation and application of correlated states in nonstationary systems at low energies of interacting particles. *J. Exp. Theor. Phys.*, 2012, 114:243-252.
16. Vysotskii VI, Adamenko SV, Vysotskyy MV. The formation of correlated states and the increase in barrier transparency at a low particle energy in nonstationary systems with damping and fluctuations. *J. Exp. Theor. Phys.*, 2012, 115:551-566.
17. Vysotskii VI, Vysotskyy MV. Formation of correlated states and optimization of nuclear reactions for low-energy particles at nonresonant low-frequency modulation of a potential well. *J. Exp. Theor. Phys.*, 2015, 120:246-256.
18. Bykov VP. Basic properties of squeezed light. *Sov. Phys. Usp.*, 1991, 34(10):910-924.
19. Mandel L, Wolf E. *Optical Coherence and Quantum Optics*. Cambridge University Press, 1995.
20. Yariv A. *Quantum Electronics*. John Sons, Inc., 1975.
21. Scully MO, Zubairy MS. *Quantum Optics*. Cambridge University Press, 1997.
22. Andreev VA, Davidović DM, Davidović LD, Davidović MD, Manko VI, Manko MA. A transformational property of the Husimi function and its relation to the Wigner function and symplectic tomograms. *Theor. Math. Phys.*, 2011, 166:356-368.
23. Andreev VA, Davidovich DM, Davidovich LD, Davidovich MD. Relationships between scaling transformed Husimi functions and symplectic tomograms describing corresponding physical states. *Phys. Scr.*, 2011, 143:01400.
24. Andreev VA, Davidović LD, Davidović Milena D, Davidović Miloš D, Manko VI, Manko MA. Operator method for calculating Q symbols and their relation to Weyl-Wigner symbols and symplectic tomogram symbols. *Theor. Math. Phys.*, 2014, 179:559-573.
25. Andreev VA., Davidović Milena D., Davidović LD, Davidović Miloš D and Davidović DM. Derivation of the Husimi symbols without antinormal ordering, scale transformation and uncertainty relations. *Physica Scripta,* 2015, 90(7):074023.
26. Vladimir A. Andreev, Dragomir M. Davidovi´c, Ljubica D. Davidovi´c, Milena D. Davidovi´c, Miloˇs D. Davidovi´c, and Sergey D. Zotov, Scaling transform and stretched states in quantum mechanics. *J. Russ. Laser Res.*, 2016, 37(5):434-439.
27. Andreev VA, Davidovi´c DM, Davidović LD, Davidović Milena D, Davidović Miloš D. The scale transformation of a phase space and stretched states of harmonic oscillator. *Theor. Math. Phys.*, 2017, 192(1):164-184.
28. Agarwal GS, Tara K. Transformation of the nonclassical states by an optical amplifier. *Phys. Rev. A*, 1993, 47(4):3160-3166.
29. Agarwal GS, Chaturvedi S, Rai Amit. Amplification of NOON States, http://arxiv.org/abs/0912.5134v1.
30. Andreev VA, Lerner PB. Supersymmetry in the Jaynes-Cummings Model. *Physics Letters A,* 1989, 134:507-511.
31. Andreev VA. Supersymmetry of two-level systems. *J. Sov. Laser Res.*, 1992, 13:268-278.
32. Schleich WP. *Quantum Optics in Phase Space*. WILEY-VCY, 2001.
33. Chernega VN. Purity dependent uncertainty relations and possible enhancement of quantum tunneling phenomenon. *J. Russ. Laser Res.,* 2013, 34(2):103-108; http://arxiv.org/abs/1303.5238v1.

UNIVERSAL MECHANISM OF REALIZATION OF NUCLEAR REACTIONS AT LOW ENERGY

Vladimir I. Vysotskii, Mikhail V. Vysotskyy

Shevchenko Kiev National University, http://www.univ.kiev.ua
64/13, Vladimirskaya str., Kyiv 01601, Ukraine
vivysotskii@gmail.com, mihas1964@gmail.com

Abstract. **A universal method of short-term and very significant attenuation and suppression of the tunneling effect in the nuclear interaction of low-energy particles by using coherent correlated states (CCS) formed with a weak controlled pulsed or periodic action on these particles or the environment is considered. This mechanism explains all the detected features of successful nuclear physics experiments conducted at low energy: an anomalously high probability of these reactions, a very significant suppression (as compared with similar reactions at high energy) of the accompanying gamma radiation, and the complete absence of radioactive daughter isotopes, formed in these reactions.**

Keywords: **nuclear reactions at low energy, coherent correlated states, the tunnel effect**

PACS: **03.65.Xp; 25.60.Pj; 25.70.−z; 25.85.Ge; 28.52.−s**

Bibliography – 18 references *Received 15.06.2017*

RENSIT, 2017, 9(1):21-36 **DOI: 10.17725/rensit.2017.09.021**

Contents

1. INTRODUCTION

Numerous successful experiments on realization of nuclear reactions at low energy (LENR), some of which have confidently emerged from the "child" age of laboratory experiments and have manifested themselves at the industrial level (this applies in particular to the experiments of A. Rossi), up to now are not based on a reliable theoretical model that adequately explains non-trivial results that are not consistent with the traditional models of nuclear physics.

Among well-known LENR problems, the most frequently considered is the reason of the anomalously high probability of overcoming the Coulomb potential barrier at interaction of charged particles with low energy. The "standard" approach of nuclear physics, which is very successful in the energy range $E > 1$ keV, is unable to answer this question taking into account that the typical equilibrium particle energy in LENR problems does not exceed $E \approx kT \approx 0.1$ eV, which leads to very small probability of a tunnel effect that is not comparable with the experimental results.

There are several dozen fairly well-developed theoretical models that, on completely different principles (including such exotic ones as taking into account the anisotropy of quark interaction, the existence of unknown elementary particles, or the presence of hypothetical super deep "Dirac" levels of electrons in a hydrogen atom) try to solve this paradox.

Other, even more exotic paradoxes (first of all, the complete absence of radioactive daughter isotopes in observed LENR reactions, which is completely unusual for "standard" nuclear physics; a very strong (by many orders of magnitude) suppression of gamma-radiation, concomitant and typical for specific nuclear reactions; very strong suppression of the neutron channel of the most studied reaction of dd fusion) in these models are practically not considered, confined to a very important but not the only problem of abnormally high transparency of the Coulomb barrier

Obviously, such one-sided approach is insufficient. The nontriviality of these unexplained paradoxes can not be ignored, since the lack of an adequate explanation of them is equivalent to the lack of understanding of these processes, and hence the impossibility of their optimization and safe large-scale use!

In [1-13], a general and rather universal mechanism for LENR optimization based on coherent correlated states (CCS) of interacting particles was considered. This mechanism provides a high probability of LENR and can be applied with the same efficiency to different experiments. It should be noted that the CCS method makes it possible to explain all mentioned above paradoxes on the basis of standard quantum mechanics and modern nuclear physics without involving fantastic heuristic models.

2. FORMALISM AND GENERAL REGULARITIES OF CCS USING IN QUANTUM-MECHANICAL SYSTEMS

In atomic and nuclear physics the well-known Heisenberg uncertainty relations are often used for the coordinate and momentum, as well as energy and time (1927)

$$\delta q \delta p \geq \hbar/2,\ \delta E \delta t \geq \hbar/2 \qquad (1a)$$

and its generalization, made in 1929 by Robertson for arbitrary dynamical variables A and B

$$\delta A \delta B \geq |<[\hat{A}\hat{B}]>|/2,$$
$$\delta K = \sqrt{\sigma_K},\ \sigma_K = \left\langle (\hat{K} - \langle K \rangle)^2 \right\rangle. \qquad (1b)$$

In 1930, Schrödinger and Robertson independently generalized the relation (1b) and obtained a more universal inequality, called the Schrödinger-Robertson uncertainty relation [14, 15]

$$\sigma_A \sigma_B \geq |<[\hat{A}\hat{B}]>|^2 /4(1-r^2),$$
$$r = \sigma_{AB} / \sqrt{\sigma_A \sigma_B},$$
$$\sigma_{AB} = (<\hat{A}\hat{B} + \hat{B}\hat{A}>)/2 - <A><B>,\ 0 \leq |r| \leq 1, \qquad (2)$$

in which the value r is the correlation coefficient between A and B. This parameter determines the degree of mutual statistical connection between the dynamic variables A and B and determines the restriction on the product of the variances of these quantities. In the special case, $A = q$, $B = p$, $<q> = 0$, $<p> = 0$, $\delta q = \sqrt{\sigma_q}$, $\delta p = \sqrt{\sigma_p}$ relations (1) and (2) reduce to the modified Heisenberg uncertainty relation with the correlation coefficient r_{pq}

$$\delta q \delta p \geq \hbar / 2\sqrt{1 - r_{pq}^2} \equiv \hbar^*/2,$$
$$\hbar^* = G_{pq}\hbar, G_{pq} = 1/\sqrt{1 - r_{pq}^2}. \qquad (3a)$$

Accordingly, at $A = E$, $B = t$, we have relation

$$\delta E \delta t \geq \hbar / 2\sqrt{1 - r_{Et}^2} \equiv \hbar^*/2,$$
$$\hbar^* = G_{Et}\hbar, G_{Et} = 1/\sqrt{1 - r_{Et}^2}, \qquad (3b)$$

which depends on the correlation coefficient r_{Et}.

According to the generally accepted terminology, the term CCS refers to states for which relations (2) and (3) become equalities, but usually the term CCS is applied to any state with $|r| \rightarrow 1$. According to the same interpretation, the quantum state, which

converts relations (2) and (3) into equalities, is traditionally called the coherent state (CS) – a synonym for the "compressed" state, which is characterized by a minimum product of variances or rms fluctuations and maximum closeness to the classical state of the particle in the potential well. The principal difference between the uncertainty relations of Heisenberg-Robertson and Schrödinger-Robertson is clearly characterized by the coefficient of correlation efficiency $G = 1/\sqrt{1-r^2}$ [9-12].

It increases from the value $G = 1$ at $r = 0$, which corresponds to the absence of correlation, up to $G \to \infty$ at full correlation (at $|r| \to 1$).

The value of G characterizes the increase of the amplitudes of the fluctuations of dynamic variables A and B, and its importance follows from the following simple example demonstrating the efficiency of CCS for optimizing nuclear reactions at low energy.

In the case $A = q$, $B = p$, $\langle q \rangle = 0$, $\langle p \rangle = 0$, the following simple estimate for the lower limit (minimum value) of the kinetic energy fluctuation of a particle of mass M localized within the spatial interval δq follows from (3a)

$$\delta T^{(\min)} = (\delta p)^2 / 2M = G^2\hbar^2 / 8M(\delta q)^2. \quad (4)$$

In particular, when a proton with a mass M_p is localized in an interatomic, typical for condensed matter, region $a \approx 1.5$Å (in this case, $\delta q \le 0.75$Å), the fluctuation of the kinetic energy of a particle that are in CCS with $1 - |r| \approx 10^{-7}$ (which corresponds to a very large (but real) correlation efficiency $G = 2240$) corresponds to the value $\delta T^{(\min)}_{|r|=1-10^{-7}} \approx 5\,keV$. It is necessary to note that this value can be obtained for an arbitrarily small (including zero) temperature of the medium in which the given potential well is located.

This value, even at this lower limit, is comparable with the optimum temperature of a thermonuclear plasma in a tokamak achieved by using of a very large real energy. If the correlation coefficient is greater, the value $\delta T_r^{(\min)}$ will be even greater. For comparison, we point out that in the absence of CCS (ie, at $r = 0$), the corresponding fluctuation of the kinetic energy $\delta T^{(\min)}_{r=0} \approx 0.001eV$ will be incomparably smaller. It should be emphasized that usually [3, 7, 8] the real value of $\delta T_{|r|\neq 0}$ is much higher $\delta T^{\min}_{|r|\neq 0}$.

For particles with a smaller mass (in particular, for an electron with a mass M_e), the minimum fluctuation under the same conditions and the presence of a CCS corresponds to large relativistic energy

$$\delta T^{(\min)}_{|r|=1-10^{-7}} = \sqrt{(\delta p)^2 c^2 + M_e^2 c^4} - M_e c^2 =$$
$$= M_e c^2 [\sqrt{1 + G^2\hbar^2 / 4M_e^2 c^2 (\delta q)^2} - 1] \approx$$
$$\approx 2.23\,MeV, \quad (5)$$

From the first hand it seems that this energy is sufficient for, for example, proton neutronization $p + \beta^- + \delta T \to n + \nu$. On the other hand, it will be shown below that such reaction due to fluctuations δT is impossible.

Another method of approximate estimation of the effectiveness of the CCS influence on the tunnel effect and subsequent nuclear transmutation is based on taking into account the formal substitution $\hbar \to \hbar^* \equiv \hbar/\sqrt{1-r^2} \equiv G\hbar$ in the expression for the tunneling probability D through a high potential barrier. In [3, 7, 8], using an example of a particle localized in a parabolic well, it was shown that the direct use of such substitution in the formula for the probability of a tunnel effect in the sub-barrier region $L(E)$ in a nuclear field of radius R

$$D_{r\neq 0} \approx$$
$$\approx \exp\left\{-\frac{2\sqrt{1-r^2}}{\hbar}\int_R^{R+L(E)} \sqrt{2M\{V(q)-E\}}dq\right\} =$$
$$= \left(D_{r=0}\right)^{\sqrt{1-r^2}} \equiv \sqrt[G]{D_{r=0}} \quad (6)$$

is in good agreement with the results of an independent strict quantum-mechanical

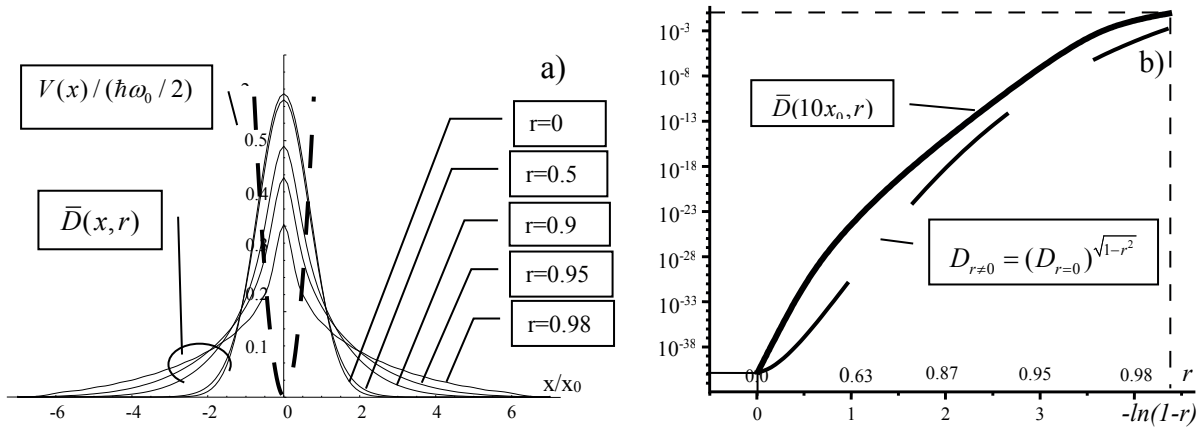

Fig. 1. *a) Average probability density* $\bar{D}(x,r)\equiv<|\Psi(x,t,r)>_t$ *in the potential well* $V(x) = (x/x_0)^2$ *and in the region under the barrier for correlated and uncorrelated states of a particle with different values; b) Dependence of the time-averaged probability density of particle localization (tunneling probability) on the correlation coefficient* $0 \le r \le 0.987$ *in the subbarrier region with the coordinate* $x = 10x_0$. *The solid line is the result of the exact calculation, the discontinuous line is the result of the approximation (6).*

calculation of $D_{r\neq0}$ under the condition $D_{r=0} << 1$.

Fig. 1*a* presents the results of the corresponding calculation showing the change in the time-averaged probability density of the subbarrier particle localization $\bar{D}(x,r)\equiv<|\Psi(x,t,r)>_t$ in the parabolic potential well $V(x) = m\omega^2x^2/2$, and Fig. 1*b* – change of this value in the test point $x = 10x_0$ deep under the barrier, depending on the correlation coefficient (here $x_0=\sqrt{\hbar/m\omega}$).

From the obtained data it follows that even with a relatively small increase in the correlation coefficient in the interval $0 \le r \le 0.987$, which corresponds to a small change in the correlation efficiency factor $0 \le G \le 6.2$, the barrier transparency increases from 10^{-36} to 0.01. In a similar way, it is easy to determine that the probability of the tunnel effect $D_{r=0,G=1} \approx 10^{-500}$, typical for a low energy and large charges of interacting particles, increases to $D_{G=100} \approx 0.3$ in the case of CCS formation, which allows to realize practically any nuclear reaction.

The physical mechanism providing such effect is associated with the formation of very large fluctuations of both momentum and energy of a particle in a potential well in a specially organized superposition coherent correlated state. This formation is related to the mutual enhancement (constructive interference) of the partial fluctuations of the kinetic energy and momentum corresponding to different eigenstates of such superposition. The result of the interference is the formation of continuously repeated giant fluctuations of the kinetic energy, sufficient for passage through a high and wide potential barrier. It is interesting to note that the formation of a CCS is not connected with an increase of the average particle energy in a given system, but is due to the synchronization of a large number of random fluctuations.

A clear and slightly simplified illustration of such process can be obtained by analyzing the features of the formation of synchronized fluctuations of the kinetic energy of a particle in a one-dimensional parabolic potential well. Each of the N eigenfunctions of the particle $\psi_n(q, t)$ in the potential well is characterized by the instantaneous value of the fluctuation of the momentum $\Delta\vec{p}_n(t)$ with the dispersion $\sigma_{pn}(t)=\left\langle\{\Delta\vec{p}_n(t)-\left\langle\Delta\vec{p}_n(t)\right\rangle\}^2\right\rangle=\left\langle[\Delta\vec{p}_n(t)]^2\right\rangle$ In such system the mean value $\left\langle\Delta\vec{p}_n(t)\right\rangle=0.$ is equal to zero. Formation of the coherent correlated state of the particle leads to phase coincidence and coherent addition (constructive interference) of the momentum fluctuations $\Delta\vec{p}(t)=\sum_n^N\Delta\vec{p}_n(t)$ for a large number $N >> 1$ of different eigenfunctions $\psi_n(q, t)$ forming a superpositional coherent

correlated state $\Psi_{corr}(q, r, t)$. A consequence of this interference is the condition $\left\langle \Delta\vec{p}_n(t)\Delta\vec{p}_m(t)\right\rangle_{corr} > 0$, that leads to the formation of very large fluctuations of the dispersion of the total momentum of the particle

$$\sigma_{p(corr)} = \left\langle \left\{ \sum_n^N \Delta\vec{p}_n(t) \right\}^2 \right\rangle_{corr} =$$
$$= \sum_n^N \sum_{m\neq n}^N \left\langle \Delta\vec{p}_n \Delta\vec{p}_m \right\rangle_{corr} + \sum_n^N \left\langle (\Delta\vec{p}_n)^2 \right\rangle \approx$$
$$\approx N^2 \left\langle \Delta\vec{p}_n \Delta\vec{p}_m \right\rangle_{corr} + N\left\langle (\Delta\vec{p}_n)^2 \right\rangle \sim N^2, \quad N >> 1. \qquad (7)$$

The presence of such fluctuations of the momentum at the moments of complete synchronization leads to a sharp increase of the probability of tunneling due to the short-term (fluctuation) formation of states with a very large kinetic energy fluctuation

$$< \Delta T(t) >_{corr} \equiv < (\Delta\vec{p}(t))^2 / 2M >_{corr} =$$
$$= N^2 \left\langle \Delta\vec{p}_n(t)\Delta\vec{p}_m(t) \right\rangle_{corr} / 2M +$$
$$+ N\left\langle (\Delta\vec{p}_n)^2 \right\rangle / 2M \sim N^2 \qquad (8)$$

at constant (small) average kinetic energy of the particle. We note that, in the absence of coherence between different eigenstates, there is an obvious condition $\left\langle \Delta\vec{p}_n \Delta\vec{p}_m \right\rangle_{noncoher} \equiv 0$, that leads to a trivial relation

$$< \Delta T(t) >_{noncoher} = N\left\langle (\Delta\vec{p}_n)^2 \right\rangle / 2M =$$
$$= N\left\langle \Delta T_n(t) \right\rangle. \qquad (9)$$

An exact calculation using the density matrix leads, naturally, to the similar results. These results are presented in a symbolic form in **Fig. 2**.

The above discussion of the CCS specifics concerns the problem of optimizing the tunnel effect, which is the main problem, but not the only one, characterizing the features of LENR.

It is easy to see that other features of LENR (first of all the absence of daughter radioactive isotopes) also follow from the specifics of CCS. In particular, from the basic relation (3b) it follows that the possibility of realizing the LENR due to the virtual kinetic energy $\delta E \equiv \delta T_{|r|\neq 0}$ is limited by the conservation laws for the entire system. Very important is the fact that this virtual energy "exists" in the given system (that is, it can have a certain influence on different processes) a finite time δt. As a consequence, any process using δE can be realized only if during the reaction carried out by this virtual energy, the reaction energy ΔE that is not less than δE is released and the time of "return" to the system under consideration of this virtual energy (in fact, the duration of the reaction with the release of energy) does not exceed the value of δt.

This result, with respect to the nuclear reaction, corresponds to the fact that the

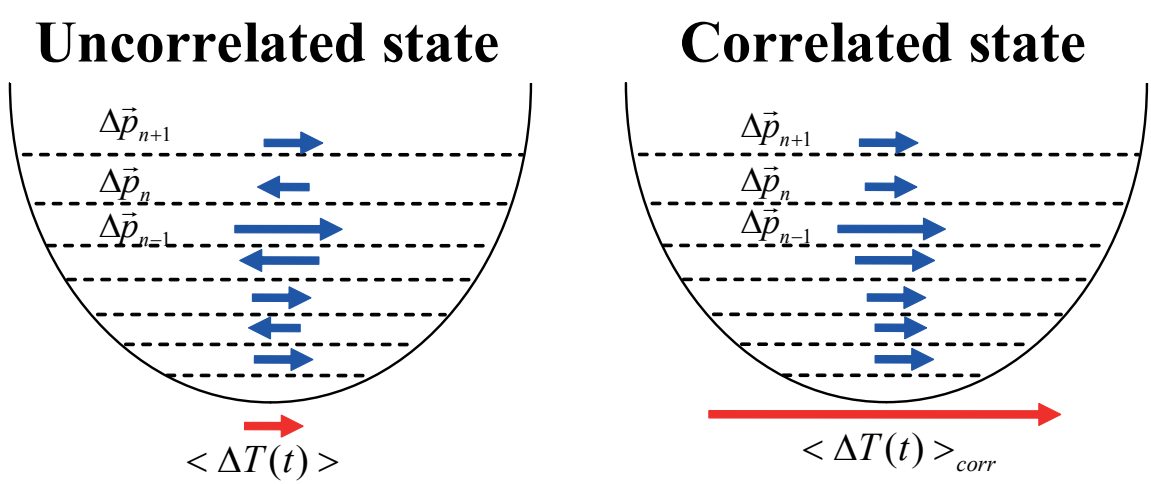

Fig. 2. *The scheme for the formation of large fluctuations of the kinetic energy of a particle in a coherent correlated state (on the right), due to the synchronization of fluctuations at different energy levels of the superposition state.*

total time of the reaction T_{total} (including the time of approach of the particle to the barrier t_1, the duration of the passage through the barrier t_2 and the time of the reaction itself with the release of T_{reac} energy) should not exceed δt. This requirement, taking into account the very short duration δt of a large fluctuation amplitude $\delta T_{|r|\neq 0}$, imposes very stringent conditions on such processes and automatically excludes the possibility of non-optimal reactions.

The scheme of this scenario is shown in **Fig. 3.**

For example, let us consider the features of the course of LENR reactions involving protons and isotopes ^6Li and ^7Li. The general scheme of these reactions is the following

$$Li^6 + p = \\ = Be^{7*}\left\{Be^{7*}: Q = 4\,MeV, T_{reac} \approx 1.3*10^{-13}\,s\right\} \rightarrow \\ \rightarrow He^4 + He^3; \qquad (10a)$$

$$Li^7 + p = \\ = Be^8 \left\{ \begin{array}{l} Be^8: Q \approx 0.1 MeV, T_{reac} \approx 6.10^{-17}\,s \\ Be^8*: Q \approx 17,255\,MeV, T_{reac} \approx 10^{-20}\,s \end{array} \right\} \rightarrow \\ \rightarrow 2He^4 + 17,255\,MeV. \qquad (10b)$$

In the "ordinary" uncorrelated state, the probability of the tunneling effect for these reactions at a low temperature of 300...1000 K is extremely small and does not exceed $D_{r=0} \approx 10^{-200}...10^{-100}$. Let us take as an estimate that for the rapid realization of these reactions it is necessary for proton to have an energy $\delta E \approx 10$KeV. In the case of using the Heisenberg uncertainty relation $\delta E \delta t_{r=0} \geq \hbar/2$, such fluctuation can exist for a time $\delta t_{r=0} \approx \hbar/2\delta E \approx 5\cdot 10^{-21}$ s. At this energy, the minimum total reaction time is equal to $T_{total} = T_{reac} + t_1 + t_2 \approx T_{reac} + L(\delta E)/v(\delta E) \approx 10^{-18}$ s.

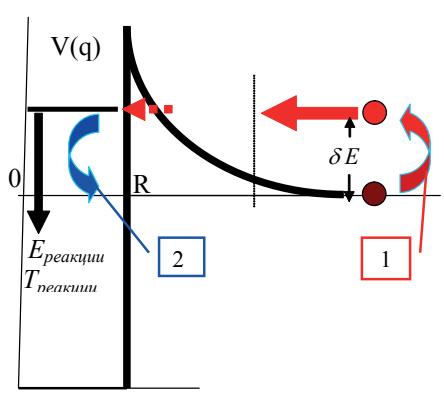

Fig. 3. *The scheme of "birth" and "disappearance" of virtual energy during the motion of a particle through the Coulomb barrier with a subsequent short-term nuclear reaction. 1 - "Birth" of virtual energy δE; 2 - "disappearance" of virtual energy δE within the interval δt after "birth".*

It is seen from the reaction schemes (10a) and (10b) that for such value of T_{total} the necessary condition $T_{total} < \delta t_{r=0}$ is not satisfied for both reactions and they are impossible.

In the correlated state, with an achievable value $r \approx 0.99999$, the same energy fluctuation $\delta E \approx 10$KeV can exist during $\delta t_{r=0.99999} \approx \hbar / 2\delta E\sqrt{1-r^2} \approx 2.5\cdot 10^{-18}$ s. Comparing this value with the total duration $T_{total} \approx 10^{-18}$s of the reaction (10b) $^7Li + p = 2^4He$, we come to the conclusion that $T_{total} \approx 10^{-18}s < \delta t$ (ie the total reaction time is less than the fluctuation time that stimulates this reaction), and the flow of such a reaction is consistent with the law of conservation of energy and the corresponding uncertainty relation.

In contrast, for reaction (10a), the opposite condition $T_{total} \approx 10^{-13}s >> \delta t$ takes place and such reaction is impossible in principle due to the formation of CCS.

These results fully coincide with the data of very detailed experiments [15] conducted for 32 days in Lugano for the examination of the A. Rossi installation, in which very efficient processing of the ^7Li isotope was observed, which is characterized by a short reaction time, and complete absence of reactions involving the ^6Li isotope.

Similarly, it is easy to show that this same selection rule prohibits the realization of LENR in reaction channels involving any other isotopes and elements that have a longer reaction time exceeding δt. It is obvious that, taking into account the smallness of δt even in systems with a large correlation coefficient, the reactions passing through the stage of formation of long-lived radioactive isotopes fully fall under this prohibition.

This mechanism also makes it possible to understand why gamma radiation is strongly suppressed in LENR reactions. The fact is that the majority of gamma transitions in nuclei are characterized by a lifetime $\tau \geq 10^{-13}...10^{-15}$ s, which significantly exceeds the duration of the existence of fluctuations for coherent correlated states, and because of this, such processes also have low probability.

It is also worth to note that the same regularities distinguish the flow of any reactions using virtual energy from reactions involving really accelerated particles. The main differences are related to the ban on both the implementation of any endoenergetic reactions and reactions with the formation of a long-lived intermediate state of the nucleus with a lifetime $\tau >> \delta t$.

3. METHODS FOR FORMATION OF COHERENT CORRELATED STATES IN REAL SYSTEMS

The basic model for the CCS analysis is the nonstationary harmonic oscillator.

It was shown in [3-13] that the simplest method of excitation of CCS for a particle is associated with a nonstationary deformation of the harmonic potential $V(q,t) = M\omega^2(t)q^2/2$, in the field of which this particle is located. In a symmetric nonstationary parabolic potential well for which $<q> = 0$, $<p> = 0$, the wave function of the particle, which was in the ground state prior to the deformation, depends on the correlation coefficient and has the form [1-3, 4, 7]

$$\Psi_0(q,t) = \frac{1}{\sqrt[4]{2\pi\sigma_q}} \exp\left[-\frac{q^2}{4\sigma_q}\left(1 - \frac{ir(t)}{\sqrt{1-r(t)^2}}\right)\right]. \quad (11)$$

The explicit form of the correlation coefficient

$$r = \mathrm{Re}\left\{\varepsilon^* \frac{d\varepsilon}{dt}\right\} / \left|\varepsilon^* \frac{d\varepsilon}{dt}\right|, \quad (12)$$

and also the compression coefficient k, which determines the ratio of the dispersions of the coordinate and momentum of the particle

$$k = \sigma_q / \sigma_p = |\varepsilon / (d\varepsilon / dt)|^2, \quad (13)$$

and the values of these dispersions

$$\sigma_q \geq (\hbar/2)\sqrt{k/(1-r^2)},$$
$$\sigma_p \geq (\hbar/2)\sqrt{1/k(1-r^2)}, \quad (14)$$

can be found on the basis of the solution of the equation of a classical oscillator with a variable frequency in the presence of an external force

$$\frac{d^2\varepsilon}{dt^2} + \omega^2(t)\varepsilon = f(t) \quad (15)$$

at initial conditions

$$\varepsilon(0) = 1, \ \left.\frac{d\varepsilon}{dt}\right|_0 = i. \quad (16)$$

In equations (11)-(16) and the following relations, $\omega(t)$ is the dimensionless frequency normalized to the characteristic oscillator frequency ω_0; t is a dimensionless (normalized to ω_0^{-1}) time; $\varepsilon(t)$ is the dimensionless (normalized to $q_0 = \sqrt{\hbar / M\omega_0}$) complex coordinate of the particle; M is the reduced mass of the particle.

In the general case, the solution of equation (14) has the form $\varepsilon(t) = e^{\varphi(t)}$, $\varphi(t) = \alpha(t) + i\beta(t)$.

Substituting this solution into (12) and (15), using the initial conditions following from (16)

$$\varphi(0)=\alpha(0)=\beta(0)=0, \ \left.\frac{d\varphi}{dt}\right|_0 = i, \ \left.\frac{d\alpha}{dt}\right|_0 = 0, \ \left.\frac{d\beta}{dt}\right|_0 = 1 \quad (17)$$

and separating the real and imaginary parts of the resulting equation, we find

$$\frac{d^2\alpha}{dt^2} + \left(\frac{d\alpha}{dt}\right)^2 - \exp(-4\alpha) = -\omega^2(t),$$
$$\beta(t) = \int_0^t \exp\{-2\alpha(t')\}dt', \quad (18)$$
$$|r| = \sqrt{\left(\frac{d\alpha}{dt}\right)^2 \exp(4\alpha) / \left\{1 + \left(\frac{d\alpha}{dt}\right)^2 \exp(4\alpha)\right\}}. \quad (19)$$

It is clear from (19) that obtaining the limiting value $|r| \rightarrow 1$ is possible only if the condition $(d\alpha/dt)^2\exp(4\alpha) >> 1$ is satisfied.

The system of equations (18), (19) is equivalent to equation (15), but it is more convenient for analysis and allows us to find the exponent of the amplitude of oscillation $\alpha(t)$

from (18), and then based on the given law of variation $\omega(t)$ to find $r(t)$ from equation (19).

A study of specific mechanisms for the formation of CCS under various modes of deformation of a potential well, as well as an analysis of the specifics of the manifestation of this state in model and real systems, was carried out in [4-13].

3.1. Formation of CCS for periodical modulation of parameters of the harmonic oscillator

In [4-8, 10], the features of the formation of CCS for the particle in the case of a weak periodic effect

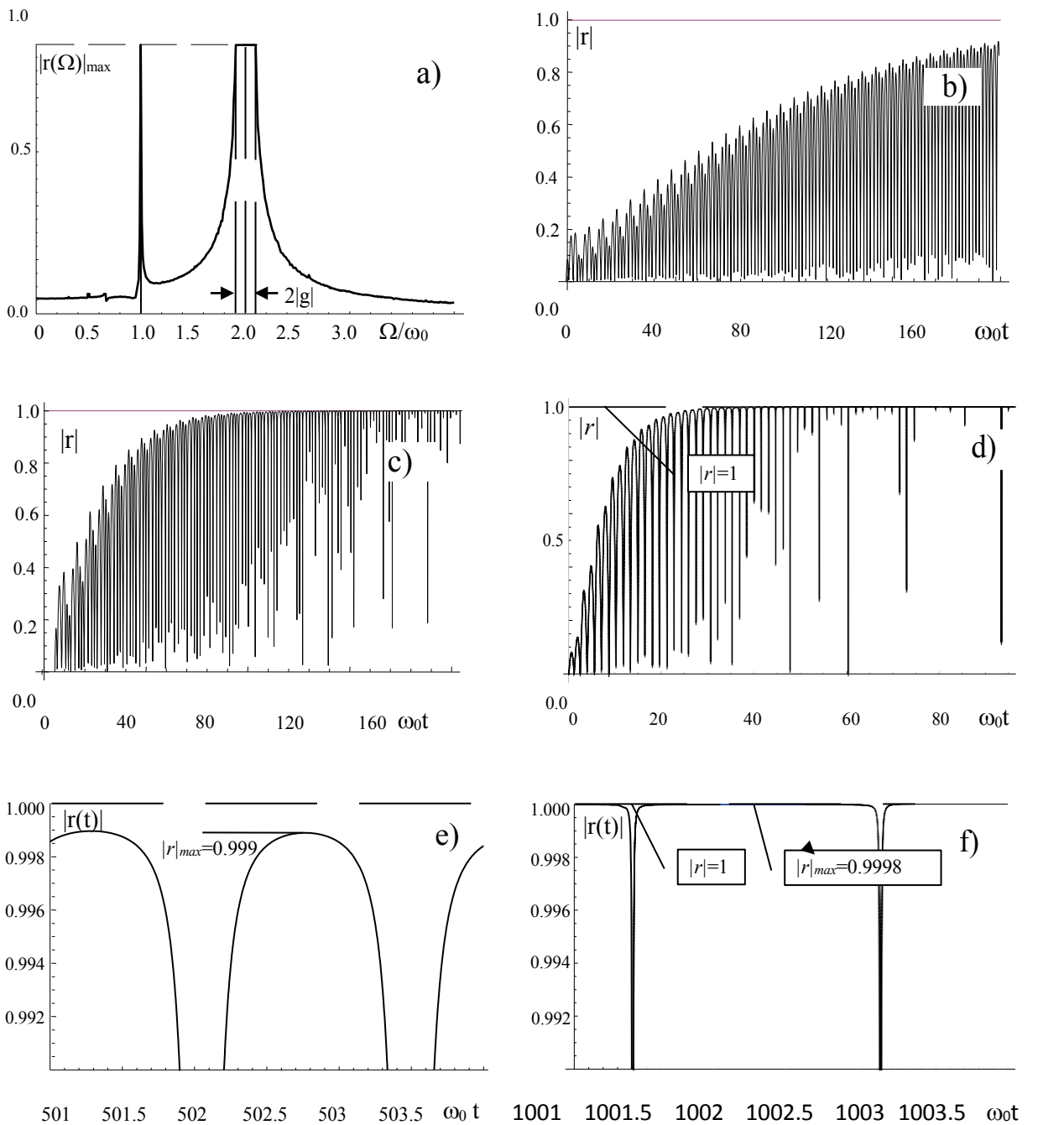

Fig. 4. *a) - resonant structure of the dependence of the maximum of the correlation coefficient on the frequency Ω for periodic modulation* $\omega(t) = \omega_0(1 + g\cos\Omega t)$ *of the potential well parameters; b) -f) are the dependence of the correlation coefficient on time for modulation at the fundamental frequency* $\Omega = \omega_0$ *at* $g = 0.1$ *and at* $g = 0.2$*(c) and the parametric resonance frequency* $\Omega = 2\omega$ *at* $g = 0.1$ *for time intervals* $\omega_0 t \leq 100$*(d),* $\omega_0 t \approx 500$*(e) u* $\omega_0 t \equiv 1000$*(f).*

on the parameters (in particular, the frequency) of the harmonic oscillator $\omega(t) = \omega_0(1 + g\cos\Omega t)$ in the case $|g| << 1$ were examined in details. It follows from the solution of Eqs. (12)-(16) that the process of CCS formation for such modulation of the parameters of the potential well is characterized by the presence of the main (for $\Omega \approx \omega_0$) and parametric ($\Omega \approx 2\omega_0$) resonances, beyond which the efficiency of this process very sharply decreases, although it remains nonzero [10]. Within these resonances $|r| \to 1$ as the modulation duration increases (see **Fig. 4**a). It is interesting to note that the frequency half-width of the main resonance is very small ($|\delta\Omega| << g\omega_0$), and the parametric resonance is characterized by a resonance curve having a flat vertex of width $|\delta\Omega| = 2g\omega_0$.

From the same calculations it follows that as the modulation duration increases, the maximum values of the correlation coefficient $r(t)_{max}$ increase rapidly. The largest rate of $r(t)_{max}$ increase corresponds to the frequency $\Omega = 2\omega_0$ and it rises sharply with the frequency modulation index g, reaching the value $|r|_{max} = 0.999$ (which corresponds to $G_{max} \approx 22$) at $\omega_0(t) \approx 500$ and $|r|_{max} = 0.9997$ ($G_{max} \approx 41$) at $\omega_0(t) \approx 1000$.

Obviously, an analogous structure with two maxima of different amplitude and area (Fig. 4a) corresponds to the dependence of the tunneling effect on the modulation frequency.

This result can explain completely the results of the experiments [16] on stimulation of LENR under the synchronized action of two laser beams generated by low-power laser diodes (P ≈ 20 mW) with close frequencies to the Pd surface of a cathode located in heavy water in an electrolytic cell (**Fig. 5**)

When the polarization of these beams coincides, the generation of a difference frequency that acts on electrons in conduction band of the cathode takes place. Action of this low-frequency field leads to the periodic modulation of the potential well parameters for localized deuterium ions in the palladium lattice. Selecting the appropriate pairs of such

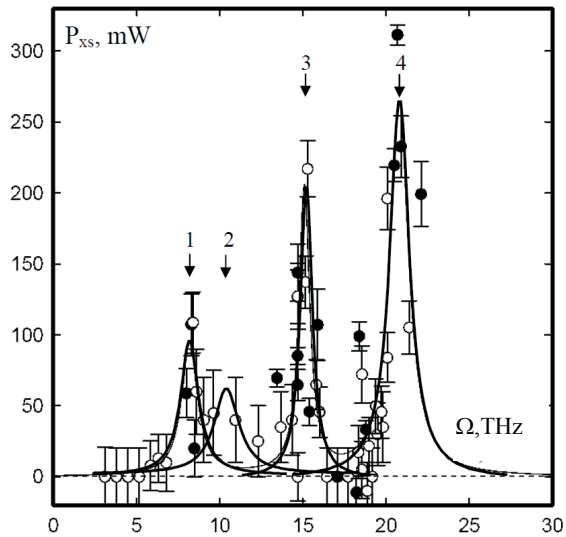

Fig. 5. *Dependence of the power released upon exposure to the surface of the palladium cathode saturated in the process of electrolysis by deuterium in the volume of heavy water, versus difference frequency Ω of radiation from two low-power laser diodes* [16].

diodes, the authors investigated the dependence of the energy release in such system on this difference frequency in the interval 5...25 THz and found 4 resonance peaks of energy release with frequencies $\Omega_1 \approx 7.8...8.2$, $\Omega_2 \approx 10.2...10.8$, $\Omega_3 \approx 15.2...15.6$ and $\Omega_4 \approx 20.2...20.8$ THz, having a different amplitude.

The authors [16] could not give any adequate interpretation of these experiments. It is easy to see that these results agree very well with the data of the calculations presented above if we assume that the energy release is associated with the stimulation of nuclear reactions at low energy

$$d + d = {}^3He + n;\ t + p,\ {}^4He \qquad (20)$$
$$Pd^A + d \to Ag^{A+2} \to ...$$

in the volume of palladium saturated with deuterium.

Analysis of the deuterium vibrational structure in the Pd matrix shows that the frequencies $\omega_1 \approx 7.8...8.2$ THz and $\omega_2 \approx 10.2...10.8$ THz correspond to the intrinsic vibrations of deuterium ions in the Pd lattice. Each of these ions is, in fact, a harmonic oscillator.

Comparing the dependences of the power output, shown in Fig. 5, and, accordingly, the structure of the frequency dependence of the correlation coefficient (Fig. 4a), it is

easy to verify that first and third peaks in Fig. 5 correspond to the pair determined by the basic $\Omega = \omega_1 \approx 7.8...8.2$ THz and parametric $\Omega = 2\omega_1 \approx 15.2...15.6$ THz frequency resonances of the correlation coefficient formation, and second and forth peaks correspond to another pair (basic $\Omega = \omega_1 \approx 10.2...10.8$ THz and parametric $\Omega = 2\omega_1 \approx 20.2...20.8$ THz frequency resonances).

The ratio of the amplitudes of the maxima of energy release in Fig. 5 fully corresponds to the results presented in Fig. 4 – the first, lower peak of each pair corresponds to the lower efficiency of the formation of the CCS at the frequency of the main resonance, and the second, higher – to greater efficiency at the parametric resonance frequency.

3.2. Features of CCS formation at limited increase or decrease of the width of a parabolic potential well

Let's find solution of equations (18)-(19) with a limited (in the range from L_0 to $L_{max} \equiv L_0(1+g^{(+)})$) increase of the width of parabolic well

$$L(t) = L_0(1 + g^{(+)})/(1 + g^{(+)}e^{-t/T}), \quad (21a)$$

which corresponds to a decrease of the frequency of the oscillator

$$\omega(t) = \omega_0^{(+)}(1+g^{(+)}e^{-t/T})/(1+g^{(+)}) \quad (21b)$$

from $\omega(0) = \omega_0^{(+)}$ to $\omega(\to\infty) \equiv \omega_{min} = \omega_0^{(+)}/(1+g^{(+)})$. Here $g(+) = L_{max}/L_0 - 1$ and $g(+) \approx L_{max}/L_0$ if $L_{max} >> L_0$.

The value of T determines the characteristic deformation time (size increase) of the well.

Fig. 6 shows the dependence of the correlation coefficient on the time of a monotonic increase of the width of the potential well in the interval $L_{max}/L_0 = 11...10^4$ for different characteristic durations $T = (10^{-1}/\omega_0^{(+)})...(10/\omega_0^{(+)})$ changes of this width. Such change of the size of the well L_{max}/L_0 corresponds to the change of interval $\omega_0^{(+)}/\omega_{min} = 11...10^4$ of oscillation frequency of the particle in the well.

From these results follows that if the interval L_{max}/L_0 increases, the amplitude of the correlation coefficient oscillations also increases greatly to the maximum possible value $|r|_{max} \to 1$. Narrow dips in the graph of $|r(t)|$ are a consequence of the rapid interference transitions between the values of $r(t)$ and $-r(t)$ with time increase. With

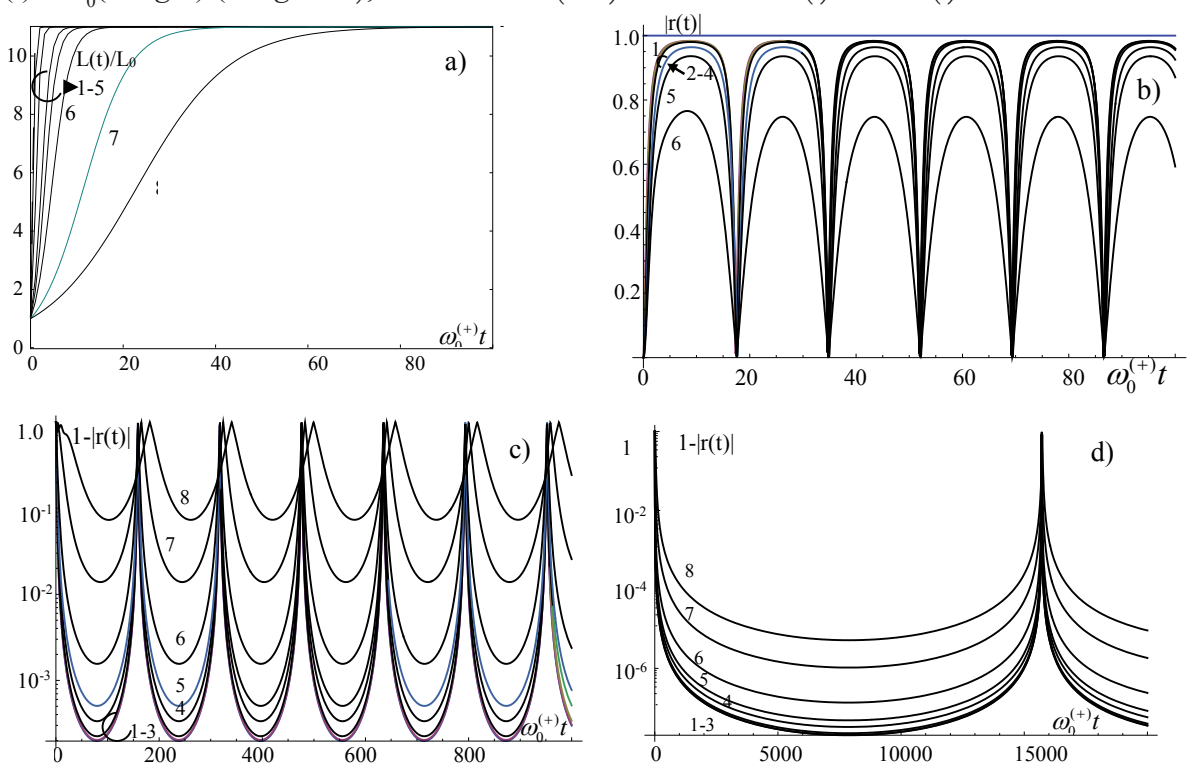

Fig. 6. *The time dependence of the width of the potential well (a) and the correlation coefficient (b) at the expansion of the well in the range: $g^{(+)} = 10$, $L_{max}/L_0 = 11$(b); $g^{(+)} = 100$, $L_{max}/L_0 \approx 100$ (c); $g^{(+)} = 10^4$, $L_{max}/L_0 \approx 10^4$(d). Graphs 1-8 correspond to the values $T\omega^{(+)} = 0.1, 0.25, 0.5, 1.0, 1.33, 2, 5, 10$.*

the increase $|r(t)|_{max} \rightarrow 1$, the width of these gaps tends to zero.

Another important factor of $|r(t)|_{max}$ increase is the use of the minimum deformation time T of the well.

In particular, for a relatively small change of the size of the well (at $L_{max}/L_0 = 11$ and $T = (0.1...1)/\omega_0^{(+)}$, the maximum values of the correlation coefficient $|r|_{max}$ and the correlation efficiency $G_{max} = 1/\sqrt{1-r_{max}^2}$ do not exceed, respectively, $|R|_{max} \approx 0.98$ and $G_{max} \approx 5$. If this interval is increased to $L_{max}/L_0 = 10^4$ (this corresponds, for example, to an increase of the width of the microcrack from the "seed" value $L_0 \approx 5...10$Å to $L_{max} \approx 5...10$ μm), we have $1 - |r|_{max} \approx 2 \cdot 10^{-7}$ and $G_{max} \approx 1600$.

The hypothetical case of even greater change $L_{max}/L_0 = 10^5$ corresponds to a CCS with close to ideal characteristics $1 - |r|_{max} \approx 10^{-9}$ and $G_{max} \approx 20000$!

We can emphasize another feature of the process of formation of the CCS. The maximum current correlation coefficient $|r(t)|_{max}$ is provided through a time interval much greater than the value of T, which determines the duration of a significant change in the width of the well. It follows directly from the analysis of the data presented in Fig. 5. In particular, the first maxima of $|r(t)|$ and $G(t)$ correspond to time of CCS formation and are equal to $t_c \approx 750/\omega_0^{(+)}$, $7500/\omega_0^{(+)}$, $75000/\omega_0^{(+)}$ for $L_{max}/L_0 = 10^3$, 10^4, 10^5, respectively. For the appearance of the following maxima of $|r(t)|_{max}$ and $G_{max}(t)$ more time is required.

These values of t_c essentially exceed the time of a significant change of the width of the well $T = (0.1/\omega_0^{(+)})...(10/\omega_0^{(+)})$. The situation corresponds to the condition $T << t_c$, at which rapid deformation of the well occurs first, and then a slow process of formation of the CCS takes place. Obviously, the process of deformation of a well with $T \rightarrow 0$, which is close to its instantaneous expansion in the interval from L_0 to L_{max} is close to the ideal case.

Examined above scenario of LENR optimization at expanding of the potential well agrees with experiments in metalhydrides (in particular, with A.Rossi's experiments), when the formation of unsteady (rapidly growing) microcracks in the volume of metal, in which hydrogen ions are localized, occurs in the process of hydrogenation. In addition, such scenario can "work" in natural dynamic systems such as cell division, when, for example, atoms or ions of hydrogen are in the space between separating cells.

b) An alternative mode of CCS formation due to the influence on the parameters of the potential well, in which the particle is located, is the reduction of its width. Let us find the solution of the system of equations (18)-(19) with a limited decrease in the width of the potential well

$$L(t) = L_0(1 + g^{(-)}e^{-t/T})/(1+ g^{(-)}) \quad (22a)$$

from L_0 to $L_{min} \equiv L_0/(1 + g^{(-)})$, which corresponds to an increase in the frequency of the oscillator

$$\omega(t) = \omega_0^{(-)}(1+g^{(-)})/(1+g^{(-)}e^{-t/T}) \quad (22b)$$

from $\omega(0) = \omega_0^{(-)}$ to $\omega_{max} \equiv \omega_0^{(-)}(1+g^{(-)})$.

Here $g^{(-)} = (L_0/L_{min} - 1)$ and $g^{(-)} \approx L_0/Lmin$ if $L_0 >> L_{min}$.

The results of calculation of the coefficient $g^{(-)} = 10, 10^2, 10^3$ for three values, which correspond to similar decreases of the size of the parabolic well, and, accordingly, an increase of the oscillation frequency within this well, as well as different values of the characteristic duration T of the well compression, are shown in **Fig. 7**. It follows from these results that the maximum value of the correlation coefficient, as in the case of expanding well, increases with the increase of the compression interval L_{max}/L_0 and decrease of the compression time T.

E.g. at a relatively small compression of the well in the interval $L_0/L_{min} = 11$ and at $T = (0.001/\omega_0^{(-)})...(0.01)/\omega_0^{(-)})$ the maximal values of the correlation coefficient and the correlation efficiency coefficient don't exceed, respectively, $|r|_{max} \approx 0.98$ and $G_{max} = 1/\sqrt{1-r_{max}^2} \approx 5$. With an increase of the compression interval to $L_0/L_{min} = 10^3$, for example, by the reducing of the width of the

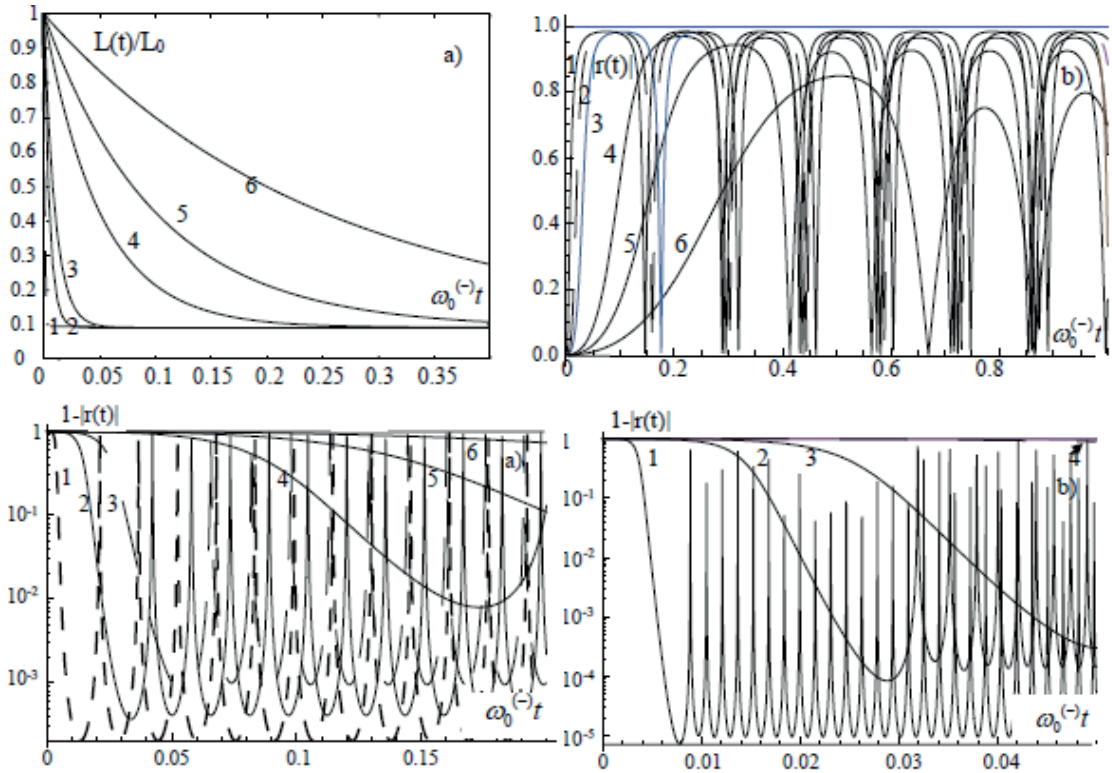

Fig. 7. *The change in the width of the compressing potential well (a) and the correlation coefficient for:* $g^{(-)} = 10$, $L_0/L_{min} = 11$*(b);* $g^{(-)} \approx L_0/L_{min} = 10^2$*(c);* $g^{(-)} \approx L_0/L_{min} \approx 10^3$*(d). Graphs 1-6 correspond to the values* $T\omega^{(-)} = 0.001, 0.005, 0.01, 0.05, 0.1, 0.25$.

microcrack in the matrix from 1 μm to 10Å, we have $1 - |r|_{max} \approx 10^{-5}$ and $G_{max} \approx 220$ at $T = 0.001/\omega_0^{(-)}$ and $1 - |r|_{max} \approx 10^{-4}$, $G_{max} \approx 70$ at $T = 0.005/\omega_0^{(-)}$.

It should be noted that if the potential well is compressed in this interval, the initial frequency $\omega_0 \equiv \omega_0^{(-)}$ (before the compression of the well) is in $L_0/L_{min} = 10^3$ times smaller than the initial frequency $\omega_0 \equiv \omega_0^{(+)}$ (before the expansion) at a similar expansion of the well in the same interval from 10Å to 1 μm. This circumstance must be taken into account when comparing graphs $r(t)$, which determine the time dependence of the process of formation of CCS with the increase and decrease of potential well sizes.

At an even larger value of the compression interval L_{max}/L_0 and with the corresponding shortening of the compression process duration T, the values of $|r|_{max}$ and G_{max} increase as effectively as in the case of an expansion of the well.

It should be noted that considered mechanism of CCS formation is realized when microcracks are "healed" in a number of materials and during the growth of biological cultures (in particular, during the division of DNA, on membrane surfaces, etc.).

3.3. Formation of CCS at pulse modulation of potential well parameters

Another alternative method of CCS excitation is connected with a pulsed change of the frequency of an equivalent harmonic oscillator – rapid deviation (usually an increase) of the frequency from a stationary value, followed by rapid return to this value. In particular, papers [11, 13] consider the features of CCS formation for different structures, durations and amplitudes of such change. **Fig. 8** shows the dependence of the maximum $|r(t)|_{max}$ and the time-averaged $<|r(t)|>$ correlation coefficient calculated on the basis of relations of the type (18)-(19) on the pulse time width τ of the frequency modulation pulse

$$\omega = \omega_0(1 + f(t)), \quad f(t) = ge^{-(t-t_0)^2/2\tau^2}, t_0 \gg \tau \quad (23)$$

at different amplitudes of this pulse.

Direct numerical calculation on the basis of equations (18)-(19) has shown that the action of such Gaussian pulse $f(t)$ leads to the rapid formation of a CCS with the maximum values of the correlation coefficient $|r(t)|_{max}$,

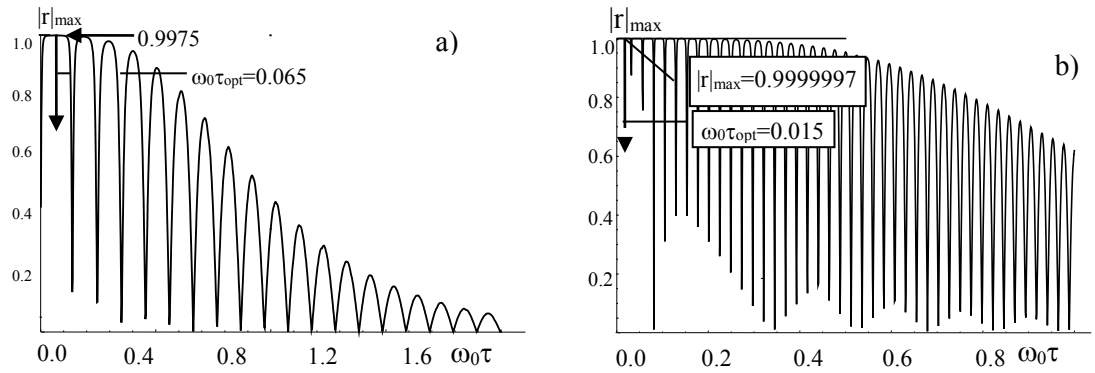

Fig. 8. *Dependence of the maximum value* $|r(t)|_{max}$ *of the correlation coefficient versus duration of the frequency modulation pulse (18) for different amplitude of this pulse:* $g = 10$ *(a);* 50 *(b).*

which correspond to a very large coefficient of correlation efficiency G, which provides great transparency of the potential barrier. In particular, at increases of the dimensionless pulse amplitude (increase of the frequency from the initial value) from $g = 10$ to $g = 50$, the value of G increases from $G \approx 14$ to $G \approx 1300$. According to the estimates made above, it provides an increase of the probability of the tunnel effect in the interaction of particles at low energy from $D_{r=0} \approx 10^{-500}$ in the absence of such action to $D_{r=0.9975} \approx 10^{-35}$ at $g = 10$ and to $D_{r=0.9999997} = 0.3$ at $g = 50$.

The mechanism of the formation of a CCS under a pulsed action on a particle [11, 13] can be realized, for example, as by the shock deformation of the lattice under the action of shock waves, as under the action of a pulsed magnetic field on free charged particles

A typical example of such external action is an electric discharge in a gas or liquid. The current $J(t)$ of the discharge is accompanied by the formation of a pulsed azimuthal magnetic field $H(\vec{r},t)$ in which the motion of the ions corresponds to tunable cyclotron resonance, and the system itself is a complete (formal) analog of the nonstationary harmonic oscillator with the same Hamilton operator with the same wave functions and energy spectrum. Used above formalism for the formation of a CCS in a nonstationary harmonic oscillator can be fully applied to such system, taking into account the obvious change of the initial frequency $\omega(t) = |q|H(t)/Mc$.

The results obtained above can be directly used for this case, if we assume that

$$\omega(t) = \omega_0(1 + f(t)), \omega_0 = |q|H_0/Mc, H(t) = H_0(1 + f(t)), H_{max} = H_0(1 + g)). \quad (24)$$

Under the action of the pulsed magnetic field, a peculiar "deformation" of this equivalent oscillator and a very effective formation of the CCS take place. Such scenario explains well [13], for example, the generation of neutrons and other isotopes in air during lightning on the base of reactions

$$d + d = T + p,\ d + d = {}^4He,$$
$${}^{12}C + n = 3{}^4He + n', d + d = {}^4He,$$
$${}^{13}C + p = {}^{14}N,\ {}^{12}C + d = {}^{14}N,\ {}^{15}N + p = {}^{16}O,$$
$${}^{14}N + d = {}^{16}O,\ {}^{18}O + p = {}^{19}F, \quad (25)$$

and also the well-known experiments of R. Mills (J. Mols, J. Lotoski, Y. Lu. Brilliant Light Power [18]) on stimulation of large energy release in an electric discharge in a gaseous medium.

3.4. The influence of damping and random force on formation of coherent correlated state of particles in parabolic well

The presence of fluctuations and damping can have a significant effect on the process of CCS formation. The most reasonable method for taking into account the attenuation of a quantum oscillator is the introduction of a thermostat and the use of a density matrix apparatus, which necessitates the use of a large number of longitudinal T_{ij} and transverse τ_{ij} relaxation times. These values are most often found semiempirically. This method greatly complicates the solution and makes it much less clear if you

stay within the framework of a model close to the classical harmonic oscillator. On the other hand, it is well known that in a classical harmonic oscillator damping can be taken into account by introducing a phenomenological braking force $\vec{F}_d = -2\gamma d\vec{q}/dt$ with a single phenomenological coefficient γ.

An acceptable alternative to the density matrix method is the simulation of a phenomenological nonstationary quantum-mechanical Hamiltonian, from which an equation of motion can be obtained, in the form corresponding to a classical oscillator with damping. This condition corresponds to the Caldirola-Kanai Hamiltonian, which takes into account the effect of the external force $\vec{F}_d$ and the phenomenological braking force on a particle in the parabolic potential, and has the form

$$\hat{H}(\hat{x},t) = \frac{\hat{p}_x^{\,2}}{2M}e^{-2\gamma t} + \frac{M\omega^2(t)\hat{x}^2}{2}e^{2\gamma t} - F(t)\hat{x}e^{2\gamma t}. \quad (26)$$

In this relation, the canonical (generalized) momentum $\hat{p}_x$ is connected with the "physical" momentum $p_{(k)x} = Mdx/dt$ by the relation $\hat{p}_x = e^{2\gamma t}\hat{p}_{(k)x}$.

This Hamiltonian is Hermitian, its eigenvalues are real, and the eigenfunctions are bounded and normalized. The use $\hat{H}(t)$ of the form (26) does not violate the canons of quantum mechanics. The validity of the use of such Hamiltonian for the analysis of systems with dissipation at a variable frequency was discussed in many papers (in particular, in [1, 2, 9-11]).

Based on the Hamiltonian (26) and taking into account the general rule for constructing the equation of motion for an arbitrary operator

$$\frac{d\hat{L}}{dt} = \frac{\partial\hat{L}}{\partial t} + \frac{1}{i\hbar}[\hat{L}\hat{H}(t)] \quad (27)$$

we can obtain the equation of motion for the coordinate operator $\hat{x}$

$$\frac{d^2\hat{x}}{dt^2} - \frac{1}{i\hbar}\frac{\partial}{\partial t}[\hat{x}\hat{H}(t)] + \frac{1}{\hbar^2}[[\hat{x}\hat{H}(t)]\hat{H}(t)] = 0, \quad (28)$$

which leads to the dimensionless equation of a classical harmonic oscillator with damping, an arbitrary external force, and the necessary initial conditions

$$\frac{d^2\varepsilon}{dt^2} + 2\gamma\frac{d\varepsilon}{dt} + \omega^2(t)\varepsilon = f(t),$$

$$\varepsilon(0) = 1,\ \left.\frac{d\varepsilon}{dt}\right|_0 = i,\ \omega(0) = 1. \quad (29)$$

This equation is an obvious generalization of equation (15).

In equation (29) and in the following relations, $f(t) = F(t)/\sqrt{\hbar M\omega_0^3}$ is a dimensionless external (including stochastic) force; γ is the dimensionless attenuation coefficient normalized to ω_0.

To solve a specific problem of the CCS formation process at the presence of damping, variable frequency, and stochastic effects, we used more simple method of equation (29) analysis, which is connected with its transformation into equations for the corresponding reciprocal and mixed moments of quantities $\hat{q}$ and $\hat{p}_q$ (in dimensionless form ε and $d\varepsilon/dt$), appearing in (29), and taking into account the correlation characteristics of the function $f(t)$. A similar method can also be used at the presence of a random perturbation of the variable oscillator frequency $\omega(t)$.

Let us consider the evolution of a nonstationary oscillator with damping under the action of a random stationary delta-correlated force $f(t)$ with characteristics

$$< f(t) >_f = 0, < f(t_1)f(t_2) >_f = 2S\delta(t_1 - t_2) \quad (30)$$

corresponding to averaging over the realization of a random force with the intensity S.

An explicit form of the dependence S on the parameters of a low-pressure plasma or gas was obtained in [9-11]

$$S = \frac{1}{2}\int_{-\infty}^{\infty} d\tau \left\langle \frac{1}{\Delta t}\int_{-\Delta t/2}^{\Delta t/2} f(t)f(t+\tau)dt \right\rangle_f \approx$$

$$\approx \frac{M^*\sigma n}{2\hbar\omega_0^2}\left\langle (\Delta v)^2 \right\rangle_f \left\langle |v| \right\rangle_f. \quad (31)$$

Here $1/\Delta t = \sigma n|v|/\omega_0$ is the dimensionless collision frequency of atoms in the medium (in this case – in a gas with a particle concentration n), $\sigma \approx 3\cdot10^{-16}$ cm^2 is the total cross section for elastic scattering of atoms at low energy, $M^* = M/(1 + M/M_a)$ is the reduced mass at

the collision of the particle with another particle of the medium, and Δν is the change of particle velocity in an elastic collision.

After introduction of the functions

$$\mu_{00} = \varepsilon^* \varepsilon, \mu_{01} = \varepsilon^* \frac{d\varepsilon}{dt},$$

$$\mu_{10} = \frac{d\varepsilon^*}{dt}\varepsilon = \mu_{01}^*, \mu_{11} = \frac{d\varepsilon^*}{dt}\frac{d\varepsilon}{dt}, \quad (32)$$

which includes a combination of dimensionless coordinates and particle pulses, it is possible to obtain a system of equations for the mixed $m_{ii} = <\mu_{ii}>$ and mutual $m_{i\neq j} = <\mu_{i\neq j}>$ moments of the quantities ε and $d\varepsilon/dt$ corresponding to the dimensionless coordinate and momentum of the particle. After additional averaging of all components of these equations by the realization of the random force $f(t)$, we can obtain the resulting system of equations for the moments $m_{ij} = <\mu_{ij}>_f$

$$\frac{dm_{00}}{dt} = m_{01} + m_{01}^*, \quad (33a)$$

$$\frac{dm_{01}}{dt} = m_{11} - 2\gamma m_{01} - \omega^2(t) m_{00}, \quad (33b)$$

$$\frac{dm_{11}}{dt} = -4\gamma m_{11} - \omega^2(t)\left\{m_{01} + m_{01}^*\right\} + 2S. \quad (33c)$$

The solutions of this system satisfy the initial conditions for the moments

$$m_{00}(0) = 1,\ m_{01}(0) = i, m_{01}^*(0) = -i,\ m_{11}(0) = 1, \quad (34)$$

directly following from the initial conditions for ε and $d\varepsilon/dt$.

The solution of the system of equations (33) and the corresponding correlation coefficient

$$r(t) = \frac{m_{01} + m_{10}}{2\sqrt{m_{00}m_{11}}} \equiv \frac{m_{01} + m_{01}^*}{2\sqrt{m_{00}m_{11}}}, \quad (35)$$

can be found for a given law of variation of the oscillator frequency $\omega(t)$. Using this coefficient and the wave function of the CCS, it is possible to calculate the fluctuation parameters of a quantum oscillator, and, using an approximate relation $D_{r\neq 0} \approx (D_{r=0})^{\sqrt{1-r^2}}$, estimate the change in the transparency of the potential barrier.

Such analysis was carried out in [9-11], where it was shown that the presence of such fluctuations (for example, due to the collision of an ion located in the field of a variable harmonic oscillator with extraneous atoms) can significantly complicate the process of CCS formation and reduce the maximum value of the correlation coefficient.

Fig. 9 presents one of the many results of the analysis of the action of random force and dephasing fluctuations on the process of CCS formation with periodic modulation of parabolic potential well (at the frequency $\omega(t) = \omega_0(1 + g\cos\Omega t)$ change) on the parametric resonance frequency $\Omega = 2\omega_0$ at the absence and presence of random force.

It can be seen that the presence of a random fluctuating force slows down the increase of the correlation coefficient, and in some cases restricts it to a fixed level. These questions are discussed in details in [5, 9, 11].

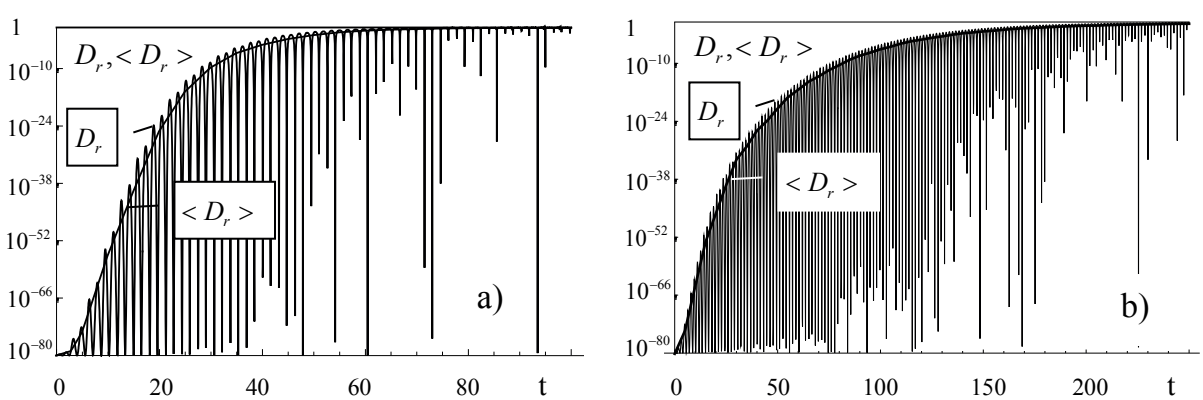

Fig. 9. *The dependence of the current D_r (oscillating function) and the averaged $<D_r>$ (monotonic function) of the tunnel effect probabilities versus duration of periodic frequency modulation in the case of: a) the absence of random force and the presence of attenuation with parameters $2\gamma = g = 0.1$; b) the presence of a random force with intensity $S = 0.05$ and damping $2\gamma = g/2 = 0.05$. The initial values $D_{r=0}$ and $< D_{r=0} >$ correspond to the value $D_{r=0} = < D_{r=0} > = 10^{-80}$.*

4. CONCLUSION

Examined above problem of LENR implementation based on the use of coherent correlated states allows us to explain, justify and numerically consider all known LENR paradoxes without applying new radical hypotheses, basing only on the powerful foundations of modern quantum theory and nuclear physics.

It is important to note that a variety of LENR effects for light, medium and heavy isotopes, observed in completely different media and systems (crystals, amorphous bodies, liquids, gases, various living systems, etc.) under different causes (hydrogenation of metals during electrolysis and thermal exposure, glow discharge, shock waves, electric discharge, natural metabolic processes with concomitant biological phenomena, etc.) are described by a single universal mechanism! Previously, different authors believed that each of the group of effects is characterized by its unique mechanism, not applicable to another group.

Another undoubtedly positive aspect of the method of coherent correlated states in application to LENR processes is the ability to predict the expected effects, as well as the possibility of preliminary assessment of the potential suitability and efficiency of new designed or newly used devices, systems and objects.

REFERENCES

1. Dodonov VV, Manko VI. Transactions of FIAN (Russia), 1987, 183:71.
2. Dodonov VV, Klimov AB, Manko VI. Transactions of FIAN (Russia),1991, 200:56.
3. Vysotskii VI, Adamenko SV. Correlated states of interacting particles and problems of the coulomb barrier transparency at low energies in nonstationary systems. *Technical Physics,* 2010, 55 (5):613.
4. Vysotskii VI, Vysotskyy MV, Adamenko SV. Formation and application of correlated states in non-stationary systems at low energy of interacting particles. *Journal of Experimental and Theoretical Physics*, 2012, 114 (2):243.
5. Vysotskii VI, Adamenko SV, Vysotskyy MV. The formation of correlated states and the increase in barrier transparency at a low particle energy in nonstationary systems with damping and fluctuations. *Journal of Experimental and Theoretical Physics*, 2012, 115(4):551.
6. Vysotskii VI, Adamenko SV, Vysotskyy MV. Subbarier interaction of channeling particles under the self-similar excitation correlated states in periodically deformed crystal. *Journal of surface investigation,* 2012, 6(2):369.
7. Vysotskii VI, Vysotskyy MV. Coherent correlated states and low-energy nuclear reactions in non stationary systems. *European Phys. Journal A49*, 2013; DOI 10.1140/epja/i2013-13099-2.
8. Vysotskii VI, Adamenko SV, Vysotskyy MV Acceleration of low energy nuclear reactions by formation of correlated states of interacting particles in dynamical systems. *Annals of Nuclear energy,* 2013, 62:618.
9. Vysotskii VI, Vysotskyy MV. Correlated states and transparency of a barrier for low-energy particles at monotonic deformation of a potential well with dissipation and a stochastic force. J*ournal of Experimental and Theoretical Physics,* 2014, 118(4):534.
10. Vysotskii VI, Vysotskyy MV. Formation of correlated states and optimization of nuclear reactions for low-energy particles at nonresonant low-frequency modulation of a potential well. *Journal of Experimental and Theoretical Physics,* 2015, 120(2):246.
11. Vysotskii VI, Vysotskyy MV. The formation of correlated states and optimization of the tunnel effect for low-energy particles under nonmonochromatic and pulsed action on a potential barrier. *Journal of Experimental and Theoretical Physics*, 2015, 121(4):559.
12. Vysotskii VI, Vysotskyy MV. Coherent correlated states of interacting particles – the possible key to paradoxes and features of LENR. *Current Science,* 2015, 108(4):30.
13. Vysotskii VI, Vysotskyy MV. The formation of correlated states and tunneling at low energy at controlled pulse action on particles. *Journal of Experimental and Theoretical Physics*, 2017, 152(8):234.
14. Schrödinger E. *Ber. Kgl. Akad. Wiss.*, Berlin, 1930, S24: 296.
15. Robertson HP. *Phys.Rev. A,* 1930, 35:667.
16. Letts D, Cravens D, Hagelstein PI. *Low-Energy Nuclear Reactions Sourcebook*. American Chemical Society, Washington DC, 2009, 2:81-93.
17. http://www.sifferkoll.se/sifferkoll/wp-content/uploads/2014/10/LuganoReportSubmit.pdf.
18. brilliantlightpower.com/suncell.

ON MECHANISMS OF LOW-ENERGY NUCLEAR-CHEMICAL PROCESSES

[1,2]Serge Timashev

[1]Karpov Institute of Physical Chemistry, http://www.karpovipc.ru
Moscow 105064, Russian Federation
[2]National Research Nuclear University MEPhI, https://mephi.ru
Moscow 115409, Russian Federation

serget@mail.ru

Abstract. **It is shown that a wide variety of low-energy nuclear transformations studied under conditions of a nonequilibrium low-temperature glow discharge plasma and laser ablation of metals in aqueous media can be understood on the basis of the concepts of the dynamic interrelation between the electron and nuclear subsystems of an atom. The initiating role in such processes belongs to electrons a sufficiently large kinetic energy E_e ~ 3-5 eV (by chemical scales), which they can acquire under the indicated conditions. Inelastic scattering of electrons by nuclei in according to weak nuclear interaction becomes possible in the collision of such electrons with ions or plasma atoms (here we assume that the nuclei are not related to "K-capture" nuclei). At the first stage of such a nuclear-chemical interaction, a nucleus arise, the charge of which is one unit less than the charge of the initial nucleus, and nuclear matter is locally disrupted: the nuclear mass in this case is insufficient to preserve nuclear matter in the base state of interacting nucleons. Under such anomalous excitations of nuclear matter, which are characterized as the states of "inner shake-up" or isu-state, the relaxation dynamics of the nuclei is initiated by weak nuclear interactions. Such nuclei, being β-active ("β-nuclei"), can have sufficiently long lifetimes and effectively participate in nuclear reactions (as the β-neutron and β-dineutron introduced into consideration). If the initial nucleus is radioactive, the decay of "β-nuclei" will occur with a probability many orders of magnitude greater than the decay probability of the original nuclei. As an example, the nuclear-chemical transformations realized in the E-CAT reactor of Andrea Rossi are also considered.**

Key words: **low-temperature plasma, laser ablation of metals in aqueous media, β-nuclei, low-energy nuclear-chemical transformation, u- and d-quarks, Feynman diagrams of the initiating radioactive decay.**

PACS 25.10.+s

Bibliography – 43 references *Received 25.5.2017*

RENSIT, 2017, 9(1):37-51 **DOI: 10.17725/rensit.2017.09.037**

Contents

1. INTRODUCTION

Beginning with the work of Fleischmann, Pons and Hawkins [1] on observation of excessive heat generation during the electrolysis of D_2O heavy water with a Pd cathode, when the generation of neutrons and tritium was recorded, it became clear that the problem of establishing the mechanism of the occurring nuclear transformations could become a key to solving the complex of problems that arose in connection with the phenomenon of low-energy nuclear reactions (LENR). One of the first attempts to solve this problem was associated with the possibility of the existence of a stable dineutron with a binding energy ε_{dn} less than

3.01 eV (for the deuteron not to be radioactive) [2]. In the experiment [1], the arising a dineutron as a result of the interaction of an activated electron with a deuteron under conditions of electrolysis of heavy water could be considered as the first stage preceding the reaction of formation of tritium during the interaction of the dineutron with the deuteron. However, there remained questions. It was unclear whether it is possible to actually activate the electrons in the conditions of electrolysis of heavy water on a palladium cathode to the necessary (what exactly?) energies, and whether there really is a dineutron. The possibility of the ^2n nucleus existence was discussed back in the early 1960s when studying the $T(d, {}^2n)^3He$ process using the $^{27}Al(^2n, \gamma)^{29}Al$ reaction for the detection of ^2n particles [3]. However, in [4], which appeared shortly after the publication of [3], the results of a similar experiment were reported and it was reported that the yield of ^{29}Al, confirming the reality of the existence of ^2n nucleus, was observed only at the background level.

Moreover, it was known, based on general considerations, that the ^2n nucleus can not exist in principle. Since there is a bound state in the neutron-proton system with a binding energy ε_D = 2.22 MeV and spin S = 1, and also there is a virtual level with energy 70 keV and spin S = 0, for the system of two neutrons only the existence of a virtual state with spin S = 0 due to the charge independence of the nuclear forces (isotopic invariance), is possible [5]. But in this state there should be a weak repulsion, and the state with S = 1 can not exist due to the Pauli principle. Nevertheless, in this review [5], based on an analysis of the experimental data available at that time (1965), an upper estimate of the cross section for the formation of a nuclear stable dineutron, s < 0.001-0.01 mb, was still given, although this estimate practically excluded the possibility of manifestation of ^2n in any experiments. This estimate was confirmed by the result of a much later experiment [6], in which for the cross section of occurring a stable dineutron in the interaction of cold neutrons with deuterons in the reaction $n + d \rightarrow {}^2n + p$, we obtained: $\sigma \leq 1$ mcb.

With time, it became clear that in order to understand the results of [1], as well as many later works on initiating low-energy nuclear reactions (LENR) and accelerating radioactive α and β decays, including under low-temperature plasma conditions [7-9], and when laser ablation of metals in aqueous media [10-13], the idea of a stable dineutron should be abandoned, and it is necessary to involve other hypotheses. At the same time, the results of [14] in which the spectrum of the "lost mass" in the process $^6Li(\pi^-, p)^5H$ (see **Fig. 1**) with the kinetic energy of π^--mesons equal to 125 MeV was investigated, continue to cause surprise. It follows from Fig. 1, a fixed maximum in the region of the lost mass from zero to –5 MeV/c^2 could well correspond to a hypothetical dineutron with a binding energy of $\varepsilon_{dn} \approx$ 3MeV. However, in this case, the probability of the occurring a dineutron in the reaction involving a π^--meson would have an order of

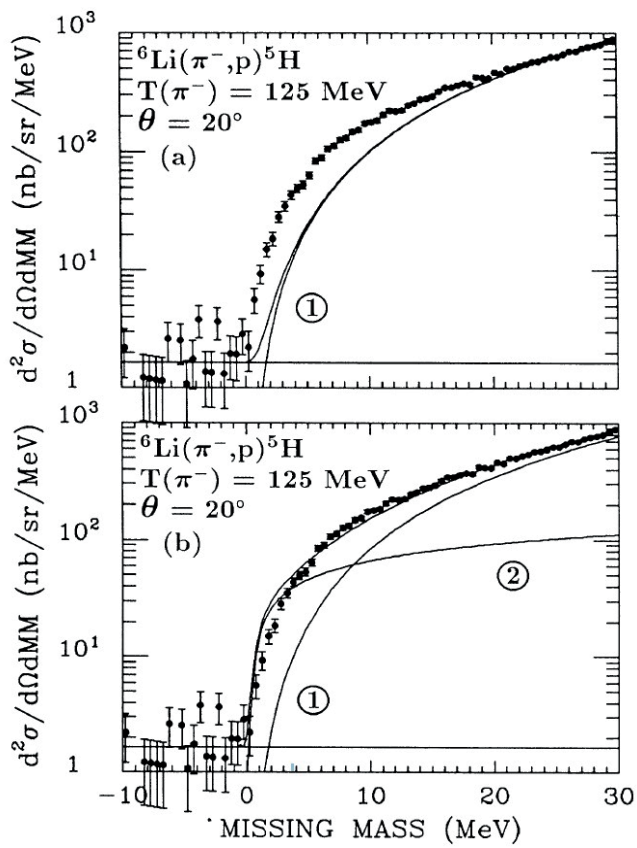

Fig. 1. *The missing-mass spectra for the reaction* $^6Li(\pi^-, p)^5H$ [14]. *The constant line at the bottom corresponds to the background. The phase-space distributions shown are as follows: (a) curve 1, fit for* $^5H \rightarrow {}^3H + n + n$; *(b) best-fit curve as sum of curve 1 for* $^5H \rightarrow {}^3H + n + n$ *and curve 2 for* $^5H \rightarrow {}^3H + {}^2n$.

magnitude higher than the values indicated above, for unknown reasons.

In subsequent years, in order to understand the results of many papers in which low-energy nuclear transformations and low-temperature plasma accelerated decays of radioactive nuclei were investigated, attempts were repeatedly made to introduce neutral particles with a baryon number of two (or one) that were the weakly coupled or resonant state of the deuteron (or proton) with an electron or a neutron with a neutrino. Such particles could participate in low-energy nuclear reactions, since for such a type of particles there would be no problem of overcoming the "Coulomb barrier" in nuclear interactions. We do not consider such possibilities here, since in accordance with the concepts of nuclear physics, electron and neutrino localization on nuclear scales ~ 10^{-13} cm would have an abnormally high, physically incredible uncertainty in the pulses [15].

In this paper, it is shown that the problems of establishing the possible mechanisms of LENR processes discussed above can be understood on the basis of the concepts of the interrelation between the electronic and nuclear subsystems of an atom [16-20], which determines the possibility of initiating the entire variety of nuclear transformations, including those studied in mentioned works [7-13], as well as realized in the Andrea Rossi E-CAT reactor [21, 22].

2. ELECTRONIC FACTOR IN INITIATING NUCLEAR PROCESSES

According to the phenomenological understanding [17-20], the dynamic interrelation between the electron and nuclear subsystems of atom, realized through the electromagnetic component of the physical vacuum, the EM vacuum, is the key factor in initiating low-energy nuclear reactions [7-13] and the processes of radioactive decay of nuclei [13, 17, 18]. A reflection of this interrelation is, in particular, the experimentally established facts showing that the possibility of radioactive decay of nuclei is determined by the positive difference between the mass of the initial nucleus together with the mass of the electron subsystem of the atom (i.e., the mass of the whole atom, not the nucleus) and the total mass of the decay products [23, 24]. Usually, when considering the mechanisms of these low-energy nuclear processes and the decay of atomic nucleus ${}^{A}_{Z}N$ (Z and A are the atomic number and mass number of the nucleus *N*, respectively), nuclear matter is represented in the form of interacting nucleons. For example, in the *K*-capture, when the electron of the inner shells of the atom interacts with the surface of the nucleus and a new daughter nucleus is formed, the nucleon structure of nuclear matter does not change. At the initial, irreversible stage of this process, the electron emits a neutrino ν when interacting with the nucleus surface. The formed virtual vector W^{-}-boson, which is introduced into the nuclear matter, is transformed into a *d*-quark when interacting with the *u*-quark of one of the protons, as a result of which this proton turns into a neutron, and the nucleus ${}^{A}_{Z-1}M$ is formed. However, the situation can drastically change when the *K*-capture is energetically forbidden (it is such cases that are considered below), but the electron has a sufficiently large (by chemical standards) kinetic energy E_e ~ 3-5 eV, as it can be realized in low-temperature plasma. Under these conditions, when the process of ionization of electron shells by such electrons is not yet realized, then, during scattering of electrons with the indicated kinetic energy and the corresponding de Broglie wavelength λ ≈ 0.5 nm, the oscillation dynamics of the electron subsystems of atoms and ions is initiated on atoms and ions and, thus, the probability of interaction between the electrons of the inner subshells of atoms and ions and the corresponding nuclei increases.

At the first, irreversible stage of such interaction, a neutrino ν is emitted and a vector W^{-}-boson is introduced into the nuclear matter of the original nucleus ${}^{A}_{Z}N$ according to the relation:

$${}^{A}_{Z}N + e^{-}_{be} \rightarrow {}^{A}_{Z-1}M_{isu} + \nu. \quad (1)$$

As a consequence, the nucleon structure of the formed nuclei ${}^{A}_{Z-1}M_{isu}$, whose charge is less than the charge of the initial nucleus by one elementary charge, turns out to be locally disrupted. Indeed, the vector W^{-}-boson, when interacting with the

u-quark of one of the protons of the ${}^{A}_{Z}N$ nucleus, can only yield the formation of a virtual *d*-quark with a subsequent chain of virtual transformations of quarks involving vector *W*-bosons, but a neutron cannot be formed due to the deficit of the total mass of such a nucleus. The emerging state of local anomaly of nuclear matter with a broken nucleon structure is characterized as a metastable state of "inner shake-up" or *isu*-state. The latter is indicated by the subscript in the notation of the nucleus in the right-hand side of the relation (1). The lower index in the notation for the electron in the left-hand side of (1) indicates the activated nature of this stage of the process. The initiated chain of virtual transformations of quarks with the participation of the vector *W*-bosons should be interrupted in the irreversible decay of the virtual W^{-}-boson with the formation of the initial nucleus, an electron, and an antineutrino $\tilde{\nu}$:

$$ {}^{A}_{Z\text{-}1}M_{isu} \rightarrow {}^{A}_{Z}N + e^{-} + \tilde{\nu}, \quad (2) $$

so that the gross process can be represented in the form of inelastic scattering of an electron on the initial nucleus:

$$ {}^{A}_{Z}N + e^{-}_{be} \rightarrow {}^{A}_{Z}N + e^{-} + \nu + \tilde{\nu}. \quad (3) $$

The nuclei with the state of nuclear matter in the metastable *isu*-state of the "internal shake" will be called the "β-nuclei". The threshold energy of such a process with the production of a $\nu\tilde{\nu}$ pair, determined by the rest masses of neutrino-antineutrinos, is about 0.3 eV [25].

As is known, the nucleus is a system of nucleons connected in a single whole by means of exchange interactions by exchanging quarks via pions. Therefore, the formation in the nucleus of three quarks unconnected into a nucleon, which can then be regarded as "markers" of new degrees of freedom, in fact, means that the intensity of nuclear forces is insufficient to provide the traditional, proton-neutron organization of nuclear matter in the system under consideration. The subsequent relaxation dynamics of the locally appeared *isu*-state, which can be transmitted to other nucleons of the nucleus by means of pions, is initiated only by weak nuclear interactions, which are realized through quarks during creation and absorption of the gauge vector neutral Z^{0}- and the charged $W^{\pm}$-bosons. In the case under consideration, such a relaxation terminates with the decay of the virtual vector W^{-}-boson with the formation of the initial nucleus during the emission of an electron and antineutrino. The lifetime of the formed β-nuclei in the metastable *isu*-state can be rather considerable, from tens of minutes to several years, and the nuclei in this state can directly participate in a variety of nuclear processes [17, 18].

It must also be taken into account here that the relaxation reorganization of nuclear matter in the process of formation of products of such nuclear transformations is carried out, first of all, by the formation of a purely nucleon structure of the nucleus, in accordance with the principle of least action. While in the nuclei with the proton-neutron, nucleon structure, the relaxation processes of de-excitation can go through the excited states of the nucleus and include the stages of emission of γ-quanta, in the β-nuclei such relaxation is practically impossible. Therefore, if the atomic nuclei with a partial "non-nucleon" state of nuclear matter participate in the processes, then the mechanism of relaxation of the formed products is inevitably associated with energy loss by the emission of neutrino-antineutrino pairs, or the URCA process [26], and not by the emission of γ-quanta by excited nuclei, as is the case during the relaxation of nuclear products having the proton-neutron organization of nuclear matter. It is for this reason that the corresponding nuclear processes are safe for the environment.

Of special interest are the cases when the formation of *isu*-states in nuclear matter is initiated in the initially radioactive nuclei, since the relaxation process with the decay of the vector W^{-}-boson can initiate a general radioactive decay of the nucleus in the *isu*-state with the creation of the daughter products of the decay of the initial radioactive nucleus. According to [18, 27], the violation of the general stability of nuclear matter in the metastable *isu*-state occurs as a result of a change in the boundary conditions for the components of the electric field intensity vector of the EM vacuum on the surface of the nucleus in whose volume such a violation of the

nucleon structure has occurred. An indicator of the instability of the ${}^{A}_{Z\text{-}1}M_{isu}$ nucleus arising during process (1) is the absolute value of the structural energy deficit ΔQ ($\Delta Q < 0$) of this nucleus in the metastable *isu*-state, defined as $\Delta Q = (m_{{}^{A}_{Z}N} - m_{{}^{A}_{Z\text{-}1}M})c^2$. In this case, the mass of the ${}^{A}_{Z-1}M_{isu}$ nucleus is taken to be $m_{{}^{A}_{Z\text{-}1}M_{isu}} = m_{{}^{A}_{Z}N} + m_e$, , where $m_{{}^{A}_{Z}N}$ is the mass of the ${}^{A}_{Z}N$ nucleus and m_e is the rest mass of the electron.

For example, during the laser ablation of metal samples in the aqueous solution of uranyl, when low-temperature plasma forms in the vapor medium adjacent to the metal surface, the initiating interaction of plasma electrons with the ${}^{238}U$ nuclei leads to the formation of the "β-protoactinium" nuclei and subsequent β-decay of the ${}^{238}_{91}Pa_{isu}$ nuclei with the formation of thorium-234 and helium-4 nuclei as the products of decay of the initial uranium-238 nucleus:

$$
\begin{aligned}
&{}^{238}_{92}U + e^-_{be} \rightarrow {}^{238}_{91}Pa_{isu} + \nu \rightarrow \\
&\rightarrow {}^{234}_{90}Th + {}^{4}_{2}He + e^- + \nu + \tilde{\nu} + Q(4.27\ MeV). \qquad (4)
\end{aligned}
$$

In this case, the effective rate constant of such initiated decays of ${}^{238}U$ nucleus, as shown in [17], increases by 9 orders of magnitude, so that a kind of "e^--catalysis" is realized. The deficit ΔQ of the structural energy of the formed nucleus of β-protoactinium is $\Delta Q \approx -3.46$ MeV. An unexpected result was obtained while carrying out experiments with a beryllium sample. It turned out that the beryllium nanoparticles, formed in the solution after the completion of the laser action for an hour, exhibited an anomalously high rate of formation of thorium-234 nuclei for more than 500 days after completion of laser ablation. The half-life period for the nuclei, initiated under laser ablation and producing thorium-234, was 2.5 years. This phenomenon could naturally be associated with the accumulation of β-protoactinium nuclei in beryllium nanoparticles during laser ablation, which lasted only for an hour.

We also give examples [17, 20] of β^--decay of ${}^{60}_{27}Co$, ${}^{137}_{55}Cs$ and ${}^{140}_{56}Ba$ nuclei, initiated by the e^--catalysis mechanism, the half-life $T_{1/2}$ of which is 1925 days, 30.1 years and 12.8 days, respectively:

$$
\begin{aligned}
&{}^{60}_{27}Co + e^-_{be} \rightarrow {}^{60}_{26}Fe_{isu} + \nu \rightarrow \\
&\rightarrow {}^{60}_{28}N + 2e^- + \nu + 2\tilde{\nu} + Q(2.82MeV), \qquad (5)\\
&{}^{137}_{55}Cs + e^-_{be} \rightarrow {}^{137}_{54}Xe_{isu} + \nu \rightarrow \\
&\rightarrow {}^{137}_{56}Ba + 2e^- + \nu + 2\tilde{\nu} + Q(1.18\ MeV), \qquad (6)\\
&{}^{140}_{56}Ba + e^-_{be} \rightarrow {}^{140}_{55}Cs_{isu} + \nu \rightarrow \\
&\rightarrow {}^{140}_{57}La + e^- + \nu + 2\tilde{\nu} + Q(1.05\ MeV). \qquad (7)
\end{aligned}
$$

In these cases, the deficit of the structural energy ΔQ, which is lacked by ${}^{60}_{26}Fe_{isu}$, ${}^{137}_{54}Xe_{isu}$ and ${}^{140}_{55}Cs_{isu}$ nuclei in the "in-shake-up" state to form the basic state of nuclear matter characteristic to ${}^{60}_{26}Fe$, ${}^{137}_{54}Xe$ and ${}^{140}_{55}Cs$ nuclei, is –0.237 MeV, –4.17 MeV and –6.22 MeV, respectively. It can be expected that the initiating influence of electrons on the β^--decay of nuclei in low-temperature plasma will be manifested to the greatest extent in the cases when the "mismatch" in the absolute magnitude of the deficit ΔQ of the structural energy for the forming nuclei in the *isu*-state is the greatest. Therefore, in the cases under consideration, the effect of accelerating radioactive decay should have been manifested for ${}^{137}_{55}Cs$ and ${}^{140}_{56}Ba$ nuclei, while for ${}^{60}_{27}Co$ nuclei, it should have been minimal. The available experimental data [28] on the initiated decays of ${}^{137}_{55}Cs$, ${}^{140}_{56}Ba$ and ${}^{60}_{27}Co$ agree with this conclusion: the half-life of β^--active cesium-137 and barium-140 nuclei, equal to 30.1 years and 12.8 days, respectively, decreased to about 380 days and 2.7 days, while the half-life of cobalt-60, equal to 1925 days, remained practically unchanged. The Feynman diagrams corresponding to the β^--decay processes, as well as the positron β^+-decays of nuclei initiated by the e^--catalysis mechanism, are shown in Fig. 1.

The unexpectedness of the presented result about the possibility of external influences on the dynamics of the decay of a radioactive nucleus is that this effect is associated with electrons that cannot interact with nucleons of the nucleus as fragments of nuclear matter, but can initiate (through the vector W^--bosons) local disturbances in the nucleon structure of the nucleus. At the same time, as experience shows, the external excitation of the radioactive nucleus as an integral system (in particular, under the influence of

γ-radiation) cannot affect the radioactive decay rate, and therefore, the discussed phenomenon of initiating the instability of the nucleus. In these cases, nuclear matter manifests itself as an integral system of interacting nucleons with their inherent individual characteristics.

The Feynman diagrams for the β^-- and β^+-decays as well as for the α-decay, initiated by the e^--catalysis mechanism, are shown in **Fig. 2 a-d**. In the analysis of the processes presented in Fig. 2, we must have in mind that weak nuclear interactions are not as weak as it is often assumed: the value of the corresponding dimensionless constant α_F is almost an order of magnitude greater than the value α_e of the fine structure constant [15, 27]. Indeed, if we take $\alpha_s = \sqrt{2}$ as the dimensionless constant of strong nuclear interaction [27], then taking into account the value of the square of the "elementary charge of weak nuclear interaction" $q_F^2 \equiv G_F / a_Z^2$ [29], where $a_Z = 2^{1/2}\hbar/m_Z c \approx 3.3\ 10^{-16}$ cm is the characteristic radius associated with the mass of the intermediate Z^0 vector boson (m_Z = 91.2 GeV/c^2 = $1.62\cdot10^{-22}$ g), and $G_F = 1.17\cdot10^{-5}(\hbar c)^3/(\text{GeV})^2$ is the Fermi constant of the four-fermion interaction, we obtain for the quantity α_F: $\alpha_F = \frac{q_F^2}{\hbar c} \approx 4.9\cdot10^{-2}$, so that $\alpha_F/\alpha_s \approx 3.45\cdot10^{-2}$. Remind that $\alpha_e = 1/137 \approx 0.73\cdot10^{-2}$, so that $\alpha_e/\alpha_s \approx 5.2\cdot10^{-3}$ and $\alpha_F/\alpha_e = 6.7$. Unfortunately, very often in the literature, in the estimation of the dimensionless constant of weak nuclear interaction, the proton mass is used as the normalization mass which is almost 100 times smaller than the mass of the Z^0 vector boson. For this reason, the value of the constant α_F is underestimated by almost 4 orders of magnitude. The real value of this constant, in accordance with the above estimates, is only 35 times, not 5 orders of magnitude less than the dimensionless constant of the strong nuclear interaction.

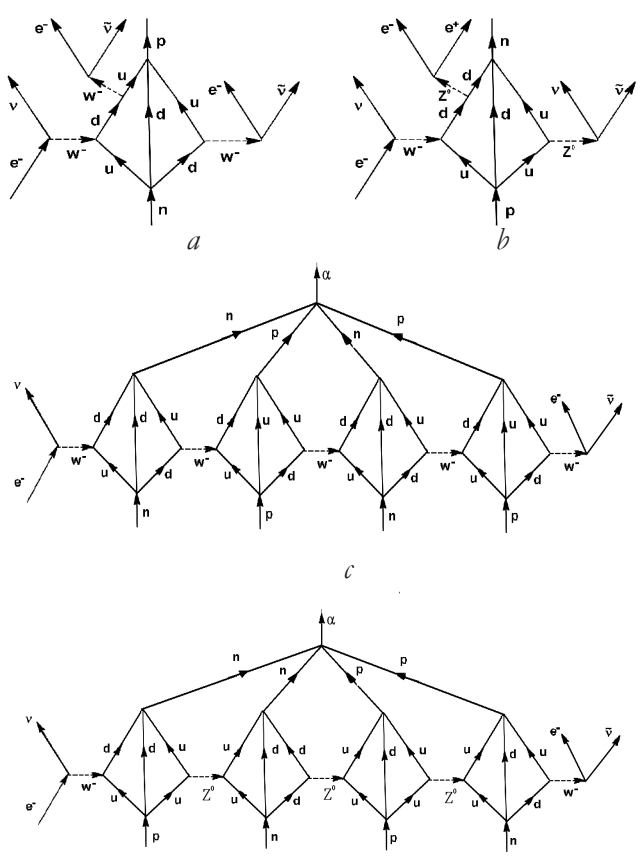

Fig. 2. *Feynman diagrams for the initiating β^--decay (a), β^+-decay (b) and the a-decay (c, d).*

In conclusion of this section, let us pay attention to some unexpectedness of the presented result about the possibility of external influences of electrons on the dynamics of the decay of a radioactive nucleus. It turns out that although the electrons can not interact with the nucleons of the nucleus as fragments of nuclear matter, they can initiate (through vector W^--bosons) local disturbances in the nucleon structure of the nucleus At the same time, as experience shows, the external excitation of the radioactive nucleus as an integral system (under the influence of γ-radiation, in particular) can not affect the rate of radioactive decay, and therefore, of the discussed phenomenon of initiating of the metastable state of the nucleus. In these cases, nuclear matter manifests itself as an integral system of interacting nucleons with inherent individual characteristics.

3. POSSIBLE MECHANISMS OF NUCLEAR-CHEMICAL REACTIONS

The simplest β-nuclei are the β-neutron and β-dineutron, which can be formed by the interaction of high-energy electrons with protons or deuterons, for example, by laser ablation of metals in ordinary or heavy water, and also under conditions of protius-containing or deuteron-containing glow discharge plasma, respectively, according to

$$p^+ + e^-_{be} \rightarrow {}^1n_{isu} + \nu, \quad (8)$$

$$d^+ + e^-_{be} \rightarrow {}^2n_{isu} + \nu. \quad (9)$$

If the half-lives $T_{1/2}$ of such β-nuclei are sufficiently long, the neutral nuclei ${}^1n_{isu}$ and ${}^2n_{isu}$, respectively, with baryon numbers equal to one and two, zero lepton charges and rest masses equal to the masses of the hydrogen atom and deuterium, can effectively participate in a variety of nuclear processes [13, 17-20].

It was shown earlier that the half-life $T_{1/2}$ of the β-dineutron:

$${}^2n_{isu} \rightarrow d^+ + e^- + \tilde{\nu} \quad (10)$$

with the formation of a deuteron, an electron, and an antineutrino, turns out to be sufficiently long, at least tens of minutes. This conclusion is based on an analysis of the experimental data on the synthesis of tritium nuclei t^+ upon the laser ablation of metals in heavy water [13]. It was assumed that the latter process occurs upon interaction between tritium nucleus t^+ and a ${}^2n_{isu}$ nucleus:

$$d^+ + {}^2n_{isu} \rightarrow t^+ + n + Q(3.25\ \text{MeV}), \quad (11)$$

where n is a neutron. At the same time, another process can take place alongside (12):

$$d^+ + {}^2n_{isu} \rightarrow {}^3_2He + n + e^- + \tilde{\nu} + Q(3.27MeV), \quad (12)$$

as a result of weak nuclear interaction.

In [13], the possibility of formation of a hypothetical β-trineutron ${}^3n_{isu}$ under the interaction of electrons with tritium nuclei t^+ was also postulated:

$$t^+ + e^-_{be} \rightarrow {}^3n_{isu} + \nu. \quad (13)$$

The rest mass of the introduced ${}^3n_{isu}$ neutral nucleus was assumed to be equal to the rest mass of the tritium atom. It is through the formation of the nucleus ${}^3n_{isu}$ that the process of initiation of decay of tritium nuclei under conditions of laser ablation of metals in aqueous media found in [13], along with the process of synthesis of tritium nuclei, can occur:

$$t^+ + e^-_{be} \rightarrow {}^3n_{isu} + \nu \rightarrow$$

$$\rightarrow {}^3_2He + 2e^- + \nu + 2\tilde{\nu} + Q(0.019MeV). \quad (14)$$

It should be noted here that according to [13], half-life $T_{1/2}$ of the decay of the ${}^3n_{isu}$ nucleus during e^--catalysis turns out to be of the same order of magnitude as the half-life of the ${}^2n_{isu}$ nucleus, which is many orders of magnitude shorter than that of the tritium nucleus ($T_{1/2}$ = 12.3 years).

As was shown in [18], the introduction of representations of sufficiently long-lived β-nuclei formed in a glow discharge in a deuterium-containing gaseous medium made it possible to understand the totality of the data [8, 9] for initiating the radioactive decay of W nuclei in the near-surface layers of a tungsten cathode (foil). Here it should be pointed out that although 5 isotopes of tungsten (${}^{180}_{74}W$, ${}^{182}_{74}W$, ${}^{183}_{74}W$, ${}^{184}_{74}W$ and ${}^{186}_{74}W$) are potentially α-radioactive nuclei:

$${}^A_{74}W \rightarrow {}^{A-4}_{72}Hf + {}^4_2He + Q_A, \quad (15)$$

they are usually considered as stable isotopes because of the anomalously large period of their half-life, $T_{1/2} = 10^{17}$-10^{19} years, which is many orders of magnitude greater than the existence time of Universe. The heat release value Q_A upon the radioactive α-decay of tungsten nuclei with mass numbers A, equal to 180, 182, 183, 184 and 186, is 2.52, 1.77, 1.68, 1.66 and 1.12 MeV, respectively. Based entirely on energy consideration, it was possible to anticipate α-decays with the formation of several α particles for the indicated stable isotopes of tungsten, including decay with the formation of nine α particles for the tungsten-180 isotope.

Within the framework of the developed ideas on the formation of nuclei in an unstable *isu* state, three mechanisms can be distinguished for initiating nuclear transformations, including radioactive decays of nuclei.

3.1. Mechanism of nuclear fusion

The fairly long-lived neutral particles (${}^An_{isu}$, A = 1, 2, 3) formed in the low-temperature plasma can diffuse along grain boundaries deep into a cathode and interact with the metal (tungsten) nuclei in its near-surface layers. Excited ${}^{A+2}_{74}W^*$ nuclei can thus appear at the initial stage upon interaction between ${}^2n_{isu}$ and ${}^A_{74}W$ isotopes and their fusion. In addition to the overall excitation energy (shows an asterisk) about of 10 MeV with respect to the main state of these nuclei, the nuclear matter of such nuclei may be partially (due to the fusion with ${}^2n_{isu}$) in an unbalanced *isu*-state with loss of stability in the nuclear bulk;

this leads to subsequent transformation with the emission of α particles and daughter isotopes. It should also be emphasized here that, in contrast to the nuclear reactions that occur upon the collision of reagents in the gaseous phase, the energy factor alone is sufficient for the considered nuclear transformations in the area of grain boundaries of a solid metal phase, due to the possible effects of the medium (without spin and parity matching conditions for the colliding and final nuclei).

When studying the processes occurring under conditions of a glow discharge in a deuterium-containing gas medium, the formation of new elements in the near-surface layer of a tungsten cathode after plasma treatment lasting 4 to 7 hours [8, 9], the formation not only the stable isotopes of erbium, ytterbium, lutetium and Hafnium, but also radioactive isotopes of ytterbium and hafnium, was detected. If the appearance of stable isotopes in this case could still be hypothetically associated with the diffusion of impurity elements from the cathode volume to the cathode surface processed in the plasma, the formation of radioactive isotopes unambiguously indicates the radioactive decay of tungsten isotopes. Since all the possible reactions of the initiated decay of different isotopes of tungsten are written out in [18], here we give for illustration a few examples:

$$^{180}_{74}W + {}^{2}n_{isu} \rightarrow$$

$$\rightarrow {}^{169}_{70}Yb + {}^{9}_{4}Be + {}^{4}_{2}He + 2e^{-} + 2\tilde{\nu} + Q\ (10.09\,\text{MeV}), \quad (16)$$

$$^{182}_{74}W + {}^{2}n_{isu} \rightarrow$$

$$\rightarrow {}^{171m}_{70}Yb + {}^{9}_{4}Be + {}^{4}_{2}He + 2e^{-} + 2\tilde{\nu} + Q\ (10.34\,\text{MeV}), \quad (17)$$

$$^{182}_{74}W + {}^{2}n_{isu} \rightarrow {}^{180m}_{72}Hf + {}^{4}_{2}He + Q\ (10.26\ \text{MeV}), \quad (18)$$

$$^{184}_{74}W + {}^{2}n_{isu} \rightarrow {}^{178}_{70}Yb + 2\,{}^{4}_{2}He + Q\ (12.28\ \text{MeV}). \quad (19)$$

Under considering the processes (16)-(19), it was taken into account that in the mass spectra of products, in addition to the major peaks with masses ranging from 169 to 180, the appearance and then the subsequent increase in the peak with mass 9 was recorded. We should also explain that the missing product with a basic mass of 4 corresponding to helium nuclei in the mass spectra obtained in [8, 9] was due to the extremely low solubility of helium in tungsten [30] and its high diffusion coefficient in the area of the foil's intergranular boundaries. It is obvious that in order for such processes to proceed, the lifetime of the ${}^{2}n_{isu}$ must be long enough for the diffusive permeation of these neutral nuclei into the near-surface areas of the foil along the grain boundaries. This agrees with the conclusion in [13] that the time must be no less than tens of minutes when synthesizing tritium under conditions of the laser ablation of metals in heavy water.

Obviously, the β-dineutron plays the same role in the realization of low-energy nuclear reactions, which previously was hypothetically assigned to a stable dineutron. And now the conclusions about the smallness of the possible contribution of the dineutron to the probability of the process $n + d \rightarrow {}^{2}n + p$ [5, 6] become clear, as well as the noticeable probability of the formation of the dineutron in the reaction ${}^{6}Li(\pi^{-}, p){}^{5}H$ initiated by the meson [14]. Indeed, in the interaction of the π^{-}-meson as a quark-antiquark pair with a nucleus, the quark structure of nucleons should manifest itself, and the possibility of forming a long-lived nucleus ${}^{2}n_{isu}$ opens up. Therefore, most likely, the maximum in the dependence shown in Fig. 1 in the region of the "missing mass" is determined precisely by the formation of a nucleus ${}^{2}n_{isu}$ whose mass is equal to the mass of the deuterium atom. The "missing mass" Δ (in MeV units) in this case, in accordance with the maximum position in Fig. 1, is $\Delta = (m_{n} - m_{p} - m_{e})c^{2} - \varepsilon_{d} \approx 3.01$ MeV, where m_{n}, m_{p} and m_{e} are the masses of the neutron, proton and electron, respectively, and ε_{d} is the deuteron binding energy. As for the nuclear reaction $n + d \rightarrow {}^{2}n + p$ involving nucleons, apparently, in this type of reaction the quark structure of the nucleons is not affected, so the probability of occurring the metastable nucleus ${}^{2}n_{isu}$ is extremely small. Therefore, estimates of the smallness of the contribution of the dineutron to this process, made in [5, 6], should be attributed to the possible contribution of the β-dineutron.

3.2. Mechanism of e⁻-catalysis

Another way of initiating the α-decay of tungsten isotopes under the conditions of glow discharge is

also possible (see above) during e⁻-catalysis, when electrons with kinetic energy E_e ~ 3-5 eV interact directly with stable isotopes of tungsten. Possible examples of such processes are given below:

$$^{183}_{74}W + e^- \rightarrow {}^{183}_{73}Ta_{isu} + \nu \rightarrow$$
$$\rightarrow {}^{175}_{71}Lu + 2\,{}^{4}_{2}He + 2e^- + 2\tilde{\nu} + \nu + Q(3.96MeV), \quad (20)$$

$$^{186}_{74}W + e^- \rightarrow {}^{186}_{73}Ta_{isu} + \nu \rightarrow$$
$$\rightarrow {}^{174}_{70}Lu + 3\,{}^{4}_{2}He + 3e^- + 3\tilde{\nu} + \nu + Q(7.17\text{MeV}). \quad (21)$$

It should be pointed out that, using the concepts of e⁻-catalysis, it can be understood that not all the new isotope products detected in the experiment are obtained. Therefore, processes involving the $^2n_{isu}$ nuclei are considered for the initiation of the W stable isotope decays as the basic ones.

The above data allow us to conclude that the nuclear decay of initially non-radioactive tungsten isotopes with the formation of lighter elements (erbium, lutetium, ytterbium, hafnium), initiated under the condition of low-temperature plasma (glow discharge), can be considered as a new type of initiated decay of nuclei that does not result from nuclear reactions, for example, with alpha particles or nucleons, but under the action of low-energy electrons. It should be remembered that stable isotopes of many nuclei, from neodymium to bismuth and including the tantalum-181 isotope in particular, for which initiated decay processes similar to the ones described were also observed in [8, 9], are potentially α-radioactive in the same sense as tungsten isotopes.

3.3. Harpoon mechanism

The extreme difficulties in understanding the mechanism of low-energy nuclear processes are the reactions between many-electron atoms. Such processes are usually considered in connection with the study of transformation processes in native systems [31-33]. However, it was recently shown [34] that reactions of this type can occur during the initiation of self-propagating high-temperature synthesis (SHS) processes [35]. The composition of condensed combustion products of thermite powder mixtures (Al + Fe_2O_3) in air was investigated in [34]. The purity of the starting materials was (99.7-99.9)% mass. It was shown that in the process of termite combustion (flame temperature exceeded 2800 K) calcium is formed and stabilized in an amount up to 0.55% mass. In the initial thermite powder systems (Al + Fe_2O_3), calcium was absent. According to [34], calcium could be formed in nuclear reactions

$$^{27}_{13}Al + {}^{14}_{7}N \rightarrow {}^{41}_{20}Ca + Q(21.8\text{MeV}), \quad (22)$$
$$^{27}_{13}Al + {}^{14}_{7}N \rightarrow {}^{40}_{20}Ca + n + Q(12.44\text{MeV}). \quad (23)$$

The phenomenon of calcium formation in experiments [34] may indicate that in the flame of iron-aluminum thermite combustion in air, the electron temperature can be much higher than the flame temperature, fixed by the energy of atoms and ions. It is the latter situation that is typical of a low-temperature glow discharge plasma. In this case, the interaction of high-energy electrons with nuclei $^{27}_{13}Al$ and $^{14}_{7}N$ could lead to the formation of nuclei $^{27}_{13}Mg_{isu}$ and $^{14}_{6}C_{isu}$, accordingly. The largest activity in nuclear interactions from these nuclei is inherent to the nucleus $^{27}_{13}Mg_{isu}$, since the deficit of its energy relative to the nucleus $^{27}_{13}Mg$ is $\Delta Q = -2.61$ MeV, whereas for the nucleus $^{14}_{6}C_{isu}$ the corresponding value is much less and equal to –0.16 MeV.

We will assume, following [20], that if the nucleus of an atom (or ion) is in a metastable, pre-decay *isu*-state (we assume that this is $^{27}_{13}Mg_{isu}$), then the lability of the electronic subsystem increases, and the probability of its partial overlap with electronic subsystems of the located near atom (in this case, the nitrogen atom), grows for this atom. It is obvious that large values of the energy releases of the gross processes (22) and (23) should act as an initiating factor to the manifestation of the spin-spin interaction of the electronic subsystems of both atoms and the formation of common "molecular" orbitals under the correcting action of spin electron-nuclear interactions for each of the atoms. The emerging bonds pull both atoms together, and the formation of common orbitals is more intense as the nuclei are brought closer together. As a result, a sort of "harpoon mechanism" is observed when a neighboring atom is captured by the atom with the nucleus in the *isu*-state. The complete integration of the electronic subsystems of both atoms initiates the fusion of the nuclear matter of

the nucleus in the isu-state (in our case ${}^{27}_{13}Mg_{isu}$) and the adjacent nucleus (in our case ${}^{14}_{7}N$). The corresponding brutto-process can be presented as:

$${}^{27}_{13}Al + {}^{14}_{7}N + e^-_{be} \rightarrow$$
$$\rightarrow {}^{41}_{20}Ca + e^- + \nu + \tilde{\nu} + Q(21.8\text{MeV}), \quad (22a)$$

$${}^{27}_{13}Al + {}^{14}_{7}N + e^-_{be} \rightarrow$$
$$\rightarrow {}^{40}_{20}Ca + n + e^- + \nu + \tilde{\nu} + Q(12.44\text{MeV}). \quad (23a)$$

Earlier, the harpoon mechanism was considered in connection with the processes of nuclear transmutations in native systems [20].

Because of the manifestation of weak nuclear interactions in the formation of the nuclear matter of the final nucleus as a set of interacting nucleons, a significant part of the energy release can also be realized by emitting neutrinos and antineutrinos if the final nucleus can be formed in the ground state by virtue of spin and parity conservation laws. Of course, in cases where the final nuclei are formed in an excited state, along with non-ionizing radiation of neutrinos and antineutrinos, X-rays or gamma quanta will be emitted. Under the experimental conditions [34], X-rays were detected.

Our phenomenological analysis shows that in order to understand the essence of the observed nuclear transformations during burning of thermite mixtures, it is actual to develop new theoretical approaches not to the calculation of the quantum mechanical probabilities of certain processes, but rather to modeling the dynamics of nuclear processes on the basis of quantum-chemical analysis. By this we mean calculations of the electronic structure of an atom upon the formation of nuclei in the *isu*-state with disturbed nucleon structure; calculations for modeling the spatial instability of the electronic subsystem of an atom that emerges due to the loss of nucleus stability; and calculations for the dynamics of the overlapping of such mobile orbitals with the electron orbitals of neighboring atoms and the formation of molecular orbitals that initiate the convergence and fusion of the respective nuclei. Kramer's activation mechanism in its discrete version (the random walk on the energy levels of the system to reach a set boundary) [36] generally used in physicochemical kinetics could be useful in analyzing the dynamics of nuclear radioactive decay. Here we mean the dynamics of the accumulation of energy by the nucleus in the unstable *isu*-state on the "last" bond, the disruption of which means the decay of the nucleus along a certain channel.

4. NUCLEAR CHEMICAL PROCESSES IN ANDREA ROSSI'S E-CAT REACTOR

Within the framework of the developed ideas on the mechanisms for initiating low-energy nuclear reactions, the results obtained in the testing of A. Rossi's energy E-Cat installations can also be understood [21]. Here we briefly discuss the test results of the E-Cat working element of the A. Rossi reactor, presented by a group of international experts [22]. The working element was a hollow ceramic tube 2 cm in diameter and 20 cm long, into which fuel was loaded – about 0.9 g of finely dispersed nickel (all stable isotopes were present, – ${}^{58}_{28}Ni$, ${}^{60}_{28}Ni$, ${}^{61}_{28}Ni$, ${}^{62}_{28}Ni$ and ${}^{64}_{28}Ni$, whose abundances were 67, 26.3, 1.9, 3.9 and 1 %, respectively), and 0.1 g of $LiAlH_4$ powder (${}^{6}_{3}Li$ and ${}^{7}_{3}Li$ isotopes, whose abundances were 8.6 and 91.4%, respectively). The tube was sealed and then heated. The tests were carried out for 32 days at element heating temperatures up to 1260°C (first half of the time) and 1400°C (second half of the time). The energy released during the tests was measured from the value of the heat flux emanating from the element. During the test, excess energy was 1.5 MWh, so the efficiency exceeded 3.5. Changes were recorded in the isotopic composition of the main components of the "fuel" – nickel and lithium, the initial abundances of the stable elements of which was close to the tabulated natural abundances. After the tests, the isotopic composition of the fixed elements has changed greatly: almost all of the nickel (more than 98%) was represented by the nickel-62 isotope (about 4% in the initial abundances), and the fraction of lithium-7 decreased to almost 8%, so that the fraction of the lithium- 6 practically increased

Table 1

The isotope abundances of the initial "fuel" and "ash" after the tests [22]

Ion	Fuel		Ash		Natural abundance [%]
	Counts in peak	Measured abundance [%]	Counts in peak	Measured abundance [%]	
$^{6}Li^{+}$	15804	8.6	569302	92.1	7.5
$^{7}Li^{+}$	168919	91.4	48687	7.9	92.5
$^{58}Ni^{+}$	93392	67	1128	0.8	68.1
$^{60}Ni^{+}$	36690	26.3	635	0.5	26.2
$^{61}Ni^{+}$	2606	1.9	~0	0	1.8
$^{62}Ni^{+}$	5379	3.9	133272	98.7	3.6
$^{64}Ni^{+}$	1331	1	~0	0	0.9

to 92%. Data on the isotope abundances of the initial "fuel" and "ash" after the tests are given in **Table 1** [22].

In accordance with the developed concepts, a fixed change in the isotopic composition of the base elements of the "fuel" – nickel and lithium in the presence of hydrogen liberated during the decomposition of $LiAlH_4$ at given temperatures may be due to the formation of protium-containing plasma in the reaction space and the formation of neutral metastable nuclei $^{1}n_{isu}$. We believe that the half-life of such nuclei, as well as of nuclei $^{2}n_{isu}$, is sufficiently large, so that such neutral nuclei, like neutrons, can interact with nuclei of elements of the elements that make up the fuel, determining the occurring changes in the elemental and isotopic composition of the fuel, which are accompanied by the corresponding energy release:

$$^{7}_{3}Li + {}^{1}n_{isu} \rightarrow 2\,^{4}_{2}He + e^{-} + \tilde{\nu} + \nu\tilde{\nu} + Q(17.35\text{MeV}) \quad (24)$$

$$^{27}_{13}Al + {}^{1}n_{isu} \rightarrow {}^{4}_{2}He + {}^{24}_{12}Mg + e^{-} + \tilde{\nu} + \nu\tilde{\nu} + Q(1.60\text{MeV}) \quad (25)$$

$$^{27}_{13}Al + {}^{1}n_{isu} \rightarrow {}^{28}_{14}Si + e^{-} + \tilde{\nu} + \nu\tilde{\nu} + Q(11.58\text{MeV}), \quad (26)$$

$$^{58}_{28}Ni + {}^{1}n_{isu} \rightarrow {}^{4}_{2}He + {}^{55}_{25}Mn + e^{+} + \nu + \nu\tilde{\nu} + Q(2.35\text{MeV}), \quad (27)$$

$$^{60}_{28}Ni + {}^{1}n_{isu} \rightarrow {}^{4}_{2}He + {}^{57}_{26}Fe + \nu\tilde{\nu} + Q(0.47\text{MeV}), \quad (28)$$

$$^{61}_{28}Ni + {}^{1}n_{isu} \rightarrow {}^{4}_{2}He + {}^{58}_{26}Fe + \nu\tilde{\nu} + Q(2.80\text{MeV}), \quad (29)$$

$$^{62}_{28}Ni + {}^{1}n_{isu} \rightarrow {}^{4}_{2}He + {}^{59}_{27}Co + e^{-} + \tilde{\nu} + \nu\tilde{\nu} + Q(0.34\text{MeV}), \quad (30)$$

$$^{64}_{28}Ni + {}^{1}n_{isu} \rightarrow {}^{65}_{29}Cu + e^{-} + \tilde{\nu} + \nu\tilde{\nu} + Q(7.45\text{MeV}). \quad (31)$$

As follows from this list of reactions, the largest specific (per unit mass of the component) energy release is associated with the nuclei of lithium-7. However, the total contribution to heat release during nuclear reactions $^{1}n_{isu}$ with all other fuel elements (aluminum and nickel isotopes) with a small mass fraction of the lithium-7 isotope in the system can be the main one. The fixed almost complete disappearance of isotopes $^{7}_{3}Li$ and $^{58}_{28}Ni$ in the ashes after monthly tests of the module indicates rather high rate constants of not only processes (24) and (27), but also of the other nuclear processes that take place with the formation of new chemical elements.

In order to understand the specific causes of the main fuel composition changes during the operation of the E-Cat unit, which consist in almost complete exhaustion of the lithium-7 isotope, and also in the overwhelming increase the nickel-62 isotope in the ash, it is necessary to indicate other nuclear reactions that also led to a change in the isotopic composition of the initial nickel. These reactions were accompanied by a significantly lower heat release than the above reactions, due to energy losses carried away by the neutrinos and antineutrinos formed:

$$^{58}_{28}Ni + {}^{1}n_{isu} \rightarrow {}^{59}_{28}Ni + \nu\tilde{\nu} + Q(8.22\text{MeV}),$$

$$T_{1/2}(^{59}_{28}Ni) = 7.6\times10^{4}\,\text{yr}, \quad (32)$$

$$^{60}_{28}Ni + {}^{1}n_{isu} \rightarrow {}^{61}_{28}Ni + \nu\tilde{\nu} + Q(7.04\text{MeV}), \quad (33)$$

$$^{61}_{28}Ni + {}^{1}n_{isu} \rightarrow {}^{62}_{28}Ni + \nu\tilde{\nu} + Q(9.81\text{MeV}), \quad (34)$$

$$^{62}_{28}Ni + {}^{1}n_{isu} \rightarrow {}^{63}_{28}Ni + \nu\tilde{\nu} + Q(6.05\text{MeV}),$$

$$T_{1/2}(^{63}_{28}Ni) = 100.1\text{yr}, \quad (35)$$

$$^{64}_{28}Ni + {}^{1}n_{isu} \rightarrow {}^{65}_{28}Ni + \nu\tilde{\nu} + Q(5.32\text{MeV}),$$

$$T_{1/2}(^{65}_{28}Ni) = 2.52\text{h}. \quad (36)$$

First of all, let us point out the large value of the half-life of the isotope $^{59}_{28}Ni$, which practically excludes the "charging" of other decaying isotopes of nickel during the tests due to the isotope $^{58}_{28}Ni$, whose fraction is 2 times that of the other isotopes of nickel. For this reason, the almost complete absence of the isotope $^{60}_{28}Ni$ in the sol should be associated with the process (33) only, because of the relatively low energy release in the process (28). It can also be assumed that the processes (29) and (34) cause the disappearance of the isotope $^{61}_{28}Ni$ in the ash, but the process (34) with high energy release thus feeds the ash with an isotope $^{62}_{28}Ni$, causing the the prevailing abundance of this

isotope among the other isotopes of nickel in the ash. The last factor is the "small" rate constant for the disappearance of the isotope $^{62}_{28}Ni$ due to reaction (30) of cobalt formation with small energy release in this process. It is also important to point out that the long half-life of the isotope $^{63}_{28}Ni$ practically excludes the completion of the ash with an isotope $^{64}_{28}Ni$ and process (31) with high energy release provides a practically complete transition of this isotope in the initial nickel to the copper-65 isotope.

Of course, here only qualitative arguments are given in favor of the fixed ash composition after the test. The comparative study of the elemental and isotopic composition of the initial fuel and ash by using mass spectrometry with inductively coupled plasma technique [37], previously effectively used in the investigation of the isotopic composition of impurities in nickel upon laser ablation of a nickel sample in an aqueous medium, could become more relevant. Here, it is important to study the changes in the isotopic ratios for different elements in the initial fuel and in the ash, primarily for the base element of nickel, as well as the elements formed in accordance with the processes (24)-(31)first of all, silicon-28 and copper-65.

5. CONCLUDING REMARKS

It is known that the results of [1] were not accepted by many physicists, not only because of difficulties in understanding the mechanism of formation of neutrons and tritium in the electrolysis of heavy water D_2O with Pd-cathode, but also because of the irreproducibility of the results [1] in various laboratories. In what can the reason, undoubtedly objective, be so irreproducible? It seems to the author that the main difficulty in reproducing the results of [1] is to create conditions under which electrons injected from the surface of the Pd-cathode participating in nuclear chemical processes must reach high (by chemical scales) kinetic energies $E_e \sim$ 3-5 eV. It can be assumed [16, 38] that under the conditions of reproducible experiments [7-13], these energies are achieved due to the presence of the spike-like random irregularities of the surface nanorelief on the metal surface that change sharply in height "roughness". The such nanoheterogeneity of the metal surface, namely, the cathode in a glow discharge in a deuterium-containing gas medium of ions and molecules, and the surface of a metallic sample during laser ablation in aqueous media [10-13] is the result of impacts of plasma ions and molecules on the surface of metallic samples.

In the latter cases, the roughness of the metal surface is sufficient to initiate nuclear transformations even in the absence of cathodic displacement. At cathodic displacement, the efficiency of nuclear chemical processes increases by orders of magnitude, as was shown in [13]. We indicate factors that cause an increase in the flux of electron emission from the surface of metals and an increase in the kinetic energy of electrons emerging from the metal in the vicinity of the spike-like random irregularities on the metal surface. First of all, increased values of mechanical tensile stresses are realized in these regions, which leads to a decrease in the work function of the electron from the metal (the Zhurkov effect [39]) and causes an increase in the flux of electrons from metals. In addition to this, electric fields of the highest intensity, which not only lower the energy barrier for the injection of electrons from the metal (the Frenkel effect [40]), but also cause the acceleration of the emitted electrons, are localized in the vicinity of the most abrupt changes in the surface profile – in the vicinity of the spike-like random irregularities. Here we also point to the paper [26], in which a decrease in the effective work function of electrons from the surface of tungsten cathodes was observed for thermionic emission initiated by laser radiation of pico- and femtosecond durations.

The conclusions about the interrelation between the efficiency of nuclear transformations observed in [10-13] and the features of the metal surface structure in the nanometer range are directly confirmed by the results of [38]. In this work, the method of atomic force microscopy was used to analyze the surface relief of metals formed under different regimes of laser ablation in an aqueous medium. It has been shown that

nuclear transformations occur only under intensive impacts of plasma ions and molecules on the surface, when the "roughness" greatly increases and the texture "spikiness factor" as one of the key 3*D* parameters of the surface relief in the nanometer range [42, 43] determining the measure of the most abrupt changes of the surface profile becomes significant.

If under the conditions of laser ablation of metals in aqueous media and in a glow discharge, the level of nanoheterogeneity of the surface necessary for the injection of high-energy electrons into the medium is maintained by the impact of ion and atom fluxes on metal surfaces, under conditions of electrolysis of heavy water with a Pd cathode there is no such factor. Probably, when carrying out appropriate studies of the surface relief and the structure of fractured near-surface layers of Pd-cathodes under conditions of D_2O electrolysis, it will be possible to find the regimes of the electrolysis process when the reproducibility of appearance of the neutrons and tritium nuclei in this process is reached.

REFERENCES

1. Fleishmann M, Pons S, Hawkins M. Electrochemically induced nuclear fusion of deuterium. *J. Electroanal. Chem*., 1989, 261:301-308.
2. Timashev SF. On possible mechanism of nuclear-chemical transformation in Pd electrode under electrolysis in heavy water. *Journal of Physical Chemistry*, 1989, 63(8):2283-2284 (in Russ.).
3. Sakisaka M, Tomita M. Experiments on the possible existence of a bound di-neutron. *J. Phys. Soc. Japan*, 1961, 16:2597-2598.
4. Katase A, Seki M, Akiyoshi, Yoshimura A, Sonoda M. Experiments on the existence of di-neutrons. *J. Phys. Soc. Japan*, 1962, 17:1211-1212.
5. Gol'danskii VI, Zel'dovich YaB, Baz' AI. Systematics of the lightest nuclei. *Phys.Usp. Advances in Physical Sciences*, 1965, 8(2):177-201.
6. Borzakov SB, Panteleev TS, Strelkov AV, Soldner T. The Search for the Dineutron at the High Flux Reactor ILL (Grenoble, France). *ISINN-10, JINR, 2003*.
7. Savvatimova I. Transmutation of elements in low-energy glow discharge and the associated-processes. *Condensed Matter Nucl. Sci.*, 2011, 8:1-19.
8. Savvatimova I. Creation of more light elements in tungsten irradiated by low-energy deuterium ions. *Proc. 13th Int. Conf. ICCF13, Sochy, Russia*, 2007:505-517.
9. Savvatimova I, Savvatimov G, Kornilova A. Decay in tungsten irradiated by low energy deuterium ions. *Proc. 13th Int. Conf. ICCF13, Sochy, Russia*, 2007:295-308.
10. Shafeev GA, Bozon-Verduraz F, Robert M. Experimental evidence of transmutation of Hg into Au under laser exposure of Hg nanodrops in D_2O. *Physics of Wave Phenomena,* 2007, 15(3):131-136.
11. Simakin AV, Shafeev GA. Initiation of nuclear reactions under laser irradiation of metal nanoparticles in the presence of thorium aqua ions. *Physics of Wave Phenomena*, 2008, 16(4):268-274.
12. Barmina EV, Sukhov IA, Lepekhin NM, Priseko YuS, Filippov VG, Simakin AV, Shafeev GA. Application of copper vapor lasers in control of activity of Uranium isotopes. *Quantum Electronics*, 2013, 43:591-596.
13. Barmina EV, Timashev SF, Shafeev GA. Laser-induced synthesis and decay of Tritium under exposure of solid targets in heavy water. *Journal of Physics: Conference Series,* 2016, 688:012106. (8th Intern. Conf. on Inertial Fusion Sciences and Applications (IFSA 2013) IOP Publishing; /http://arxiv.org/abs/1306.0830[physics.gen-ph]).
14. Seth KK, Parker B. Evidence for dineutrons in extremely neutron-rich nuclei. *Phys. Rev. Lett.*, 1991, 66(19):2448-2451.
15. Akhiezer AI, Rekalo MP. *Elementarnye chastitsy* [Elementary particles]. Moscow, Nauka Publ., 1986, 256 p.
16. Timashev SF. Physical vacuum as a system manifesting itself on various scales – from nuclear physics to cosmology; http://arxiv.org/abs/1107.1799v7.

17. Timashev SF, Simakin AV, Shafeev GA. Nuclear–Chemical processes under the conditions of laser ablation of metals in aqueous media (Problems of "cold fusion"). *Russian Journal of Physical Chemistry A.*, 2014, 88(11):1980-1988).
18. Timashev SF. Radioactive decay as a forced nuclear chemical process: phenomenology. *Russian Journal of Physical Chemistry A.*, 2015, 89(11):2072-2083.
19. Timashev Serge. Nuclear-chemical processes in the solar atmosphere. *International Journal of Astrophysics and Space Science*, 2014, 2(6):88-92.
20. Timashev SF. Initiating nuclear-chemical transformations in native systems: phenomenology. *Russian Journal of Physical Chemistry A,* 2016, 90(10):2089-2095.
21. United State Patent – *US 9,115,913 B1*, Aug. 25. 2015; https://animpossibleinvention.files.wordpress.com/2015/08/us9115913b1.pdf; Andrea Rossi.
22. Levi G, Foschi E, Höistad B, et al. Observation of Abundant Heat Production from a Reactor Device and of Isotopic Changes in the Fuel. http://amsacta.unibo.it/4084/1/LuganoReportSubmit.pdf.
23. Jung M, Bosch F, Beckert K, et al. First observation of bound-state decay. *Phys. Rev. Lett.*, 1992, 69:2164-2167.
24. Bosch F, Faestermann T, Friese J, et al. Observation of bound-state β^--decay of fully ionized ^{187}Re: ^{187}Re–^{187}Os cosmochronometry. *Phys. Rev. Lett.,* 1996, 77:5190-5193.
25. Thomas SA, Abdalla FD, Lahav O. Upper Bound of 0.28 eV on Neutrino Masses from the Largest Photometric Redshift Survey. *Phys. Rev. Lett.*, 2010, 105(3):031301.
26. Lattimer JM, Pethick CJ, Prakash M, Haensel P. Direct URCA process in neutron stars. *Phys. Rev. Lett.*, 1991, 66:2701-2704.
27. Timashev Serge F. The Planck numbers and the essence of gravity: phenomenology. http://arxiv.org/abs/1701.08073 [physics.gen-ph].
28. Vysotskii VI, Kornilova AA. Microbial transmutation of Cs-137 and LENR in growing biological systems. *Curr. Sci.*, 2015, 108:636-640.
29. Donnelly TW, Formaggio JA, Holstein BR, Milner RG, Surrow B. *Foundations of Nuclear and Particle Physics.* Cambridge, University Press, 2017, 745 p.
30. Sharapov VM, Kanashenko SL. *Vopr. At. Nauki Tekh., Ser. Termoyad. Sintez.* 2008, 2:20 (in Russ.).
31. Kervran CL. *Biological Transmutation.* Happiness Press, USA, Magalia, California,1998.
32. Biberian J-P. Review Article Biological Transmutations: Historical Perspective. *J. Condensed Matter Nucl. Sci.*, 2012, 7:11-25.
33. Vysotskii VI, Kornilova AA. *Nuclear Transmutation of Stable And Radioactive Isotopes In Biological Systems.* Pentagon Press, New Delhi, 2010.
34. Gromov AA, Gromov AM, Popenko EM, et al. Formation of calcium in the products of iron–aluminum thermite combustion in air. *Russian Journal of Physical Chemistry A*, 2016, 90(10):2104-2106.
35. Borisov AA, De Luca LT, Merzhanov AG. *Self-Propagating High-Temperature Synthesis of Materials.* CRC Press, Taylor and Francis, 2000, 400 p.
36. Tunitskii NN, Kaminskii VA, Timashev SF. *Metody fisikokhimicheskoy kinetiki* [Methods of Physicochemical Kinetics]. Moscow, Khimiya Publ., 1972, 198 p.
37. Revel'skiy IA, Buryak AK, Sajti PL, et al. Isotopic ratio changes of several trace elements in nickel as a result of laser ablation in aqueous medium, *in press*.
38. Serkov AA, Akovantseva AA, Barmina EV. Influence of the Surface Structure on the Initiation of Nuclear Chemical Processes Under Laser Ablation of Metals in Aqueous Media. *Russian Journal of Physical Chemistry A,* 2014, 88(11):1989-1995.
39. Timashev SF. On the thermofluctuation nature of the strength of solids. *Reports of the USSR Academy Science*, 1984, 276:898-902 (in Russ.).
40. Bonch-Bruevich VL, Kalashnikov SG. *Fizika poluprovodnikov* [Physics of Semiconductors]. Moscow, Nauka Publ., 1990, 678 p.
41. Barmina EV, Fotakis C, Stratakis E, Stolyarov VN, Stolyarov IN, Shafeev GA, Serkov AA.

Nano-textured W shows improvement of thermionic emission properties. *Appl. Phys. A*, 2012:1-4.

42. Timashev SF, Polyakov YuS, Lakeev SG, Misurkin PI, Danilov AI. Fundamentals of fluctuation metrology. Russian *Journal Physical Chemistry A.,* 2010, 84(10):1807-1825.
43. Mirsaidov U, Timashev SF, Polyakov YuS, Misurkin PI, Polyakov SV, Musaev I. Analytical method for parameterizing the random profile components of nanosurfaces imaged by atomic force microscopy. *Analyst*, 2011, 136(3):570-576; http://arxiv.org/abs/1010.6232.

SYNTHESIS AND TRANSMUTATION OF STABLE AND RADIOACTIVE ISOTOPES IN BIOLOGICAL SYSTEMS

Alla A. Kornilova

Lomonosov Moscow State University, http://www.msu.ru
1/2, Leninskie gory, Moscow 119991, Russian Federation
prfnart@mail.ru

Vladimir I. Vysotskii

Shevchenko Kiev National University, http://www.univ.kiev.ua
64/13, str. Vladimirskaya, Kyiv 01601, Ukraine
vivysotskii@gmail.com

Abstract. **The work considers the background, theoretical assumptions and results of experiments on nuclear transmutation of stable and radioactive isotopes in growing biological objects. It is shown that such fundamental transformations are based on nuclear-physical processes, the course of which is stimulated by the catalytic influence of non-stationary spatial inhomogeneities in the volume of growing living objects. This process can be used both for the accelerated utilization of stable and radioactive nuclei, and for the production of rare isotopes. The conditions for optimizing the deactivation process are investigated. It was found that in the most optimal case the rate of activity decrease in aqueous solutions of radionuclides is accelerated by 35...200 times in relation to the natural decay. The physical and biological reasons of these processes are considered.**

Keywords: **isotopes, microbiological systems, low energy nuclear reactions, deactivation of radionuclides**

PACS: 25.60.Pj; 25.70.−z; 28.41.Kw; 28.52.−s; 28.60.+s; 82.90.+j; 87.17.−d; 87.17.Ee; 87.80.−y; 89.60.−k

Bibliography – 23 references *Received 13.06.2017*

RENSIT, 2017, 9(1):52-64 **DOI: 10.17725/rensit.2017.09.052**

Contents

1. INTRODUCTION

The hypothesis of the possibility of nuclear transmutation of chemical elements and their isotopes in biological systems is one of the most mysterious in the history of science, it has often been discussed in recent decades and has its own history and mythology, its own supporters and critics. This problem arose in the "pre-nuclear period" and the initial stages of its emergence are closely connected with alchemy. A brief background of this phenomenon is presented in [1, 2].

Among the many predecessors, a series of works by L. Kervran [3-6] occupies a special place in the chronology of studies on the transmutation of chemical elements and isotopes in biological objects. In fact, he was the first scientist of the "nuclear age," who conducted a systematic study of the processes of transmutation of

chemical elements in biological objects. In particular, Kervran investigated the potassium transmutation reaction in calcium $^{39}K + {}^{1}p \rightarrow {}^{40}Ca$ in a biological system containing hydrogen. He also investigated many other reactions of isotope transmutation, among which one should especially note those that lead to the formation of vital micro- and macroelements Ca, K, Mg, P. Many of the experiments of Kervran are very convincing if we consider them without analysis at the micro level.

At the same time, Kernran's scientific views were far enough from the requirements of nuclear physics. For example, it allowed the reversibility of the nuclear reaction $^{39}K + {}^{1}p \leftrightarrow {}^{40}Ca$ and the possibility of the reactions of the Cl – O → F, P – Li → Mg, Ca – O → Mg, Fe – H → Mn decay, which are incompatible with energy conservation laws, since for their realization requires a giant energy $Q \approx 5...20$ MeV, whose sources are absent in the biological environment! Kervran in his works treated such processes as a specific "biological transmutation," claiming that this is a very special process stimulated by an unknown enzyme. Such an interpretation (linking incomprehensible processes with yet another unknown enzyme) is quite common in biology, but it does little to understand and use these processes.

In our opinion, there is no reason to consider the process of isotope conversion in growing biological systems as a "biological transmutation" and separate it from the general physical concept of transmutation as a process of isotope conversion completely "controlled" by the laws of physics and stimulated by certain structural features of the biological system. Unfortunately, Kervran did not carry out in any of his experimental studies an analysis of the ratio of isotopes in the initial and final states. This is the basic error of Kervran's experiments, because nuclear physics is the science of isotopic (non-elemental!) transmutations – in other words, "nuclear physics is the chemistry of isotopes"!

2. BIOLOGICAL ASPECTS OF THE PROCESS OF TRANSMUTATION OF ELEMENTS

Specific biophysical aspects of the process of transmutation of isotopes in biological systems have been considered in detail in monographs [7, 8]. It is possible to note only some of them. Experiments to study the transmutation of isotopes in growing biological systems should be conducted taking into account the specific of the problem and the following requirements:

- The synthesized isotope must be included in the number of micro- and macroelements vital to the biosystem of or their biochemical analogs, and the medium in which growth occurs should not contain these elements, but must contain those isotopes from which these elements can be formed without irreversible additional energy generation.
- In order for experiments to be conducted in a short time, the growth rate of the biological object under study must be large, and the isotope formed must be adapted to this object and must accumulate in an amount sufficient for reliable registration.
- The living object must be sufficiently resistant to the action of the products of vital activity in order to avoid the phenomenon of self-intoxication.
- When working with radioactive isotopes, the living object must be sufficiently resistant to the action of strong radiation fields formed by the utilized isotopes.
- It is desirable (and for stable isotopes – mandatory) the possibility of analyzing the isotope composition of a biological object before and after the transmutation process.
- The requirements related to the environment and to the problems of humanism (we are talking about living objects) must be met.

The best objects for such experiments are microbiological cultures, the characteristics

of which meet the above requirements to the maximum extent. As a rule, "pure" microbiological cultures can effectively grow only under certain environmental conditions (acidity, temperature, the presence of toxins, radiation background, etc.), and if these conditions are violated, growth is sharply inhibited or becomes impossible. The typical dose that conventional microbiological cultures can withstand corresponds to a level of about 30 KRad, and the pH parameter is not lower than 3.

Synrotrophic microbiological associations, including sets of different strains that are in a symbiotic state, are more effective. These microorganisms are not in the form of a simple mechanical mixture. They coexist in a synrotrophic association in such a state of joint symbiosis, when, in fact, they form a single macroorganism (although with separate systems of internal metabolism). In its scope, every member and every physiological group of the community is maximally adapted to the joint life activity and is in a state of collective mutual assistance and mutual protection. This system has a high degree of adaptation to various variations and "aggressive" manifestations of the external environment.

Obviously, such a system proves to be maximally adapted to changing aggressive conditions, which corresponds to their growth, including under the conditions of radiation. The effectiveness of this "collective defense" is extremely high. For example, in an acidic medium with pH = 2 (sufficiently concentrated hydrochloric acid) no "pure" strains can growth. At the same time, the synrotrophic association grows fine in such an environment after a certain transitional period. The same applies to large doses of radiation. Approximately, we can assume that the time interval of adaptation corresponds to a change of 5-10 generations, which allows us to estimate this interval from 10 hours to several days.

3. EXPERIMENTS ON SYNTHESIS OF STABLE ISOTOPES IN MICROBIOLOGICAL SYSTEMS

We began studying the nuclear processes in biological systems in the early 90s. The basis of the proposed experiments was the principle of "looking for what was lost under the street lamp" – which corresponds to the rule: if you have lost something in the dark, then you should look under the street lamp, because in other (dark) places you will not find anything! This principle gave priority to a reliable method of recording products of potential nuclear reactions, supplemented by the possibility of accumulating of these products. Based on our understanding of these processes, we investigated the reality of transmutation of stable isotopes based on the basic reaction $^{55}Mn + d = {}^{57}Fe$ (see patent [9] and articles [10-11]), leading to the formation of a rare Mössbauer iron isotope ^{57}Fe in a medium based on heavy water, where along with the microorganisms and macronutrients necessary for the growth of microbial cultures, there was a manganese salt, but completely (or with a minimal admixture), there was no iron. The advantage of this reaction is that the final product can be identified by both "standard" and Mössbauer mass spectrometers. The nutrient composition is shown in **Table 1**.

Initial experiments were carried out on the basis of pure microbiological cultures of *E. coli* and *Saccharomyces cerevisiae T-8*. This reaction was successfully realized and identified with the help

Table 1.
Nutrient medium for transmuting manganese into iron.

Components	Concentration in medium (%)	Relative admixture of iron (no more), %	Absolute admixture of iron (no more), g
Sucrose	3	10^{-4}	$3\cdot10^{-7}$
$(NH_4)_2$tartrate	1	$5\cdot10^{-4}$	$5\cdot10^{-7}$
$MgSO_4\cdot7H_2O$	0.25	$2\cdot10^{-4}$	$5\cdot10^{-8}$
$CaHPO_4\cdot7H_2O$	0.008	$1.5\cdot10^{-3}$	$1.2\cdot10^{-8}$
K_3PO_4	0.5	$5\cdot10^{-4}$	$2.5\cdot10^{-7}$
$MnSO_4\cdot7H_2O$	0.01	$5\cdot10^{-4}$	$5\cdot10^{-9}$
D_2O (experiment) H_2O (control)	100·(10ml)	10^{-7}	10^{-8}

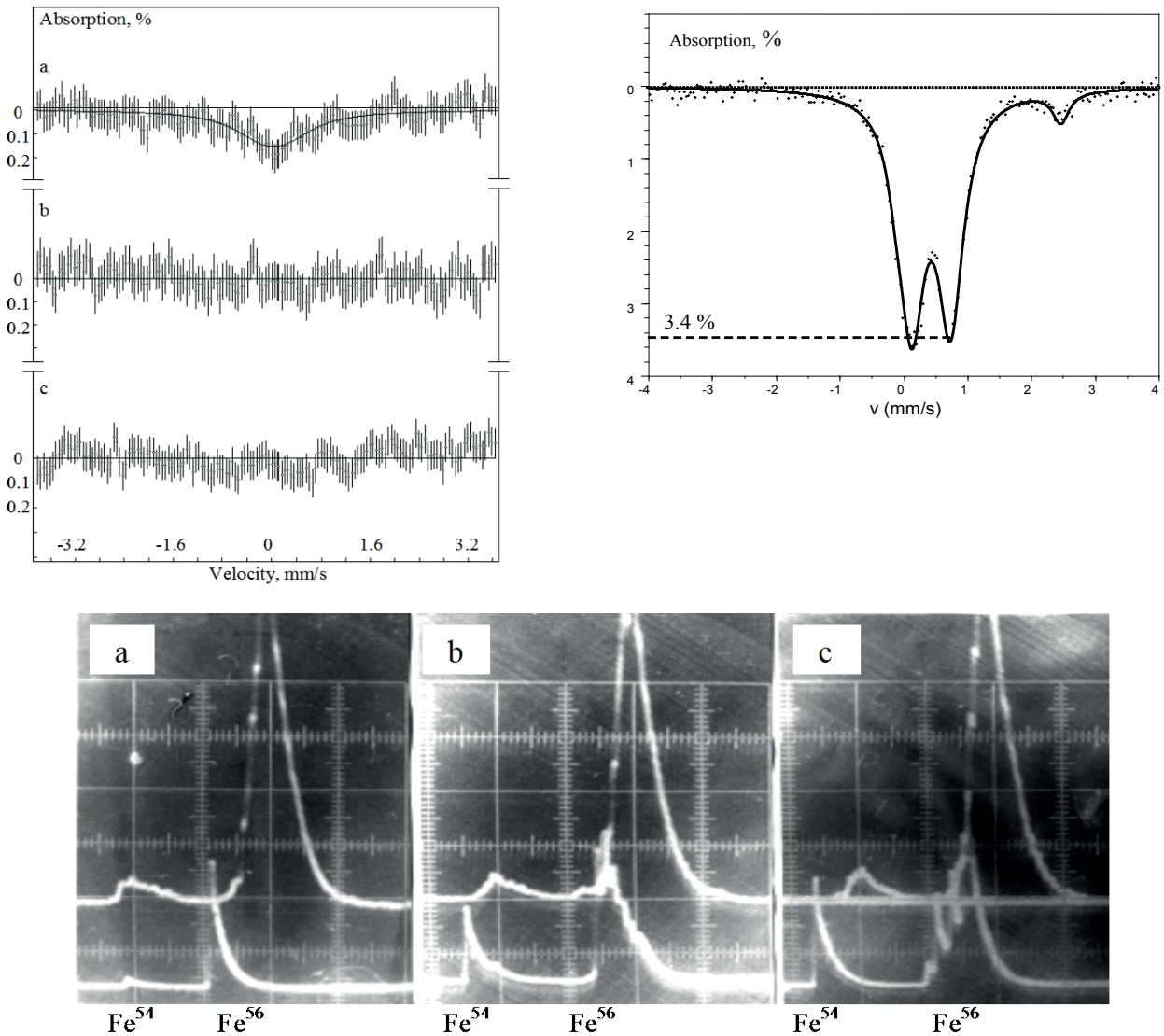

Fig. 1. *The upper left is the Mössbauer spectrum of the dried microbiological culture of Saccharomyces cerevisiae T-8, grown in a liquid nutrient medium on the basis of: a) heavy water D_2O in the presence of the ^{55}Mn isotope; b) light water H_2O in the presence of ^{55}Mn; c) heavy water D_2O in the absence of the ^{55}Mn isotope. At the top right – Mössbauer spectrum of MCT granules grown in a nutrient medium on the basis of heavy water D_2O in the presence of the ^{55}Mn isotope and the absence of iron (or its minimum amount as an impurity). Below – a fragment of the mass spectrum of the same culture, grown in a nutrient medium based on H_2O in the presence of ^{23}Na and ^{31}P (b), (c) and the absence of ^{31}P (a). The upper graphs on each of the photos below correspond to the control spectrum of the natural iron masses obtained in the same series as the corresponding lower graphs.*

of Mössbauer and time-of-flight spectrometers (**Fig. 1**).

The typical duration of these experiments was 2...3 days, after which growth was stopped due to a change in acidity and self-intoxication of cultures by metabolic products.

The experimental efficiency of these reactions corresponded to the value $\lambda = \Delta N(^{57}Fe)/N(^{55}Mn)\Delta t \approx 10^{-8}$ of the synthesized ^{57}Fe nuclei per one ^{55}Mn nucleus per second.

Further, another $^{23}Na + {}^{31}P = {}^{54}Fe$ reaction was realized and investigated, with the formation of another rare iron isotope ^{54}Fe. In transmutation experiments, K_2HPO_4 salt was present, and in control experiments it was absent. Corresponding results of mass-spectrometric analysis are presented in Fig. 1. The efficiency of this reaction was approximately the same as in the case of the synthesis of the ^{57}Fe isotope.

These experiments were further optimized by using microbial syntrophic associations of MCT ("microbial catalyst-transmutator"). The basis of MCT granules is the synthrophic association (superassociation) of many thousands of

different types of microorganisms belonging to different physiological groups that represent different groups of microbial metabolism and are characterized by different mechanisms of microbial accumulation.

On the same Fig. 1, the Mössbauer spectrum of the dried MCT granules is presented. These granules grew for 30-50 days in a medium similar to the above discussed case of pure cultures. It is seen that the efficiency of transmutation in such a system is much higher.

Estimations made on the basis of analysis of these samples show that in the case of using of synrotrophic associations, the transmutation efficiency reaches a value $\lambda = \Delta N(^{57}Fe)/N(^{55}Mn)\Delta t \approx 10^{-6}$ (synthesized ^{57}Fe nuclei per one ^{55}Mn nucleus per second).

Subsequent experiments were aimed at studying the possibility of transmutation not only of light and medium-weight isotopes, but also of heavy nuclei. The reaction of transmutation of a stable isotope of cesium into the barium isotope $^{133}Cs + p = {}^{134}Ba$ was chosen as the object of research [12]. The expediency of such studies was due to the subsequent possibility of transmutation and deactivation of the ^{137}Cs radioactive isotope.

During the research, different types of synthrophic associations were used, adapted to aerobic or anaerobic conditions. The light-water nutrient medium contained glucose, dissolved base salts of the main macro- and microelements (including NH_4NO_3, $CaSO_4$, $MgSO_4$), as well as stable cesium as the Cs_2CO_3 salt, but did not contain the potassium vital for the growth of the crops included in these associations. Barium is a biochemical analogue of potassium and in its absence it can be used for the growth of microbiological cultures.

In the process of growth, samples were taken from the experimental cuvettes periodically, which were used to study the dynamics of the transmutation process. The results of these studies are shown in **Fig. 2**.

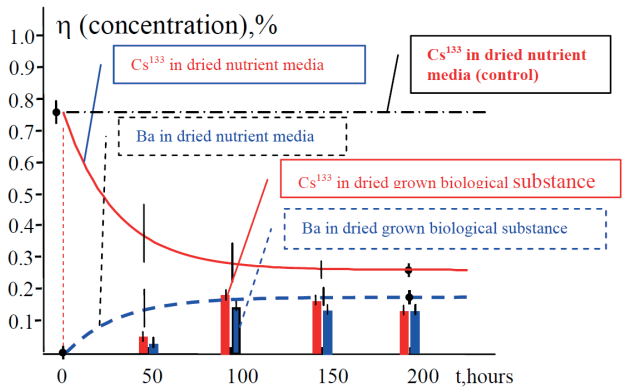

Fig. 2. *The time dependence of the transmutation of a stable ^{133}Cs isotope into an ^{134}Ba isotope in a growing syntrophic association and in a nutrient medium.*

From the obtained data it follows that the average efficiency of the transmutation reached the value $\lambda = N(^{134}Ba)/N(^{133}Cs)\Delta t \approx 10^{-6}$ synthesized nuclei of ^{134}Ba per core of ^{133}Cs per second.

The total amount of the ^{133}Cs isotope decreased from $M_{133Cs} \approx 13$ mg/cell to $M_{133Cs} \approx 6.5$ mg/cell for 192 hours.

4. EXPERIMENTS ON TRANSMUTATION AND DETECTION OF RADIOACTIVE ISOTOPES IN MICROBIOLOGICAL SYSTEMS

Currently, the task of safe storage, utilization and deactivation of radioactive waste from nuclear power plants is one of the main factors of the entire nuclear power industry. The urgency of this problem follows from simple digits.

The world currently has about 400 thousand tons of spent fuel elements (TVELs), more than 1 million tons of medium-level waste, the same amount of highly active water and more than 10 million tons of wastes of low activity. For example, in the territory of Hanford nuclear storage in the United States, there are 177 burial tanks (radwaste storage tanks) for liquid high-level waste with a total volume of 204000 m³. According to estimates conducted in 2013, about 2% of these liquid wastes have already been released into the environment due to uncontrolled leaks from burial grounds.

Each year, these values increased by 5-7%, and after the accident at the NPP in Fokushima,

"reserves" of highly active water increase even faster.

By and large, the problem of utilization of radioactive waste has not yet been solved by anyone, and for spent fuel elements, there is no alternative for their storage for an indefinitely long period of storage after primary processing.

All the newest programs to create systems for utilization based on methods of "burning out" spent fuel with intensive neutron fluxes are extremely costly (each of several tens of billions of dollars) [13-17]. The analysis shows that a large number of new radionuclides will be formed in this case. This problem is well known in the problem of controlled thermonuclear fusion as a "first wall problem".

There is another direction of research related to the possibility of nuclear transformations under normal (not extreme) conditions in a substance, for example, at room temperature. In the 90s of the 20th century this trend was called "cold nuclear fusion". At present, the term LENR ("nuclear reactions at low energy") is more used and closer to the essence of the processes. It is necessary to note the extremely ambiguous attitude of scientists towards such processes.

Most "classical" specialists in nuclear physics believe that the probability of nuclear transformations, if considered by the method of direct approximation of the physics of high-energy two-particle nuclear reactions to low energies, is very small, and such effects can not be a priori meaningful.

There is another point of view. It is actively developing recently and is based on a number of fundamental provisions of quantum mechanics. Its essence lies in the fact that direct approximation is not legal, since many nuclear physics processes at low energy are collective (not pairwise), are subject to the influence of the environment and can proceed with a fairly high probability, which makes them quite suitable for practical use. These results, in particular, directly follow from the specific behavior of the particle in a non-stationary potential well (in particular, in a nonstationary oscillator).

In recent years it has been shown [18-20] that one of the effective methods for a very significant increase in the transparency of a potential barrier at low particle energies is associated with the use of coherent correlated states (CCS) of particles interacting with the atoms (nuclei) forming this barrier. The most characteristic property of CCS is the possibility of forming controlled giant energy fluctuations of a particle whose amplitude can be thousands and millions times greater than the average (thermal) energy of a particle and reach values $\delta E \approx$ 10-50 keV. In a concentrated form, this is reflected in the modified uncertainty relations, called the Schrödinger-Robertson $\delta p \delta q \geq \hbar / 2\sqrt{1-r_{pq}^2}$, $\delta E \delta t \geq /2\sqrt{1-r_{Et}^2}$, uncertainty relations, in which the product of the fluctuations of the corresponding dynamic variables (coordinate, momentum, energy, time, ...) is determined by the corresponding correlation coefficients, the magnitude of which is limited by the interval $0 \leq r_{pq}^2 \leq 1$, $0 \leq r_{Et}^2 \leq 1$,... [18-20].

In a stationary state in any system $r_{pq}^2, r_{Et}^2 \ll 1$, these relations take the form of well-known Heisenberg uncertainty relations. Another situation in dynamic systems (including living objects). It is well known that the growth front of any biological object is never ideally homogeneous - local heterogeneities are always formed (in fact, these are potential nano-wells), which are leveled and eliminated during the growth process. Each of these nano-wells is a nonstationary oscillator for particles that are localized in it. In the process of dynamically changing of the parameters of these wells, CCS can be formed for these particles with a large value of the correlation coefficient $r_{pq}^2, r_{Et}^2 \to 1$ and, accordingly, with unlimitedly increasing fluctuations of momentum and energy, which is enough to pass through the potential barrier [18-20]. From this point of view, the growth zone of any biological object represents a collection of potential nanoreactors, in each of which a

reaction involving these particles is possible, as well as the nuclei of atoms forming the "walls" of the dynamic nano-brain. Similar processes can occur in the space between cells during fission, in mitochondria, at the entrance to biological membranes, etc.

The correct interpretation and possible use of the experiments discussed below can change the view on the relationship between wildlife and the diversity of chemical elements and isotopes on Earth. The question concerns the possibility of nuclear transformations in biological systems under "non-reactor" conditions (room temperature, normal (atmospheric) pressure, absence of neutrons and charged particles of high energy). These issues, in particular, are considered and formalized in the patent [21].

Note that from the point of view of the possibility of catalytic effect on nuclear transmutations, the growing biological environment is no worse (and, most likely, better) than, for example, the usual crystal, which is most often used in LENR experiments. It is better in the sense that, unlike a static crystal, the growing biological system is a dynamic object, which allows us to consider each of its elements as a microscopic system of non-stationary potential wells and barriers.

4.1. Experiments on utilization of the reactor isotope ^{140}Ba

The realization of phenomena of heavy stable isotopes transmutation led to the formulation of the question about transmutation of radioactive nuclei. The first series of experiments was devoted to the possibility of influencing the activity of reactor water samples extracted from the first circuit of the water-water nuclear reactor, which is located in the Institute of Nuclear Research in Kiev.

The water under study had an activity of about 10^{-4} Curie/L and contained a number of highly active unstable isotopes (in particular, ^{24}Na, ^{40}K, ^{60}Co, ^{91}Sr, ^{131}I, ^{135}Xe, ^{140}Ba, ^{140}La, ^{141}Ce, ^{239}Np). The gamma-radiation spectrum of the reactor isotopes contained in this water is shown in **Fig. 3**. Water samples of the same volume (about 5 ml) were placed in the same glass thin-walled closed cuvette with a volume of about 10 ml. In a part of the cuvettes with active water, the same mass of MCT granules was placed.

The remaining cuvettes with water (but without granules) were controls. The essence of the research consisted in a periodic (after 5 days) study of the gamma spectrum of active water. To eliminate the influence of the distance factor (it may be associated with a small increase

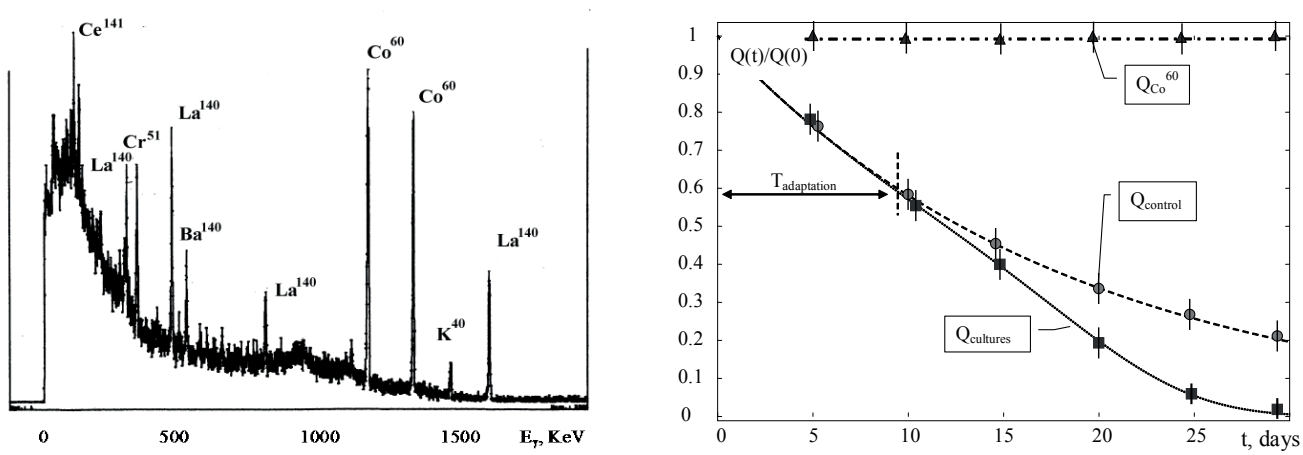

Fig. 3. *Left: spectrum of gamma radiation of distilled water from the first circuit of the water-water nuclear reactor. The data correspond to the tenth day after the sampling of water from the core of the reactor. On the right is the dependence of the Q(t) activity of ^{140}Ba, ^{140}La and ^{60}Co reactor isotopes in reactor water samples in the transmutation experiment (here $Q_{cultures}$ is activity of cuvettes at the presence of metabolically active microorganisms) and in control cuvettes without microorganisms ($Q_{control}$ activity): $Q_{control}$–decay of ^{140}Ba and ^{140}La in control experiments without MCT granules, $T_{adaptation}$ – time of internal adaptation of microbial synthrophic association to action of radiation, $Q_{cultures}$ – deactivation of ^{140}Ba and ^{140}La isotopes in transmutation experiments with presence of MCT granules, $Q_{Co\text{-}60}$ – activity of ^{60}Co isotope in control and experimental cuvettes with MCT.*

in the volume of a mixture of water and granules with the growth of microbiological cultures or their spatial redistribution), we used an amplitude germanium detector with a large size of germanium crystal, in which the cells under study were arranged in turn exactly in the center.

Fig. 3 shows the averaged results of the dependence of the activity of the isotopes ^{140}La and ^{60}Co in cuvettes with MCT granules ($Q_{cultures}$) and in control cells ($Q_{control}$) from the time after the beginning of the experiments.

From the data obtained it follows that the activity of the long-lived ^{60}Co isotope remains constant throughout the measurement period (about 40 days) (both in the control cuvettes and in cuvettes with MCT granules). This indicates that systematic methodological errors (a change in the volume of the liquid, a change in the position of the cell relative to the center of the crystal of the detector, etc.) did not have a significant effect on the result.

At the same time, a fundamentally different law for the reduction of the activity of the isotope ^{140}La in both types of cuvettes was discovered. This isotope has a relatively short lifetime (τ_{La} = 40.3 hours) and is a daughter unstable isotope of the longer-lived ^{140}Ba isotope, whose lifetime is τ_{Ba} = 12.7 days.

The initial activities of the ^{140}Ba and ^{140}La isotopes (on the 10th day after extraction the water from the reactor core) for each of the cuvettes was, respectively, $Q_{Ba\text{-}140} = 1.46 \cdot 10^{-7}$ Curie/L and $Q_{La\text{-}140} = 2.31 \cdot 10^{-7}$ Curie/L. Since $\tau_{La} << \tau_{Ba}$, the observed decrease in ^{140}La activity reflected a decrease in activity of ^{140}Ba.

It was found that the decrease in activity of ^{140}La in control cuvettes approximately corresponded to the law of "standard" decay of the ^{140}Ba isotope with a "tabulated" lifetime. Approximately the same law of decreasing activity of ^{140}La was observed in cuvettes with granules up to 10 days of the experiment. However, after this, periodic measurements showed that the rate of decrease in activity of ^{140}La (and hence of activity ^{140}Ba) is equivalent to a more accelerated decay. Extrapolation shows that the effective lifetime of this isotope is reduced by about 2 times in relation to the lifetime of the ^{140}Ba isotope.

These results can be explained on the basis of the assumption that the ^{140}Ba isotope could be converted in a cuvette with MCT granules to another, non-radioactive isotope. In this case, the presence of an initial, unchanged region in the law of decay can be explained by the processes of adaptation of the microbiological association to the action of radioactive irradiation in a cell with active water. This time (about 10 days) correlates well with the expected time of the change of 10 generations of microbiological cultures.

Analysis of possible isotope transformations has shown that in this case the following transmutation reaction of the radioactive ^{140}Ba isotope to a stable nucleus of another type ^{140}Ba + ^{12}C = ^{152}Sm + ΔE is possible. This reaction is energy-efficient and is characterized by a positive reaction energy

$$\Delta E = E(A_{Ba}Z_{Ba}) + E(A_C, Z_C) - E(A_{Sm}, Z_{Sm}) = 8.5 \text{ MeV}.$$

The carbon required for this reaction is abundant in the volume of MCT granules.

There is one more question about the biochemical aspects of the expediency of the course of this particular reaction in the living system. For answer to this question, it should be noted that the law of constancy of the chemical composition of biological objects is one of the fundamental properties of living matter. If we proceed from this circumstance, then it is obvious that according to the analysis of biochemical aspects of nuclear processes [11, 12], the isotope transmutation reaction in the biological system will be possible if the result of the reaction is an isotope corresponding to such a chemical element that either itself is included in the number of vital chemical elements (such as H, O, C, K, Ca, N, P, Fe, ...), or it is a biochemical analogue of such an element. In the latter case, it should have approximately the same ionic radius and, preferably, the same valence. In this case,

the reaction efficiency will be great only when the vital chemical element or its biochemical analogue is not contained in the nutrient medium or is contained in a small amount.

A simple comparison shows that Sm^{2+} and Ca^{2+} ions are biochemical analogues and have a close ionic radius in the divalent state ($R_{Sm} \approx 1.2$Å, $R_{Ca} \approx 1.06$Å). As you know, calcium is among the vital elements, and its concentration in the volume of granules was small. In this case, we can assume that the growing microbiological association could fill the lack of calcium with a synthesis of its biochemical analog (samarium). At the same time, the unchanged activity and the number of nuclei of the ^{60}Co isotope can be explained by the fact that in this system there is no possible energy-efficient transmutation reaction in which ^{60}Co participates and whose product would be an isotope of that vital chemical element that is absent in the nutrient medium. In other words, ^{60}Co may simply be "not in demand".

4.2. Experiments on utilization of the long-lived reactor ^{137}Cs isotope in growing associations of microbiological structures

Nontrivial results, indicating an abnormal decrease in the activity of ^{140}Ba and ^{140}La isotopes in experiments with reactor water in the presence of microbiological cultures, stimulated the setting up of special experiments to study the possibility of utilization of long-lived "fuel" isotopes formed during the operation of nuclear reactors. These works were conducted with the participation of our colleagues V.N. Pavlovich and A. Odintsov from the Institute for Nuclear Research and the Institute for Nuclear Safety Problems in Kiev [22]. The microbiological granules of MCT were prepared by our colleague A.B. Tashirev from the Institute of Microbiology in Kiev.

The utilization of such isotopes is of the greatest practical interest. Consider these experiments in more detail. In these experiments we have used the same closed glass cuvettes, each containing 10 ml of distilled water, in which the salt containing ^{137}Cs was dissolved. The total activity of each of the cuvettes was about $2 \cdot 10^4$ bq.

The scheme of investigations is shown in **Fig. 4**. The same mass of MCT granules was placed in 7 cuvettes. In 6 cuvettes, purified salts of K, Ca, Na, Fe, Mg and P were added to the active water. These chemical elements are among the most vital for any living system. The main purpose of using of such additives was to find ways to block possible channels of transmutation because if a specific chemical element is present in the system from the number of vital ones, then the assimilation of its biochemical analogue during transmutation becomes unlikely. In addition, such substitutions were carried out with the goal of creating the optimal composition of microelements for rapid growth of microorganisms. The results obtained below confirm the importance of such substitutions. Two additional cuvettes were used

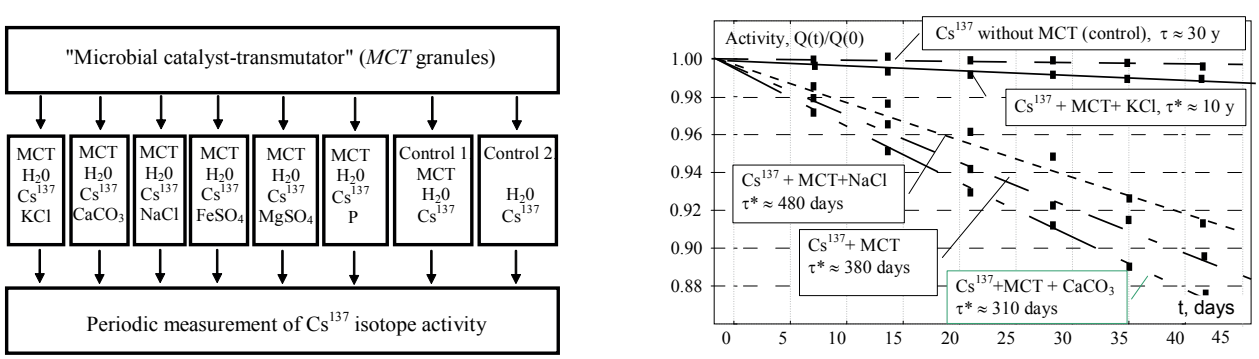

Fig. 4. *Scheme of studies of the utilization of active isotopes under different conditions and the results of experiments on the accelerated utilization (deactivation) of the ^{137}Cs isotope in "biological cells" in the presence of MCT and various chemical elements.*

for monitoring: one contained active water and MCT (but did not contain additional salts), and the other – only active water.

All the cuvettes were closed and kept at a temperature of 20°C. The amplitude gamma-ray spectrum of the cuvette was measured every 7 days on the same detector, in which a Ge crystal was used. Particular attention was paid to reducing the influence of errors associated with the measurement process. For this purpose, we have used cuvettes with a low height, and the detector with a large Ge crystal. The cuvettes were set at the same position in the center of the crystal of the detector for each measurement.

The results of the change in the relative activity of the ^{137}Cs isotope are shown in Fig. 4 and in **Table 2.**

From the obtained data it follows that during a 100-day observation period, a steady decrease in ^{137}Cs isotope activity was recorded in all cuvettes containing active water and MCT. In the control cuvette containing only active water, the change in the activity of ^{137}Cs isotope corresponded to the standard spontaneous decay with a lifetime of about 30 years. For other investigated isotopes, the changes were much weaker.

The fastest decrease in activity (it was equivalent to a decrease in the lifetime of ^{137}Cs by a factor of 35 to $\tau^* \approx 310$ days) was observed in a cuvette containing a calcium salt. This decrease in activity was not related to the accelerated decay, but was the result of reaction of transmutation the radioactive ^{137}Cs isotope to the stable isotope of another element.

Table 2.

Changes in the activity of ^{137}Cs in the "optimal" medium (MCT + active water + $CaCO_3$ salt)

Izotope	Energy, keV	The beginning of the experiment. N_1 - the number of events 10^3 sec.	The end of the experiment (100 days). N_2 - the number of events 10^3 sec.	Spon-taneous decay	Change of activity
^{137}Cs	661.7	266900	216800	-0.6%	-24%

An analysis of possible ways of transmutation should be based on several fundamental logical premises:

- this process should be energy-efficient, i.e. transmutation should be characterized by a positive reaction energy $\Delta E \geq 0$;
- the transmutation reaction must in a certain sense be adapted to the biological system, the result of the reaction must be an isotope corresponding to one of the vital elements or its biochemical analogue;
- the initial isotope of the transmutation reaction should reflect (correlate) the quantitative composition of the medium;
- among the different initial isotopes that can participate in reaction, preference should be given to the lightest isotopes for which the effect of potential barriers should be the smallest among the possible ones.

Based on these conditions, we can expect that the utilization of ^{137}Cs is related to the reaction $^{137}Cs + {}^{1}p = {}^{138}Ba + \Delta E$, flowing with the participation of water protons. The result of the reaction is the stable isotope ^{138}Ba. The reaction energy is positive and equal to $\Delta E = 5.58$ MeV.

Concerning the "biological expediency" of such a hypothesis, it can be noted that Ba^{2+} and K^+ ions are biochemical analogs: they have approximately the same ionic radii in the divalent state ($R_{Ba} \approx 1.4$Å, $R_K \approx 1.33$Å). Since the replaceable element (potassium) is one of the vitally important trace elements, the probability of such a substitution is quite large and the ions of the synthesized barium can replace potassium ions in metabolic processes with the growth of cultures. Such a substitution appears to be more effective than the "direct" replacement of potassium by cesium in the case of potassium deficiency (this can be seen from the large difference in the ionic radii of cesium $R_{Cs} \approx 1.65...1.69$Å and potassium $R_K \approx 1.33$Å). It should be noted that a similar replacement of ions was previously observed and analyzed in experiments with

the microbiological culture of *Blastocladiella emersonii* [23]. In these experiments, a fairly effective replacement of K^+ ions by Rb^+ and Ba^{2+} ions was recorded. These ions can replace each other in the processes associated with ion transport through the membrane into the cell.

Another interesting question relates to the cause of increased efficiency of utilization when using an additional calcium salt. Apparently, this effect is associated with the general pattern of the metabolism of microbiological cultures: the optimal growth of culture corresponds to the necessary balance of all micro- and macroelements. It is possible that it was calcium deficiency that was the "bottleneck" that inhibited the growth process and accompanying transmutation in a particular growing microbiological system.

In recent years, further improvements in bio- and nuclear technology has led to significant progress of these processes using more optimal biological substances and their modes of growth. Recent experiments have shown that the recycling process can be accelerated many times. In particular, the mean (according to parallel experiments) decrease in ^{137}Cs concentration over 14 days was 23%, which corresponds to an acceleration of deactivation more than 200 times. In some cases, a decrease in the concentration of ^{137}Cs in these experiments reached 40% and even 70% (**Fig. 5**) [12].

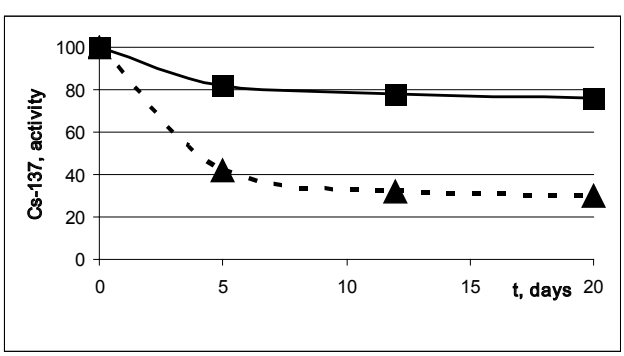

Fig. 5. *Reduction of the activity of the aqueous solution of ^{137}Cs in the optimized syntrophic association (the upper graph is the average data for the series of experiments, the lower is the most optimal case).*

5 CONCLUSION

The obtained results testify to the reality of the process of transmutation of both stable and radioactive isotopes accompanying the growth of microbiological cultures. The authors are aware that the totality of the observed phenomena and, especially, their interpretation do not coincide with the traditional notions and can cause serious criticisms. On the other hand, such processes have a purely physical basis and are not directly related to the specific features of the growth of living organisms, although they are stimulated by such a process. The authors have several patents (including international ones) on this modern technology.

In our minds, certain stereotypes are firmly fixed, among which the question of the "industrial" character of nuclear transformations is one of the most stable. Based on previous experience in the creation and operation of large-scale nuclear power, it is difficult to imagine that such processes (but in incomparably smaller scales) can take place in a living organism. However, by and large, there is no significant opposition. The whole question is only in the appropriateness of such transformations and in their very low efficiency caused by mutual repulsion of the nuclei due to the presence of the Coulomb barrier. At the molecular level, the specificity of the interaction and motion of microparticles is fully described by the laws of quantum mechanics and electrodynamics for both living and non-living objects. From this point of view, there is no difference between them! As the analysis [18-20] shows, in nonstationary systems of the potential well type, an interference short-term suppression of such repulsion is possible due to the formation of large fluctuations of momentum and kinetic energy in the process of formation of coherent correlated states. Such processes can be successfully implemented in

any system if the necessary prerequisites are met.

It is obvious that such nuclear reactions can not be called a semi-mystical term "biological transmutation". These processes are ordinary nuclear reactions, but they are realized in growing biological systems and under the catalytic effect of dynamic electric fields accompanying atomic-molecular processes that take place with the growth of these systems. In any case, the experiment plays a decisive role. Such a process can be called "nonstationary dimensional nuclear catalysis."

In our understanding, the influence of the biological object itself on the process of nuclear transformation is in the following circumstances:

- the dynamic spatial structure of the growing bioobject at the molecular and atomic levels acts as a "spatial catalyst" for the nuclear reaction, which ensures a short-term elimination of the Coulomb barrier factor of the reaction;
- specificity of the growth of a particular biological object provides selective functions that characterize the effectiveness of a particular reaction.

In conclusion, we can say a few words about the biological specifics of the observed phenomena. The very phenomenon of the transformation of chemical elements and isotopes in biological systems is based, first of all, on the repeatedly verified condition of constancy of the elemental composition of microorganisms. From this fact follows the heuristic assumption that in the case when some of the required macro- or microelements are missing in the system, there are prerequisites that they will be synthesized and fixed in a finite form as a result of physically grounded nuclear reactions.

In conclusion, we note that the words of V.I. Vernadsky that the biosphere is a nature-forming and relief-forming factor in the evolution of the Earth can be supplemented by the observation that it can be an isotope-transforming factor that significantly changes the distribution and quantity of different elements and isotopes.

REFERENCES

1. Biberian JP. Biological transmutations. *Current science*, 2015, 108(4):633.
2. Biberian JP. Biological transmutations: historical perspective. *Journal Condens. Matter Nucl. Sci.*, 2012, 7:11.
3. Kervran CL. Transmutations Biologiques, Métabolismes Aberrants de l'Azote, le Potassium et le Magnésium. *Librairie Maloine S.A.*, Paris, 1963.
4. Kervran CL. A la Découverte des Transmutations Biologiques. *Librairie Maloine S.A.*, Paris, 1966.
5. Kervran CL. Preuves Relatives à l'Existence de Transmutations Biologiques. *Librairie Maloine S.A.*, Paris, 1968.
6. Kervran CL. *Biological Transmutations.* Happiness Press, USA, Magalia, California, 1998.
7. Vysotskii VI, Kornilova AA. *Nuclear fusion and transmutation of isotopes in biological systems.* Moscow, Mir Publ., 2003.
8. Vysotskii VI, Kornilova AA. *Nuclear transmutation of stable and radioactive isotopes in biological systems.* India, Pentagon Press, 2010.
9. Vysotskii VI, Kornilova AA. Sposob polucheniya stabilnykh izotopov za schet yadernoy transmutatsii tipa nizkotemperaturnogo yadernogo sinteza elementov v mikrobiologicheskikh kulturakh [A method of producing stable isotopes due to nuclear transmutation type low-temperature nuclear fusion of elements in microbiological cultures]. *Patent RU* 2052223C1, 1995 (https://patents.google.com/patent/RU2052223C1/ru) (in Russ.).
10. Vysotskii VI, Kornilova AA. Transmutation of stable isotopes and deactivation of radioactive waste in growing biological systems. *Annals of Nuclear Energy*, 2013, 62:626.
11. Vysotskii VI, Kornilova AA. Microbial Transmutation of Cs-137 and LENR in

growing biological systems. *Current Science,* 2015, 108:142.
12. Vysotskii VI, Kornilova AA, Gaidamaka S, Kashcheev V, Zhura E, Tserbaev A. Biotransmutation of Cs133 and Biodeactivation of Cs137 by Aerobic Microorganisms of Methanogenic Sea Ooze. *20th Int. Conf. on Condensed Matter Nuclear Science* (*ICCF*-20), 2-7 Oct 2016, Japan, Sendai. Book of Abstracts, p. A91.
13. Minato K, Ikegami T, Inoue T. Recent research and development activities on partitioning and transmutation of radioactive nuclides in Japan. *Actinide and Fission Product Partitioning and Transmutation. Eight Information Exchange Meeting*. USA, Las-Vegas, November 2004, p.29-47.
14. Savage C. Overview of United States P&T Programme. *Ibid*, p. 49-56.
15. Ponomarev LI. Overview of Russia P&T Programme. *Ibid*, p. 79-90.
16. Stanculescu A. IAEA Activities in the aria of partitioning and transmutation. *Ibid*, p.101-108.
17. Radioactive Waste Management. *World Nuclear Association*. July 2015. Retrieved 2015-08-25.
18. Vysotskii VI, Adamenko SV, Vysotskyy MV. Acceleration of low energy nuclear reactions by formation of correlated states of interacting particles in dynamical systems. *Annals of Nuclear energy*, 2013, 62:618.
19. Vysotskii VI, Vysotskyy MV. Coherent correlated states and low-energy nuclear reactions in non stationary systems. *European Phys. Journal*, 2013, A49:99.
20. Vysotskii VI, Vysotskyy MV. Coherent correlated states of interacting particles – the possible key to paradoxes and features of LENR. *Current Science*, 2015, 108:524.
21. Kornilova AA, Vysotskii VI. Method for purifying water of radionuclides. *Intern. patent WO 2015156698 A1*, 11 April 2014.
22. Vysotskii VI, Odintsov A, Pavlovich VN, Tashirev AB, Kornilova AA. Experiments on controlled decontamination of water mixture of long-lived active isotopes in biological cells. *Proc. 11th Int. Conf. on Condensed Matter Nuclear Science*, 2004, France, Marseilles, World Scientific, Singapore, 2006, p. 530-536.
23. Van Brunt J, Caldwell JH, Harold FM. Circulation of potassium across the plasma embrane of Blastocladiella emersonii: K-chanel. *J. Bacteriol.*, 1982, 150(3):1449.

NONLINEAR QUENCHING OF THE RADIOACTIVITY OF AQUEOUS SOLUTIONS OF SALTS OF NUCLIDES BY LASER ABLATION OF NANOPARTICLES OF METALS

Stepan N. Andreev, George A. Shafeev

A.M. Prokhorov General Physics Institute, Russian Academy of Sciences, http://www.gpi.ras.ru
Moscow 119991, Russian Federation
nauka@gpi.ru, shafeev@kapella.gpi.ru

Abstract. **Laser ablation of metal nanoparticles in a solution containing radioactive nuclides, initiate their transformation into a stable state. This paper presents a brief review of studies of the dissolution of salts of radioactive uranium and cesium, where a significant acceleration of their decay is experimentally observed. Also it is proposed a possible mechanism of suppression of radioactivity, for example, salts of cesium. The obtained results allow us to hope for the establishment of effective technologies for disposal of liquid radioactive wastes containing cesium-137 and other dangerous isotopes.**

Keywords: **copper vapor laser, gold nanoparticles, laser ablation, radionuclides**
PACS 42.62.–b; 61.46.–w; 78.66.–w

Bibliography – 13 references *Received 10.05.2017*

RENSIT, 2017, 9(1):65-73 **DOI: 10.17725/rensit.2017.09.065**

Contents

1. INTRODUCTION

Development of any area science passes certain stages. At the beginning stage of science direction are discussed the most bold theories and hypotheses and everything that could, is be checked experimentally. When science is in the process of blossoming, side hypotheses are discarded and the emphasis is on the general direction. Finally, when this direction reaches its peak and when it seems that just about everything openly and understood, appear a strange experimental results that do not fit into the framework of conventional theory: paradoxes, the resolution of which is only possible outside of that framework. Then occur return to the side directions, that were once discarded and forgotten, and sometimes - breakthrough into an entirely "new dimension" of science.

So it was with mechanics, thermodynamics, optics. A similar story will be repeated still not once with different areas of science. Is no exception, and the nuclear physics.

In the period formation of nuclear physics was put forward and discussed a most different hypotheses about what is the atomic nucleus, what are its properties, is it possible to extract from it the energy. If very to simplify, we can say that in the initial phase stood out and competed two directions of development of nuclear physics. One is the high-energetic, and the other is low-energetic.

The high-energy direction promised very large dividends - are weapons and energy, and medicine. But at the same time, it carried and the danger, in the first place associated with radiation. The second direction is a low-energy – at first actively was developed, but then came to naught and was even banned.

However, it has always attracted talented and outstanding researchers. The great Igor V. Kurchatov in 1956 he was invited to Britain, where he gave a lecture at the nuclear center in Harwell. The lecture was entitled "On the possibility of creating thermonuclear reactions in gas discharge" [1]. It was about the under his leadership experiments, on powerful electrical discharges in tubes filled with gaseous hydrogen, deuterium or helium. The strength of the discharge current has reached two million amperes. The discharge was nourish with a voltage of several dozen kilovolts.

This is a very and very small voltage by the standards of nuclear physics. Nevertheless, was reliably recorded acts of thermonuclear reactions in this discharge. Of course, now we can say that it can't be, because it can't be never, but at that time, in the far 1956, Igor Vasilievich did not hesitate to tell about it in England.

Another example is associated with the name of the famous academician Yevgeny I. Zababakhin, the creator of the russian thermonuclear weapon. The Russian Federal Nuclear Center in Snezhinsk is named after his. Yevgeny Ivanovich worked on the development of the theory of unlimited cumulation in the cavitation bubbles and mathematically strictly solved this problem [2]. His decision was not lost relevance to this day. He proved that for the energy concentration in the bubbles of a certain size there are no restrictions: neither viscosity nor thermal conductivity can lead to limiting the temperature rise in the bubble. From here directly follows the possibility of bubble fusion. Academician Zababakhin considered the idea of a simple experiment that was to demonstrate this phenomenon: in a cauldron filled with heavy water (D_2O) and placed on the fire; the water boils, it bubbles; the bubbles collapse, causing a thermonuclear reaction in deuterium. Unfortunately, we have no information about the fact, whether were conducted and to what led these experiments.

There are many other examples of studies of low-energy nuclear reactions, conducted eminent scientists, including academicians of the an USSR and the RAS. Manifestations of low-energy nuclear reactions was discovered in very various experimental productions. This are and the reactions in the crystal lattice of metals induced by electrolysis, and reactions in the crystal lattice, induced by impact, the different reactions at diffusion through the membrane. This is a whole class of experiments using electric discharge, electric explosion, of ultrasound in a gas or liquid. This are reactions induced corpuscular and wave action on condensed media, and finally, reactions in biological systems.

Summarizing the known experimental data we can conclude that low energy nuclear reactions are not a synthesis, and are not a decay, but apparently, this are some collective nuclear transformations, which take place at energies unacceptably low for conventional nuclear reactions, and give the change of the isotopic composition, as well as quite a large heat generation in the full absence of residual radioactivity.

2. LASER ABLATION OF GOLD NANOPARTICLES IN SOLUTIONS OF SALTS URANIUM AND CESIUM

At the Prokhorov Institute of General Physics of RAS, in the laboratory of macrokinetics of non-equilibrium processes of the Scientific center of wave researches (a branch GPI) in the recent years intensively investigate ablation (removal of the substance from the surface by a laser pulse) of solids in the liquid. The basis of this phenomenon is light-hydraulic effect, discovered by G.A. Askar'yan, A.M. Prokhorov,

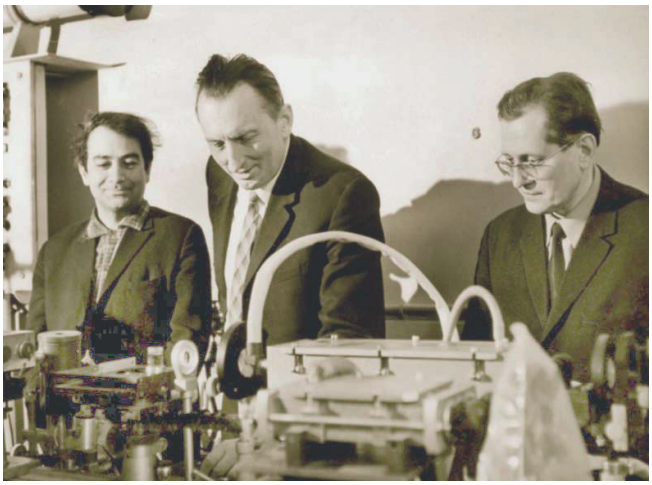

Fig. 1. *G.A. Askar'yan, A.M. Prokhorov and G.P. Shipulo (left to right) beside experimental setup for the study light-hydraulic effect.*

and G.P. Shipulo (**Fig. 1**) at the beginning of the laser era in 1963 [3, 4].

If the laser beam acts on the absorptive target, located in a transparent fluid, at a sufficiently high intensity of laser exposure, on the target surface the nanorelief arises, and into the surrounding liquid stand out nanoparticles from the material of the target (**Fig. 2**). In principle, this technique allows to generate nanoparticles of any kind – metallic, dielectric, semiconductor.

It was shown that laser irradiation of nanoparticles of metals in aqueous solutions of salts of uranium leads to a significant deviation of activity of the radionuclides of this family from the equilibrium values [5, 6]. Change of activity of radionuclides occurs in the process of laser irradiation of metal targets in aqueous solutions of salts of uranium. Herewith an acceleration of the spontaneous α - and β-decay nuclides belonging to the family of uranium-238 is observed. This effect was investigated in a wide range of wavelengths of the laser radiation and pulse durations [7, 8]. Laser ablation of targets in aqueous solutions of salts of nuclides accompanied by the formation in solution of nanoparticles of the target material and, apparently, is a necessary condition for changes in the activity of the nuclides. This conclusion can be drawn from observing the growth of activity of a number of nuclides (thorium-234) for a long time after laser irradiation - up to 100 days [9].

In the present work we will focus on the irradiation by the pulsed laser of an aqueous solution of a salt of cesium-137 (**Fig. 3**) with placed in it by gold nanoparticles (**Fig. 4**) which form in water a fairly stable colloidal solution [10].

Glass cuvette with an aqueous salt solution of the radioactive isotope cesium-137, in which added gold nanoparticles at a concentration of 10^{12} units per milliliter, was irradiated through

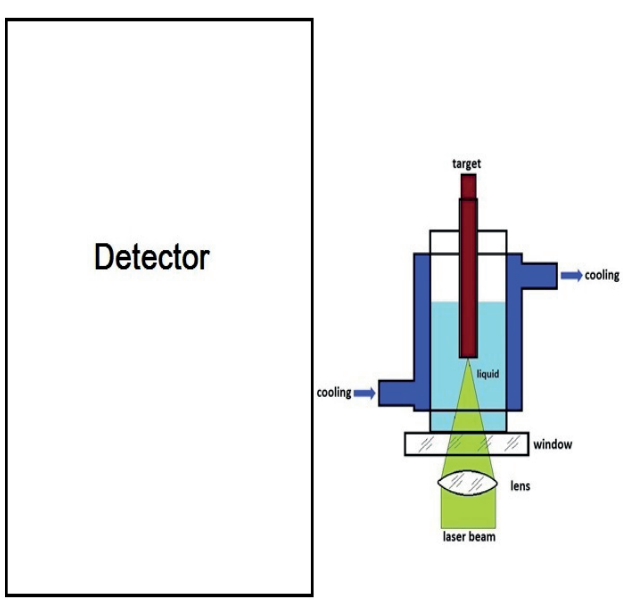

Fig. 2. *Laser ablation of solids in liquid.*

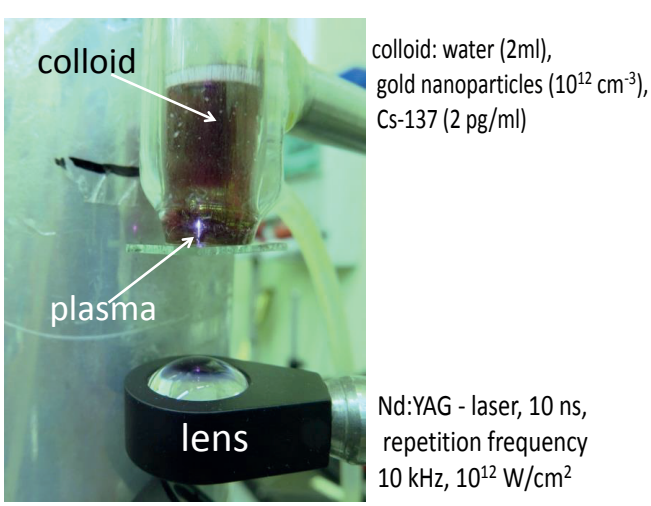

Fig. 3. *The irradiation of pulsed laser radiation of an aqueous solution of a salt of caesium-137 placed in him by the gold nanoparticles.*

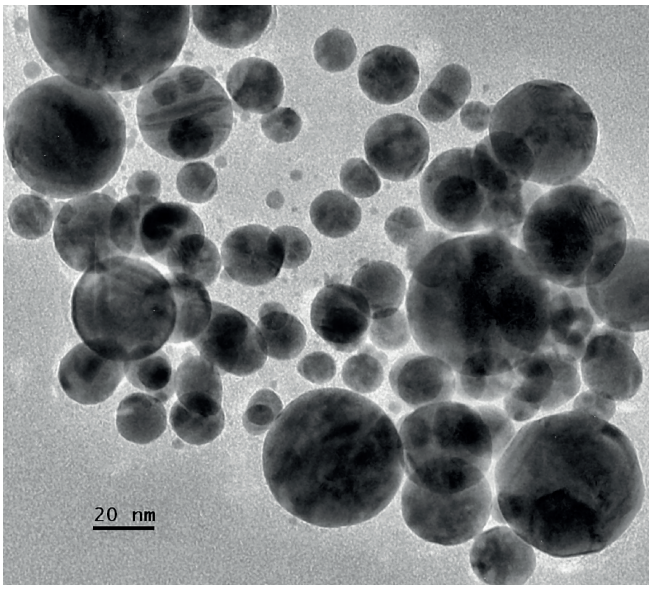

Fig. 4. *Gold nanoparticles obtained by ablation of a gold target in aqueous solution of salt of cesium-137.*

the transparent bottom by the pulses of the copper vapor laser. The energy of each pulse was 2 mJ, duration 10 ns, repetition frequency 10 kHz. The characteristic time of irradiation - ten hours. In order to the transparent bottom of the cuvette is not quickly destroyed, the laser beam is focused not at the same place, and scanned over the surface of the cuvette. External cooling of the cuvette with running water prevented the boiling in it a radioactive solution.

In contrast to the nuclides of family of uranium-238, at cesium-137 there is only one

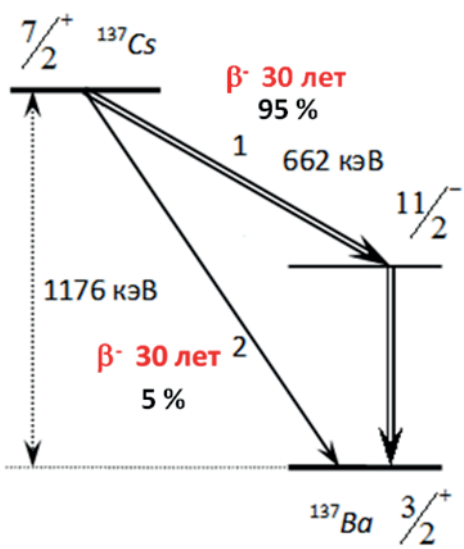

Fig. 5. *Diagram of the beta decay of the isotope cesium-137.*

channel of decay – β-decay. There are two channels of β-decay (**Fig. 5**). The first channel, which is realized with a probability of 95%, is the beta decay of cesium-137 to an excited state of barium-137, the loss of excitation by a nucleus of barium results in the emission of gamma-quant with energy 662 keV. I.e., in fact, in the experiment measured the number of excited nuclei of barium. But because this transition is very rapid compared to beta decay (half-life of cesium-137 is 30 years), in fact, the intensity of the gamma-quants determines the concentration of nuclei of caesium-137. Measurement of the intensity of the flux of gamma-quants is a very reliable method of measuring the concentration of nuclei of caesium, as gamma-quanta with energy 662 keV are not absorbed into either the liquid or the nanoparticles or glass of cuvettes.

There is a second channel of the beta decay of cesium-137 that is implemented with a probability of 5%. In it beta-electron is emitted from the nucleus of a cesium with energy of order 1 MeV, and the nucleus of the barium is in the unexcited, ground state. This channel is nonradiative and cannot be used for measurements in this scheme of the experiment for the reason that electrons with an energy of about 1 MeV can not leave the cuvette - they are completely braked in water, not reaching the walls of the cuvette.

Gamma radiation from the fixed cuvette was measured by semiconductor gamma spectrometer Ortec-65195-P with an accuracy of ±5% continuously for 15 hours before laser irradiation, 10 hours during the experiment, and 15 hours after irradiation.

A typical gamma spectrum from the cuvette with a solution of caesium-137 is shown in **Fig. 6.** The solution activity was measured by area under the spectral peak of gamma-quant with energy 662 keV using a special program. Activity values were saved in computer memory

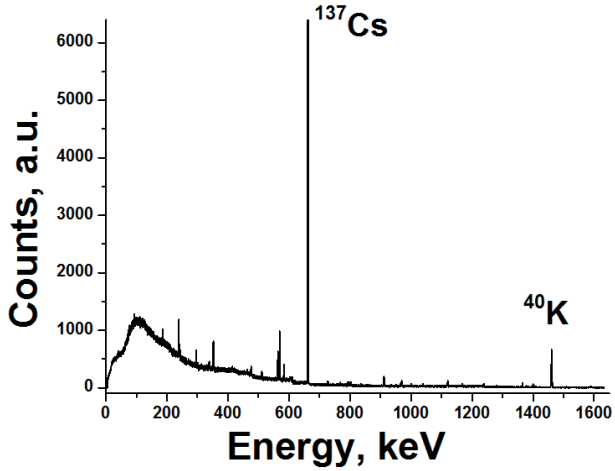

Fig. 6. *A typical gamma spectrum from the cuvette with a solution of cesium-137.*

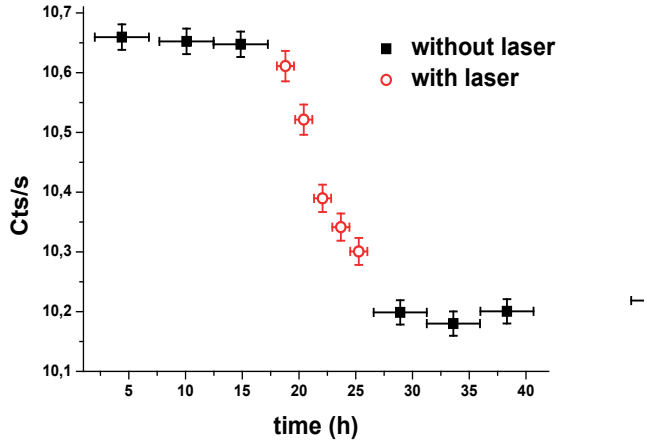

Fig. 7. *The dependence of the intensity of the flux of gamma rays with energy of 662 Kev from the time before, during, and after irradiation by laser pulses of the cuvette with a solution of radioactive cesium-137.*

with a frequency of 1 time per second, and the time of signal accumulation was selected such that the measurement error did not exceed 0.5%. The peak contrast relative to the background was 120:1.

Preliminary measurements of gamma spectrum of the cuvette, with radioactive cesium-137 for 15 hours before laser irradiation showed that the concentration of cesium in the cuvette during this time has not changed (which, on the one hand, to be expected, because the period of half-decay of cesium-137 is a lot more observation time, and on the other hand, this fact indicates the absence of possible care paths of caesium from the cuvette).

The main result of the experiment, conducted jointly with specialists from Dubna, lies in the detection by they the monotonic decrease of the flux of gamma quanta with energy 662 keV on 5% at the time of laser irradiation of the cuvette, with a solution of radioactive cesium-137 for 10 hours (**Fig. 7**).

Subsequent measurements of gamma spectra for 15 hours showed that after switching off the laser the gamma activity of the cuvette with the solution remains at a constant level.

Thus, for 10 hours of laser exposure, the concentration of radioactive cesium in the cuvette decreased by 5%. Formally, this corresponds to the acceleration beta-decay of cesium-137 is not less, than 1200 times. However, in reality, here we are faced with manifestation of the another nuclear process. The effect we called "nonlinear quenching of the radioactivity of cesium-137" – similar to the quenching of luminescence in laser crystals.

3. POSSIBLE MECHANISMS OF REDUCTION OF CESIUM RADIOACTIVITY

The discovered effect is not the acceleration of beta-decay. This is easily seen by following the method of the proof "by contradiction". Without going into the mechanism of the process, assume that during laser exposure, for whatever reason, the acceleration of beta-decay of the nucleus of caesium-137 occur. Herewith this realizes the decay channel into the excited state of the barium nucleus. Now its half-decay period is already not 30 years, and just 9 days (this figure is obtained taking into account the fact that for 10 hours, the decrease of the radioactivity of the solution was 5%). What then will be the result? The nuclei of cesium will go to an excited level of the nuclei of barium 1200 times faster. Consequently, the intensity of the flux of gamma quanta with energy 662 keV should increase by 1200 times. However, gamma-ray spectrometer does not register that. On the contrary, it shows a

monotonous decrease in the intensity during laser irradiation. So, talk about the acceleration of the beta decay of cesium in this case is incorrect.

Consider another possibility, when beta decay accelerated by non-radiative channel of the caesium into the ground state of barium. To explain the experimental data, its half-life must equal total of 11 hours, as the radiationless transition occurs only in 5% of cases. Beta decay of cesium on this channel will not give an increase in the intensity of gamma quanta with energy 662 keV, instead there will be a large number of electrons with energy around 1 MeV. These electrons, scattered on the surrounding atoms will give to gamma-quanta of bremsstrahlung radiation with a continuous spectrum of energies from a high of 1176 keV and below. Their emergence one may register with the help of gamma-spectrometer, however, this task is connected with considerable experimental difficulties. In particular, it is necessary to eliminate the effect of cosmic gamma background on the measurement results. Work in this direction is underway, but so far the achieved measurement accuracy does not allow to make certain conclusions.

The third possibility of reducing the radioactivity of cesium lies in the implementation of nuclear reactions during laser irradiation of solution. As we know from nuclear physics, nuclear reactions must overcome the Coulomb barrier of repulsion of the positively charged nuclei involved in the reaction. This requires a temperature of millions of degrees, or a high-energy accelerator. It is obvious that in our experiment none of these possibilities is not possible. Therefore, about the occurrence of the usual nuclear reactions in this case is not out of the question.

However, we cannot exclude the possibility of exotic nuclear processes, the theory of which develop in the works of doctors of Phys&Math Sciences V.I. Man'ko [11] and V.I. Vysotskii [see, for example, on pages 21-36 of this issue and the bibliography in it]. From their theory it follows that for the implementation of exotic low-energy nuclear reaction it is necessary that the nuclei were correlated in a coherent quantum state. Recall that these are the states in which fluctuations of momentum and coordinates of a quantum particle are not independent, and therefore, the ratio of uncertainty of Heisenberg is written for them in the form of an equation of the Schrödinger-Robertson [12, 13]. It takes into account the correlation coefficient, which in the usual uncorrelated quantum states is equal to zero (then this formula reduces to the ratio of the Heisenberg uncertainty), but may be and very close to unity. Then the product of the fluctuations of the coordinate and momentum of a particle can increase substantially. Formally, this corresponds to increasing the "effective" Planck's constant by several orders of magnitude, which in turn leads to a multiple increase in the probability of tunneling of a quantum particle through the Coulomb barrier.

There is a fundamental difference of correlated particles in the coherent condition compared with the particles having high kinetic energy.

If the particle with high kinetic energy collides with an atomic nucleus, this nucleus, as a rule, enters an excited state, the decay of which is usually accompanied by the emission of gamma quanta, neutron yield, electrons, or other nuclear particles. As a result, the kernel acquires the residual radioactivity.

If the particle is in a coherent correlated state, then she may have high energy because of the fluctuations on very short time, that is determined by the uncertainty relation Schrödinger-Robertson. A particle with such energy would react with the nucleus, but

this happens only if the excited state of the nucleus, which arises herewith, relaxed during the time less than the lifetime of fluctuations of the energy of the particle.

I.e. not every nuclear reaction can be come true, but only one in which the products have a very short relaxation time to the ground state. In other words, those new nuclei that occur in these exotic nuclear processes do not have residual radioactivity, i.e., are stable.

As shown by V.I. Vysotskii, for the formation of coherent correlated state the quantum particle must be in a potential pit, the walls of which experience a rapid changes. Potential pit must either monotonically expand or shrink, or experience periodic perturbations. An example of such a potential pit can serve as a nano-cavity in the crystal lattice of a solid body subjected to shock compression or rupture. Another example, of direct relevance to experiment [10], is a nano-sized cavitation bubble in the liquid, the volume of which fluctuates under the action of external forces. Such nanoscale bubbles appear in laser irradiation of colloidal solution of gold nanoparticles.

It is possible to give some estimates. The average size of the nanoparticles in the experiment [10] is of the order of 10 nm. With long-term laser exposure the nanoparticles are fragmented and their size can be smoothly reduced to 3 nm. The concentration of nanoparticles in solution – 10^{12} units per ml, the average distance between them – of about 1 micron.

What happens to a nanoparticle trapped in the focus of the laser pulse? It absorbs the laser energy, heats up and becomes the center of nucleation – on it arise nanoscale cavitation bubble. The surface of these bubbles are charged. With the growth of nanobubble on its surface there is a separation of charges, and inside it formed a sufficiently large electric field, which causes electrical breakdown of a gas-vapor mixture inside the bubble and the formation of a plasma consisting primarily of electrons and protons. The resulting plasma then absorbs the laser radiation, which leads to further growth of the bubble. According to our calculations, the electric field inside the bubble can reach values of the order of 10 kVcm^2. This is sufficient to breakdown the gas.

We conducted special experiments in which we measured the duration of the individual flashe from nanobubble and the spectrum of its radiation. It is obtained that the flash duration is around 10 ns – this coincides with the duration of a single laser pulse. Spectrum of flash continuous, that matches the spectrum of the bremsstrahlung of the electrons in the plasma. Evaluation of plasma temperature give a value of the order of several electron volts.

It should be emphasized that the characteristic distance between nanobubbles of the order of 1 μm is large enough to consider them independent from each other. It is well known that the cavitation processes are most intense when the bubbles are separated from each other. Once they merge, the efficiency of cavitation drops sharply. From this follows an important condition for the intensity of the laser pulses: it must be high enough for the formation of cavitation bubbles on the gold nanoparticles, but not to exceed such values, when the bubbles merge with each other.

So, as a result of the impact of laser pulse on gold nanoparticle is formed nanobubble containing electron-proton plasma. In fact, the bubble is proton potential well, the walls of which are deformed due to the fact that the bubble grows or shrinks. Therefore, the protons can be in a coherent correlated States. Fluctuations of the proton energy in these States can be sufficient to proton react with a nearby nucleus of caesium-137 with the

formation of non-radioactive barium-138 in ground state.

Thus, a third possible mechanism for reducing the radioactivity of a solution of cesium lies in the occurrence of nuclear reactions between protons, which are in coherent correlated states in nanobubbles, and nuclei of caesium-137, with the formation of non-radioactive barium-138.

4. CONCLUSION

Obtained results extend the list of radionuclides (^{232}Th, ^{238}U, ^{3}H), the accelerated decay of which can be initiated with the aid of laser radiation. These data are of practical interest, since cesium-137 is one of the most hazardous radionuclides due to its rapid spread in water and soil.

At the present time there are approximately two hundred nuclear power plants, in which operate almost 450 power unit. Many of them have almost exhausted their resource and prepare for decommissioning. In this regard, the acute question of disposal of liquid radioactive waste (RW), first of all, water under the reactor. Currently, the solution to the problem of disposing of radioactive waste in fact confines to their long-term storage, in which radioactive isotopes disintegrate naturally over tens or hundreds of years. In fact — is shifting the solution of environmental problems of the present generation on the shoulders of its immediate and distant descendants. Even more acute problem of disposal of radioactive waste arises in case of emergencies at nuclear facilities (Chernobyl, Fukushima), and in the case of military conflicts with the use of nuclear weapons, as a result of which extensive territories undergo by radiation contamination. Therefore, the development of technologies accelerated deactivation of the radiation contaminations and the utilization of radioactive waste is an urgent and priority task of nuclear physics.

The relative simplicity of the technological realization of the laser quenching of radioactivity gives a real possibility of its use for the decontamination of radiological contaminants and adjustment of the composition of radioactive waste of atomic energetics.

REFERENCES

1. Kurchatov IV. About possibility of creation of thermonuclear reactions in gas discharge. *Advances in physical Sciences*, 1956, 59(4):603-618.
2. Zababakhin EI, Zababakhin IE. *Yavleniya neogranichennoy kumulyatsii* [The phenomena of unlimited cumulation]. Moscow, Nauka Publ., 1988, p. 161.
3. Askar'ian GA, Prokhorov AM, Chipulo GP, Chanturia GF. Luch OKG v zhidkosti [The ray of optical quantum generator in fluid]. *Pis'ma v Zhetf*, 1963, 44(6):2180-2182 (in Russ.).
4. Askar'ian GA, Prokhorov AM, Chipulo GP. Sbetogidravlicheskiy effekt [The light-hydraulic effect]. Diploma No. 65. Priority 28.2.1963. *Otkrytiya, izobreteniya, promyshlennye obraztsy, tovarnye znaki* [Discoveries, inventions, industrial designs, trademarks], 1969, 19:4 (in Russ.).
5. Simakin AV, Shafeev GA. Initiation of nuclear reactions under laser irradiation of Au nanoparticles in the aqueous solution of Uranium salt. *Appl. Phys. A*, 2010, 101(1):199.
6. Simakin AV, Shafeev GA. The influence of laser irradiation of nanoparticles in aqueous solutions of uranium salts on the activity of the nuclides. *Quantum electronics*, 2011, 41(7):614.
7. Barmina S, Sukhov IA, Lepekhin NM, Priseko YuS, Filippov VG, Simakin AV, Shafeev GA. The use of copper vapor lasers for controlling activity of uranium isotopes. *Quantum electronics*, 2013, 43(6):591-596.

8. Shafeev GA, in: *Uranium: Characteristics, Occurrence and Human Exposure*. Ed. by A. Ya. Vasiliev, M. Sidorov. New York, Novapubl. Inc., 2012, pp 117-153.
9. Kirichenko NA, Simakin AV, Shafeev GA. Long-term variation in nuclide activities under laser ablation of metallic targets in aqueous solutions of uranium salt. *Phys. Wave Phenomena*, 2014, 22(2):81.
10. Barmina EV, Simakin AV, Shafeev GA. Laser-induced decay of cesium-137. *Quantum electronics*, 2014, 44(8):791-792.
11. Dodonov VV, Manko VI. Invarianty i evolutsiya nestatsionarnylh kvantovykh sistem [Invariants and evolution of nonstationary quantum systems]. *Trudy FIAN*. Moscow, Nauka Publ., 1987, 183:286-351.
12. Robertson HP. A general formulation of the uncertainty principle and its classical interpretation. *Physical Review*, 1930, 35(5):667.
13. Schrödinger E. Zum Heisenbergschen Unscharfeprinzip. *Berl. Königlich Akad. Wiss.*, 1930, 24:296-303.

NICKEL-HYDROGEN REACTORS: HEAT GENERATION, ISOTOPIC AND ELEMENTAL COMPOSITION OF FUEL

Alexander G. Parkhomov, Sergey N. Zabavin, Timur R. Timerbulatov
Experimental-design laboratory "K.I.T."
Moscow 121108, Russian Federation
alexparh@mail.ru, sergeyzabavin@gmail.com, konfi1@konfi.ru

Kirill A. Alabin, Stepan N. Andreev
Prokhorov General Physics Institute of the Russian Academy of Sciences, http://www.gpi.ru
Moscow 119991, Russian Federation
alabin.kirill@gmail.com, naukagpi@yandex.ru,

Alexander G. Sobolev
Lebedev Physical Institute of the Russian Academy of Sciences, http://www.lebedev.ru
Moscow 119991, Russian Federation
asob09@gmail.com

Abstract. **At the interaction of hydrogen with a number of metals, including Nickel, are observed not only mechanical and chemical changes, but also such extraordinary phenomena as the anomalously large heat generation and the change in isotopic and elemental composition. An overview of experiments that explore these phenomena is presented. Also the results of analysis of the isotopic and elemental composition of the fuel and substances near the active zone of nickel-hydrogen reactors before and after work with the production of excess energy to 790 MJ are presented. Reliable changes in the isotopic composition of nickel and lithium are not detected. A significant increase in the concentration of impurities of a number of nuclides discovered, not only in fuel but also in structural elements adjacent to the active zones of reactors.**

Keywords: **hydrogen, nickel, heat generation, isotopic composition, radiation**

UDC 53.043

Bibliography – 30 references *Received 19.06.2017*

RENSIT, 2017, 9(1):74-93 **DOI: 10.17725/rensit.2017.09.074**

Contents

1. INTRODUCTION

In March 1989 Fleishmann M., and S. Pons demonstrated the device, in which during the electrolysis of heavy water in the presence of a palladium cathode, emitted energy was several times more than supplied [1]. The authors explained this by the fact that released at the cathode deuterium penetrated into palladium, which has high ability to absorb hydrogen (deuterium). High concentration of deuterium nuclei, introduced into the crystal lattice of palladium, makes possible the fusion of two deuterium nuclei into the nucleus of helium or of tritium with the release of large energy.

Usually the history of studies of the anomalously large heat generation and other phenomena occurring at the feeding of some

materials with hydrogen, one start with this demonstration, although the results indicating the existence of these phenomena were obtained before. For example, in 1950-ies I.S. Filimonenko has created an installation in which there was an unusually large heat generation at temperatures up to 1150°C [2]. The main part of Filimonenko reactor was a metal pipe made of an alloy containing palladium and filled of the deuterium.

Reaction of scientific community to the demonstration of Fleischmann and Pons was very boisterous. In scientific laboratories of different countries, attempts were made to repeat these experiments. But the poor reproducibility and the lack of clear explanation have led to the fact that a significant portion of the scientific community began to relate to the works in this area skeptical or even strongly negatively. Dislike was also contributed by the fact that this kind of phenomenon was called "cold fusion", though, from the point of view of the existing system of scientific knowledges, transformation of matter at the nuclear level at energies of the order of 1 eV are impossible. But even if we assume the existence of some obscure mechanism of such nuclear transformations, they, according to existing ideas, inevitably must be accompanied by deadly gamma and neutron radiation. The fact that the researchers were not perish, it would seem, clearly demonstrated the fallacy of their experiments.

However, researches in this direction were continued [3-9]. The technique of such experiments is usually composed in saturating with hydrogen (deuterium) substances that have the ability to greedily absorb this gas (commonly used palladium, titanium or nickel). For this, in addition to just detention in the atmosphere of hydrogen are used electrolysis or electrical gas discharge. The hydrogen-saturated samples are subjected to different influences. In this case, are made a measurements, which may indicate the processes of the changes at the nuclear level. On the nuclear changes may indicate heat generation, exceeding the possibilities of chemical reactions, the appearance of neutrons, gamma and x-ray radiation, the appearance of tritium, the change in isotopic composition. In addition, we studied the possibility of occurrence of nuclear transmutations in biological systems was studied [10, 11].

In this article presents information on the results of the analysis of the heat generation and changes in the fuel and in construction materials that occurred in several nickel-hydrogen reactors created by our team.

2. FIRST EXPERIMENTS WITH THE HYDROGEN-SATURATED NICKEL

Until recently, among the researchers of the phenomenon of anomalous heat generation received the most attention the palladium or titanium, with the most striking ability to absorb hydrogen. Although already in 1992 at the physics faculty of the University of Siena (Italy) by a group of researchers led by Francesco Piantelli experiments were conducted in which it was found anomalously large heat in the interaction with hydrogen with nickel [12].

In **Fig. 1** the layout of the experimental set-up is shown. Reactor chamber of length 100 mm has a diameter of 50 mm. In the chamber is a heater of platinum wire. Inside the heater is placed, or a rod of Nickel with a length of 90 mm with a diameter of 5 mm, or alternatively, an appropriate dummy stainless-steel rod of

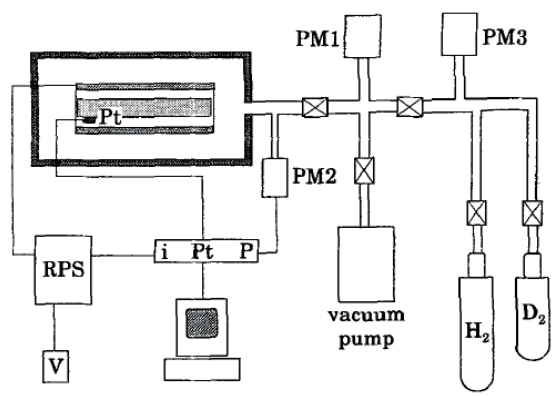

Fig. 1. *Scheme of setup for the saturation of nickel with hydrogen and of study of heat generation* [12].

the same size. The temperature of these rods was measured by a platinum thermometer. The chamber can be evacuated by means of a turbomolecular vacuum pump and filled with hydrogen or deuterium from gas bottles. The pressure inside the chamber is measured by a piezomanometer. The heater coil is powered DC stabilized power supply. The values of the gas pressure, the heater current and the temperature are continously monitored by a PC operated data logger.

Calibration measurements of the temperature dependence of the stainless steel rod upon heating power at pressures in the range from the maximum attainable vacuum up to atmospheric was made. Further, in setup placed a rod of nickel and cyclically carried out the pumping out and filling of the chamber with hydrogen (natural mixture of protium and deuterium) up to a pressure of about 0.55 bar at a temperature of 440°C. Every time the pressure stabilized an hour after reducing the pressure about on 0.05 bar as a result of absorption of hydrogen by the nickel.

In one of the cycles of pumping-filling, the temperature suddenly rose from 440° to 480°C at a constant power of electric heating. Using the calibration curve heating power-temperature, the authors concluded that unto the electrical heating has become add heat, to the power of about 20W. After several additional cycles the excess power reached 50 watts (**Fig. 2**).

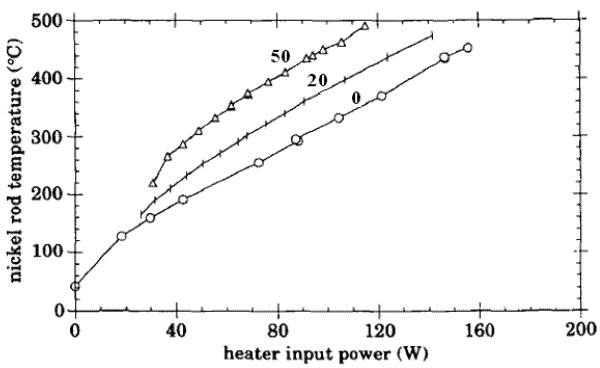

Fig. 2. *The temperature of the rod in depending on the power of the electrical heating at different values of the anomalous energy release 0 W, 20 W, 50 W* [12]. *The dependence in "0" is obtained for the stainless steel rod and rod of nickel is not saturated with hydrogen.*

Fig. 2 shows that the same temperature of nickel rod, which saturated with hydrogen, is achieved at a power of about two times smaller than when using the dummy or nickel, which not saturated with hydrogen.

The setup work lasted continuously for 24 days, with an average excess power of 44 watts. In total for this time produced about 90 MJ of thermal energy in excess of electricity consumed.

In the future, were created a similar, but more advanced setups [13-15]. One of them, producing 68 watts of excess capacity, worked for 278 days, producing 900 MJ of heat, above of electricity consumed. Other, producing 18 watts of excess capacity, worked 319 days, producing about 600 MJ of heat in excess of electricity consumed. So much heat is released during the combustion of more 10 kg of oil products. Note that the mass of hydrogen absorbed by nickel, and partially reacted, is less than 100 mg.

After operation of the reactor for 22 days (produced 35 MJ surplus energy) surface of the nickel sample was subjected to analysis using scanning electron microscope [13]. It revealed the presence of chromium and manganese, the presence of these was not noticeable prior to being in the reactor.

For clarification of the radiation situation around reactors were carried out special researches with the involvement of experts in the field of registration of nuclear radiation. To measurement of a possible neutron radiation were used three 3He counter surrounded by a paraffin retarders, and also an activation method using gold foil [14]. With the excessive power of heat generation 22-38 W was registered the unstable emission to 6.000 neutrons per second. It this to 1011 times less than would be emitted if the excess power was called the known mechanisms of nuclear reactions.

The possible gamma radiation was detected by the scintillation NaI(Tl) and also the semiconductor germanium detector.

The measurement results differed little from natural background radioactivity [15]. In later experiments, it was discovered weak radiation with an energy of 511 Kev, which indicates the occurrence of β^+-decays. Description of the experiments of the Italian physicists, continue to the present time, can be found on the website [16]. One of the setups worked for several months without additional power supply and without added hydrogen, is continuously allocating 70 watts of thermal power.

The radiation of neutrons was registered as well by the Russian researchers during heating in the temperature range 250-350°C the nickel powder in a hydrogen environment at a pressure to 100 bar [17]. The radiation of neutrons took place in the form of short bursts or series of bursts lasting up to several tens of minutes. The total neutron yield reached 500000. For registration of neutrons was used 3He counter with a water retarder as well as an activation technique using indium. The results of the measurements by both methods are within the possible errors are the same.

From other studies in which it was registered the heat generation in excess of electricity consumed, it should be noted the researches of team led by the fellow worker of Italian national Institute of nuclear physics Chelani Francesco [18], as well as Akito Takahashi (Osaka University) and Akira Kitamura (Kobe University) [19], studied the nanopowder alloy nickel-copper in the matrix of ZrO_2. They registered the release of energy up to 800 eV per one absorbed hydrogen atom, which is hundreds times greater than the energy release, which is possible in chemical reactions.

3. ANDREA ROSSI'S HEATGENERATORS

Despite these successes, until recently, the study of these anomalous phenomena professionals nuclear was not taken seriously. The situation changed when the Italian engineer Andrea Rossi and Professor of the University of Bologna Sergio Focardi managed to move from research mock-ups to setups that produce energy on an industrial scale [20].

For the first time a device which produces a heat to capacity of 12.5 kW, were demonstrated January 15, 2011. "Fuel" of the reactor is the nickel and hydrogen. The structure of this device is described in patent [21], but the detailed description is a trade secret. During public demonstrations, observers were allowed only to inspect the unit outside, measure the input and output of energy and to monitor the level of radiation.

October 28, 2011, Rossi demonstrated the reactor, which for 5.5 hours had give power 470 kW in self-sustaining mode. Careful measurements of the radiation around the working installation have not revealed any noticeable differences from the background. Although achieved in the tests the results are impressive, the design of setup cannot be considered perfect, as it consisted of 300 modules, housed in a cargo container. For her work needed the balloons with hydrogen and a lot of water.

Reactors of other design Rossi demonstrated in December 2012, March 2013 and March 2014. These devices appeal to compactness and simplicity. The operation of these reactors was controlled by an international Commission of competent scientists who released two lengthy report [22, 23]. Of particular interest is the last report. Although it did not disclose the internal structure of the reactor shown, the detail observation of the device operation and the thoroughness of the tests allow you to guess a lot. The study was performed in Barbengo (Lugano, Switzerland) with the use of equipment which, according to experts, does not in any way connected with Andrea Rossi or his partners. In the work took part Giuseppe Levi (Bologna University, Italy), Evelyn Foschi (Bologna, Italy), Bo Höistad, Roland Pettersson and Lars Tegnér (Uppsala University, Sweden), and Hanno Essén (Royal Institute of Technology, Sweden), David Bianchini (expert in radiation measurements).

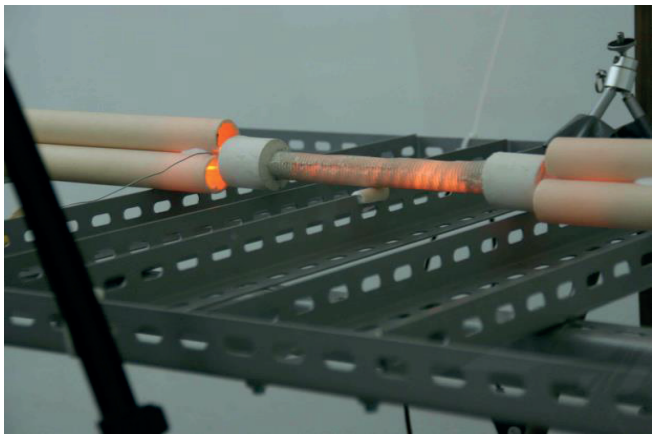

Fig. 3. *The Rossi's reactor during the test. On each side there are three ceramic tubes with wires for which power is supplied, required for the preliminary heating of the reactor.*

The presentment of this report was published in Russian [24].

The reactor weighs 450 g. The appearance of the reactor is a ceramic cylinder of diameter 2 cm length 20 cm with overhangs that improve convective heat transfer (**Fig. 3**). On both sides this cylinder ends with two ceramic tips diameter 4 cm, long 4 cm. On the tips there are the clamps of three heaters. In one of the tips there is a hole with a diameter of 4 mm. Into the hole is inserted ceramic plug in which is mounted the thermocouple probe. Through this hole is loaded the fuel.

Three phase power to the heaters is supplied from two sides via copper wires, located in ceramic tubes. To adjust the electric power programmable power supply was used, which uses to maintain the set mode the signal from the thermocouple probe.

For determining the consumed energy used power meters and spectrum analyzers, and digital multimer. The power generated was determined by measuring the surface temperature using thermal imaging cameras and calculation on this basis, the energy losses by radiation and convection. All used measuring equipment were tested at the manufacturing companies and cross-checked at the application site. The information coming from all sensors were recorded in the computer memory for later careful analysis.

All testing stages were under the continuous supervision of experts. In the first stage the reactor was investigated at idling speed (without fuel). In this case, the thermal energy dissipated by the reactor is equal to the amount of electricity supplied. This allowed to make calibration measurements, using the results of which it is possible to determine the energy release of the reactor in the operating mode.

After a 23-hour operation without fuel, the reactor was turned off and disconnected from electrical cables, which allowed to load fuel mass of about 1 g, having the form of a fine powder. Before that, the powder to be loaded was poured into a special container, and its radioactivity was measured in a low-background lead chamber. After loading the fuel, the hole was closed with a ceramic stopper containing the thermocouple probe, and sealed with alumina cement. Were connected by electric cables and gradually increasing heating was included. The increase in heating power lasted as long as the average surface temperature of the reactor reached 1260°C at a power consumed by the heater of 810 watts. The operation in this mode lasted almost 10 days. At the end of this period the experts decided to increase the capacity, and raised it up to 900 watts. As a result, in a few minutes the temperature of the reactor was increased to 1400°C. Such an increase in temperature corresponds to an increase in heat dissipation for 700 W, although power of electric heating increased less than 100 watts. Further work took place when the electrical heating power of about 900 watts up to a pre-scheduled time shutdown (32 days after switching the reactor with fuel). The reactor was off by gradually decreasing the power of the electric heating. Until that time the reactor operation occurred without a noticeable reduction of the power of heat generation that indicates that the service life of the reactor after 32 days operation was not exhausted.

The measurements showed that the heat dissipation of the reactor is much more energy consumption. When power consumption of 790 watts in the first 10 days of operation of the reactor, the additive to the power consumed,

on average, is 1650 watts. After increasing the power consumption to 900 watts the value of supplements in an average of 2300 watts.

The report made the calculation of the energy produced during the reactor operation in excess of the consumed electric power: 1.6 MW h or 5800 MJ. Attributing this value to the mass of fuel 1 g, we estimate the density of energy release 1.6·109 W·h/kg = 5.8·106 MJ/kg. It is in hundreds of thousands times more than what can be obtained with the combustion of petroleum products.

After cooling of reactor the hole on the tip was opened, spent fuel extracted, poured into a container and checked for radioactivity similarly to testing of the fuel before loading. After that, the spent fuel has been subjected to various tests.

The analysis of the elemental and isotopic composition of the fuel was made by three independent groups of researchers specializing in the application of various techniques. Were used scanning electron microscope (SEM) to study the surface morphology of the fuel powder. Were using methods of x-ray photoelectron spectroscopy (XPS), dispersive x-ray spectroscopy (EDS), time-of-flight mass spectrometry of secondary ions (ToF-SIMS), mass spectrometry with inductively coupled plasma (ICP-MS) and atomic emission spectroscopy (ICP-AES). The application of the complex of these methods allows to give quite extensive information about the properties of fuel before and after operation of the reactor.

The conducted analyzes allowed to draw the following conclusions.

The original fuel is mainly composed of nickel powder in the form of pellets the size of a few microns, having a natural isotopic composition. In addition to the nickel in the fuel is detected admixture of Li, Al, Fe and H. The analysis of ICP-AES showed that the ratio of the contents of Li and Al corresponds to the molecule of lithium aluminum hydride, $Li[AlH_4]$. This component is likely used to produce free hydrogen by heating. In addition, EDS and XPS analyses revealed the presence of O and C. The analysis of the ToF-SIMS showed the presence of protium, but did not notice the presence of deuterium. The amount of most elements differs greatly in different granules.

The spent fuel has granules of a different kind than the initial fuel. The elemental and isotopic composition of granules is different, however, it is obvious that the isotopic composition of Li and Ni in spent fuel is radically different from the measured isotopic composition of the initial fuel (**Table 1**).

Although the results of measurements of the isotope composition by the two methods do not completely coincide, the following conclusions can be drawn.

1. The ratio of isotopes of lithium and nickel in the original fuel is within the possible error does not differ from the natural.

2. In the spent fuel the relative content of ^{6}Li increased significantly and the content of ^{7}Li decreased.

3. In spent fuel, the content of all isotopes of nickel, except ^{62}Ni, has decreased very much. The content of this isotope increased from 3.6% to 99%.

Such a strong change in the isotopic ratio of lithium and nickel, after 32 days of reactor work suggests that the registered anomalously large energy release is associated with changes at the nuclear level.

Table 1.
The isotopic composition of lithium and nickel in the source and spent fuel (%), measured by methods ToF-SIMS and ICP-MS, as well as the natural ratio of isotopes in these elements

	Initial fuel		Spent fuel		Nature
	ToF-SIMS	ICP-MS	ToF-SIMS	ICP-MS	
^{6}Li	8.6	5.9	92.1	57.5	7.5
^{7}Li	91.4	94.1	7.9	42.5	92.5
^{58}Ni	67	65.9	0.8	0.3	68.1
^{60}Ni	26.3	27.6	0.5	0.3	26.2
^{61}Ni	1.9	1.3	0.0	0.0	1.8
^{62}Ni	3.9	4.2	98.7	98.3	3.6
^{64}Ni	1.0		0.0		0.5

To check the possible ionizing radiation were used scintillation detectors and Geiger counters, as well as thermoluminescent dosimeters. This allowed registration of alpha, beta, gamma radiations and neutrons near working reactor. In addition, it was measured the radioactivity of the fuel before the filling of the reactor and after completion of work. None of these devices had not registered the difference from the background during operation of the reactor or in the study of the initial and spent fuel.

4. ATTEMPTS TO REPRODUCE ROSSI REACTOR

Researches in the field of cold nuclear transmutations – pretension on experiments, showing the path to acquiring fundamentally new knowledge and discovery new possibilities for the human community. But from the point of view of established scientific knowledge, the nuclear transmutation at low energies, without nuclear radiation, is absolutely impossible. In such circumstances, the first thing need to do is to make sure that such unusual results – not the result of errors or deliberate falsifications. Even the most strict and fair examination is insufficient. It is necessary to independently reproduce these results by other people, in other laboratories, with other equipment.

After the publication of the report of experts on the work of last version of Rossi reactor, its structure became in general clear, and it was finally possible to reproduce it. This reactor, in fact, is ceramic tube, sealed of heat-resistant cement, in which there is the nickel powder with the addition of lithium aluminum hydride $Li[AlH_4]$. To initiate the process, the tube has slowly heated to a temperature of 1200-1400°C. First of all, when heated, occurs decomposition of lithium aluminum hydride. The liberated hydrogen cleans the surface of nickel from oxides. After that, the hydrogen starts to dissolve in the nickel. After reaching a sufficiently high temperature in nickel with dissolved in it hydrogen, lithium and aluminum, begins a process with a high heat release.

Realizing this, many researchers around the world began to try to reproduce the heat generator Rossi. But it was not as simple task as it seems at first glance. Need to find a constructive materials that can withstand a corrosive environment at high temperature and elevated pressure, and to provide sealing. Need heaters, which operate at high temperature continuously. It is necessary to provide temperature measurement of the order of 1400°C, and to work out the control techniques of power of operating reactor.

A report on the first successful test of the Rossi reactor analogue was made as early as December 2014. [25]. For the manufacture of reactor used a tube of corundum ceramics 120 mm in length, an outer diameter of 10 mm and an inner diameter of 5 mm (**Fig. 4**). On tube is wound an electric heater of heat-resistant wire. Inside the tube is 1 g powder of nickel, mixed with 0.1 g of lithium aluminum hydride. On the outer surface tube there is thermocouple. The ends of the tube are sealed with heat-resistant cement. The same cement covers the whole surface of the reactor.

As the power source for the heater was used the transformer with switched windings. Switching was both manual and automatic

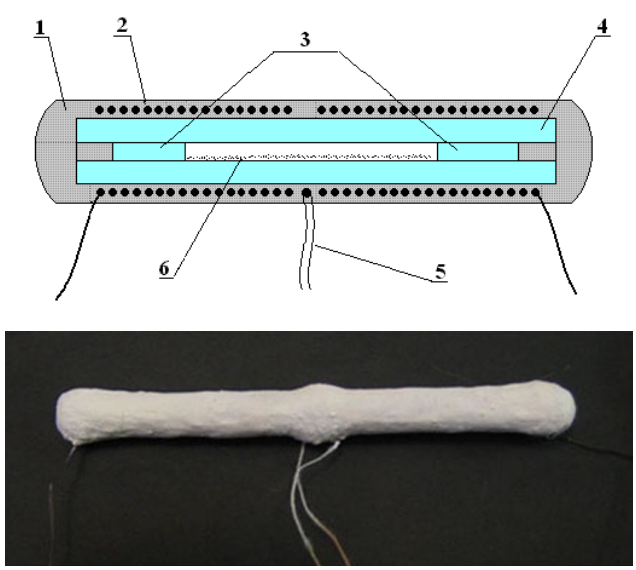

Fig. 4. *The scheme of Rossi's reactor analogue* [26]*: 1 – cement, 2 – electric heater, 3 - ceramic bungs, 4 – ceramic tube, 5 - thermocouple, 6 – powder of* $Ni + LiAlH_4$*. Below - foreign view.*

with using the regulator controlled by the thermocouple signal. Heating up to operating temperature lasted 10-12 hours. For measuring consumption of electricity are used the voltmeter and the ammeter, and the meter, allowing you to transfer data to the computer. To control the level of radiation used Geiger counter SI-8B, the dosimeter DK-02 and neutron activation technique, using indium.

The method used to measuring the power of heat generation, based on the readings of thermal imagers [24], used by experts for testing the Rossi reactor is too complicated. In this experiment used a methodology based on the amount of evaporating water. This technique worked and repeatedly verified in various experiments. The reactor is in closed metal vessel (**Fig. 5**). This vessel is immersed in water. Part of water goes away as steam. By measuring the loss of water, by a known value of heat of vaporization (2260 kJ/kg) is easy to calculate the separated heat. A correction for heat loss through insulation can be calculated using the cooling rate after shutdown of the reactor.

A detailed description of the progress of the experiments and of technic of results processing can be found in [25]. Here are only a summary of the results obtained in experiments conducted in December 2014 and January 2015 (**Table 2**). In addition to the experiments with reactors, which loaded with a mixture of Ni + $Li[AlH_4]$, were carried out experiments with models of the reactor without fuel.

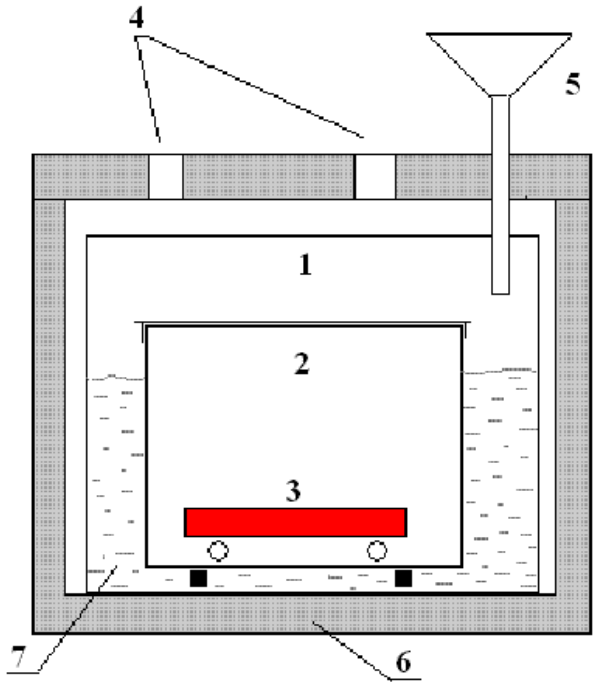

Fig. 5. *The scheme of the calorimeter with evaporating water: 1 – vessel for the water, 2 – vessel for the reactor, 3 reactor, 4 – holes for the escape of steam, 5 – funnel for adding water, 6 – heat insulation, 7 – water.*

A significant excess of released heat energy over the absorbed electrical energy was observed only in reactors with fuel at temperatures about 1080°C and above. In cases with models reactor, as well as with reactors with fuel at a temperature below 1080°C, the ratio of the emitted heat energy to absorbed electric power close to 1.

Table 2.

The ratio of emitted heat to electricity consumed (COP) in the experiments in December 2014 and January 2015

Reactor with fuel					
Date	Temper.	Duration	Consump.	Gener.	COP
	°C	min	W	W	
20.12.2014	970	38	301	297	0.99
20.12.2014	1150	50	395	758	1.92
20.12.2014	1290	40	499	1365	2.74
04.01.2015	940	131	304	305	1.00
04.01.2015	1020	75	377	407	1.08
10.01.2015	1080	73	161	281	1.77
18.01.2015	800	90	308	293	0.95
18.01.2015	1080	38	78	135	1.73

Reactor without fuel					
Date	Temper.	Duration	Consump.	Gener.	COP
	°C	min	W	W	
02.01.2015	210	56	211	227	1.07
02.01.2015	470	88	433	414	0.95
02.01.2015	1050	16	328	1035	1.12
21.01.2015	1000	69	297	296	1.00
21.01.2015	1080	43	306	297	0.97
28.01.2015	900	65	955	105	1.08
28.01.2015	1100	66	116	116	1.00
28.01.2015	1200	50	151	147	0.97

Thus, these experiments showed that a mixture of nickel and lithium aluminum hydride, with heated in hermetic ceramic tube to a temperature above 1080°C, indeed, produces much more heat than it consumes. The level of ionizing radiations during reactor operation is not appreciably higher than the background indicators. The density of neutrons flux is not higher than 0.2 neutr./см^{2}с.

Later it was created a lot of experimental installations, confirming the presence of excess heat generation in devices similar to the heat generator Rossi. In the paper [26] described 15 devices of this kind created in Russia, USA and China. In this article we will give a description of some of the many devices, created in our team.

5. ESTIMATION OF POSSIBLE CHANGES IN THE ISOTOPE COMPOSITION OF FUEL

We can estimate the possible changes in the isotopic composition of the fuel assuming that the excess heat release occurs as a result of nuclear transmutations in accordance with the law of conservation of energy. For example, in nickel, containing hydrogen, a nuclear reaction may occur

$$^{58}Ni + {}^{1}H + 2e^- \rightarrow {}^{59}Co + 10.32\ MeV \quad (1)$$

Since 1 MJ is equal to $6.3 \cdot 10^{18}$ MeV, about $6 \cdot 10^{17}$ nickel nuclei (0.00006 g) are consumed as a result of this reaction to release 1 MJ of energy, and the same amount of cobalt is formed. Nickel-hydrogen reactors usually contain about 1 g of fuel. It is quite possible, using modern technology, to detect 0.00006 g of cobalt in 1 g nickel (0.006%).

It is more difficult to detect changes in the isotopic ratios. Conventional mass spectral analyzers allow one to capture changes in isotopic ratios of elements of the order of 1%. It is not possible to detect a change of the order of 0.01% that occurs when 1 MJ of energy released into 1 g of fuel as a result of the reaction (1). To reduce the content of the isotope ^{58}Ni by 1%, an excess energy of the order of 100 MJ is necessary.

If the fuel contains lithium, a nuclear reaction is possible

$$^{7}Li + {}^{1}H \rightarrow 2{}^{4}He + 17.35\ MeV \quad (2)$$

As a result of this reaction, in a mixture of lithium isotopes (the natural mixture contains 92.6% of ^{7}Li and 7.4% of ^{6}Li) the content of ^{7}Li decreases and, accordingly, the content of ^{6}Li increases. Suppose that all excess energy release is associated with reaction (2). To release 1MJ of energy, $4 \cdot 10^{17}$ ^{7}Li nuclei are required ($4.2 \cdot 10^{-6}$ g). A typical reactor with fuel mixture of lithium-aluminum hydride and nickel contains about 0.02 g of ^{7}Li. Therefore, when 1MJ is released, only 0.02% ^{7}Li is removed. It is almost impossible to detect such a change. With the release of 1000 MJ of energy, 20% of ^{7}Li is removed. This leads to an increase in the content of ^{6}Li from 7.4 to 10%. This change is quite possible to detect, although not easy because of the small mass of the material available for analysis.

Thus, the appearance of nuclides that are absent in the initial fuel can be detected with excess energy of the order of 1 MJ per gram of fuel. To reliably detect changes in the ratios of isotopes in elements that originally are a part of fuel, excess energy exceed 100 MJ/g is required. It is natural that a thorough analysis of the fuel of the GS3 reactor made by Alan Goldwater did not reveal any noticeable isotope changes, since the excess energy production in it was about 50 MJ/g [3, 4]. The excess energy production in the high-temperature heat-generator of Rossi, according to [1], was 5800 MJ/g. This is quite sufficient for radical changes in the isotopic composition of both nickel and lithium. Further, we will present the results of an analysis of isotope changes in fuel and in structural materials that occurred in several nickel-hydrogen reactors created in our laboratory.

6. REACTOR AP2

Reactor AP2 [28] was charged with a fuel mixture of 640 mg Ni + 60 mg $LiAlH_4$ (**Fig. 6**).

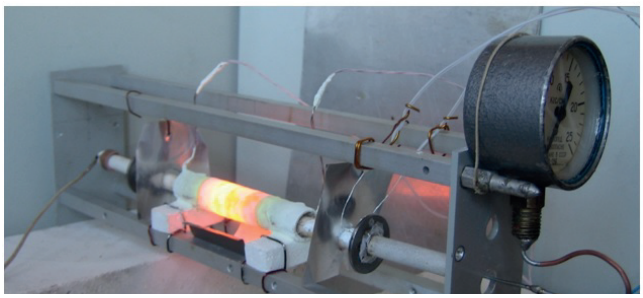

Fig. 6. *Reactor AP2.*

It worked from March 16 until March 22, 2015, and produced about 150 MJ of excess heat.

Analyzes of fuel before and after the experiment were made using several methods in different organizations. The analysis of the elemental composition using an electron scanning microscope was made at the Prokhorov General Physics Institute, Russian Academy of Sciences and All-Russian Research Institute of Experimental Physics (VNIIEF, Sarov). Two fractions confidently differ in the fuel mixture measured before experiment: gray crystals and white granules. Gray crystals mainly contain Al, O, and Cl. White granules consist of nickel with a small admixture of iron, aluminum and oxygen. In the fuel after the experiment, white molten and gray slag-like structures are visible. White structures contain mainly nickel with an admixture of Fe, Al, Cr, Mn, Si and O. Slag-like structures consist mainly of Al and O.

Analysis of the elemental composition of the fuel before and after experiment using laser atomic emission spectrometer was made at the Kurnakov Institute of General and Inorganic Chemistry, Russian Academy of Sciences. It showed that the content of K and Cr increased tens of times after the experiment. The content of Si, Na, Mg, Ca, Ti, and V increased manifold. The content of Al, Ni, Cl, Mn, Cu, Zn decreased. It should be noted, that this method of analysis, as well as analysis using a scanning electron microscope, provides information on the atomic composition only on the surface of the test substance.

Table 3.

Analysis of AP2 reactor fuel by the ICP-MS method at Uppsala University (Sweden)

%	^{6}Li	^{7}Li	^{58}Ni	^{60}Ni	^{61}Ni	^{62}Ni	^{64}Ni
Before	7.4	92.6	68.1	26.2	1.14	3.63	0.93
After	15.4	84.6	63.4	27.6	1.3	5.2	2.5
Nature	7.6	92.4	68.0	26.2	1.14	3.71	0.93

Analysis of the isotope composition of the fuel before and after the experiment in AP2 reactor was made using ICP-MS method, which gives information on the isotopic composition on average over the sample. Such analysis was made in Vernadsky Institute of Geochemistry and Analytical Chemistry of Russian Academy of Sciences. Total content of aluminum and lithium after the experiment decreased, while the relative content of ^{6}Li increased slightly. However this increase (by 0.5%) fall within the range of possible measurement error. There are no significant changes in the isotopic composition of nickel.

The analysis of AP2 reactor fuel by the ICP-MS method was also made at Uppsala University (Sweden). The results of these measurements are shown in **Table 3**.

According to these measurements, the relative content of ^{6}Li in the sample of spent fuel has more than doubled. Quite noticeable changes have occurred also in the ratio of nickel isotopes. These results differ from the results obtained in Vernadsky Institute of Geochemistry and Analytical Chemistry RAS. This difference can be explained, perhaps, by the unevenness of the changes in the sample volume. It should be noted that reliable results for lithium are difficult to obtain because of a very low concentration of lithium in spent fuel (<0.01%).

7. REACTOR PROTOK-6

Reliable measurement of generated heat is a key challenge in creating devices, which prove the existence of excess heat generation. The technique with running water is considered the most accurate, so we used the flow-through calorimeter to measure the heat generation in the twelve reactors. This article describes one

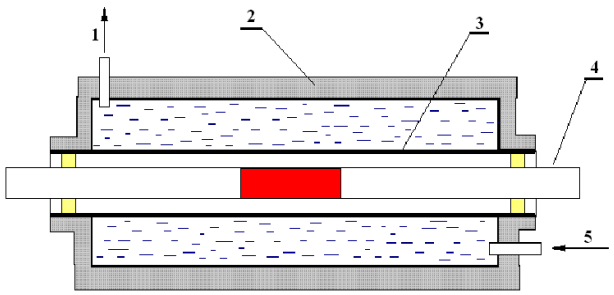

Fig. 7. *Device flow-through calorimeter: 1 – flowing in water, 2 – insulation 3 – copper tube, 4 – reactor, 5 – flowing out water.*

of them [29], who has worked for more than a month (**Fig. 7**).

We used a flow-through calorimeter in which the generated heat absorbed by the water which washed around the copper pipe, in which reactor is located. Power of heat generation is determined by the formula $W = c(dm/dt)(T-T_0)(1+\alpha)$, where c is the specific heat of water, (dm/dt) is the mass of water flowing per second, α is the correction for heat loss, T_0 is the temperature at the inlet to the calorimeter, T is the temperature at the outlet.

In **Fig. 8** shows the structure of the reactor. The fuel (1.8 g of nickel powder mixed with 0.2 g of lithium aluminum hydride) was located in a ceramic tube of length of 80 mm, external diameter of 7.5 mm, inner diameter of 5 mm. On the tube is wound a spiral of tungsten wire 0.5 mm in diameter. In the tube is inserted the ceramic rods, which by centering washers holding the inner tube in the middle of the reactor. In the longitudinal hole of one of the rods inserted W-Re high temperature thermocouple, which measures the temperature of the fuel end. Another thermocouple (type K) controls

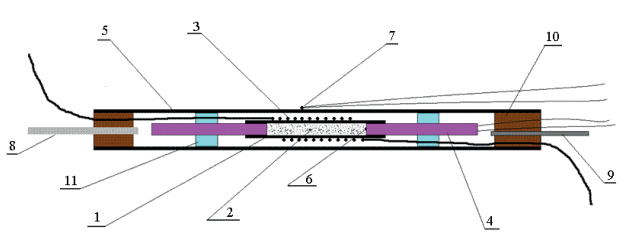

Fig. 8. *Scheme of the "Protok-6" reactor: 1 – inner ceramic tube, 2 – fuel, 3 – heater W, 4 – ceramic rods, 5 – external ceramic tube, 6 – termokcouple W-Re, 7 – termocouple K, 8 – tube for manometer, 9 – pumping tube, 10 – sealant, 11-centering washers.*

the temperature of the outer surface of the outer ceramical tube. This tube has an outer diameter of 18 mm and inner 14 mm. Due to the great length of the outer tube (350 mm) and the low thermal conductivity of ceramics during reactor operation, the temperature of its ends does not exceed 50°C, which allows for sealing use the epoxy compound. Of the ends of the reactor, in addition to the wiring of the heater, metal tube goes out for connecting the manometer and the glass tube for pumping air.

The power supply to the reactor was carried out from the secondary winding of transformer capacity of 630 watts. The switch taps of the secondary winding allows you to set the desired heating power. The thermocouple that measures the temperature of the end fuel, is connected to the thermostat TRM-500, which keeps the heater on until the temperature reaches the set value, and disables it when exceeding a predetermined temperature. Heating power is measured by voltmeter and ammeter directly on the heater, and also by a power meter, installed on the inlet of the transformer. Mapping power on the heater with the power on the primary winding allows to determine the losses in the transformer and wires. This is necessary to amend the results of the measurements of pulses power consumption by electric meter, that is registering by a computer. In addition to energy consumption, the computer registers the temperature at the inlet and outlet of calorimeter, as well as information about water consumption coming from the flow meter.

To verify the device was used similar to the above described reactor, which does not contain fuel. These measurements showed that the deviation of the data of the calorimeter from the results of measurement of electric power does not exceed 3%.

In the preparatory phase of measurements out of reactor, who was heated to 120°C, by the roughing pump was pumped air, to remove residual water and other volatile contaminants.

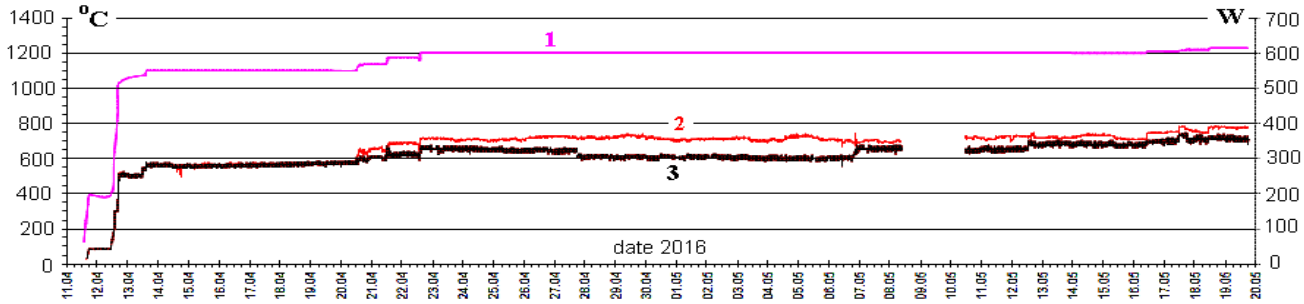

Fig. 9. *Change of temperature (1), power heat generation (2) and of power of electrical heating (3) during operation of the reactor.*

Next the vacuumed reactor was disconnected from the vacuum pump by melting in the flame of a gas burner glass tube connecting the reactor with a vacuum pump. Next as a result of heating the inner tube to a temperature of 180-200°C occurred the decomposition of lithium aluminum hydride, and the reactor was filled with hydrogen to a pressure of 4.25 bar. Then the temperature was increased to 400°C and kepted at this level for about 20 hours. By means of opening the valve located on the tube connecting the reactor pressure gage, the pressure was reduced to 0.4 bar. In the process of gradual increase in temperature after small increases of pressure at a temperature of 1100°C, in despite of a further increase in the temperature, pressure began to fall and on the fourteenth day from the beginning of the experiment has become below atmospheric.

In **Fig. 9** it is showen how varied during the 38 days from beginning to end of the experiment, the power of electrical heating, the temperature on the end of fuel and power heat generation, as measured by the calorimeter.

It is seen that at temperatures up to 1100°C power heat generation, measured by the calorimeter, almost equal to the power, emitted by the electric heater. Starting from a temperature of 1150°C, the power heat generation is clearly higher of the power of the electric heater. Change of difference between the power of heat generation (excess capacity) and of capacity for energy consumption shown in **Fig. 10**. It is also shown how varied for the experiment, the power ratio of allocated heat to power consumed by the electric heater (COP).

It is seen that the emergence of excess power of about 30 watts, significantly exceeding the possible error of the measurements, occurred after reaching a temperature of 1150°C. Approximately such excess capacity is produced at the beginning and with increasing temperature up to 1200°C. But after 5 days without external intervention there was a sharp increase of excess power to 50-60 watts. 9 days after this occurred an equally sharp decrease

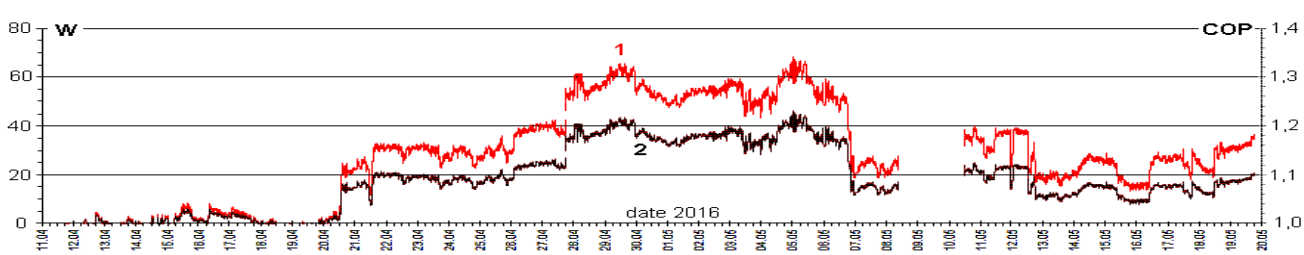

Fig. 10. *Change of excess power (1) and ratio of the produced heat power to power consumed by the electric heater COP* (2).

to 20-30 watts. In the last week fluctuations in excess capacity within the limits of 15-30 W were observed with a period of about 2 days. A gradual increase in temperature up to 1230°C led to a rise in excess capacity of 35 watts, but the work in such mode through the day led to the exit of the reactor down due to burnout of the electric heater. For total time of the experiment was produced about 100 MJ of excess heat.

After the experiment was over, the reactor was opened (**Fig. 11**). It was found that the inner surface of the outer tube near the heater was covered with

Fig. 11. *Reactor "Protok-6" after opening.*

lumpy gray glassy coating. The physical configuration of the inner tube and the heater winding was preserved. However, the changes inside were significant: a vitreous mass with inclusions of metal balls measuring about 0.1 mm was formed. Several

Table 4.

Relative content of isotopes (atomic %) in fuel and near the core of the "Protok-6" reactor before and after reactor operation. Isotopes with a content > 0.1% are shown.

Before reactor operation					
Initial fuel		Ceramics		W wire	
^{7}Li	0.74	^{23}Na	7.01	^{23}Na	5.37
^{23}Na	1.90	^{24}Mg	1.61	^{24}Mg	0.24
^{24}Mg	0.12	^{25}Mg	0.23	^{27}Al	0.31
^{27}Al	3.63	^{26}Mg	0.28	^{29}Si	1.88
^{29}Si	1.04	^{27}Al	65.05	^{31}P	0.18
^{39}K	1.60	^{29}Si	1.55	^{39}K	6.09
^{44}Ca	0.28	^{31}P	0.16	^{44}Ca	1.06
^{45}Sc	0.22	^{39}K	8.36	^{45}Sc	0.80
^{51}V	0.68	^{44}Ca	0.94	^{54}Cr	0.40
^{53}Cr	0.22	^{45}Sc	0.61	^{56}Fe	10.46
^{55}Mn	0.17	^{48}Ti, Ca	0.15	^{182}W	18.50
^{56}Fe	0.99	^{54}Cr	0.41	^{183}W	9.52
^{58}Fe, Ni	65.91	^{56}Fe	10.00	^{184}W	21.48
^{60}Ni	23.58	^{58}Fe, Ni	0.15	^{186}W, Os	21.29
^{61}Ni	1.10	^{89}Y	0.25	^{200}Hg	0.20
^{62}Ni	3.63	^{90}Zr	0.44	^{202}Hg	0.21
^{64}Ni, Zn	1.24	^{92}Sr, Mo	0.16	^{198}Hg	0.21
^{66}Zn	0.16	^{94}Sr, Mo	0.16		
^{68}Zn	0.12	^{138}Ba, Ce	0.33		
^{79}Br	0.13	^{206}Pb	0.13		
^{81}Br	0.12	^{208}Pb	0.29		
^{138}BaLaCe	0.25				
^{206}Pb	0.32				
^{207}Pb	0.25				
^{208}Pb	0.69				

After reactor operation							
Metal ball in spent fuel		Coating on inner surface of outer tube		Substance appeared between inner and outer tubes			
^{11}Ba	0.19	^{23}Na	1.56	^{11}B	0.44	^{75}As	0.43
^{23}Na	5.07	^{24}Mg	1.16	^{23}Na	14.70	^{76}Ge, Se	0.16
^{24}Mg	0.21	^{25}Mg	0.16	^{24}Mg	0.82	^{77}Se	0.17
^{27}Al	0.22	^{26}Mg	0.17	^{26}Mg	0.15	^{79}Br	0.97
^{29}Si	3.94	^{27}Al	0.23	^{27}Al	0.92	^{81}Br	1.03
^{31}P	0.14	^{29}Si	0.77	^{29}Si	9.37	^{90}Zr	0.16
^{39}K	3.51	^{39}K	0.86	^{31}P	0.32	^{116}In, Sn	0.26
^{43}Ca	0.14	^{44}Ca	0.71	^{39}K	9.89	^{120}Sn, Te	0.12
^{44}Ca	1.08	^{45}Sc	0.24	^{43}Ca	0.35	^{127}I	0.15
^{45}Sc	0.91	^{51}V	0.10	^{44}Ca	2.15	^{138}Ba, La, Ce	0.36
^{51}V	1.56	^{52}Cr	0.57	^{45}Sc	1.95	^{140}Ce	6.54
^{52}Cr	0.14	^{53}Cr	0.10	^{48}Ti, Ca	0.13	^{142}Ce, Nd	0.85
^{53}Cr	0.51	^{54}Cr	1.17	^{51}V	6.08	^{182}W	3.50
^{54}Cr	0.46	^{56}Fe	19.10	^{52}Cr	0.48	^{183}W	1.77
^{55}Mn	0.14	^{57}Fe	0.45	^{53}Cr	2.07	^{184}W, Os	4.09
^{56}Fe	7.36	^{58}Fe, Ni	32.31	^{54}Cr	0.61	^{186}W, Os	3.82
^{57}Fe	0.18	^{59}Co	0.40	^{55}Mn	0.28	^{206}Pb	0.21
^{58}Fe, Ni	45.07	^{60}Ni	13.93	^{56}Fe	6.48	^{207}Pb	0.19
^{59}Co	19.81	^{61}Ni	0.68	^{57}Fe	0.18	^{208}Pb	0.49
^{60}Ni	0.86	^{62}Ni	2.10	^{58}Fe, Ni	8.25		
^{61}Ni	2.97	^{64}Ni, Zn	5.06	^{60}Ni	3.30		
^{62}Ni	0.14	^{66}Zn	2.88	^{61}Ni	0.15		
^{64}Ni, Zn	1.62	^{67}Zn	0.47	^{62}Ni	0.54		
^{66}Zn	0.52	^{68}Zn	2.02	^{63}Cu	0.17		
^{68}Zn	0.40	^{88}Sr	0.11	^{64}Ni, Zn	1.48		
^{75}As	0.15	^{115}In, Sc	0.13	^{66}Zn	0.81		
^{79}Br	0.35	^{140}Ce	0.37	^{67}Zn	0.15		
^{81}Br	0.36	^{182}W	2.81	^{68}Zn	0.63		
^{138}Ba,La,Ce	0.14	^{183}W	1.54				
^{184}W, Os	0.12	^{184}W, Os	3.52				
^{208}Pb	0.17	^{186}W, Os	3.24				

balls had a diameter of up to 1 mm. At the ends of the filling, the fuel took the form of a sintered mass containing small metal balls. Furthermore, powder from the inner tube poured out. Using a magnet, a fraction was extracted from this powder consisting of filaments with a transverse dimension of about 0.1 mm and length up to 5 mm.

Several samples were subjected to mass-spectroscopic analysis at Vernadsky Institute of Geochemistry and Analytical Chemistry RAS using the ICP-MS method. The following were investigated: the initial fuel mixture, the metal ball from the spent fuel, the fuel at the edge of the filling, the substance accumulated between the inner and outer tubes, and the coating on the inner surface of the outer tube. Due to the large amount of information received, it is not possible to present it completely. Partially, the results of the analysis are shown in **Table 4**. In addition to the data for samples recovered from the reactor after its operation, information is given on the content of isotopes in the fuel, as well as in the ceramic and tungsten wire, before the experiment. This information is important, since the appearance of new elements can be associated not with transmutations, but with migration from structural materials, which is quite possible at high temperatures. Unfortunately, the ICP-MS method can not determine the content of isotopes with masses of 1-5, 12-22, 32, including isotopes of carbon, oxygen, nitrogen, fluorine and sulfur.

The obvious result is an increase in the content of many nuclides in comparison with their content in the initial fuel and structural materials. The exception is lithium (decrease in about 100 times) and aluminum in fuel (decrease in more than 10 times). We note a particularly great increase in the presence of boron, iron, gallium, cerium, zirconium, strontium and bismuth. The most significant anomalies are found in the powder accumulated in the space between the inner and outer tubes. Especially great amount of ^{140}Ce appeared: 6.3% (in the initial fuel <0.0001%). A significant amount of tungsten found in the samples after being inside the reactor is probably due to the migration of this element from the incandescent tungsten coil.

Table 5.

The ratio of nickel isotopes in fuel and near the core of the "Protok-6" reactor before and after the experiment.

%	^{58}Ni	^{60}Ni	^{61}Ni	^{62}Ni	^{64}Ni
Initial fuel	65.78	27.74	1.29	4.28	0.91
Metal ball	65.00	28.57	1.24	4.29	0.91
Fuel at edge	65.58	27.88	1.27	4.36	0.91
Coating on ceramics	65.32	28.16	1.37	4.24	0.91
Powder between tubes	66.74	26.71	1.23	4.41	0.91
Natural ratio	68.27	26.1	1.13	3.59	0.91

The investigation of possible changes in the isotopic composition of lithium and nickel is of great interest. Unfortunately, the very low content of lithium in the samples after experiment did not allow us to make reliable measurements. The results obtained for nickel are presented in the **Table 5**. Since the data on ^{64}Ni is unreliable due to the uncontrolled additive of ^{64}Zn, when compiling the table, the value from the reference book [30] was used for the ^{64}Ni fraction. Since this fraction is small, such an assumption can change the fractions of the remaining isotopes only slightly.

It can be seen that the data for the various samples studied differ somewhat from the natural ratio [30], but differ insignificantly between different measurements. A noticeable increase in the ^{62}Ni fraction, due to a decrease in the fraction of the remaining isotopes, that was found in the experiment in Lugano [1, 2] was not observed in any of the samples studied. It is possible that the effect is not visible due to the fact that the excess energy production in Lugano experiment was 60 times greater than in the described one.

8. REACTOR VV3

Reactor VV3 (**Fig. 12**) differs from the "Protok 6" reactor with a different heater design and

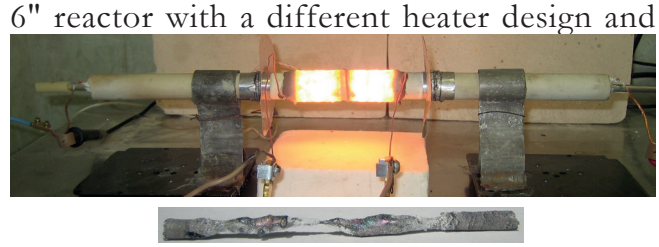

Fig. 12. *Reactor VV3 and spent fuel extracted from it.*

Table 6.
Isotope content (atomic %) in the reactor fuel "VV3" before and after reactor operation. Isotopes with a content > 0.1% are shown.

Fuel in the reactor VV3							
Before		After					
Initial fuel		Surface		Surface		Deep layer	
^{23}Na	2.61	^{10}B	0.15	^{75}As	0.17	^{10}B	0.14
^{24}Mg	0.15	^{11}B	0.67	^{79}Br	0.11	^{11}B	0.66
^{27}Al	2.93	^{24}Mg	1.50	^{81}Br	0.21	^{23}Na	3.72
^{29}Si	1.22	^{25}Mg	0.12	^{88}Sr	0.23	^{27}Al	1.02
^{39}K	2.52	^{26}Mg	0.27	^{90}Zr	0.20	^{28}Si	0.25
^{44}Ca	0.44	^{27}Al	1.14	^{107}Ag	1.13	^{51}V	2.14
^{45}Sc	0.34	^{28}Si	0.54	^{109}Ag	2.01	^{52}Cr	0.30
^{51}V	0.55	^{44}Ca	0.16	^{127}I	0.43	^{53}Cr	0.73
^{53}Cr	0.18	^{45}Sc	0.18	^{140}Ce	0.72	^{54}Cr	0.21
^{55}Mn	0.14	^{51}V	2.41	^{182}W	3.34	^{56}Fe	2.55
^{56}Fe	2.92	^{52}Cr	0.31	^{183}W	1.61	^{58}Fe, Ni	44.47
^{58}Fe, Ni	45.09	^{53}Cr	0.81	^{184}W, Os	3.39	^{60}Ni	18.23
^{60}Ni	19.01	^{56}Fe	0.42	^{185}Re	0.26	^{61}Ni	0.87
^{61}Ni	0.88	^{58}Fe, Ni	46.08	^{186}W, Os	2.91	^{62}Ni	2.83
^{62}Ni	2.93	^{60}Ni	19.34	^{187}Re, Os	0.60	^{64}Ni, Zn	0.87
^{64}Ni, Zn	1.00	^{61}Ni	0.96	^{206}Pb	0.18	^{75}As	0.12
^{66}Zn	0.13	^{62}Ni	3.02	^{207}Pb	0.13	^{79}Br	0.19
^{68}Zn	0.10	^{63}Cu	0.39	^{208}Pb	0.34	^{81}Br	0.19
^{79}Br	0.10	^{64}Ni, Zn	1.31			^{90}Zr	0.39
^{7}Li	0.60	^{65}Cu	0.16			^{92}Sr, Mo	0.14
^{81}Br	0.10	^{66}Zn	0.37			^{94}Sr, Mo	0.16
^{138}Ba, La, Ce	0.20	^{68}Zn	0.20			^{107}Ag	1.37
^{182}W	3.73					^{109}Ag	1.39
^{183}W	1.92					^{140}Ce	0.78
^{184}W	4.33					^{142}Ce, Nd	0.10
^{186}W, Os	4.29					^{182}W	3.49
^{206}Pb	0.26					^{183}W	1.90
^{207}Pb	0.50					^{184}W, Os	4.17
^{208}Pb	0.56					^{185}Re	0.38
						^{186}W, Os	3.72
						^{187}Re, Os	0.60
						^{208}Pb	0.17

the absence of a calorimeter. A mixture of nickel powder with lithium aluminum hydride weighing 1.5 g was used as fuel. The fuel contained pieces of tungsten wire with a total mass of 0.77 g. The reactor operated from June 14 to July 24, 2016, producing surplus power up to 330 W. A total of 790 MJ of excess heat was generated.

After the experiment was finished, the spent fuel, which looked like a drop-shaped ingot, was extracted from it. It was analyzed at Vernadsky Institute of Geochemistry and Analytical Chemistry RAS using the ICP-MS method, with separate analyzes of the surface and deeper layers. Partially the results of the analysis are shown in **Table 6**. In addition to the data for the samples recovered from the reactor after its operation, information is given on the content of isotopes in the initial fuel, including tungsten wires embedded in it.

It can be seen that the isotopic composition of fuel as a result experiment has changed noticeably. The content of boron, copper, cerium and silver increased significantly.

Just as in the above-described reactors, the data on the investigated samples, although slightly different from the natural ratio, differ insignificantly between each other (**Table 7**).

Table 7.
The ratio of nickel isotopes in fuel VV3 before and after reactor operation.

%	^{58}Ni	^{60}Ni	^{61}Ni	^{62}Ni	^{64}Ni
Initial fuel	65.93	27.98	1.19	3.98	0.91
Surface	65.79	27.61	1.37	4.31	0.91
Deep layer	66.36	27.20	1.29	4.23	0.91
Natural ratio	68.27	26.10	1.13	3.59	0.91

9. REACTOR KV3

KV3 reactor (**Fig. 13**) operated from December 20, 2016 until January 31, 2017, with an excess power of 100-200 watts. The integrated excess energy during the whole operating time of KV3 reactor is about 400 MJ. The main difference from the previous reactors is that it was loaded with 1.8 grams of nickel powder without an admixture of lithium aluminum hydride. Saturation with hydrogen was carried out by keeping it in hydrogen gas. In addition, unlike the above-described reactors, it had not a ceramic but a quartz outer tube. The heater

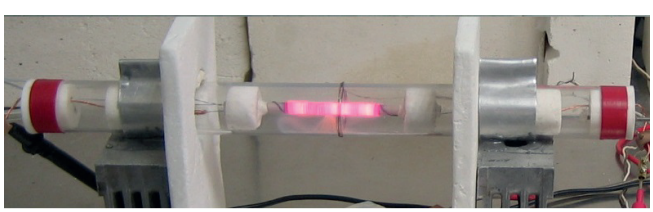

Fig. 13. *Reactor KV3 at the beginning of work.*

Table 8.

Isotope content (atomic %) in fuel and near the active zone of the KV3 reactor before and after reactor operation. Isotopes with a content > 0.1% are shown.

Before					
Initial fuel		Ceramics		Heater wire	
^{23}Na	0.33	^{27}Al	88.15	^{23}Na	0.47
^{39}K	0.38	^{23}Na	1.98	^{29}Si	0.27
^{56}Fe	0.45	^{24}Mg	0.82	^{39}K	0.40
^{58}Fe, Ni	64.49	^{25}Mg	0.12	^{44}Ca	0.12
^{60}Ni	27.63	^{26}Mg	0.14	^{56}Fe	0.21
^{61}Ni	1.18	^{29}Si	0.37	^{58}Fe, Ni	0.12
^{62}Ni	3.88	^{39}K	2.10	^{182}W	20.24
^{64}Ni, Zn	1.21	^{44}Ca	0.21	^{183}W	11.02
		^{47}Ti	0.88	^{184}W, Os	24.39
		^{48}Ti, Ca	0.18	^{185}Re	6.97
		^{54}Cr	0.14	^{186}W, Os	22.23
		^{56}Fe	3.17	^{187}Re, Os	11.85
		^{58}Fe, Ni	0.28	^{198}Hg, Pt	0.12
		^{60}Ni	0.11	^{200}Hg	0.14
		^{89}Y	0.13	^{202}Hg	0.13
		^{138}Ba, Ce	0.17	^{208}Pb	0.18

After						Substance appeared between inner and outer tubes	
Fuel central zone		Ceramics		Ceramics			
^{23}Na	0.13	^{11}B	0.13	^{64}Ni, Zn	0.22	^{23}Na	5.53
^{31}P	0.11	^{23}Na	15.61	^{66}Zn	0.11	^{24}Mg	0.50
^{39}K	0.14	^{24}Mg	1.06	^{76}Ge, Se	0.20	^{27}Al	0.32
^{56}Fe	0.23	^{25}Mg	0.13	^{88}Sr	0.21	^{29}Si	1.42
^{58}Fe, Ni	65.39	^{26}Mg	0.24	^{89}Y	0.22	^{31}P	0.16
^{60}Ni	26.15	^{27}Al	6.05	^{90}Zr	0.42	^{39}K	6.93
^{61}Ni	1.18	^{29}Si	4.26	^{92}Sr, Mo	0.22	^{44}Ca	0.88
^{62}Ni	3.99	^{39}K	15.26	^{94}Sr, Mo	0.17	^{45}Sc	0.82
^{63}Cu	0.84	^{43}Ca	0.26	^{109}Ag	0.10	^{54}Cr	0.26
^{64}Ni, Zn	1.14	^{44}Ca	3.15	^{127}I	0.16	^{56}Fe	7.04
^{65}Cu	0.42	^{45}Sc	2.04	^{138}Ba, Ce	0.39	^{58}Fe, Ni	1.80
		^{48}Ti, Ca	0.23	^{182}W	4.32	^{60}Ni	0.74
		^{51}V	0.22	^{183}W	2.35	^{62}Ni	0.10
		^{54}Cr	0.96	^{184}W	5.01	^{63}Cu	0.13
		^{55}Mn	0.10	^{185}Re	5.95	^{64}Ni, Zn	0.15
		^{56}Fe	21.14	^{186}W, Os	4.77	^{182}W	18.29
		^{57}Fe	0.15	^{203}Tl	0.15	^{183}W	10.44
		^{58}Fe, Ni	0.91	^{206}Pb	0.15	^{184}W	21.36
		^{60}Ni	0.37	^{207}Pb	0.15	^{186}W, Os	20.90
		^{63}Cu	0.14	^{208}Pb	0.40	^{198}Hg	0.17
						^{200}Hg	0.20
						^{202}Hg	0.18
						^{208}Pb	0.15

was made not from pure tungsten, but from a tungsten-rhenium alloy.

The ICP-MS analysis by Vernadsky Institute of Geochemistry and Analytical Chemistry RAS was used to investigate: fuel and structural materials prior to operation of the reactor, as well as fuel in the central zone and near the edge, powder from the space between the inner and outer tubes, and structural materials after work of the reactor. The results are partially shown in **Table 8**.

Just as in the reactors Protok 6 and VV3, a lot of tungsten appeared in the space between the inner and outer tubes. In addition to tungsten, a lot of iron, sodium, potassium, nickel, silicon, calcium, scandium and a number of other elements have accumulated there.

Comparing fuel before and after the experiment, one can see a decrease in the content of sodium, potassium and iron. Attention is drawn to the appearance of a significant amount of copper.

A lot of tungsten and rhenium appeared in the inner ceramic tube with fuel, which was wrapped with a heater. **Table 9** shows nuclides, the relative content of which in the ceramic tube has increased more than 10-fold.

It can be seen that in addition to tungsten and rhenium, the appearance of which can be

Fig. 14. *Reactor KV3 opened after ending of experiment.*

Table 9.

Relative content of nuclides (atomic %) in the ceramic tube before and after the operation of the KV reactor. Nuclides are shown whose content has increased more than 10 times.

	Before	After	After/ before		Before	After	After/ before
^{10}B	0.0008	0.0318	41.8	^{114}Cd, Sn	0.0005	0.0064	11.9
^{11}B	0.0054	0.1277	23.4	^{116}Cd, Sn	0.0022	0.0275	12.8
^{29}Si	0.3709	4.2603	11.5	^{117}Sn	0.0011	0.0129	12.0
^{43}Ca	0.0158	0.2638	16.7	^{118}Sn	0.0024	0.0422	17.9
^{44}Ca	0.2123	3.1461	14.8	^{119}Sn	0.0014	0.0165	11.7
^{45}Sc	0.0507	2.0384	40.2	^{120}Sn, Te	0.0034	0.0670	19.5
^{46}Ti, Ca	0.0074	0.0836	11.3	^{122}Te	0.0007	0.0101	15.0
^{51}V	0.0028	0.2151	78.0	^{127}I	0.0062	0.1589	25.7
^{53}Cr	0.0057	0.0753	13.3	^{128}Te	0.0002	0.0046	22.8
^{64}Ni, Zn	0.0186	0.2224	12.0	^{124}Te	0.0008	0.0092	11.4
^{66}Zn	0.0099	0.1102	11.1	^{130}Te	0.0006	0.0101	16.7
^{67}Zn	0.0014	0.0211	15.0	^{182}W	0.0076	4.3168	567.8
^{68}Zn	0.0080	0.0808	10.1	^{183}W	0.0035	2.3489	671.7
^{72}Ge	0.0001	0.0037	27.2	^{184}W	0.0076	5.0087	658.8
^{75}As	0.0001	0.0138	102.2	^{185}Re	0.0006	5.9469	9827.0
^{76}Ge, Se	0.0115	0.1976	17.2	^{186}W, Os	0.0089	4.7748	537.6
^{77}Se	0.0001	0.0055	82.2	^{198}Hg	0.0001	0.0321	238.5
^{78}Se, Kr	0.0028	0.0542	19.7	^{199}Hg	0.0007	0.0248	33.5
^{79}Br	0.0028	0.0560	20.3	^{200}Hg	0.0004	0.0560	138.9
^{81}Br	0.0040	0.0790	19.6	^{202}Hg	0.0005	0.0606	128.8
^{83}Kr	0.0001	0.0009	13.7	^{203}TI	0.0015	0.1498	101.2
^{107}Ag	0.0067	0.0863	13.0	^{204}Pb, Hg	0.0010	0.0101	10.0
^{109}Ag	0.0071	0.1020	14.3				
^{113}Cd, In	0.0001	0.0009	13.7				

explained by its migration from the heater coil, the boron content in the ceramic tube greatly increased, as well as nuclides with atomic masses of 43-53, 64-83, 107-130, 198-208.

Table 10 shows the results of an analysis of the ratio of nickel isotopes in fuel, as well as in the surrounding ceramic and in the substance accumulated between the inner and outer tubes, before and after the reactor operation. When analyzing the isotope composition, in order to avoid the errors associated with the registration of ^{64}Zn, the ^{64}Ni share was taken from the reference book [30].

Table 10.

The ratio of nickel isotopes in fuel and near the core of the KV3 reactor before and after reactor operation.

%	^{58}Ni	^{60}Ni	^{61}Ni	^{62}Ni	^{64}Ni
Initiak fuel	65.93	27.98	1.19	3.98	0.91
Fuel after work	65.74	28.17	1.20	3.98	0.91
Substance between tubes	66.66	27.33	1.30	3.79	0.91
Ceramics	67.65	27.37	0.82	3.26	0.91
Natural ratio	68.27	26.10	1.13	3.59	0.91

It can be seen that the isotopic composition of nickel in fuel before and after the experiment remained practically unchanged. Some differences are noticeable in the results obtained for the ceramic tube and the substance between the tubes. But these results can not be considered accurate, since the concentration of nickel in the samples studied is not high enough for reliable analysis.

In addition to the Vernadsky Institute of Geochemistry and Analytical Chemistry RAS, the analysis of KV3 fuel before and after the experiment, as well as the substance from the space between the inner and outer tubes, was made by the research company Coolescence LLC, Boulder, Colorado, USA. EDS analyzes were performed using an electronic scanning microscope, as well as analyzes using the ICP-MS method. These studies confirmed the insignificant changes in the isotopic composition of the fuel, the appearance in the fuel of about 1% of copper and the presence of many nuclides in the substance from the space between the tubes10.

10. DISCUSSION

Thus, a significant change in the nuclide composition as a result of the operation of the investigated nickel-hydrogen reactors occurs not only in the fuel, but also in the ceramics surrounding the reactor core. In addition, a substance containing sodium, potassium, silicon, iron, boron, calcium, zinc and many other elements accumulates in the cavity between the inner and outer tubes. Especially great amount of tungsten appeared. It is reasonable to assume that the source of tungsten is the hot spiral of the heater. The most understandable mechanism of substance migration is evaporation in places with high temperature and condensation in less heated places. As the measurements show, the temperature of the heater wire reaches 1700° C. But even at this temperature, the density of tungsten vapor ($<10^{-10}$ Pa) is too low for such mechanism to

work with a noticeable intensity. Obviously, more complex physicochemical processes take place with the participation of hydrogen and other reagents that may be present in the reactor. It is possible that a number of other elements appear as a result of migration from structural materials, since sodium, potassium, silicon, calcium, iron and a number of other elements are contained in appreciable quantities in the heater wire, thermocouples and in ceramics. However, there are some elements (cobalt, cerium, gallium, germanium, arsenic, selenium, cadmium, tellurium) that appeared in significant quantities, which are practically not presented in the initial fuel and structural materials. This indicates the possibility of their appearance as a result of nuclear transmutations. For example, cerium can be a product of the fission of tungsten

$$^{182}W \rightarrow {}^{140}Ce + {}^{42}Ca + 4e + 76{,}04\ MeV \qquad (3)$$

Attention is drawn to the appearance of a significant amount of copper in the fuel of the KV3 reactor (0.84% ^{63}Cu and 0.42% ^{65}Cu) with a total mass of about 20 mg. It can be assumed that this is due to the course of nuclear reactions given below

$$^{62}Ni + {}^{1}H \rightarrow {}^{63}Cu + 6.125\ MeV$$
$$^{64}Ni + {}^{1}H \rightarrow {}^{65}Cu + 7.450\ MeV \qquad (4)$$

About 200 MJ are released as a result of the reactions (4), when 20 mg of copper is formed. This energy release does not contradict the total excess heat release in the KV3 reactor (about 400 MJ). In addition to heat generation, the appearance of such a quantity of copper should cause a decrease in the relative content of ^{62}Ni by 0.8% and ^{64}Ni by 0.4%. The data presented in Table 8 does not show such changes. It should be noted that the predicted changes lie within the limits of a possible measurement error, and the ^{64}Ni content is generally difficult to measure reliably due to uncontrolled additions of ^{64}Zn.

11. CONCLUSION

Numerous experiments conducted in different laboratories, confirm the allocation in Nickel-hydrogen systems, thermal energy, many times exceeding the heat dissipation possible in chemical processes. The level of accumulated empirical knowledge in this area allows us to reflect on the transition from experimental models to a variety of practical applications, extremely efficient and environmentally friendly technologies.

In the course of processes in nickel-hydrogen systems, the changes of the elemental and isotopic composition of matter are detected. This indicates that an anomalously high heat generation in these systems is probably related to transformations at the nuclear level. The fact that such transformations occur at very low nuclear standards, temperatures, and the lack of hard nuclear radiations and radioactivity, indicates the need to look for unusual approaches to explain the detected effects. The problem is that the explanation is not confined to finding ways of overcoming the Coulomb barrier to the close approach and merging of the nuclei [13]. The most mysterious is the absence (or very small intensity) of nuclear radiation in the process of cold transmutations and education only isotopes that do not exhibit radioactivity.

1. The isotopic and elemental composition of the substance in four nickel-hydrogen reactors of various designs with an excess energy output from 100 to 790 MJ has been analyzed. Not only the changes in fuel, but also the materials adjacent to the active zone have been investigated. In addition, the composition of the substance accumulating in the cavity of the reactor near the active zone has been studied.

2. There were no significant changes in the isotopic composition of nickel and lithium, except for the analysis of the fuel of the AP2 reactor at Uppsala University (Sweden).

3. A significant increase in the concentration of impurities of a number of nuclides has been detected not only in fuel, but also in structural

elements adjacent to the active zones of the reactors. In addition to tungsten and rhenium, the appearance of which can be explained by migration from the heater coil, the content of boron increased greatly, as well as nuclides with atomic masses of 43-53, 64-83, 107-130, 198-208.

4. In the substance that was found in the cavity of the reactor near the active zone, in addition to tungsten, a lot of iron, sodium, potassium, nickel, silicon, calcium, scandium and a number of other elements accumulated.

REFERENCES

1. Fleishmann M, Pons S, Hawkins M. Electrochemically induced nuclear fusion of deuterium. *J. Electroanal. Chem.*, 1989, 261:301-308.
2. Filimonenko IS. Demonstratsionnaya termoemissionnaya ustanovka dlya yadernogo sinteza [Demonstrational therm-emission device for nuclear fusion]. *Materials 3 Sci. Symp. "Perestroyka estestvoznaniya* [Restructuring of Natural history"-92, Volgodonsk, Russia, 17-19 apr. 1992 (in Russ.).
3. Velikodny VYu, Eremeev AV, Kazennov AYu, etc. Experiments on the registration of abnormally high relative heat output during high-voltage electrolysis of heavy water. *Materials 12 Ross. Conf. on cold transmutation of nuclei of chemical elements,* Sochi, 19-26 Sept. 2004, p.98-109 (in Russ.).
4. Pan'kov VA, Kuzmin BP. Demonstrational technique of synthesis of elements from water in the plasma of electric discharge. *Actual problems of modern science,* 2008, 5(44):112-116 (in Russ.).
5. *Vzaimoprevrashcheniya khimicheskikh elementov* [Interconversion of chemical elements]. Under the editorship of V.F. Balakirev. Ekaterinburg, Ural Branch of RAS Publ., 2003, 64 p.
6. *Controlled Nucleosynthesis. Breakthroughs in Experiment and Theory.* Series: Fundamental Theories of Physics. Vol. 156. Eds. Adamenko S, Selleri F, Merwe A., 780 p., Springer, 2007.
7. Urutskoev LI, Liksonov VI. Observation of transformation of chemical elements during electric discharge. – http://arxiv.org/ftp/physics/papers/0101/0101089.pdf.
8. Bazhutov YuN, Velikodny VYu, Grishin VG et al. Neutrons, Gamma-Rays & Tritium Diagnostic at Electrolysis in Water Solutions. *Proc. 13 Intern. Conf. on Condensed Matter Nuclear Science* (*ICCF-13*). Sochi, June 25-July 1, 2007, p. 156-169.
9. Parkhomov AG. Cold transmutation of nuclei: strange results and attempts at their explanations. *Zhurnal formiruyushchikhsya napravleniy nauki* (*ZhFNN*) [Journal of unconventional science], 2013, 1(1):71-76 (in Russ.).
10. Kervran C. *Transmutations Biologique et Physique Moderne*. Paris, Librairie Maloine S.A., 1982.
11. Vysotskii VI, Kornilova AA. *Nuclear fusion and transmutation of isotopes in biological systems.* Wiley, New York, 2003, p. 161.
12. Focardi S, Habel R, Piantelli F. Anomalous Heat Production in Ni-H Systems. *Nuovo Cimento,* 1994, 107A(1):163-167.
13. Focardi S, Gabbani V, Piantelli F et al. Large excess heat production in Ni-H systems. *Nuovo Cimento,* 1998, 111A(11):1233-1242.
14. Battaglia A, Daddi L, Focardi S et al. Neutron emission in Ni-H systems. *Nuovo Cimento,* 1999, 112A(9):921-931.
15. Focardi S, Gabbanib V, Piantelli F et al. Evidence of electromagnetic radiation from Ni-H Systems. *Proc. 11 Intern. Conf. on Condensed Matter Nuclear Science* (*ICCF-11*), 2004, Marseille, France. - http://www.nichenergy.com.
16. http://www.nichenergy.com.
17. Bazhutov YyN, Koretsky VP, Parkhomov AG. Research of radiation effects at saturation $LaNi_5$, nickel and beryllium with hydrogen. *Materials 19 Ross. Conf. on cold transmutation of nuclei and ball lightning.* Krinitsa, Krasnodarsky Krai, 3-10 September 2012, pp. 129-142 (in Russ.).
18. Celani F, Marano EF, Spallone A. Cu-Ni-Mn alloy wires, with improved sub-micrometric surfaces, used as LENR device by new transparent, dissipation-type, calorimeter. *J. Condens. Matter Nucl. Sci.*, 2014, 13:56-67.
19. Takahashi A, Kitamura A, Taniike A et al. Anomalous exothermic and endothermic data observed by nano-Ni-composite samples. – https://mospace.umsystem.edu/xmlui/handle/10355/36494.
20. Bazhutov YuN. The heat generator Rossi and Focardi. *Izobretatelstvo*, 2012, 12(1):49-59 (in Russ.).
21. *Patent 0001387256, Italy.* International application WO/2009/125444. Date: Aug.04, 2008.

22. Levi G, Foschi E, Höistad B. et al. Indication of anomalous heat energy production in a reactor device. – arXiv:1305.3913v3 [physics.gen-ph].
23. Levi G, Foschi E, Höistad B. Observation of abundant heat production from a reactor device and of isotopic changes in the fuel. – http://www.sifferkoll.se/sifferkoll/wp-content/uploads/2014/10/LuganoReportSubmit.pdf.
24. Parkhomov AG. Otchet mezhdunarodnoy komissii ob ispytanii vysokotemperaturnogo teplogeneratora Rossi [Report of the international Commission on the testing of high-temperature heat generator Rossi]. *ZhFNN*, 2014, 2(6):57-61 (in Russ.). – http://www.unconv-science.org/pdf/6/parkhomov2-ru.pdf.
25. Parkhomov AG. Issledovanie analoga vysokotemperaturnogo teplogeneratora Rossi [The study analogue high-temperature heat generator Rossi]. *ZhFNN*, 2015, 3(7):68-72 (in Russ.) – http://www.unconv-science.org/pdf/7/parkhomov-ru.pdf.
26. Parkhomov AG. Nikel-vodorodnye reaktory, sozdannye posle publikatsii otcheta ob eksperimente v Lugano [Nickel-hydrogen reactors, created after the publication of the report on the experiment in Lugano]. *ZhFNN*, 2016, 11(11):58-62 (in Russ.) – http://www.unconv-science.org/n11/parkhomov.
27. Alabin KA, Andreev SN, Parkhomov AG. Rezultaty analiza izotopnogo i elementnogo sostava topliva nikel-vodorodnykh reatorov [The results of the analysis of the isotopic and elemental composition of the fuel Nickel-hydrogen reactors]. *ZhFNN*, 2015, 3(10):49-53 (in Russ.) – http://www.unconv-science.org/pdf/10/alabin-ru.pdf.
28. Parkhomov AG. Rezultaty ispytaniy novogo varianta analoga vysokotemperaturnogo teplogeneratora Rossi [The results of the tests of the new version of analogue high-temperature heat generator Rossi]. *ZhFNN*, 2015, 3(8):34-38 (in Russ.) – http://www.unconv-science.org/pdf/8/parkhomov-ru.pdf.
29. Parkhomov AG. Dlitelnye ispytaniya nikel-vodorodnykh teplogeneratorov v protochnom kalorimetre [Long-term testing of Nickel-hydrogen generators in a flow calorimeter]. *ZhFNN*, 2016, 4(12-13):74-79 (in Russ.) – http://www.unconv-science.org/pdf/12/parkhomov-ru.pdf.
30. *Fizicheskie velichiny. Spravochnik* [A physical values. Handbook]. Edited by I. S. Grigoriev and E. Z. Meilikhova Moscow, Energoatomizdat Publ., 1991, 1232 p.

In memory of Alexander Didyk

MULTINUCLEAR REACTIONS IN CONDENSED HELIUM

Gennady V. Mishinsky

Joint Institute for Nuclear Research, http://www.jinr.ru/
6, str. Joliot Curie, Dubna, Moscow Region 141980, Russian Federation
mysh@jinr.ru

Abstract. **Helium high-pressure chambers filled with gaseous helium at pressures of about 1.1 and 3 kbar were irradiated by bremsstrahlung gamma rays with a maximum energy of 10 MeV during ~10^5 s. Inside the reaction chambers "extraneous" chemical elements are found which were absent prior to the onset of irradiation. To explain the appearance of synthesized elements, a new mechanism is proposed: multinuclear reactions. These reactions are due to the creation of nuclear molecules which consist of several helium nuclei. Nuclear molecules are formed by the fusion of several orthohelium atoms. It is proposed to execute experiments aimed at recording multinuclear reactions by passing electric discharges through helium or through a mixture of helium and hydrogen at a pressure of several bars.**

Keywords: **condensed matter nuclear science, low energy transmutation, multinuclear reactions, nuclear molecules, Bose–Einstein condensate**

PACS: 03.75.Mn; 03.75.Nt; 25.70.Jj; 31.15.xg

Bibliography – 17 references *Received 25.04.2017*

RENSIT, 2017, 9(1):94-105 **DOI: 10.17725/rensit.2017.09.094**

Contents

1. INTRODUCTION

The phenomenological model of low energy nuclear reactions implies fusion of multiple atomic nuclei into one single formation with its subsequent decay into multiple nuclei [1-3]. This model assumes that such reactions take place due to the appearance in the excited condensed matter of local regions or capsules containing a large number of atoms [4]. Inside of such capsules, conditions for physical processes and the structures of atoms and nuclei may change. Herein it is not important how exactly the matter is excited and the capsules are formed, whether it occurs under explosion-induced compression or electric discharge, through cavitation or electrolysis, a chemical or biochemical reaction, or due to radiation.

In a series of studies carried out by A.Yu. Didyk et al. at the Flerov Laboratory Nuclear Reactions of JINR [5-7, over 40 papers], metallic specimen in gaseous deuterium, hydrogen or helium under pressures of hundreds and thousands of bars were irradiated by braking gamma rays with E_{max} of 10 MeV and 23 MeV. Under such pressures, the density of atoms in the gas is comparable with the density of atoms in solids or liquids. Therefore, from here on we shall use such a term as *condensed gas*. Similar investigations were done using chambers filled with pure condensed gases as hydrogen, helium [8-11] and xenon [12] under irradiation by gamma rays with E_{max} of 10 MeV. In all of these experiments, extraneous chemical elements which had not been present prior to irradiating were found in the reaction chambers upon completion of irradiation. Such foreign elements range from hydrogen up to bismuth. This paper presents results of experiments on the synthesis of chemical elements under the action of braking radiation with E_{max} of 10 MeV in condensed ^{4}He (99,999) under pressures of 1.1 kbar

and 3.05 kbar. In order to explain the appearance of extraneous chemical elements in these experiments, a new mechanism of multinuclear reactions is introduced.

2. EXPERIMENTS ON THE SYNTHESIS OF CHEMICAL ELEMENTS IN HELIUM

The helium high-pressure chamber (HeHPC) is shown in **Fig. 1**. The chamber body (3) and entrance-window plug (2) are made of beryllium bronze. A liner (6) and a sleeve (7) made of copper with 99.9% purity are placed inside the chamber. The chamber filled with helium (5) has the following inner dimensions: the length is 15mm; the diameter is 8 mm; and the volume is 0.754 cm^3. Upon filling of the HeHPC and prior to its irradiation, the helium pressure was monitored using a strain gauge pressure sensor (8) during several weeks.

Irradiation of the HeHPC was carried out by braking gamma rays (1) with a maximal energy of 10 MeV at the MT-25 electron accelerator at the FLNR JINR. The electron current at the tungsten convector shaped as a disk of 40 mm diameter and 2.5 mm thickness and used to transform the electron flux into gamma rays was $(1\text{-}1.5)\cdot10^{14}$ s^{-1}. The electron beam was 6-7 mm in diameter. The beam spread of gamma quanta at the intensity half-height amounted to $10°\pm1°$ in horizontal and $8°\pm1°$ in vertical direction. Right behind the convector, an electron absorber of 25 mm thickness made from D16T duralumin was placed. Irradiation was performed during 7-8 hours a day. The irradiation parameters [8-11] are given in **Table 1**: № - experiment number; P – helium pressure at the start of irradiation; ΔP – helium pressure difference between the start and end of irradiation; T – irradiation duration; I – electron current.

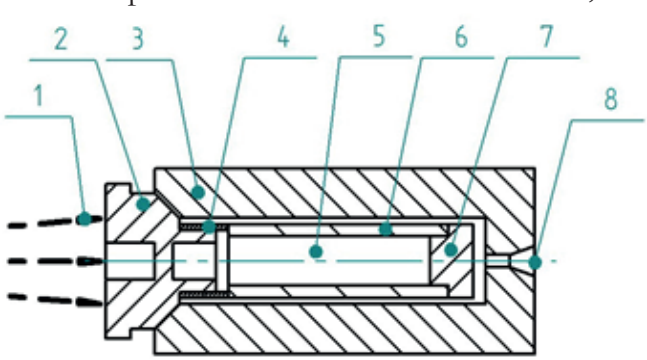

Fig. 1. *The high-pressure chamber HeHPC.*

Table 1

Parameters of the radiation

№	P, kbar	ΔP, bar	ρ, atm/sm^3	T, s $\cdot10^{-5}$	I, s^{-1} $\cdot10^{-14}$
1	1.1	666	$1.5\cdot10^{22}$	1.02	1.2-1.5
2	3.05	63	$2.6\cdot10^{22}$	1.0	1-1.2

Upon completion of irradiation, helium was released from the HeHPC to the surrounding environment and the chamber was opened. The most impressive result in the first experiment under 1.1 kbar pressure was the observation of thin black foils of cylindrical shape and considerable size (4) inside the HeHPC. The foils (**Fig. 2**) were composed predominantly of carbon and left oily stains on paper. The latter fact points to the presence of liquid oils on the foils such as hydrocarbons and to the synthesis of hydrogen.

In the second experiment under 3.05 kbar no carbon foils were observed. This is suggestively due to a small drop of pressure in the chamber during the irradiation: in the second experiment, it amounted to 63 bar, and in the first one was 666 bar (Table 1). Using scanning electron microscopy (SEM) and x-ray microprobe analysis (MPRA) studies were made of the element compositions of the "window plug" from beryllium bronze, anomalous structures and microparticles (objects) formed on the inner surfaces of the

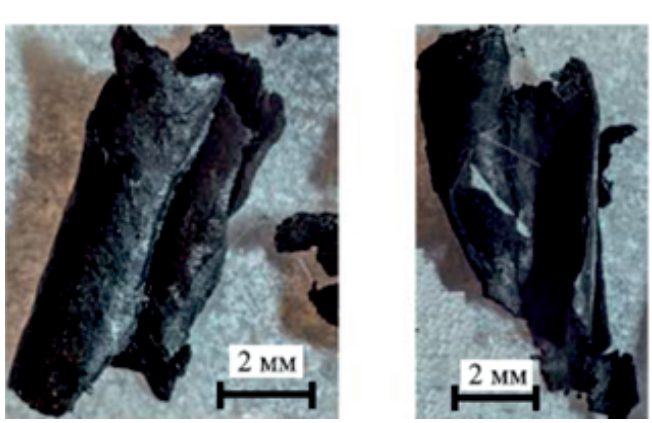

Fig. 2. *Pictures of black foils*

liners and sleeves under irradiation. All of the SEM and MPRA studies were organized at two independent certified laboratories: at the analytical centre of the Skobeltsyn Laboratory of Lomonosov Moscow State University and at the Research Institute for Perspective Materials and Technologies in Moscow. MPRA of the obtained structures and microparticles was done with the electron beam excitation area ~ 1-4 μ^2. In some cases the investigated object was scanned with a microscope electron beam along the band where several x-ray spectra were obtained.

Figs. 3 and 4 display averaged element concentrations of K in atomic %, obtained in the experiments under helium pressures of 1.1 kbar and 3 kbar, as a function of the nucleus charge *Z*. In the case with 1.1 kbar averaging was done over 11 measurements of various objects, and in the case with 3 kbar, over 17 measurements. When comparing the images, one can see that the set of elements in the first experiment under 1.1 kbar is more diverse than in the second experiment under 3 kbar pressure. Both element distributions are characterized by presence of the group of light elements from $_{6}$C to $_{30}$Zn. In the first experiment, along with light chemical elements such elements as $_{33}$As (arsenic), $_{50}$Sn (tin), $_{52}$Te (tellurium), $_{56}$Ba (barium), $_{73}$Ta (thantalum) and $_{82}$Pb (lead) were obtained. However, these chemical elements were not found in the second experiment. Only one element with the nucleus charge $Z > 30$ as $_{47}$Ag (silver) was present. This distinction is apparently also due to the small drop of pressure in the chamber during the irradiation in the second experiment under 3 kbar.

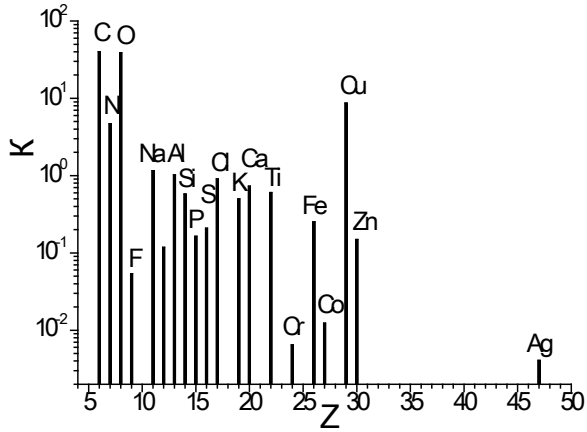

Fig. 4. *Concentrations of elements on P = 3 kbar.*

On the basis of the facts that carbon foils and chemical elements with $Z > 30$ were obtained in the experiment under 1.1 kbar pressure while they were almost not observed in the experiment under 3 kbar, it can be assumed that the synthesis rate for the chemical elements depends on the helium pressure. Synthesis reactions proceed at 1.1 kbar more intensively than at 3 kbar pressure. This apparently points to the existence of an optimal value of gas pressure under which the reaction rate becomes maximal, with all other conditions being equal.

3. MULTINUCLEAR REACTIONS

Fig. 5 shows averaged concentrations of chemical elements determined by 5 measurements (black dots). Two measurements were done at the carbon foil and the other three, at the microparticles [9, Tables 3, 4]. This figure was drawn and

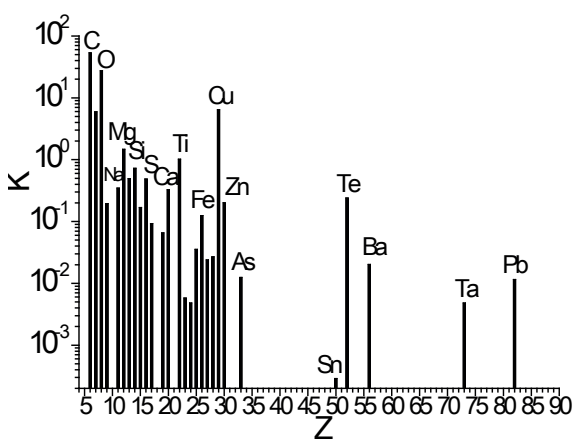

Fig. 3. *Concentrations of elements on P = 1.1 kbar.*

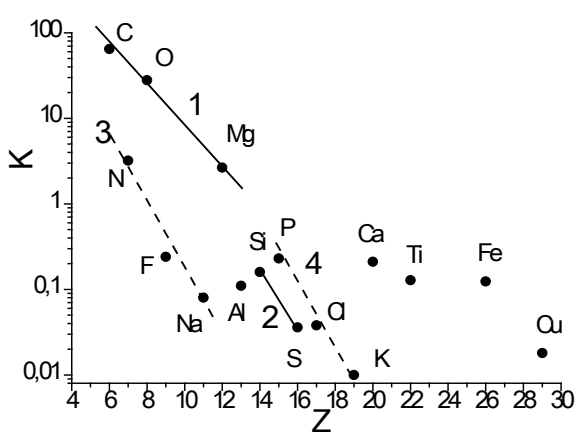

Fig. 5. *The concentration of the elements in five dimensions.*

analyzed first, along with figures 3 and 4. Conspicuous here are the groups of elements. The first and second ones are the groups of chemical elements which are even by the nucleus charge. They are represented by the elements such as carbon-oxygen-magnesium and silicon-sulfur. The third and fourth are the groups of chemical elements which are odd by the nucleus charge. They include such elements as nitrogen-fluorine-sodium and phosphorus-chlorine-potassium. One can draw a straight line through the dots of every group. All lines of such groups are numbered in Fig. 5.

Since the elements in the groups fall behind each other by a charge that is a multiple of two, i.e. by ${}^{4}_{2}He$ nucleus, it can be assumed that under the action of gamma rays multinuclear reactions proceed in condensed helium.

The emergence of even chemical elements ${}^{N}_{Z}A$ can be presented as a result of fusion into a compound of $(n - 1)$ helium nuclei from a common formation comprised of "n" helium nuclei, with simultaneous emission of one helium nucleus:

$$n \cdot {}^{4}_{2}He \rightarrow {}^{4(n-1)}_{2(n-1)}A + {}^{4}_{2}He + Q.$$

Odd chemical elements ${}^{N}_{Z}B$ are then a result of fusion into a compound of "n" helium nuclei, but with the emission of a proton:

$$n \cdot {}^{4}_{2}He \rightarrow {}^{4n-1}_{2n-1}B + p + Q,$$

where Q is the energy released in the reaction. The common formation produced from individual helium nuclei is a nuclear molecule, or the so-called transmolecule [4]. It is believed that the existence of a transmolecule consisting of helium nuclei is due to nuclear and electromagnetic interactions. The reaction with emission of helium from a transmolecule will have a larger cross section than the reaction with emission of a proton because the outgoing helium nucleus is not involved in the fusion process. The possibility of formation of transmolecules decreases exponentially as the number of helium nuclei in the transmolecule increases

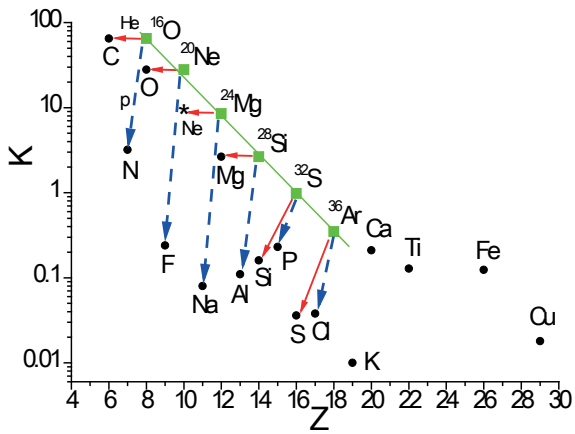

Fig. 6. *Transformation of transmolecules ($n \cdot {}^{4}He$) emission of helium or proton.*

(**Fig. 6,** shown by the green line). If during the fusion of helium nuclei into a compound the ratio of the cross section with helium emission to the cross section with proton emission is preserved, the yields of the respective products have to decrease exponentially as well. Such behavior in the product yields can be observed in Fig. 5, lines 1-4. In Fig. 6 the reactions of transformation of transmolecules from ${}^{16}O$ to ${}^{36}Ar$ (the green squares) with the emission of helium (solid arrow) or a proton (dotted arrow) are schematically shown by arrows. The ${}^{16}_{8}O$ transmolecule consisting of four helium nuclei transforms into ${}^{12}_{6}C$ with the emission of helium or into ${}^{15}_{7}N$ with the emission of a proton. The ${}^{20}_{10}Ne$ transmolecule composed of five helium nuclei transforms into ${}^{16}_{8}O$ with the emission of helium or into ${}^{19}_{9}F$ with the emission of a proton, etc. During the fusion of helium nuclei into a compound, it can evaporate neutrons. For the yields of final products, neutron evaporation and subsequent β^{+}-decay of the compound are equivalent to the emission of a proton from this compound. Beginning with the ${}^{20}_{10}Ne$ transmolecule the reactions with the production of two or more fragments become possible, for example: $5 \cdot {}^{4}He \rightarrow {}^{12}C + 2 \cdot {}^{4}He$ and $6 \cdot {}^{4}He \rightarrow {}^{12}C + {}^{12}C$.

A nuclear transmolecule is formed due to the successive capture of orthohelium nuclei or other transmolecules. The average spacing between helium atoms at a temperature of

300 K under pressures of 1 kbar and 3 kbar is $4.1 \cdot 10^{-10}$ m and $3.4 \cdot 10^{-10}$ m, while the mean time between the collisions of helium atoms is ~ $3 \cdot 10^{-13}$ s. Therefore, a transmolecule is a stable formation on a nuclear time scale of $10^{-20\text{-}22}$ s. It should be assumed that nuclear forces binding the nuclei together and Coulomb repulsive forces preventing the nuclei from instant fusion coexist in a nuclear transmolecule in balance.

The characteristics of multinuclear reactions are displayed in **Table 2.** № indicates the line number. The second column presents reaction products − the isotopes of elements produced in the reactions. The content of the respective isotope in the natural mixture is shown in the brackets. The isotopes with the plus sign A^+ are β^+-radioactive isotopes emanating e^+ (positrons). Their lifetime is also given here. In the third column multinuclear reactions with the formation of the $n \cdot {}^4He$ transmolecule are displayed. The binding energy ($\mathcal{E}$) of the reaction products is given in the fourth column, and the calculated energy (Q) released in the reaction, in the fifth column. The sixth column presents recoil energy (q) for the helium, proton, and neutron.

Table 2

Multinuclear reactions in helium

№	Reaction product	Reaction $n \cdot {}^4He$	$\mathcal{E}$, keV	Q, keV	q, keV
1	^{7}Li (92.5%)	2·^{4}He - p	39245	-17347	
2	^{8}Be	2·^{4}He - eγ	56500	-92	
3	^{9}Be	3·^{4}He - ^{3}He	58165	-19004	
4	^{11}B (80.0%)	3·^{4}He - p	76205	-8682	
5	^{11}C+ 20.4 m	3·^{4}He - n	73440	-11447	
6	^{12}C (98.9%)	3·^{4}He - eγ	92162	7275	
7	^{12}C	4·^{4}He - ^{4}He	92162	7275	5 456
8	^{15}N (0.37%)	4·^{4}He - p	115492	2309	2 165
9	^{15}O+ 2 m	4·^{4}He - n	111956	1227	1 150
10	^{16}O (99.8%)	5·^{4}He - ^{4}He	127619	14437	11 549
11	^{19}F	5·^{4}He - p	147801	6323	6 007
12	^{19}Ne+ 17 s	5·^{4}He - n	143781	2302	2 187
13	^{20}Ne(90.5%)	6·^{4}He - ^{4}He	160645	19166	15 972
14	^{23}Na	6·^{4}He - p	186564	16790	16 090
15	^{23}Mg+ 11 s	6·^{4}He - n	181725	11951	11 453
16	^{24}Mg(79.0%)	7·^{4}He - ^{4}He	198257	**28483**	**24 922**
17	^{27}Al	7·^{4}He - p	224952	26882	25 922
18	^{27}Si+ 4 s	7·^{4}He - n	219357	21287	20 527
19	^{28}Si(92.23%)	8·^{4}He - ^{4}He	236537	38467	34 193
20	^{31}P	8·^{4}He - p	262917	36551	35 409
21	^{31}S+ 2.6 s	8·^{4}He - n	256738	30373	29 424
22	^{32}S (95.02%)	9·^{4}He - ^{4}He	271781	45415	40 369
23	^{35}Cl (75.8%)	9·^{4}He - p	298290	43549	42 339
24	^{35}Ar+ 1.8 s	9·^{4}He - n	291462	36801	35 779
25	^{36}Ar (0.34%)	10·^{4}He -^{4}He	306716	52055	46 849
26	^{39}K(93.26%)	10·^{4}He - p	333724	50767	49 498
27	^{39}Ca+ 0.9 s	10·^{4}He - n	326411	43454	42 367

It is seen from Table 2 that such chemical elements as lithium, beryllium and boron are not produced in simple reactions with the emission of helium-3 and a proton since $Q < 0$. These elements emerge paired with the radioactive isotopes of nitrogen, oxygen, fluorine and others in the reactions with participation of five or six helium nuclei. Such reactions require an essential reorganization of the compound formed through fusion of all helium nuclei in the transmolecule. That is why respective reaction cross sections are suppressed.

In Table 2 attention should be paid to the reactions presented in lines 2 and 6. Transmolecules consisting of two and three helium nuclei can be relatively stable. In the first case, stability of the ^{8}Be (beryllium) transmolecule results, first and foremost, from the impossibility of fusion of two helium nuclei due to the energy causes, with $Q < 0$. In the second case, notwithstanding that the bond energy of ^{12}C equal to 92161.7 keV is greater than the sum of bond energies of three helium nuclei, $3 \cdot {}^4He$ = 84887 keV, by the value ~7274.7 keV, the reaction $3 \cdot {}^4He \rightarrow {}^{12}C + 6e-$ is suppressed. This is due to the retardation in the redistribution of the released energy resulting only from the electromagnetic interaction between carbon and six atomic electrons [13]. The six electrons are bound into the Bose condensate. Their bond energy is ~ 3 keV. Apart from this reaction, the following reaction

can take place as well: $3 \cdot {}^4He \rightarrow {}^{12}C + 6e^- + \gamma$. A gamma quantum with an energy of 4438keV is produced in this reaction through the decay of the ^{12}C excited state.

Now, let us have a look at line 16 in Table 2. The bond energy of the ^4He nucleus equal to 28295.6745 keV is lower than the energy released in the reaction $7 \cdot {}^4He(^{28}Si) \rightarrow {}^{24}Mg + {}^4He +$ 28483 keV; however, it is greater than the ^4He recoil energy of 24922 keV. Thus, the reaction energy is not enough to destroy the produced ^4He nucleus. Therefore, the Mg point in Fig. 5 remains at line 1. However, the cross section of the reaction with the emission of a proton $7 \cdot {}^4He(^{28}Si) \rightarrow {}^{27}Al + p + 26882$ keV increases, and the Al point shifts from line 3 upwards in Fig. 5.

In line 19 from Table 2, in the reaction $8 \cdot {}^4He(^{32}S) \rightarrow {}^{28}Si + {}^4He + 38467.2$keV, the released energy and recoil energy of ^4He is already larger than the bond energy of the ^4He nucleus. Consequently, it is the reaction with the emission of a proton and production of P (phosphorus) that chiefly takes place here. The reaction with the escape of helium and formation of Si (silicon) is suppressed, with the Si point in Fig. 5 shifting from line 1 downward. The same happens in the event of the reaction with nine helium nuclei, $9 \cdot {}^4He(^{36}Ar)$, with the production of S (sulphur) and Cl (chlorine). Under changed conditions, when reactions with helium emission are suppressed, we can observe a new systematics in the reaction cross sections. This is reflected in the fact that the values of chemical element yields in the reactions shift to other lines, 2 (Si-S) and 4 (P-Cl-K) (Fig. 5).

The production of chemical elements starting from chlorine with $Z > 19$ (Fig. 5) is apparently governed by secondary processes. Under such processes, multinuclear interactions take place with the participation of transformed atoms (transatoms [15]) of chemical elements obtained in the preceding reactions. The 100-percent production of ^{15}N and ^{36}Ar in multinuclear reactions, lines 8 and 25 in Table 2, should be given special attention. In the natural mixture their presence amounts to 0.37% and 0.34%. Therefore, in mass analyses predominant registration of ^{15}N and ^{36}Ar isotopes provides evidence of the multinuclear reactions proceeding in condensed helium.

4. FORMATION OF TRANSMOLECULES. ELECTRON BOSE-CONDENSATE

For the formation of a transmolecule from helium nuclei, helium atoms have to transform into helium transatoms (**Fig. 7**). Helium atoms are unique for such transformation. As is known, helium atoms have two stable basic states: parahelium 1^1S_0 and orthohelium 2^3S_1. The existence of orthohelium [14] and transhelium [15] is due to the exchange interaction associated with the indistinquishability of the electrons (identity principle). The exchange interaction is characterized by the exchange energy ("A"). As opposed to the electrostatic energy "C", the contribution of exchange energy into the total energy of the system may be of different signs depending on whether the spin part of the wave function is symmetric or antisymmetric. The correction ΔE to the total energy of system (1) connected with the electron interaction is determined in frames of the perturbation theory:

$$\Delta E = C \pm A, \quad (1)$$

where the sign "+" refers to the antisymmetric ↑↓ spin state S = 0; and the sign "–" indicates the symmetric ↑↑ spin state S = 1. In an atom, the energy of Coulomb repulsion between the electrons "C" and the exchange energy "A" (exchange integral) are positive. This is why due to the exchange energy attractive forces between the electrons (orthohelium) and repulsive forces (1) are present in a helium atom concurrently. The spins of electrons in parahelium are antiparallel ↑↓, while in

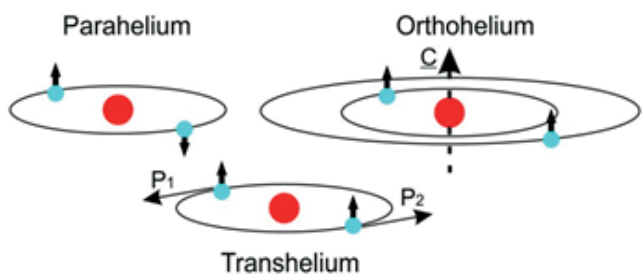

Fig. 7. *Main states of a helium atom.*

orthohelium they are parallel ↑↑ (Fig. 7). As distinct from parahelium, the electrons in orthohelium cannot be present in the same state according to the Pauli principle. Therefore, in orthohelium the electrons are found in different states, at different energy levels (Fig. 7). The main states of parahelium and orthohelium differ by 19.77 eV. The parahelium lines are singlets (S = 0), and orthohelium lines are triplets (S = 1). The characteristic lines in the optical spectrum have a wavelength of 501.6 μm in parahelium, and of 587.6 μm in orthohelium. The transition with two-photon emission $2^3S_1 \rightarrow 1^1S_0 + 2\gamma$ between ortho- and parahelium is strongly suppressed and has a lifetime of $2.5 \cdot 10^8$ s. The one-photon, magnetic-dipole decay of the 2^3S_1-state has a lifetime of $8 \cdot 10^3$s. However, radiationless transitions during an interaction with an incident electron or another atom are also possible.

Orthohelium, unlike parahelium, has a strong magnetic field since magnetic moments of its electrons are always parallel. The radius R_1 of the first electron in orthohelium (or in a parahelium atom) is $3.1 \cdot 10^{-11}$ m; and the radius R_2 of the second orthohelium electron is $8.76 \cdot 10^{-11}$ m. The magnetic moment of the electron $\boldsymbol{\mu}_e$ produces a magnetic field with the magnetic induction vector $\mathbf{B}_\mu$ equal to [16]:

$$\mathbf{B}_\mu = \mu_0 \frac{3\mathbf{n}(\boldsymbol{\mu}_e \cdot \mathbf{n}) - \boldsymbol{\mu}_e}{r^3}, \qquad (2)$$

where $\mu_0 = 1.26 \cdot 10^{-6}$ H/m is the magnetic constant; $\mu_e = 9.29 \cdot 10^{-24}$ J/T = $5.79 \cdot 10^{-5}$ eV/T; r is the distance from the electron up to the point where the field is calculated; $\mathbf{n}$ is a unitary vector in the direction r. At the centre of an orthohelium atom, the magnetic field near the nucleus $\mathbf{B}_0$ is calculated using the formula (2): $\mathbf{B}_0 = -\mu_0\boldsymbol{\mu}_e/R_1^3 - \mu_0\boldsymbol{\mu}_e/R_2^3 = -393 - 17 = -410T$. The negative sign indicates that magnetic field at the atom's centre is directed in the opposite direction to the magnetic moments of the electrons. The magnetic field B_{R2} at the point located on the C axis (Fig. 7) at the distance R_2 from the nucleus is ~ 70 T and directed parallel to the magnetic moments of the electrons $\boldsymbol{\mu}_e$. The C axis is restored perpendicularly to the electron orbitals and passes through the atom's centre. At the distance $c^2 \gg R_2^2$, on the C axis the magnetic induction vector for orthohelium from expression (2) is $\mathbf{B}_C = \frac{4\mu_0\boldsymbol{\mu}_e}{c^3}$ and parallel to $\boldsymbol{\mu}_e$. Consequently, two orthohelium atoms are attracted to each other with magnetic self-focusing along the axis C. The energy of their magnetic interaction along the axis C is: $E_\mu = 4\mu_e \cdot B_C$. At a distance R_2, the magnetic interaction energy is equal to ~ 0.016 eV. As two orthohelium atoms approach each other, the energy of their interaction enhances.

With a decreased distance between the orthohelium atoms, the motion of the electrons in one orthohelium will synchronize owing to the electromagnetic interaction with the motion of the electrons in the second orthohelium. As a consequence of such synchronization, both inner- and outer-shell electrons of the orthohelium atoms will be located at the orbitals in diametrally opposite positions (**Fig. 8**). Due to this, the sums of momenta of the outer- and inner-shell electrons separately are equal zero, $\mathbf{P}_1 = -\mathbf{P}_2$ (Fig. 7), which is one of the conditions for the electron pairing. Moreover, due to the additionally arising attractive exchange interaction between the electrons of different orthohelium atoms and to strong magnetic field, such electrons form Cooper pairs with S = 1 (Fig. 8) bound into a boson. These electron bosons are common for the two helium nuclei. So, an excited nuclear transmolecule of ^{8}Be has one Cooper electron pair at the outer orbital and another Cooper pair at the inner orbital (Fig. 8). Because the outer pair represents a boson, it

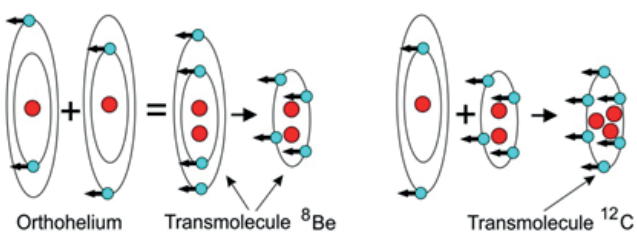

Fig. 8. *The formation of transmolecules ^{8}Be and ^{12}C.*

immediately passes into the ground state with the emission of two photons. Consequently, this leads to electron Bose condensate around the transmolecule. The radius of a ^{8}Be transmolecule is $R_{Be} = 1.32 \cdot 10^{-11}$m. The magnetic field B_0 at the centre is $2 \cdot 10^4$ *T* and at the distance $1.2 \cdot R_{Be}$ from the centre the magnetic field B_R equals $4 \cdot 10^3$ *T*.

The magnetic interaction of an orthohelium atom and a ^{8}Be transmolecule, as well as exchange interaction between their electrons result in the transformation of the orthohelium atom into a transhelium atom (Fig. 8). The radius R_{He} of transhelium is $2.64 \cdot 10^{-11}$ m, $B_0 = 1.3 \cdot 10^3$ *T*. Further interaction of transhelium with the ^{8}Be transmolecule leads to the formation of a ^{12}C (carbon) transmolecule. The radius of the ^{12}C transmolecule is as follows: $R_C = 0.89 \cdot 10^{-11}$m. The magnetic field B_0 at the centre is 10^5T and at the distance $1.2 \cdot R_C$ from the centre the magnetic field B_{Rc} equals $2 \cdot 10^4$T. The possibility of existence of transmolecules is due to nuclear forces and ultrastrong inhomogeneous magnetic fields of 10^4–$3 \cdot 10^8$ T at their centres [15].

As was noted in section 3, ^{8}Be and ^{12}C transmolecules can be stable. Therefore, they can interact both with orthohelium, transforming it into transhelium, and with each other. These interactions result in the formation of other, heavier nuclear transmolecules. **Fig. 9** displays a few combinations composed of orthohelium atoms, ^{8}Be and ^{12}C transmolecules, which lead to the production of: A – an ^{16}O (oxygen) transmolecule; B – a ^{20}Ne (neon) transmolecule; C – a ^{24}Mg (magnesium) transmolecule; and D – a ^{28}Si (silicon) transmolecule. For example, an ^{16}O transmolecule can be obtained by combining a ^{12}C transmolecule with orthohelium or by combining two ^{8}Be transmolecules. The arrows on the right (Fig. 9) show the isotopes of chemical elements produced in multinuclear reactions with the emission of a helium (^{4}He) nucleus, a proton (**p**) and a neutron (*n*) (Table 2).

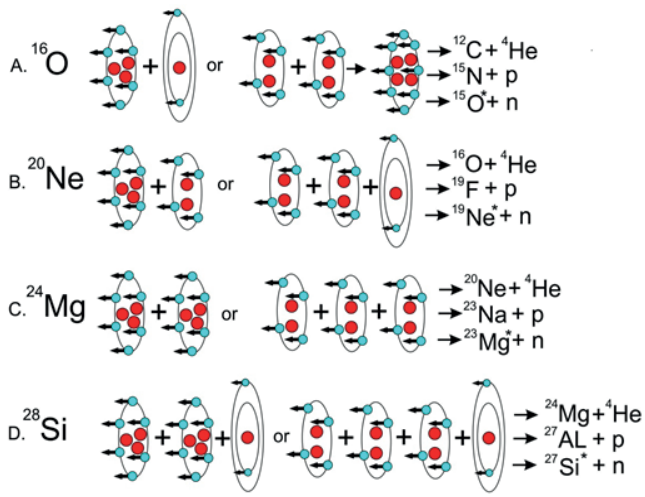

Fig. 9. *The formation and collapse of transmolecules.*

Thus, production of transmolecules depends on the orthohelium formation cross section and its spatial density. Upon formation of transmolecules multinuclear reactions proceed automatically. Consequently, the cross sections of multinuclear reactions are comparable with the cross sections of atomic processes!

5. NUCLEAR PROCESSES IN IONIZED HELIUM

It is evident from the earlier sections that gamma quanta are not involved in multinuclear reactions. They only ionize helium atoms. The ionization potential of a helium atom is equal to 24.59 eV. During the recombination – capture of free electrons by helium ions – a mixture of two "gases" of parahelium and orthohelium is formed. Since the level densities for orthohelium are thrice greater than with parahelium, the probability for orthohelium formation in the course of ion recombination ought to be also three times greater. The orthohelium density should be such that the magnetic attraction forces between them can lead to the formation of transmolecules. This is attained, firstly, due to the small interatomic spacing in condensed helium, and, secondly, as Compton electrons of large recoil energy produced by intensive fluxes of gamma rays generate in helium "plasma tracks" with a high density of ions and electrons.

The greater the ion density, the greater is the density of orthohelium. With increasing density of the electrons, the radiationless

transitions of orthohelium into parahelium grow more intensive. So, there are two contrary processes. Thus, with the given electron density of specific ionization, there exists apparently an optimal density, condensed helium pressure, with which the orthohelium density is maximal.

In condensed gases, a "plasma track" represents a "capsule" inside which the conditions for physical processes and the atomic and nuclear structures are subject to change. The use of intensive fluxes of gamma quanta proves to be the most suitable method for ionization of condensed helium owing to their high penetrability through the thick walls of the reaction chamber. Other radiations, coupled with high ionization, do not have such a penetrating power. It should be noted that the products of multinuclear reactions such as fragments, alpha particles and protons have a higher density of specific ionization than the electrons. Therefore, they, in their turn, produce along their tracks plasma of higher density than the one generated by the electrons. So, it is likely that the conditions for a chain reaction are thereby created!

Since the multinuclear reactions are connected with ionization of helium, attempts should be made to register nuclear radiations, for example, gamma quanta, by passing electric discharge through helium under pressure up to several bar.

As stated in section 3, the following reaction may proceed in the ^{12}C transmolecule during the fusion of three helium nuclei: $3\cdot{}^4He \rightarrow {}^{12}C + 6e^- + \gamma$. A gamma ray with an energy of 4438 keV is emitted in this reaction due to the decay of the excited state of ^{12}C. A gamma ray of the same energy may be produced in the reaction: $4\cdot{}^4He \rightarrow {}^{12}C + {}^4He + \gamma$. In multinuclear reactions with evaporation of a neutron (Table 2), β^+-radioactive isotopes emitting e^+ positrons are produced. A positron-electron annihilation results in the emission of two gamma rays, each of energy 511 keV.

An attempt should be made to register the above gamma quanta during the irradiation of helium by a powerful alpha or beta source placed inside a gas chamber under a pressure of ~ 1 kbar.

It must not be ruled out that in experiments [17] conducted in the fifties of the previous century under the leadership of Igor Kurchatov with the aim of exploring the possibility of thermonuclear reactions in gaseous atmosphere of hydrogen, deuterium, helium and their mixture, the emergence of neutrons and powerful x-radiation in the energy range 300-400 keV is due to multinuclear processes. – Plasma must not be heated, and it is very bad to do so!

Clearly, the synthesized chemical elements during their excitation by electric discharge will produce characteristic radiation in the optical region. For this reason, considerable interest is attracted to experiments aiming to register characteristic optical radiation produced by nuclear reaction products and, what is more interesting, by transmolecules.

All the electrons in the even-charge, light transmolecules are bound into bosons and have a binding energy in the transmolecule and an energy of transitions between the excited levels of hundreds electron-volt [15]. That is why it would be of interest to study odd-charge transmolecules which have one electron not bound into the boson. Supposedly, such a transmolecule can be obtained from a mixture of hydrogen and helium. Indeed, ^8Be and ^{12}C transmolecules produced under the action of electric discharges may merge with a protium atom and its nucleus (proton) due to magnetic attraction and strong central magnetic fields, thereby forming an odd transmolecule. The magnetic field B_0 of the protium atom (hydrogen) at the centre is equal to 79 T; and at the distance $1.2\cdot R_H$ from the centre, $B_{RH} = 16$ T. In the case when the proton adds to the ^8Be transmolecule, a ^9B (boron) transmolecule is formed. When the proton adds to the ^{12}C transmolecule, this

results in the formation of a ^{13}N (nitrogen) transmolecule. The ^{13}N transmolecule is less stable than the ^{12}C one. It decays according to the reaction $^{13}N \rightarrow {}^{12}C + p$, possibly with the emission of a gamma ray with the energy 4438 keV.

Such nuclear transmolecules are hydrogen-like atoms with heavy multinuclear formations at the centre. The outer-shell electron in such transmolecules moves around in its orbital in the strong magnetic field produced by paired electrons. In the approximation when the radii of orbitals of the outer-shell electron in ^{9}B and ^{13}N transmolecules are equal to the hydrogen atom radius $R_H = 5.29 \cdot 10^{-11}$ m, the magnetic induction vector B_{RH} of the ^{9}B transmolecule at R_H is equal to 316 T, whereas for the ^{13}N transmolecule B_{RH} equals 474 T ($\mathbf{B}_r = \frac{P_e \mu_0 \boldsymbol{\mu}_e}{r^3}$, where P_e is the number of paired electrons [15]). For these reasons the outer-shell electron orbitals at the ^{9}B and ^{13}N transmolecules are displaced relative to the hydrogen atom orbitals in accordance with the corrections for the given masses to the Rydberg constant (3) and split into two sublevels by formula (4):

$$R_A = R/(1 + m_e/M_A), \quad (3)$$

$$\Delta E = \pm \mu_e \cdot B_{RH}, \quad (4)$$

where R_A is the Rydberg constant for an atom with the nucleus of mass M_A; R is the Rydberg constant; m_e is the electron mass. In our case, M_A equals: 2 or 3·^{4}He nuclei plus a proton. In **Table 3**, the main Balmer lines ($n \rightarrow 2$, n is the principal quantum number) in the visible range are given in nanometers for the hydrogen atom

Table 3

Balmer's lines of transmolecules ^{9}B, ^{13}N

	H_α 3→2	H_β 4→2	H_γ 5→2	H_δ 6→2	H_ε 7→2	H_ζ 8→2
λH	656.279	486.133	434.047	410.174	397.007	388.9
λ^{9}B	655.961	485.898	433.837	409.976	396.815	388.7
λn ^{9}B	655.853 655.870 656.052 655.069	485.844 485.952	433.794 433.880	409.937 410,015	396.779 396.851	388.67 388.73
λ^{13}N	655.952	485.890	433.830	409.969	396.809	388.7
λn ^{13}N	655.759 655.816 656.088 656.114	485.809 485.971	433.765 433.895	409.911 410.027	396.755 396.863	388.65 388.75

(λH), displaced (λ_{MA}) for the ^{9}B (λ^{9}B) and ^{13}N (λ^{13}N) transmolecules and split for the ^{9}B (λn^{9}B) and ^{13}N (λn^{13}N) transmolecules. Displacement of transitions, according to (3), is calculated by the formula: $\lambda_{MA} = \lambda_H M_H (M_A + m_e)/M_A (M_H + m_e)$, where M_H is the proton mass. All of the levels of the outer-shell electrons of ^{9}B and ^{13}N transmolecules are not only displaced but split, according to (4), into two states. For a ^{9}B transmolecule the ground state splitting (n = 1) by energy is $\Delta E = \pm 1.83 \cdot 10^{-2}$ eV and for a ^{13}N transmolecule the ground-state splitting is $\Delta E = \pm 2.74 \cdot 10^{-2}$ eV (4).

Since the radii of hydrogen electron orbitals: $r_n = \hbar \cdot n^2/2 \cdot m_e^2$, then $r_2 = 2.1 \cdot 10^{-10}$ m, $r_3 = 4.8 \cdot 10^{-10}$ m. The magnetic fields of the ^{9}B transmolecule at r_2 and r_3 are B_{r2} = 4.91 T and B_{r3} = 0.43 T, and for the ^{13}N transmolecule, B_{r2} = 7.37 T and B_{r3} = 0.65 T. Correspondingly, r_2 and r_3 level splitting for the ^{9}B transmolecule is $\Delta E_{r2} = \pm 2.85 \cdot 10^{-4}$ eV and $\Delta E_{r3} = \pm 2.51 \cdot 10^{-5}$ eV; and for the ^{13}N transmolecule level splitting at r_2 and r_3 is $\Delta E_{r2} = \pm 4.26 \cdot 10^{-4}$ eV and $\Delta E_{r2} = \pm 3.6 \cdot 10^{-5}$ eV. Consequently, one can observe four lines in the spectrum which are doublets Hα of the split levels r_2 and r_3. Because at the orbitals with $n \geq 4$ the magnetic fields produced by the paired electrons are small, two lines will be observed in the spectrum for H_β, H_γ and other transitions. It is seen from Table 3 that the distances between the split states are considerable and must be well registered by spectroscopic instrumentation.

Thus, there is a relatively simple nuclear and spectral methods by which you can try to register in electric discharges flow multinuclear reactions in helium or mixtures of helium with hydrogen when the pressure up to several bar.

6. CONCLUSION

When irradiation of condensed helium at pressures of 1.1 and 3.05 kbar braking gamma quanta with a maximum energy of 10 MeV, the volume of the reaction chamber discovered the chemical elements missing before the start of the exposures.

The emergence of extraneous chemical elements can be explained by multinuclear reactions. Multinuclear reactions take place due to the formation of nuclear transmolecules composed of several helium nuclei. Primary nuclear transmolecules of ^{8}Be with electrons that are pairwise bound into bosons with S = 1 are produced through fusion of two orthohelium atoms. Heavier transmolecules are formed via fusion of orthohelium and lighter transmolecules with each other.

The atoms of orthohelium are produced in helium during its ionization by gamma radiation with subsequent recombination of the emerged ions. So, the cross sections of low-energy multinuclear reactions directly depend on the special density of orthohelium, i.e. on the cross sections of the atomic processes.

Further experiments should be conducted to register multinuclear reactions by passing electric discharges through helium or a mixture of helium and hydrogen under pressure up to several bar. In the case of their registration, it is proposed to revert to the idea of power production using electric discharges in condensed light gases such as hydrogen, deuterium, helium and their mixtures [17].

REFERENCES

1. Kuznetsov VD, Mishinsky GV, Penkov FM, Arbuzov VI, Zhemenik VI. Low energy transmutation of atomic nuclei of chemical elements. *Annales de la Fondation Louis de Broglie,* 2003, 28(2):173-214.
2. Mishinsky GV, Kuznetsov VD. Element distribution in the products of low energy transmutation. Nucleosynthesis. *Annales de la Fondation Louis de Broglie*, 2008, 33(3-4):331-356; *Materials of 14-th Russian Conf. on cold transmutation of nuclei of chemical elements,* 2008, Moscow, pp. 79-97.
3. Urutskoev LI, Filippov DV. On the possibility of nuclear transformation in low-temperature plasma from the viewpoint of conservation laws. *Annales de la Fondation Louis de Broglie,* 2004, 29(3):1187-1205.
4. Mishinsky GV. Transatoms – Transnuclei, and their properties. *The materials of the 18th Russian conference on cold transmutation of nuclei of chemical elements*, 2012, Moscow, pp. 94-106.
5. Didyk AYu, Wiśniewski R. Nuclear reactions, induced by gamma quanta, in palladium saturated with deuterium surrounded by dense deuterium gas. *Europhys. Lett*, 2012, 99(2):22001.
6. Didyk AYu, Wiśniewski R. Results of irradiation of aluminum and a homogeneous alloy YMn_2 γ-quanta with energy of 23 MeV in the atmosphere of molecular deuterium at a pressure of 2 kbar. *Particles and nuclei, letters,* 2014, 11, 3(187):284-298.
7. Didyk AYu. Nuclear reactions of fusion and fission chemical elements and the formation of new structures in dense gases H_2, D_2 and He at irradiation 10 MeV-tion of γ-quanta. *Physics and chemistry of materials processing,* 2015, 2:5-19.
8. Didyk AYu, Wiśniewski R and Wilczynska-Kitowska T. The carbon-based structures synthesized through nuclear reactions in helium at 1.1 kbar pressure under irradiation with braking γ-rays of 10 MeV threshold energy. *Europhys. Lett.*, 2015, 109(22001):1-6.
9. Didyk AYu, Wiśniewski R., Properties of structures based on carbon synthesized in nuclear reactions in helium at 1.1 kbar pressure under irradiation with braking γ-quanta with a threshold energy of 10 MeV. *Particles and nuclei, letters,* 2016, 13, 4(202):777-792.
10. Didyk AYu, Wiśniewski R. Nuclear reactions, synthesis of chemical elements and new structures in dense helium at 1.1 kbar pressure under irradiation with braking γ-quanta with a threshold energy of 10 MeV. *Preprint P15-2014-50. JINR*, Dubna, 2014, 40 p.
11. Didyk AYu, Wiśniewski R. Synthesis of new structures and formation of chemical elements in dense helium at a pressure of 3.05 kbar under irradiation with braking γ-quanta with a threshold energy of 10 MeV. *Preprint P15-2014-87, JINR*, Dubna, 2014, 23 p.
12. Didyk AYu, Gulbekian HS, Mushinski GW, Sabelnikov AV. The synthesis of micro

particles of complex composition in the chamber high-pressure xenon (550 bar) when irradiated by bremsstrahlung with maximum energy of 10 MeV. *Preprint P15-2016-19, JINR*, Dubna, 2016, 49 pages.
13. Kalman P, Keszthelyi T. Lattice effect in solid state internal conversion. *Phys. Rev. C*, 2009, 79(0316026):1-4.
14. Heisenberg W. Über die Spektra von Atomsystemen mit zwei Elektronen. *Z. Phys.*, 1926, 39(7):499-518.
15. Mishinsky GV. Magnitnye polya transatomov. Spinovy-nuklidny-elektronny kondensat [Magnetic fields of transatoms. Spin-nuclide-electronic condensate]. *International Journal of Unconventional Science*, 2017, 15-16(5):6-25 (in Russ.).
16. Landau LD, Lifshitz EAT. *Field theory.* Moscow, Nauka Publ., 1973, 138 p.
17. Kurchatov IV. About possibility of creation of thermonuclear reactions in gas discharge. *UFN*, 1956, 59(4):603-618.

TRANSITION OF BISMUTH TO LEAD IN THE PULSE ELECTROMAGNETIC FIELD

Vladimir F. Balakirev

Institute of Metallurgy of the Ural Branch of the Russian Academy of Sciences, http://www.imet-uran.ru
Ekaterinburg 620016, Russian Federation
vfbal@mail.ru

Valeriy V. Krymsky, Nataliya V. Plotnikova

South Ural State University, http://www.susu.ru
Chelaybinsk 45408, Russian Federation
krymskiivv@susu.ru, plotnikovanv@susu.ru

Absract. **Impact of powerful nanosecond electromagnetic impulses (NEMI) on fusions containing lead and bismuth is considered. The main controlled property is chemical composition. Special pulse generators are used for influence. They produce pulses of the positive polarity with duration of 1 nanosecond on a half-height, with amplitude of 6-10 kV and repetition frequency of 1 kHz. Processing of NEMI is carried out directly in a crucible into which the copper tube or a core is inserted. Outputs of the generator connect with a crucible and a tube. Time of processing is tens of minutes. The level of α-radiation and β-radiation of solid metal is measured before and after processing. There are given the results of 4 experiences in which the reduction of amount of bismuth by 8-10% and the same in size increase of amount of lead is noted. For one of experiences the analysis of the chemical composition is carried out on three devices, various on type. The theory of electronic capture under the influence of NEMI and change of isotope structure without change of mass of a kernel are offered as theoretical base. Results which describe transformation of tens of grams of bismuth into the same amount of lead are absent in available literature.**

Keywords: **impulse, field, nanosecond, transition, bismuth, lead**

UDC 544.032

Bibliography –12 references *Received 28.03.2017*

RENSIT, 2017, 9(1)106-112 **DOI: 10.17725/rensit.2017.09.106**

Contents:

1. INTRODUCTION

Some results of influence of powerful nanosecond electromagnetic impulses (NEMI) on fusions of metals and solutions of salts are given [1-3]. The essence of the method is that fusion of metal is affected by influence of unipolar electromagnetic impulses lasting less than 1 ns with an amplitude more than 5 kV without carrier frequency. Impulses are generated by special generators which have small dimensions and weight, consume the power from a network less than 100 W. In our researches we used generators with next parameters: amplitude of impulses is 7-10 kV, duration is 1 ns, the frequency of repetition is 1 kHz.

The impulse from the generator exit is transferred on the radiator. We used radiators in the form of a piece of the coaxial line. The crucible performs function of the external conductor and has to be

the current conductor, for example, graphite. The nonconducting crucible is inserted into carrying-out screen. The central conductor is made from copper or graphite and located in a protective tube. It separates a radiator from fusion and is made from quartz. It can not be used at low temperatures of fusion.

Many mechanical properties change at the hardened metal after processing of fusions of metals by NEMI. For example, durability and plasticity increase at the same time, impact strength at low temperatures increases [1-4]. Questions of change of the chemical composition of fusions and solutions under the influence of big pulse currents are considered in [5-7].

The purpose of work is experimental research of impact of powerful NEMI on change of the chemical composition of lead-bismuth fusion.

2. EXPERIMENTAL RESEARCHES

Experience 1. Radiation of Roze alloy (Pb, Bi, Sn). Alloy is standard. The composition of elements according to the passport (masses%) is the next: Pb – 32.87; Bi – 49.11; Sn – 17.95; Sb – 0.04; Cu – 0.01; As – 0.01; Fe – 0.006.

Experimental conditions: the mass of an alloy is 0.5 kg, the crucible graphite Ø45 with internal dimensions, depth is 90 mm. Radiator is the copper rod Ø5 160 mm long in a quartz test tube of Ø10 mm. Alloy melting is made, stirring is carried out by a quartz stick and test taking of the initial test (No. 3) is carried out in a ceramic tank. Radiation of the melt was executed out of the furnace. Generator parameters: amplitude was 6 kV, frequency was 1 kHz. Time of radiation was 15 min. Initial temperature of radiation was 350ºC, finite – 135ºC. Irradiated test was selected in a ceramic tank after melt agitation (test No. 4).

Sawdust was made from the received castings of tests 3 and 4 by a file. The analysis of a chemical composition of sawdust was carried out on the atomic and adsorption spectrophotometer "Quantum-2A". The atomic and adsorption spectrophotometer "Quantum-2A" was certified in the state system. The relative error of the analysis makes ±2%, with confidential probability 0.95. Elements Bi, Cd, Sn, Sb, Cu, Zn, Fe are defined. The Pb element is defined as "remaining to 100%". Analysis results are presented in **Table 1**.

It is visible that good data fits on the initial test with passport data and good coincidence of balance of transmutation of elements takes place. Also coincidence of balance of elements conversion – the sums of minuses (–7.4) and pluses (+7.4) – is observed.

Experience 2. Radiation of an alloy of Pb, Bi. The alloy is prepared independently. Lead is granulated, composition in % masses: Pb – 99.88, Sb – 0.1, other Bi, Fe, Cu, Sn, Ag, As less than 0.06); Bismuth is granulated (composition: Bi – 97.9, Pb – 1.8, Ag – 0.08, other Cu, Fe less than 0.001).

The hinge plate from Lead of 0.55 kg and Bismuth of 0.45 kg was used for preparation of the melt. The crucible is graphite Ø55, height is 95 mm. Lead was heating to 400ºC, then Bismuth was added, stirring was made, a test taking of the initial test (No. 21) was carried out. Radiation of a melt was made out of the furnace. The radiator is the copper

Table 1

Composition of Elements, % masses

Element	Pb	Bi	Sn	Sb
Initial, No.3	32.3	50.0	17.5	0.2
Irradiated, No. 4	39.66	43.1	17.0	0.24
Change	+7.36	-6.9	-0.5	+0.04

rod Ø5, length is 120 mm in a quartz test tube of Ø10 mm. Generator parameters: 6 kV, 1 kHz. Time of radiation is 15 min. Initial temperature is 400ºC, finite – 250ºC. The irradiated test (No. 22) was molded after melt agitation. The analysis of tests 21 and 22 in the form of sawdust was carried out on the atomic and adsorption spectrophotometer "Quantum-2A". Results are presented in **Table 2**.

It is visible that the composition of elements in the initial sample is very close to the value determined by the weight composition of 55% Pb and 45% Bi with the accounting of the additional composition of 1.8% of Lead in Bismuth. Transformation of 8% of Bismuth into Lead is watched after radiation. The rule of balance is observed.

Measurement of radioactivity of Lead and Bismuth in the form of sawdust in mass of 1 g was carried out on low-background installation of UMF-2000. Results of measurements are the next: exceeding of a α-radiation background for Lead – by 15 times, for Bismuth – by 7 times. Results of the measurements of activity for initial and irradiated tests are the next: exceeding of a α-radiation background for the initial test No. 21 by 6.25 times, for the irradiated test No. 22 – by 14.7 times. There was the significant increase in the β-radiation level of the irradiated sample after radiation. Measurements of radioactivity of these samples in the year gave background exceeding in the initial test by 5.6 times, in irradiated – by 3.6 times. Level change of β-radiation is in error limits.

Experience 3. Radiation of Roze alloy (Pb, Bi, Sn). The alloy was bought from the manufacturer. Experimental conditions: the mass of an alloy is 0.5 kg, the alundovy crucible with Ø55 internal dimensions, depth is 70 mm in the screen from a copper foil. Radiator is the copper rod Ø5, 160 mm long in a quartz test tube of Ø10 of mm. Heating of an alloy is made to 400ºC, stirring and a test taking of the initial test (No. 23) are carried out. Generator parameters are 6 kV, 1 kHz, time of radiation is 15 min. Initial temperature is 400ºC, finite − 215ºC. Irradiated test (No. 24) was selected after stirring.

The analysis of tests 23 and 24 in the form of sawdust was carried out on the atomic and adsorption spectrophotometer "Quantum-2A". Results are presented in **Table 3**.

It is visible that a large amount of Bismuth passed into Lead after radiation. Transition of small part of Tin to Lead is also watched. The rule of balance is observed: –12.9→+12.9.

Results of radioactivity measurements of initial and irradiated tests are the next: exceeding of a α-radiation background for the initial test – by 115 times, for irradiated test – by 82 times. There was the considerable reduction of the α-radiation level of the irradiated sample after radiation. Measurements of radioactivity of these samples in the year gave background exceeding in the initial test by 35.6 times, in

Table 2

Composition of Elements, % masses

Element	Pb	Bi	Sn	Sb
Initial, No.21	57	43.0	0.005	0.014
Irradiated, No. 22	65	35.0	0.006	0.014
Change	+8.0	-8.0	+0.001	0

Table 3

Composition of Elements, % masses

Element	Pb	Bi	Sn	Sb
Initial, No.23	15.4	67.0	17.4	0.2
Irradiated, No. 24	28.26	55.1	16.4	0.24
Change	+12.86	-11.9	-1.0	+0.04

the irradiated by 29.6 times. Level change of β-radiation is in error limits.

Experience 4. Radiation of an alloy of Pb and Bi. The alloy is prepared independently. The chemical composition of Lead and Bismuth is given in Experience 3. The hinge plate from Lead of 0.17 kg (39%) and Bismuth of 0.27 kg (61%) was used for melting. The crucible is graphite, Ø45, height is 95 mm.

Heating of Lead was carried out to 400ºC, then bismuth was added, an exposure was carried out at a temperature 300ºC, stirring, a test taking of the initial test (No. 31). Radiation mode: the radiator is the graphite rod Ø6 of mm without protective tube, depth of dipping is 85 mm. Generator: amplitude is 10 kV, keyboard speed of 1 kHz. Time of processing is 10 min. Initial temperature is 260ºC, finite − 210ºC. Irradiated test (No. 32) was selected after agitation.

Researches of a chemical composition were conducted on the raster electronic microscope of JEOL JSM-6460LV firm (Japan) with system of microanalysis JXFORD INCA EWC453 (Great Britain). Measurements were made on fresh cross cutoffs of samples. Three sites of 2×3 mm in size were researched in case of increase equal 30.

Distinctions on a chemical composition between the initial and irradiated samples by the results of mean values of three measurements are presented in **Table 4**.

It is visible that there is a considerable change of chemical composition that exceeds the measurement error by 11 times.

Table 4

Mean values of a chemical composition, % masses

Element	Pb	Bi
Initial	30.34	69.66
Irradiated	41.96	58.04
Change	+11.62	-11.62
Error	1.02	1.05

Results of radioactivity measurements are the next: exceeding of α-radiation background for Lead – by 2.9 times, for Bismuth – background level. Results of activity measurements of initial and the irradiated tests are: exceeding of α-radiation background for the initial test is absent, for irradiated – by 3.6 times. There was an insignificant increase in the α-radiation level of the irradiated sample after radiation.

3. ANALYSIS OF RESULTS

All our experiments were made using one technique. Melt agitation after preparation was carried out by a quartz stick and then a test "initial" was selected in a ceramic tank. It is known [8] that Lead in case of a melting temperature 327ºC has density of 10678 kg/m^3, and in a solid status – 11350 kg/m^3. Bismuth has density 10050 kg/ m^3 in a liquid status in case of a melting temperature 271ºC, and in solid – 9747 kg/m^3, respectively. Therefore, density of Lead will decrease and density of Bismuth will increase in case of extension a melt temperature above a melting temperature. It is possible that these densities will be close at melt temperatures of 350ºC-400ºC under which process of radiation begins and test "initial" is molded. The maximum error can be counted at the expense of a density difference for Lead density of 10.678 and 10.050 for Bismuth. If melt is not absolutely mixed, the density difference will make 628 kg/m^3, this will make 5.9% in relation to Lead. Receiving of the initial test with the raised content of Bismuth is possible in case of insufficient agitation at the expense of density difference.

The place where test is molded is one more factor influencing on the quality of test. In our experiences tests were selected to

the ceramic tank of 10×10×70 mm in size. There is a melt crystallization in it.

The status chart of Bi-Pb alloy is used for the characteristic of crystallization process [9]. Crystallization of Lead-Bismuth alloys happens in the range of temperatures. Therefore, a composition of the crystals which are forming at the beginning of solidification can significantly differ from composition of last straws of a crystallizing melt. The temperature interval of alloy crystallization is wider, the segregation develops more strongly. The single alloy of Lead-Bismuth system crystallizing in case of continuous temperature (125°C) is the alloy of the eutectic composition containing 56% (at.) Bi.

The following operation was carried out for the analysis of a chemical composition of samples "initial No. 31" and "irradiated No. 32". Research of a transverse section of samples 31 and 32 in the direction from a sample bottom to its top in 8 areas was carried out by means of micro ray spectral analysis by a Carl Zeiss firm microscope. The area of measurement surface makes ≈0.5×0.5 mm. An exception method of results connected with casting boundaries – upper and lower is used when processing of analysis results of metal castings. Mean values on 6 layers are given in **Table 5**.

These values are less than the data specified in Table 4.

All abovementioned results belonged to analyses of solid samples. The raster electron microscope allows to analyze the samples in the form of powders and sawdust. Sawdust from samples 31 and 32 in the cross direction was saw by a small-sized file for results comparison. This sawdust on a neutral glue basis was pasted on the end face of the rod Ø4 mm which was set in the analysis camera. The area of an analyzable surface made ≈10 mm^2. Data of the carried-out analysis are given in **Table 6.**

These data are very close to data given in Table 4.

An analysis of samples 31 and 32 was carried out also on the atomic and emissive spectrometer "Spektroflame Modula S" with the inductive and connected plasma. Hinge plate of an alloy of 0.22 g before the analysis dissolved in imperial vodka (HCl : HNO_3 = 3 : 1) in case of heating up. The hinge plate was received by shaving drilling by a drill with a diameter of 3 mm in the vertical direction of a sample. Solution was transferred to measured flasks after full dilution of a hinge plate and then measured volumes used for the analysis were taken. Concentration measurements were carried out with the use of standard components method. It was carried out in two measurements. Analysis data are presented in **Table 7**.

All data of the content measurement of Lead and Bismuth in samples 31 and 32

Table 5

Chemical composition of samples, % masses

Element	Pb	Bi
Initial, No. 31	49.6	50.4
Irradiated, No.32	59.6	40.1
Change	+10.0	-10.3

Table 6

Chemical composition of samples 31 and 32 (sawdust), % masses

Element	Pb	Bi
Initial, No. 31	29.1	70.9
Irradiated, No.32	40.97	59.3
Change	+11.87	-11.6

Table 7

Average composition of elements, % masses

Element	Pb	Bi
Initial, No. 31	34.5	65.65
Irradiated, No. 32	44.6	55.15
Change	+10.1	-10.5

under different conditions of measurement are given together below for convenience of comparing (**Table 8**).

Data in Table 8 unambiguously specify the reduction of the Bismuth content and increase of the Lead content during radiation.

4. THEORETICAL SUBSTANTIATIONS

The theory of electron capture is one of hypotheses for theoretical reasons for transmutation of Bi→Pb under the influence of NEMI [3]. According to this theory change of atomic mass doesn't happen, and one of bismuth protons becomes a neutron. We will use the table from [10] for the analysis of isotope composition of long-living isotopes of lead and bismuth.

The new result about an isotope ^{209}Bi is received [11]. It is revealed its α-radiation with energy 3.13 keV and the half-life period of 1.9×10^{19} years is defined. The isotope ^{204}Pb is specified as stable in literature. However, it is specified as radioactive with a half-life period of 1.4×10^{17} years [10]. Existence α-activity of the initial and irradiated samples in experiences 3, 4, 5 and its change within the time in experiences 3 and 4 specify existence and change of the isotopic composition after NEMI radiation.

Table 8

Changes of the composition of Pb and Bi of samples 31 and 32, % masses

Element	Pb	Bi	Analyzer
Metal, 3 platforms	+11.97	-11.97	JEOL
Sawdust, 10 mm^2	+11.87	-11.6	JEOL
Metal, 6 platforms	+10.0	-10.3	Carl Zeiss
Shaving, 2 measurements	+10.1	-10.5	Spektroflame Modula S

From table data [10] it's visible that if there are isotopes ^{210m}Bi, ^{208}Bi and ^{207}Bi in a melt before radiation, they will give a long-living isotope of Lead ^{210}Pb or stable isotopes ^{208}Pb and ^{207}Pb after NEMI radiation. The isotope ^{209}Pb has small time of half-life. There would be the considerable change of analysis results during time in case of its existence. This effect wasn't watched. Unfortunately, we had no instruments for measurement of the isotopic composition of Bismuth and Lead. Therefore, it is necessary to consider the offered transitions ^{210m}Bi→^{210}Pb, ^{208}Bi→^{208}Pb and ^{207}Bi→^{207}Pb as a scientific hypothesis.

5.CONCLUSION

The provided data of experimental researches indicate a possibility of transformation of tens of grams of bismuth into lead under the influence of pulse fields with big degree of reliability. Data are easily checked. It is possible to get generators of impulses in "Fid-Tekhnologiya" firm (St. Petersburg). It is necessary to pay special attention to bismuth choosing initial materials. It is possible to receive coefficient of transformation of bismuth into lead about 3% if the choice of bismuth is unsuccessful. All other conditions of experiences are described above in detail.

From the analysis of experiences on water solutions it is possible to specify one more couple of elements – copper and nickel in which the similar phenomena can occur.

REFERENCES

1. Balakirev VF, Krymsky VV, Kulakov BA, Ri Khosen. *Elektroimpul'snye nanotekhnologii* [Electropulse Nanotechnologies]. Ekaterinburg, Ural Office of Russian Academy of Sciences Publ., 2009, 141 p.
2. Shaburova NA. *Obrabotka metallov i splavov nanosekudnymi elektromagnitnymi impul'sami* [Processing of Metals and Alloys by

Nanosecond Electromagnetic Impulses]. Chelyabisk, TsNTI Publ., 2011, 94 p.
3. Balakirev VF, Krymsky VV, Shaburova NA. *Nanoimpul'snye tekhnologii* [Nanopulse Technologies]. Chelyabisk, TsNTI Publ., 2012, 124 p.
4. Krymski VV, Shaburova NA, Filimonov IE. Pulse electromagnetic effect on metal melts. *J. of Chemistry and Chemical Engineering,* 2012, 6(11):967.
5. Urutskoev LI, Liksonov VI, Tsinoev VG. *Prikladnaya fizika*, 2000, 4:83-100 (in Russ.).
6. Krymsky VV, Balakirev VF. *Doklady RAN* [Reports of Russian Academy of Sciences], 2002, 385(6):786-787 (in Russ.).
7. Balakirev VF, Krymsky VV, Bolotov BV, Vasil'eva NV, Vachaev AV, Ivanov NI, Kazbanov VI, Pavlova GA, Solin MI, Trofimov VI, Urutskoev LI. *Vzaimoprevrasheniya khimicheskikh elementov* [Interconversions of Chemical Elements]. Ekaterinburg, Ural Office of Russian Academy of Sciences Publ., 2003, 93 p.
8. Emsley J. *The Elements*. Oxford, Clarendon press, 1991, 256 p.
9. Budberg PB, Alisova SP. *Diagrammy sostoyaniya dvoynykh i mnogokomponentnykh system na osnove zheleza* [Charts of a Condition of Double and Multicomponent Systems on the Basis of Iron]. Moscow, Metallurgiya Publ., 1986, 525 p.
10. Shirokov YuM, Yudin NP. *Yadernaya fizika* [Nuclear Physics]. Moscow, Nauka Publ., 1980, 727 p.
11. Varcillac P, Coron N, Dambier G, Leblanc J, Moalik JP. Experimental detection of alpha-particles from the radioactive decay of natural bismuth. *Nature*, 2003, 422(6934):876-878.

RUSSIAN CONFERENCE ON COLD TRANSMUTATION OF NUCLEI (1993-2017)

Yuri N. Bazhutov

Scientific-research centre for engineering and physical problems "Erzion"
Moscow 109451, Russian Federation
erzion@mail.ru

Abstract. **The information about the Russian conferences on cold transmutation of nuclei of chemical elements and ball lightning (RCCTN&BL) is presented, which occurring in the Krasnodar coast of Black sea (Abrau-Dyurso, Sochi, Lazorevskoe, Dagomys, Loo, Krinitsa), annually since 1993.**

Keywords: **coordination council, conference, cold transmutation of nuclei of chemical elements, ball lightning**

UDC 061.053, 539.172

References – 4

Received 20.06.2017

RENSIT, 2017, 9(1):113-115

DOI: 10.17725/rensit.2017.09.113

Contents

1. INTRODUCTION

From the first steps of nuclear physics by the its low-energy direction is not lucky: E. Rutherford, captivated by prospects development nuclear power, declared as the incorrect the first works on nuclear reactions at low energy [1], and they went underground. However, after the publication in 1989 M. Fleischmann and S. Pons (USA) in Journal of Electroanalytical Chemistry [2] and their interview at a press conference on March 23, 1989, published to the newspaper "Financial Times" in which they stated that it is possible to create energy source of the industrial scale based on the fusion of nuclei of heavy hydrogen at room temperature, studies of low-energy nuclear reactions has been obtain widely developed in many laboratories of the world. In countries such as USA, Japan, Italy, China and other, these studies are funded by the state programs and the largest firms (Toyota, Honda, Mitsubishi, Fiat, etc).

Since 1990, annual International Conference on Cold Fusion (ICCF, 2007 - International Conference on Condensed Matter Nuclear Science) in the United States, Canada, Japan, Italy, France, China, Korea, India and other countries is conducted. There are an electronic journal http://newenergytimes.com, sites (one of the largest - www.lenr-forum.com) on low-energy nuclear reactions [3].

In Russia, these studies became involved Kurchatov Institute of atomic energy (Moscow), JINR (Dubna) and other institutes of Academy of Sciences of the USSR, universities, Scientific-research institute scientific-production association "Luch" (Podolsk) and other research institutes of our country. In 1991, all-Union conference "Cold nuclear fusion" at JINR-Dubna - MSU-Moscow under the chairmanship of the academician of the AN USSR Y.M. Kolotyrkin is conducted. In 1992, the UFN publishes a review of Dr Sci Phys&Math V.A. Tsarev (Lebedev Physical Institute). In 1993 the Coordinating board on anomalous nuclear phenomena in condensed matter, the Chairman - Dr Sci Chem, academician of the AN USSR Baraboshkin A.N. (IECh UrF USSR Academy of Sciences, Yekaterinburg) is organized. This Board provided the two-year state grant for these studies. The First Russian conference on cold nuclear fusion in Abrau-Dyurso, 1993 was conducted. In 1994, in Sochi the 2nd conference was held already under the name "Cold fusion and transmutation of nuclei". In 1996, after the death of academicians Baraboshkin A.N. and Kolotyrkin Y.M. the Interdepartmental coordination board on the problem of "Cold fusion" under the Vice-President of RAS, Dr Sci Chem O.M. Nefedov, Chairman of the Board Dr Sci Chem, academician V.E. Kazarinov (Frumkin IPCE RAS) is organized. 5th Russian conference in

Dagomys (1997) is conducted under the name "Cold transmutation of nuclei of chemical elements". In 2004, the Interdepartmental coordination Board on the problem of "Cold transmutation of nuclei" under the Russian physical society is organized (until 2012). Since the tenth conference (2002) it is called Russian conference on cold transmutation of nuclei of chemical elements and ball lightning (RCCTN&BL). In 2007, in Dagomys (Sochi) the 13th International Conference on Cold Transmutation of Nuclei of chemical elements (ICCF-13) was conducted. In September 2017 in Sochi will be held the next annual 24th RCCTN&BL.

Since 2017, the Coordinating Board on the problem of "Cold transmutation of nuclei" (CB CTN) was registered in the Russian Academy of Natural Sciences (RANS) and operates in the following composition.

1. Chairman CB CTN - Henri Amvrosievich Rukhadze, Dr. Sci Phys&Math, Professor, academician of RANS, chief researcher of Prokhorov GPI RAS, Moscow, Russia.

Co-Chairmans CB CTN:

2. Victor Victorovich Apollonov, Dr Sci Phys&Math, Professor, academician of RANS, Prokhorov GPI RAS, Moscow, Russia;

3. Yuri Nikolaevich Bazhutov, PhD Phys&Math, senior researcher, corresponding member of RANS, Scientific-research center for engineering and physical problems "Erzion" (SRC EPP "Erzion"), Moscow.

Vice-Chairman CB CTN:

4. Runar Nikolaevich Kuzmin, Dr. Sci Phys&Math, Professor, Lomonosov Moscow State University, Physical Faculty;

5. Nikolay Vladimirovich Samsonenko, PhD Phys&Math., corresponding member of RANS, associate Professor of the Russian University of friendship of peoples (RUFP).

6. Scientific Secretary - Albina Ivanovna Gerasimova, PhD Chem, associate Professor, corresponding member of RANS, SRC EPP "Erzion", Moscow.

Members of the coordinating Board of the cold nuclear transmutation:

7. Stepan Nikolaevich Andreev, Dr Sci Phys&Math, Prokhorov GPI RAS, Moscow;

8. Dmitry Sergeevich Baranov, PhD Phys&Math, Joint Institute for High Temperatures of the Russian Academy of Sciences (JIHT RAS)

9. Vsevolod Valerievich Botvinovsky, PhD Phys&Math, senior researcher, corresponding member of RANS, Novosibirsk plant of industrial instrumentation (NPII), Novosibirsk, Russia;

10. Aleksandr Nikolaevich Vlasov, Dr Sci Phys&Math, Professor, corresponding member of Academy of electrotechnical Sciences of the Russian Federation, Ryazan state radio engineering University (RSREU), Ryazan;

11. Sergey Mikhaylovich Godin, LLC Lokterm, Moscow;

12. Igor Vitalievich Goryachev, Dr Sci Techn, Professor, Moscow;

13. Valery Nikolaevich Zatelepin, PhD Techn, LLC "Inlis", Moscow;

14. Pyotr Vasilyevich Zakharov, PhD Phys&Math, SRC EPP "Erzion", Moscow;

15. Mikhail Yakovlevich Ivanov, Dr Sci Phys&Math, Professor, corresponding member of RANS, Central institute of aviation motors (CIAM), Moscow;

16. Vitaliy Alekseevich Kirkinsky, Dr Sci Geol-Min, Institute of Geology and Mineralogy SB RAS, Novosibirsk;

17. Anatoly Ivanovich Klimov, Dr. Sci Phys&Math, academician of RANS, Joint Institute for High Temperatures RAS, Moscow;

18. Alla Aleksandrovna Kornilova, PhD Phys&Math, Lomonosov Moscow State University, Moscow;

19. Alexei Ivanovich Laptukhov, PhD Phys&Math, associate Professor, Pushkov Institute of Terrestrial Magnetism, Ionosphere and Radio Wave Propagation of RAS (IZMIRAN), Troitsk, Moscow;

20. Alexander Georgievich Parkhomov, PhD Phys&Math, corresponding member of RANS, Experimental-Design Laboratory "K. I. T.", Moscow;

21. Boris Ustinovich Rodionov, Dr. Sci Phys&Math, Professor, academician of RAEN, Institute of content and methods of education Russian Academy of education, Moscow;

22. Alexey Sergeevich Rusetsky, PhD Phys&Math, Lebedev Physical Institute of RAS, Moscow;

23. Irina Borisovna Savvateeva, PhD Techn, Scientific Research Institute "Luch", Podolsk, Moscow region;

24. Sergey Alekseevich Tsvetkov, PhD Techn, pensioner, Ekaterinburg;

25. Ivan Petrovich Chernov, Dr. Sci Phys&Math, Professor, Tomsk Polytechnic University, Tomsk;

2. ORGANIZING COMMITTEE OF 24th RCCTN&BL-2017

Bazhutov Yu.N. - Chairman, SRC EPP "Erzion";
Bychkov V.L. - Vice-Chairman, Lomonosov Moscow State University;
Samsonenko N.V. - Deputy Chairman, RUFP;
Gerasimova A.I. - Secretary, SRC EPP "Erzion";
Prosvirnov A. A. - editor of the Russian web site, JSC VNIIAES (Moscow);
Shestopalov A.V. - editor of video web site, Melnikov Research Institute of Comprehensive Exploitation of Mineral Resources RAS, Moscow.

Members of the organizing Committee:

Klimov A.I. - JIHT RAS, Moscow;
Kornilova A.A. - Lomonosov Moscow State University;
Parkhomov A.G. - EDL "K. I. T.";
Famina N. V. – STU MADI.

3. THE MAIN DIRECTIONS OF RESEARCHES

1. Physics of cold transmutation of nuclei of chemical elements.
2. Experimental studies and theoretical models of cold nuclear transmutation.
3. Environmental issues associated with the phenomenon of cold transmutation of nuclei.
4. Physics of ball lightning. Pilot studies. Reviews and theoretical models.

4. ORGANIZATIONAL ISSUES

The conference, usually is conducted in autumn, in September, in Sochi, Dagomys settlement, Krasnodar area, boarding house "Olympic-Dagomys" [3].

The conference gathers for weekly your from 20 to 50 participants from 20-30 different scientific organizations of Russia – Moscow and the Moscow region, St-Petersburg, Novosibirsk, Armavir, Volgograd, Rostov-on-Don, Krasnodar, Sochi etc. Are presenting about 40 reports – overview, experimental and theoretical. Including up to a quarter of the reports on the problem of ball lightning.

Its regular participants are foreign researchers from the USA, Japan, Italy, China, France, Belgium and other countries.

The conference takes place at the expense of the organizing Committee and authors of articles. Episodically the Russian and foreign firms involve in the sponsorship.

The conference proceedings are published at the expense of the organizing Committee of RCCTN&BL and articles authors. The conference proceedings are indexed in Russian Science Citation Index (RSCI) and registered in Book Chamber of the Russian Federation.

The conference informs about its activities the Nuclear Society of Russia, Mendeleev Russian Chemical Society, Lomonosov Moscow State University, the Russian University of Friendship of Peoples.

5. CONCLUSION

The systematic conduct of the conference, the activity of its participants, saturation of an annual programme attested to the relevance of the existence of the conference as a working platform, promoting the development of researches the problem of cold transmutation of nuclei of chemical elements.

REFERENCES

1. Rutherford E. Identification of a missing element. *Nature,* London, 1922, 109:781.
2. Fleishmann M, Pons S, Hawkins M. Electrochemically induced nuclear fusion of deuterium. *J. Electroanal. Chem.*, 1989, 261:301-308.
3. Ehrlich G.V., Andreev S.N. *The history of nuclear physics in the mirror of alchemy: from the beginning of the twentieth century to the sensational discoveries of present days*. Moscow, LENAND Publ., 2017, 232 p.
4. The problems of cold transmutation of nuclei of chemical elements and ball lightning. *Materials of 23nd Russian conference on RCCTN&BL*. June 2016, Dagomys, Sochi, 2016, 310 s.

SEMINAR ON COLD FUSION AND FIREBALL IN RUDN

Nikolay V. Samsonenko
Peoples' Friendship University of Russia, http://eng.rudn.ru
Moscow 117198, Russian Federation
nsamson@bk.ru

Abstract. **Information on the seminar of cold transmutation of nuclei, held every month in Moscow at the Peoples' Friendship University of Russia (RUDN University), in Faculty of physical-mathematical and natural sciences since 1992, is provided.**

Keywords: **RUDN university, seminar, low-energy nuclear reactions, cold transmutation of nuclei**

UDC 061.053, 539.172

Bibliography – 6 references *Received 06.06.2017*

RENSIT, 2017, 9(1):116-117 **DOI: 10.17725/rensit.2017.09.116**

Seminar "Cold fusion and fireball" in RUDN University was arise, in 1992 from FIAN monthly seminar "Low-temperature nuclear fusion" that had existed in the Lebedev Physical Institute of USSR Academy of Sciences since 1989. FIAN seminar was heding under the leadership of Vladimir Alexandrovich Tsarev, Dr Sci Phys&Math, Professor, head of the Department of cosmic radiations and of the Laboratory of elementary particles in the Division of nuclear physics and astrophysics of Lebedev Physics Institute. V.Tsarev is known for his publications on the subject in the Central academic journals (see, eg., [1]). I regularly attended this seminar, and over time our with V.A. Tsarev relationship evolved into friendly (shared research interests - neutrino physics, the proximity of residence, etc.). And V.A. Tsarev, when him it came time to go into a long scientific trip abroad, he was suggested me to organize conduct of his seminar in the RUDN University, helped by a lightweight access to the RUDN and his international status. In addition in our group at the chair of theoretical physics and mechanics, Faculty of physics, mathematics and natural sciences of RUDN University after several years of experimental research, within one of the main scientific directions of faculty - research in the field of interaction of the electromagnetic radiation with matter, particle physics, physics of metals and alloys aimed at creation of energy-saving technologies and environmentally friendly energy, - for the first time managed to observe the neutrons emitted by deuterated ferroelectric in the process of repolarization in an electric field [2], the world's first work on the initiation of nuclear reactions in ferroelectrics. Moreover, the experiment was reliable reproducible. The experimental successes stimulated our theoretical surveys [3].

V.A. Tsarev seminar continued in RUDN (**Fig. 1**) University. And when V.A. Tsarev returned from Italy, and then from Japan, it became clear that return of seminar in FIAN is impossible due to the sharp opposition to this scientic direction in the Russian Academy of Sciences, where soon was established the Commission on pseudoscience. So the seminar remained in the RUDN University, where it continue to work until now (**Fig. 2**).

After the First Russian conference on cold nuclear fusion in 1993 in Abrau-Dyurso, seminar of RUDN was visited such famous explorers like Jean-Pierre Vigier, Professor of the Paris University P. and M. Curie, France; Michael McKubre, Director of the Energy research centre of the international Stanford research Institute, USA; Reiko Natoa – senior chemist-researcher at the Centre for catalysis Hokkaido University, Japan.

Fig. 1. *The building of the RUDN University on Ordzhonikidze Str., 3.*

Fig. 2. *Seminar on cold fusion and fireball in the conference hall of the Faculty of physico-mathematical and natural Sciences, RUDN University.*

Academician Baraboshkin A.N., becoming in 1993 the head of the coordination Council of Russian Academy of Sciences on Anomalous nuclear phenomena in condensed matter, approved our Seminar in RUDN as All-Russian.

After the closing of seminar on ball lightning in Lomonosov Moscow State University, its participants together with their supervisor Dr Sci Phys&Math, Professor V.L. Bychkov joined our seminar, which is reflected in its title.

Among the regular participants of the seminar – Rukhadze Henri Amvrosievich, Dr Sci Phys&Math, Professor (Prokhorov GPI RAS, Moscow), Apollonov Viktor Viktorovich, Dr Sci Phys&Math, Professor (Prokhorov GPI RAS, Moscow), Vysotskii Vladimir Ivanovich, Dr Sci Phys&Math, Professor (Shevchenko Kiev National University (Kyiv, Ukraine), Bazhutov Yuri Nikolaevich, PhD Phys&Math (IZMIRAN, SRC EPP "Erzion", Moscow), Parkhomov Alexander Georgievich, PhD Phys&Math (Experimental design laboratory "K.I.T.", Moscow), Goryachev Igor V., Dr Sci Tech, Professor (Moscow), Zatelepin Valery Nikolaevich, PhD Techn (LLC"Inlis", Moscow) Zakharov Pyotr Vasilyevich, PhD Phys&Math (SRC EPP "Erzion", Moscow), Mikhail Ya. Ivanov, Dr Sci Phys&Math, Professor (CIAM, Moscow), Klimov Anatoly Ivanovich, Dr Sci Phys&Math (JIHT RAS, Moscow), Kornilova Alla Aleksandrovna, PhD Phys&Math (M.V. Lomonosov MSU, Moscow), Laptukhov Alexei Ivanovich, PhD Phys&Math, associate Professor (IZMIRAN, Troitsk, Moscow), Rodionov Botis Ustinovich, Dr Sci Phys&Math, Professor (ISMO RAO, Moscow), Rusetsky Alexey Sergeevich, PhD Phys&Math (FIAN, Moscow), Savvateeva Irina Borisovna, PhD Techn (NII NPO "Luch", Podolsk, Moscow region).

In different years the seminar were attended by foreign scientists from the USA, France, Italy, Germany, Belgium, Japan, Korea, China and other countries of Europe, Asia and Africa. Among them were such authors as a pupil and nearest co-worker of Louis de Broglie, President of his Foundation Georges Lochak (France), Fulvio Frizone (Deaptmen of Physics, Catania State University, Italy), Philippe Hatt (European Comission Brussels, Belgium) and Fidel Ndahauo (Univetsity of Rwanda, Kigali, Rwanda) and many others.

In 2014, after the publication of the reports of the European experts on the evaluation of the generator Rossi [4-6] works on the cold nuclear transmutation intensified worldwide. At the seminar of RUDN University are presented results in abnormally excessive heat generation and synthesis of isotopes in a variety of experimental productions. A variety of methods and technologies – a feature of Russian research on cold transmutation of nuclei. In 25 years of existence in the RUDN University of monthly seminar on the cold transmutation of nuclei more than 500 reports were presented and discussed. Ie in spite of the well-known Russian specificity of the existence of researches on cold transmutation of nuclei in the country, this area of nuclear physics was not stood and does not stand still on the spot. There are appropriate technologies in which Russia is the undisputed world leader. Activities of the seminar contributes to expand communications among researchers and raise the level of experiments on cold transmutation of nuclei and to improve theoretical models.

REFERENCES

1. Tsarev VA. Low-temperature nuclear fusion. *UFN,* 1990, 160(11):1-53 (in Russ.).
2. Dougar-Jabon VD, Fedorovich GV, Samsonenko NV. Catalitically Induced D-D Fusion in Ferroelectrics. *Brazilian J. of Phys.*, 1997, 27(4):515-521.
3. Samsonenko NV, Tahti DV, Ndahayo F. On the Barut-Vigier Model of the Hydrogen Atom. *Phys. Lett.*, 1996, A220:297-301.
4. Levi G., Foschi E, Höistad B. et al. Indication of anomalous heat energy production in a reactor device. – *arXiv*:1305.3913v3 [physics.gen-ph].
5. Levi G, Foschi E, Höistad B. Observation of abundant heat production from a reactor device and of isotopic changes in the fuel. – http://www.sifferkoll.se/sifferkoll/wp-content/uploads/2014/10/LuganoReportSubmit.pdf..
6. Parkhomov AG. Report of the international Commission on the testing of high-temperature heat generator Rossi. *ZhFNN*, 2014, 2(6):57-61. – http://www.unconv-science.org/pdf/6/parkhomov2-ru.pdf.

DEVYATKOV NIKOLAY DMITRIEVICH

(TO 110 ANNIVERSARY OF BIRTH)

UDC 929.53

DOI: 10.17725/rensit.2017.09.118

110 years ago, on 11 April (29 March, old style), 1907, in Vologda, in an old house on quay of the Zolotukha river, in the big family of the artisan merchant of Dmitry Kirillovich Semenov-Devyatkov and a native of Yaroslavl Poshehonie Lidia Ivanovna was born last-born Kolya, Nikolay Dmitrievich Devyatkov - the future physicist, who fate has chosen to be a Patriarch of Soviet Electronics. The childhood and youth of Nicholay were held in Vologda, with 8 years he studied at the real school, loved to paint with watercolors and pastels, painted scenery for school performances. But most of all he liked electrical engineering - transformers, generators, electrical distribution systems, power transmission problems. A year after school graduation, in 1925, the family moved to Leningrad, where Nicholay entered the Leningrad Polytechnic Institute, while working as a lab technician in X-ray Institute. Its Director, A. F. Ioffe suggested to the inquisitive young man a place in the laboratory known electrical engineer of the 20-30-ies, one of the pioneers of radar, the future academician A. A. Chernyshev, which became its first scientific Head. Here the student N. Devyatkov published in 1930 his first article in the journal "Electricity" called "Powerful gas arrestors for protection of lines of communication."

After institute graduation, from 1931 to 1942, Nikolai Dmitrievich worked in LFTI and in its branch NII-9 on defence thematics. During this time he performed important research in various fields of technology, published 12 publications and has received 6 patents for inventions. Beginning in 1935 Devyatkov carries out pioneering research in the field of generation of ultra-high frequencies. To him belongs the priority in the creation of the microwave triode with plane – parallel electrodes- low-power generator lamps with almost the inertialess output of grid. Original ideas embodied in the design of microwave triodes, served as the basis for creating many types of such lamps, as well as amplifiers and generators on their basis not only in the USSR but also in England, USA and Germany. Continuing work in this direction, in 1940, he with employes comes to outstanding invention – reflective klystron, which later became the main industrial type of vacuum devices used so far in various electronic systems.

Since 1942 N. D. Devyatkov has been worked in Moscow the development of the domestic (instead of english existing) radars - stations weapon aiming. By now November 1942 it had completed the development and manufactured two pilot specimen of the radar which have been successfully tested under Moscow in battle front. In 1943 he was transferred to research Institute-160, that was created on the basis radio plant in Fryazino near Moscow (now NPP Istok), where he led work on the development and production of electronic devices for radar equipment until the end of his life. The first award order of the Red Star he received in 1944 for participation in the development and production of radars for gun aiming. Air defense troops equipped with these stations have greatly increased its effectiveness in the protection of Moscow and other large cities, victims of Nazi air raids.

Since 1954 N. D. Devyatkov – the scientific header of the Department of microwave electronics, Institute of radio engineering and electronics, USSR Academy of Sciences, the formation of which is associated with his name. Since 1960 – head of the Department of emission and quantum electronics of the Moscow Institute of Physics and Technology. In the postwar

years under his guidance were created lamps of the backward wave in millimeter and submillimeter wavelength ranges and based on them, first in a world, had begun works on the development of MM-range of wavelengths.

To impressive achievements of the last decades are pertain his works in the field of application of microwave electron devices and quantum generators in the economy and medicine.

Nikolay Dmitrievich creates a unique creative teams for joint work of experts in such diverse fields as electronics, medicine, biology, etc. The main works carried out under his leadership in this direction: the use of lasers in surgery and therapy, the use of hyperthermic heating of tumors for their destruction, the establishment of a number of devices for gastroenterology, diagnostic thermal imaging equipment, setups for the irradiation of seeds with the aim of increasing crop yields.

Particularly striking are obtained by N.D. Devyatkov with employees the results of the study the specific impact of electromagnetic waves of millimeter range on biological structures and organisms for the effective therapeutic treatment of diseases by improving the immunological ability of the body.

In April 1997, was held the 11th Russian Symposium "Millimeter waves in medicine and biology" with international participation, dedicated to the 90th anniversary of the founder of MM-therapy, academician N.D. Devyatkov.

Nikolay Dmitrievich worked at the state scientific production enterprise Istok 54 years, including 39 years was Deputy Director for scientific work. Herewith never was the member of communist party. He is the author (coauthor) of more than 250 scientific works and inventions.

In 1952 he was awarded the academic title of associate Professor, while he read a course of lectures in the Moscow Power Engineering Institute. In 1953 he was elected corresponding member in the Department of technical Sciences of the USSR, while still a Professor. In 1957 he was awarded the degree of doctor of technical Sciences, and in 1958 – the title of Professor. Nikolay Dmitrievich Devyatkov - academician of the USSR (1968), Hero of Socialist Labor (1969), winner of the Stalin (State) prize of the USSR (1949) and Lenin prize (1965), two government awards (1984, 1996), cavalier of two orders of Lenin, order of October Revolution, two orders of Labor red banner and order of the red Star. Awarded a gold medal. A. S. Popov (1986).

N.D. Devyatkov was spending the big scientific-community work. The decision of the Presidium of the USSR in 1975 he was appointed Chairman of the Council on the issue of physical electronics. Since 1950-ies he worked in Higher Certification Commission, for two terms (5 years each) was a member of the Bureau of the Department of General physics and astronomy of the USSR, was a member of the editorial Board of the "Great Soviet encyclopedia". He was the chief editor of the journal "Radioengineering and electronics", headed the editorial Board of the collection "Elektronnaya Tekhnika. Series 1. SVCH-Tekhnika".

Nikolay Dmitrievich Devyatkov possessed a rare combination of the qualities of an outstanding original academic, that paving new paths in science, and an excellent organizer. A scholar with world forename, he is one of the founders of many scientific fields: modern electronic engineering, physical electronics, electronics of ultrahigh frequencies, vacuum technology, medical electrical engineering. The scope and importance of his scientific work are so great that it is impossible to briefly reflect them accordingly. Estimation outstanding multi-faceted activities of N. D.Devyatkova is inseparable from the answer to the eternal questions of the relation between imagination and rigor, intuition, and mathematics, "algebra" and "harmony" in physics and microwave technology and other natural Sciences.

Nikolay Dmitrievich Devyatkov lived a long and productive life, which he described in his book "Memories" (Moscow, Nauka Publ., 1998). He married in August 1933 on the Zoya Vasilievna Sterlyadkina, also vologzhanka, and lived with her in love and harmony for almost 70 years. Son Michael, doctor of physical and mathematical Sciences, untimely died in 1984 Nikolay Dmitrievich died on 1 February 2001 on 94-m to year of life, buried at Vostryakovskoye cemetery.

Nikolai Dmitrievich was a sampling of the Russian intelligent, ready to come to the aid of anyone who needed it, a man of great intelligence and high internal culture.

The memory of this amazing man will forever remain in our hearts. His dealing lives on in the collectives, by which he directed, his principles and style are remain as leading for his former employees and for the next generations of scientists.

Editorial board

GUBIN SERGEY PAVLOVICH

(TO 80 ANNIVERSARY OF BIRTH)

UDC 929.53

DOI: 10.17725/rensit.2017.09.120

On May 8, 2017 Sergey Pavlovich Gubin, Doctor of Chemical Sciences, Professor, Head of the Laboratory of Chemistry of Nanomaterials of N.S. Kurnakov Institute of General and Inorganic Chemistry of the Russian Academy of Sciences, Laureate of the State Prize of the USSR, Honored Scientist of Russia, Academician of the Russian Academy of natural Sciences, the known expert in the field of solid state chemistry, nanoscience and nanotechnology celebrated his 80th birthday.

S.P. Gubin was born in 1937 in Moscow in a family of engineers Gubin Pavel Fedorovich (after the Moscow Institute of Transportation Engineers - in the Subway) and Romashko Lyudmila Kondradovna (after Moscow Institute of Steel and Alloys – plant "Salute", Moscow), both hailing from the Vologda region. In school he fascinated by chemistry and since 7th grade (1951) each year participated in city Chemical Olympiads at the Chemical faculty of Moscow state University, always getting the first prizes. In 1954 he entered chemistry faculty of M.V. Lomonosov Moscow State University. In the same year began to specialize in the chair of organic chemistry, in laboratory of chemistry of organometallic compounds under the guidance of academician Alexander Nikolaevich Nesmeyanov, at that time President of the Academy of Sciences of the USSR.

Diploma and postgraduate studies at the chemical faculty of MSU was completed in 1963 with a dissertation on competition of a scientific degree of candidate of chemical sciences "redox-potentials of substituted ferrocenes", performed under the guidance of academician of the USSR Academy of Sciences A.N. Nesmeyanov and doctor of chemical sciences E. G. Perevalova..

Since 1963, S.P. Gubin – fellow, Institute of Organoelement compounds (INEOS) Academy of Sciences of the USSR. Due his research on the chemistry of organometallic compounds and π-transition metal complexes S.P. Gubin acquired prominence in the native and world science. He conducted extensive studies of reactivity and electronic effects in π-complexes of transition metals; proposed and substantiated the hypothesis of the participation of the electrons of σ-skeleton of the organic ligands in the bond formation with transition metals in the π-complexes. S. P. Gubin established the basic laws of oxidation-reduction reactions of π-complexes of transition metals. In In 1971, the scientific council INEOS, assigns to S. P. Gubin the degree of doctor of chemical Sciences (dissertation "Electronic effects and reactivity of π-complexes of transition metals", scientific consultant academician A.N. Nesmeyanov).

A lot of attention in this period of time S.P. Gubin was given to use of π-complexes of transition metals in electronics, nonferrous metallurgy, petrochemistry and oil refining. In 1976, S.P. Gubin in the composition of the team of authors was awarded the State Prize of the USSR for work in the application of organometallic compounds in electronics technics.

Since 1977, Sergei Pavlovich in Novosibirsk, Deputy Director of the Institute of inorganic chemistry of SB of Academy of Sciences. In 1978, S.P. Gubin accepts the offer akademician G. K. Boreskov, agreed with the academician G.I. Marchuk, who was the Chairman of SB AS USSR, about the organization in the Krasnoyarsk branch of the USSR Academy of Sciences, chemical Institute. S.P. Gubin is the founder (1979) and the first Director of the Institute of chemistry and chemical technology, Siberian branch of the USSR Academy of Sciences in Krasnoyarsk. He carried out extensive work on the involvement into the newly created Institute of skilled research personnel and

equipping it with instruments and equipment, identifies the major scientific areas in which the Institute operates successfully up to the present time. In Krasnoyarsk under the direction of S.P. Gubin developed theoretical bases of complex processing of coals of the Kansk-Achinsk basin by the method of supercritical extraction by alcohols. In the subsequent, on this basis, developed the original technology for producing liquid fuel from these coals. Here S. P. Gubin first in our country began a systematic researches on the use of supercritical fluids as reagents, successfully developing at present time. In Krasnoyarsk started the first studies in the field of chemistry of clusters.

In 1980-1983 S. P. Gubin – the Director of the Institute of inorganic chemistry of SB of Academy of Sciences in Novosibirsk. Here S. P. Gubin continued systematic research in the field of chemistry of clusters. He have been developed research on key topics in this new scientific direction – the synthesis, the study of the reactivity and structure, to identify possible ways of implementation of clusters in materials science, catalysis, etc.; revealed peculiarities of coordination of ligands on multiple metal centres in the cluster.

Since 1983, Sergei Pavlovich in Moscow, in Kurnakov Institute of general and inorganic chemistry of the USSR Academy of Sciences. Work was delivered on a broad front: supercritical fluids, clusters, synthesis of nanoparticles, including magnetic. Are conducted researches on theoretical problems of chemistry of clusters and created the foundations of the classification of cluster compounds based on the topology of the metal skeleton. The overall results of this working are generalized in the monograph of S. P. Gubin, "Cluster Chemistry" (Moscow, Nauka Publ., 1987), which has no analogues neither in native nor in foreign literature; she played a outstanding role in the development of this field in our country.

On the basis of studies of the electrochemistry of the clusters and the distinguishing features of clusters as reservoirs of electrons, in collaboration with the staff of the Physical faculty of MSU and Institute of radio engineering and electronics of RAS created the world's first single-electron transistor on the clustered molecule, operating at room temperature.

S.P. Gubin has been a pioneer in the synthesis of magnetic nanomaterials; magnetic characteristics of the material consisting of isolated from each other in a nonmagnetic solid dielectric matrix magnetic nanoparticles (3-10 nm), were first described by he in the publication 1980. In future these works were successfully continued and led to the creation of a new class of nanomaterials based on metal-containing nanoparticles in dielectric matrices. In 2002, S. P. Gubin has created in Kurnakov IGIC RAS the first in our country the laboratory of Chemistry of nanomaterials, that has been working successfully in this direction. In 2009 S.P. Gubin as the scientific head participates in the creation at the territory of scientific research Institute "Diamond", startup company, LLC "AkKoLab", where works are carried out on the use of nanotechnology in the creation of supercapacitors, Li-ion batteries, nanosensors, etc. In 2011 S. P. Gubin in collaboration with his graduate student S. V. Tkachev had published a small but very informative book "Graphene and kindred nanoforms of carbon", which came out already by 4th edition. Professionals, working with graphene, team up and create in 2011 on the basis of the Institute "Diamond" and OOO AkKoLab the monthly Moscow seminar "Graphene: a molecule and a 2D crystal", led by Professor S.P. Gubin., that soon developed into the all-Russian with international participation. Finally, in 2015 S. P. Gubin has organismal and successfully conducted the first in Russia all-Russian conference on graphene "Graphene - molecule and a 2D-crystal" in Novosibirsk at Nikolaev Institute of inorganic chemistry SB RAS.

S.P. Gubin is a Professor of the Department of chemistry and technology of nanosized and composite materials, Lomonosov Moscow Institute of fine chemical technology and as such pays much attention to upbringing young scientists. S.P. Gubin is a Professor of chair of solid state physics on faculty of physics, Lomonosov MSU.

S.P. Gubin – academician of the Russian Academy of natural Sciences in Department of Radioelectronics, Nanophysics and Information technologies problems. Under his leadership defended their dissertations 6 doctors and over 30 candidates of Sciences. He has published more than 550 articles in scientific journals, 5 books and about 40 patents. S. P. Gubin, member of the editorial boards of the journals "Inorganic materials", "Coordination chemistry", Deputy editor-in-chief of the journal "Radioelectronics. Nanosystems. Information technologies" (RENSIT).

Professor S.P. Gubin is widely known specialist in scientific circles; he is an honoured man of science of the Russian Federation, his students work in a number of research organizations and educational institutes.

Sergei Pavlovich has an inexhaustible scientific potential and creative activeness, which undiminished with the years. He is full of optimism and new creative ideas..

A talented scientist, organizer and leader of science, attentive and demanding teacher, a charming and sympathetic person, Sergey Pavlovich Gubin deserved respect and authority among the scientific community in Russia and abroad.

Friends, colleagues, and disciples sincerely congratulate Sergei Pavlovich Gubin on his glorious jubilee and wish him good health, luck and success in scientific and pedagogical activity.

The editorial office of RENSIT journal cordially joins these wishes.

Editorial board

BUSHUEV
VLADIMIR ALEKSEEVICH

(TO 70 ANNIVERSARY OF BIRTH)

UDC 929.53

DOI: 10.17725/rensit.2017.09.122

On May 13, 2017 Vladimir Alekseevich Bushuev, Doctor of Physical and Mathematical Sciences, Professor of the Department of Solid State Physics of the Physics Department of the M.V. Lomonosov Moscow State University, member of the Russian Academy of Natural Sciences, well-known specialist in the fields of X-ray optics, phase contrast tomography, X-ray diagnostics of multilayer nanostructures, photonic crystals and free-electron X-ray lasers, and distinguished Professor at Moscow University celebrated his 70th birthday.

V.A. Bushuev was born in 1947 in Moscow, to military academy cadet Alexei Efimovich Bushuev from the Pskov region and MAI student Nadezhda Trofimovna Bushueva from the Zaporozhye region. After graduating from high school in Smolensk in 1965, he entered the Physics Department of Moscow State University. Vladimir Alekseevich entered the realm of physics at a time when the Physics Faculty was making breakthroughs in nonlinear processes in all fields, especially in optics and in radiophysics. In his third year, VA. Bushuyev was assigned to the sub-faculty of Wave Processes of the department of Radiophysics of the faculty of Physics. At that time, the sub-faculty of Wave Processes, founded and headed by Academician Rem Viktorovich Khokhlov, became a powerful global research center for nonlinear optics, nonlinear acoustics, laser physics and nonlinear spectroscopy. Here, under the guidance of his first teacher, the creator of the school of quantum optics, author of the discovery of the spontaneous parametric luminescence effect, Ph.D., David Nikolaevich Klyshko, VA. Bushuyev carried out graduate work devoted to the study of nonlinear scattering of light in crystals. Based on the results of these studies, V. Bushuyev made a report at the All-Union Conference on Nonlinear Optics in 1970, which became the beginning of his scientific biography.

In 1971, V.A. Bushuyev graduated from the Physics Department of Moscow State University and entered the graduate school of the Department of Solid State Physics, where the vector of his scientific interests shifted to X-ray and gamma-ray ranges. Under the guidance of Dr.Sc. D.N. Klyshko and Dr.Sc. R.N. Kuz'min, in 1975, he defended his dissertation, "Dynamic theory of inelastic scattering of X-rays in crystals," followed by a series of articles and speeches on the themes of X-ray optics and gamma-laser.

VA. Bushuev has been a member of the Department of Solid State Physics at the Physics Department of the Moscow State University since 1974, from 1974 to 1986 as a junior researcher, from 1986 to 1988 as a researcher, from 1988 to 1993 as a senior researcher, and since 1993 as a Professor. In 1978, for his series of works "Mathematical Models of the Kinetics of a Nuclear Gamma-Laser", V.A. Bushuev (along with A.V. Andreev and O.Yu. Tikhomirov) received the First R.V. Khokhlov Prize at the competition of scientific works of young scientists of the Moscow State University.

Vladimir Alekseevich teaches the special courses "Dynamic theory of X-ray scattering", "Secondary processes in X-ray optics", "Three-crystal X-ray diffractometry", "X-ray phase contrast tomography", the course "Inelastic X-ray scattering", the faculty courses "Problems of creating X-ray and gamma lasers" and "Nonlinear X-ray optics", produces relevant monographs, and supervises undergraduate and graduate students.

In 1990, V.A. Bushuev defended his doctoral dissertation "Coherent and diffraction phenomena in inelastic X-ray scattering in crystals". In 1999, by decision of the State Committee of the Russian Federation for Higher Education, V.A. Bushuev was awarded the academic title of Professor.

The scientific interests of V.A. Bushuev include X-ray optics, diffractometry, reflectometry and phase contrast tomography, the theory of X-ray scattering in microstructures with defects, photonic crystals, and X-ray and gamma lasers. He is an expert in nonlinear optical phenomena, and the author of the principal works on the diffraction of ultrashort X-ray and laser pulses. He developed the theory of X-ray phase contrast imaging and the theory of coherent and diffuse scattering in nano-sized crystalline and porous structures. V.A. Bushuev created a statistical dynamical theory of X-ray diffraction in crystals with structural defects and the theory of second-harmonic generation and diffraction splitting of laser pulses in linear and nonlinear photonic crystals. The scientific interests of V.A. Bushuyev are also associated with the creation of medical phase-contrast X-ray diagnostics, patented in 1998, about which he repeatedly spoke with interviewers on television and on the pages of the mass media.

In recent years, V.A. Bushuev has obtained results on the effect of thermal self-action on the diffraction of powerful X-ray pulses and the dynamic theory of ultracold neutron diffraction on a moving grating.

V.A. Bushuev is Laureate of the "Basic Element" Company for his series of works "Coherent and diffraction phenomena in the scattering of X-rays in amorphous, crystalline and nanoporous structures and laser radiation in nonlinear photonic crystals" (2003). His results also received recognition in the form of the Certificate of Honor of the Ministry of Education and Science of the Russian Federation (2005). Among his publications are more than 270 articles in authoritative scientific journals (the number of citations in the journals according to the Web of Science: 510, Scopus: 416). He is the co-author of several monographs and a number of books and schoolbooks devoted to various aspects of X-ray optics and diffractometry. V.A. Bushuev is a member of two dissertational councils of the Physics Department of Moscow State University, since 2003 a member and from 2008 to 2014 chairman of the Russian Foundation for Basic Research expert council for scientific discipline 02-211 "Interaction of X-ray, synchrotron and neutron radiation with condensed matter".

V.A. Bushuev is a member of the program and organizational committees of National and International conferences, and symposiums and meetings on X-ray optics, nanophysics and nanoelectronics. For many years he has supervised the work of the "Physics" section at the International Conference of Moscow State University "Lomonosov", and also chairs the program committees of the periodic International Scientific Seminars and youth schools-seminars "Modern methods of analysis of diffraction data and actual problems of X-ray optics" in Veliky Novgorod.

V.A. Bushuyev is a member of the editorial boards of the scientific journals "Crystallography Reports", "Surface: X-ray, synchrotron and neutron investigations", "Bulletin of the Moscow University: Series Physics, Astronomy", Deputy Chief Editor of the journal "Radioelectronics, Nanosystems, Information Technology (RENSIT)".

In 2006, he was awarded the honorary title of "Honored Professor of Moscow University." He was awarded the medal "To commemorate the 850th anniversary of Moscow", the Emblem "Honored Worker of Higher Professional Education of the Russian Federation" (2008), the anniversary breastplate "250 years of M.V. Lomonosov MSU".

Our portrait of V.A. Bushuev would be incomplete without mentioning his rare passion - the collection of historical video recordings of the legendary performers of the "golden age" of rock music. In this sphere of human enthusiasm, he occupies a very prominent place - his collection ranks among the top ten in the world. Vladimir Alekseevich generously shares by his recordings, bringing joy to the everyday life of numerous scientific conferences to which he is brought to participate.

HIs high scientific erudition, efficiency, adherence to principles and responsibility have given V.A. Bushuev deserved authority and wide popularity among the scientific community.

Friends, colleagues and students sincerely congratulate Vladimir Alekseyevich Bushuev on his birthday and wish him good health, luck, success in scientific and pedagogical activity

The Editorial Office of RENSIT magazine of the Branch of the Russian Academy of Natural Sciences cordially joins these wishes.

Editorial board

RUSAKOV VYACHESLAV SERAFIMOVICH

(TO 70 ANNIVERSARY OF BIRTH)

UDC 929.53

DOI: 10.17725/rensit.2017.09.124

On May 25, 2017 Vyacheslav Serafimovich Rusakov, Doctor of Physical and Mathematical Sciences, Professor of the Chair of General Physics of Physical Faculty of Lomonosov Moscow State University, full member of the Russian Academy of Natural Sciences, the known specialist in the field of Mössbauer spectroscopy, nuclear and radiation physics, condensed matter physics and hyperfine interactions, honored Professor of MSU celebrated his 70th birthday.

V.S. Rusakov was born in 1947 in Moscow, to family of employees Seraphim Semenovich Rusakov and Galina Alexandrovna Rusakova. After graduating 154 school of Moscow in 1965, he entered the physical faculty of Lomonosov MSU. In his third year, V.S. Rusakov was assigned to the Chair of solid state physics of Division of solid state physics of the Faculty of physics. At that time, the Chair of solid state physics, one of the oldest chairs of the faculty, was headed by Professor Herman Stepanovich Zhdanov. Here, under the guidance of his first teacher, then yet a PhD Phys&Math, Vladimir Ivanovich Nikolaev, V.S. Rusakov performs scientific work devoted to the study of crystal and magnetic structure of ferrites. Via the results of this research, the student Rusakov publishes an article in the journal "Solid State Physics", which became the beginning of his scientific biography.

In 1971, V.S. Rusakov graduated from the physical faculty of MSU and entered the postgraduate school at the Chair of General physics. The vector of his scientific interests shifted to the area of Mössbauer spectroscopy. Under the leadership of V.I. Nikolaev in 1974 he defended his PhD dissertation "Study of dynamic properties of nuclei in solid using the Mössbauer spectroscopy", behind which followed by a series of presentations at conferences articles and publications on Mössbauer spectroscopy, its hardware and software.

From 1974 to the present time V.S. Rusakov – an employee of the Chair of General physics of the Division experimental and theoretical physics of Faculty of physics, MSU, from 1974 to 1982 – assistant, from 1982 to 1994 – senior lecturer, from 1994 to 2001 – associate Professor, from Jan 2002 – Professor.

Vyacheslav Serafimovich teaches courses in General physics: "Electricity and magnetism" and "Optics", special courses "Physical principles of Mössbauer spectroscopy" and "Methods of Mössbauer spectroscopy", conducts general and special physics workshop at the faculty, publishes scientific monographs and teaching books and manuals, and guides the post-graduate and students. He has guided more than 30 diploma theses and 11 PhD dissertations.

In 1999 V.S. Rusakov defended his doctoral dissertation "Mössbauer spectroscopy of locally nonhomogeneous systems". In 2006, the decision of the State Committee of the Russian Federation for higher education V.S. Rusakov awarded the academic title of Professor.

Area of scientific interests of V.S. Rusakov – Mössbauer spectroscopy, condensed matter physics, hyperfine interactions, local atomic, crystalline, electronic and magnetic structure of matter. He is a specialist on the spectroscopy of locally

nonhomogeneous, including the phases of variable composition, amorphous, defective, and multiphase systems, the author of fundamental works on ion-beam and ion-plasma modifikacii materials. He developed methods for Mössbauer investigations of the spatial spin-modulated structures, hyperfine interactions, phase formation in layered systems, the kinetics of low-temperature crystallization of minerals. V.S. Rusakov developed and implemented the complex of methods of processing and analysis of Mössbauer data: quality improvement, and modelling decryption of Mössbauer spectra, reconstruction of distributions of hyperfine parameters, processing theirs the temperature, field and time dependencies. Rusakov scientific interests are also connected with the study of biogenic transformations and crystal chemistry of minerals.

In recent years, V.S. Rusakov obtained new results on the magnetic structure and hyperfine interactions in iron-cobalt and iron-Nickel nanotubes, successfully developing the diagnostics of spatial spin-modulated structures of multiferroics by methods nuclear magnetic resonance and Mössbauer spectroscopy

Of particular note are long-term, fruitful cooperation V.S. Rusakov with Institute of nuclear physics of Eurasian national University named after L.N. Gumilev, Republic of Kazakhstan. Joint researches, lectures, his expert activity continues to the present.

V.S. Rusakov is laureate of the prize of MSU in the nomination "Achievements in the scientific-research activity" (2016). Rusakov V.S. published more than 900 publications. Among his publications, about 300 papers in prestigious scientific journals (number of citations articles in journals according to Web of Science: 586, Scopus: 529), 4 scientific monographs, 43 manuals, 2 certificates on registration of the rights to the software.

V.S. Rusakov is member of the scientific council of physics Faculty and scientific council of the Division of experimental and theoretical physics of faculty of physics of MSU, chairman of the methodological commission of this Division. His active teaching activity is noticed the highest award of the native University – the Lomonosov prize of MSU (2011) and the hot recognition of students of the faculty of physics.

V.S. Rusakov is member of program and organizing committees of International Conferences "Mössbauer spectroscopy and its applications" and "Nuclear and radiation physics".

V.S. Rusakov is member of the editorial Board of the scientific journal "Radioelectronics. Nanosystems. Information technology" (RENSIT).

In 2013 he was awarded the honorary title "Honored Professor of the Moscow University". He was awarded the medal "In commemoration of 850th anniversary of Moscow", commemorative badge "250 years of Lomonosov MSU", commemorative badge "Honored workman of atomic industry of the Republic of Kazakhstan of I degree (gold mark)" (2009).

The high scientific erudition, working capacity, adherence to principles, responsibility brought V.S. Rusakov well-deserved prestige and wide fame in the science community.

Friends, colleagues, and pupils sincerely congratulate Vyacheslav Serafimovich Rusakov on his glorious jubilee and wish him good health, luck and success in scientific and pedagogical activities.

The editorial board of RENSIT journal cordially joins these wishes.

Editorial board

GRAFENIKA [GRAPHENICS] RUSSIAN GUBIN'S SEMINAR (MOSCOW)

Elena Yu. Buslaeva

VNIIAlmaz, http://www.vniialmaz.ru, Ltd. AkKoLab, http://www.akkolab.ru
Moscow 107996, Russian Federation
Kurnakov Institute of General and Inorganic Chemistry, Russian Academy of Sciences, http://www.igic.ras.ru
Moscow 117991, Russian Federation
eyubuslaeva@inbox.ru

Russian Seminar "GRAPHENE: MOLECULE AND CRYSTAL (material, physics, chemistry, electronics, photonics, biomedical applications)" under the direction of prof. SP Gubin operates from November 2011. Seminar sessions are held once a month, mainly in the boardroom VNIIAlmaz in Gilyarovskogo str., 65 (metro station "Rizhskaya"). The seminar is supported by LLC "AkKoLab" and the VNIIAlmaz. Programms of seminars are available at http://www.akkolab.ru. The seminar organizers see it as a discussion platform to discuss new ideas and concepts, review the results and the exchange of experience of researchers in the booming grafenika - an interdisciplinary field of modern science. Anticipated publication of an annual compendium of seminar materials, creating Programs of research in this area with possible access to financing. The seminar was attended by officials from various scientific institutions of Moscow - Kurnakov Institute of General and Inorganic Chemistry RAS, Nesmeyanov Institute of Organoelement Compounds of RAS, Semenov Institute of Chemical Physics RAS, Kotel'nikov Institute of Radio Engineering and Electronics RAS, National Research Centre "Kurchatov Institute", Moscow State University Department of Chemistry, Moscow Institute of Physics and Technology, National Research Nuclear University "MEPhI", People's Friendship University of Russia, LLC "AkKoLab", Open Joint Stock Company (JSC) "VNII ALMAZ", LLC "Karbonlayt", JSC NIIgrafit and others, as well as invited members of scientific institutions in Russia, Commonwealth of Independent States (CIS) and foreign countries. The audience for each session - about fifty participants. In the four- hour meeting with a break heard and discussed the 3-4 reports, news review and submitted poster presentations.

The journal RENSIT is published semi-annual reports of this seminar: list of reports indicating affiliated authors and submitted abstracts.

PACS: 01.10 Fv

RENSIT, 2017, 9(1):118-119 **DOI: 10.17725/rensit.2017.09.126**

TWENTY-EIGHT SEMINAR, 15.01.2016

1. Bocharov G.S., Mel'nikov V.P., **Eletskii A.V.**, Dr Sci Techn., Professor (MEI, Moscow). *The nonlinear heat-conductivity of the recovered graphene oxide.*

2. Obraztsova E.D., PhD Phys&Math, Tonkikh A.A., TsebroV.I., Rybkowski D.V., Obraztsova E.A., Chuvilin A.L., Kauppinen E. (CENI GPI RAS) *Film from the filled single-walled carbon nanotubes - a new material for optoelectronics.*

3. **Chervonobrodov S.P.**, PhD Phys&Math, Moscow. *On the application of nano-materials in electrochemical energy storage (according to the discussions at the expert session, held in RUSNANO 15 and 21 December 2016).*

TWENTY-NINTH WORKSHOP 22.03.2017

1. Zhuravlev V.V., Dr Sci Techn (JSC VNIIALMAZ)**.** *New materials based on graphene oxide and graphene; the work of the* VNIIALMAZ *for 2015-2016.*

2. Burmistrov I.S., Dr Sci Phys&Math (Landau ITP RAS). *Quantum graphene elasticity: coefficient of thermal expansion and heat capacity.*

THIRTIETH WORKSHOP 24.05.2017

1. **Gall N.R**., Dr Sci Phys&Math, prof.; Rudikov E.V. (Ioffe FTI RAS, Saint-Petersburg). *The problem of "ideality" of graphene, obtained by CVD and high temperature diffusion from the bulk.*

2. **Danilov E.A**., Samoilov M.V., Dmitriev V.S., Nikolaeva A.B., Ponomarev D.V., Timoshchuk E.I. (JSC NIIgrafit). *Obtaining a transparent conductive films based on graphene and metal nanoparticles by the method of Langmuir-Blodgett films.*

3. **Korolev V.V.,** Dr Sci Chem (Institute of solution chemistry of RAS, Ivanovo), Koksharov Yu.A., Gubin S.P. (IGIC RAS). *Magnetocaloric effect in graphene.*

4. DIFFERENT.

Second Russian Conference

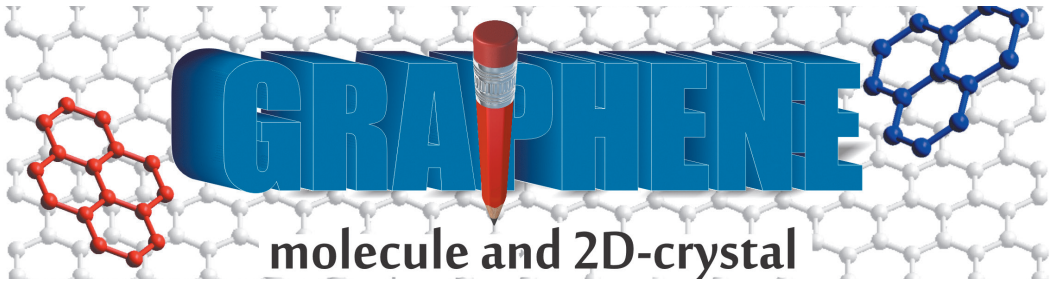

August 7-11, 2017
Novosibirsk 630090, Russian Federation

http://grapheneconf.ru

PACS: 01.10 Fv

DOI: 10.17725/rensit.2017.09.128

Novosibirsk State University
Nikolaev Institute of Inorganic Chemisry SB RAS
Kurnakov Institute of General and Inorganic Chemisry RAS
Boreskov Institute of Catalysis SB RAS
Rzhanov Institute of Semiconductor Physics SB RAS

The conference implements a national platform for discussion of scientific and practical achievements in the field of synthesis and application of graphene and related structures, identify current issues and prospects of research in this area. The conference will bring together nearly 150 leading experts from major research centers and universities of Russia and will be attended by foreign scientists.

The official conference language - Russian

SUGGESTED TOPICS:

- CVD-synthesis of graphene
- Diagnosis of graphene
- Graphene electronics
- Mechanical properties and applications
- Microelectromechanical systems
- Chemical derivatives of graphene: synthesis, structure, properties
- Electrochemical materials
- Optical properties
- Hybrid materials based on graphene

RELATED SEMINARS:

- Non-carbon 2D materials
- Related sp^2-carbon materials
- Theoretical methods in the annex to grafene materials

KEY DATES

The deadline for registration and abstract submission	**is April 15. 2017**
Notification of inclusion in the program	**- May 01. 2017**
The deadline of registration fee payment	**- July 01. 2017**
Conference program	**- August 01. 2017**
Deadline for submission of papers to the Journal of structural chemistry	**- September 30.2017**

VENUE

Novosibirsk, Academgorodok, Novosibirsk state university, aud. 3307.

ACCOMODATION OF PARTICIPANTS

Novosibirsk, Pirogova str., 1; Hotel "Golden Valley"

Radioelectronics. Nanosystems. Information Technologies (abbr. RENSIT)
Certificate El. no. FS77-60275 on 19.12.2014 of the Ministry of Telecom and Mass Communications of Russian Federation, Moscow
ISSN: 2414-1267online. Http://www.rensit.ru. Publisher - Vladimir I. Grachev. 2017, 30 Juni.
Computer printing, page-proofs, graphics, photos of work - the editors RENSIT.